CHARACTERIZATION OF AMINOPEPTIDASE N AND ENDOPEPTIDASES E, O, O2, O3 FROM *LACTOBACILLUS HELVETICUS* WSU19, A LACTOBACILLI WITH INDUSTRIAL SIGNIFICANCE

By

ELLY SOERYAPRANATA

A dissertation submitted in partial fulfillment of the requirements for the degree of

DOCTOR OF PHILOSOPHY IN FOOD SCIENCE

WASHINGTON STATE UNIVERSITY
Department of Food Science and Human Nutrition

AUGUST 2005

To the Faculty of Washington State University:

The members of the Committee appointed to examine the dissertation of ELLY SOERYAPRANATA find it satisfactory and recommend that it be accepted.

_____

Chair

_____

_____

_____

ACKNOWLEDGMENTS

I would like to express my genuine appreciation to my major advisor, Dr. Joseph R. Powers, for his expertise, interest, and support throughout my Ph.D. program. He opened the opportunities for me to learn technical skills in various fields, which shaped me to be a well-rounded scientist. I extend my appreciation to Dr. Gülhan Ü. Yüksel, for sharing her expertise in molecular biology and her willingness to discuss my lab work; Dr. Stephanie Clark, and Dr. Herbert H. Hill, for their suggestions to improve my dissertation; and Dr. Lloyd O. Luedecke, for his friendship and constant support.

I would like to thank the United Dairymen of Idaho, Western Center for Dairy Research, Washington State Dairy Products Commission, and Department of Food Science and Human Nutrition at Washington State University for providing financial supports to this project. In addition, I would like to thank the Washington State University Creamery, Dr. Barry G. Swanson, and Department of Food Science and Human Nutrition at Washington State University for providing assistantships throughout my Ph.D. program.

Special thanks are given to my parents, Dean and Mary Guenthers, Dustin and Mary Bakers, Jodi Anderson, Jean Taylor, Kitty Anderson, and Sarmauli Manurung for their endless love and encouragement especially during the difficult times at the end of my study. Also, I thank Dewi Scott, Shantanu Agarwal, and Claudia Ionita for their supports.

CHARACTERIZATION OF AMINOPEPTIDASE N AND ENDOPEPTIDASES E, O, O2, O3 FROM *LACTOBACILLUS HELVETICUS* WSU19, A LACTOBACILLI WITH INDUSTRIAL SIGNIFICANCE

Abstract

by Elly Soeryapranata, Ph.D.
Washington State University
August 2005

Chair: Joseph R. Powers

Lactobacillus helveticus WSU19 is the adjunct culture of Cougar Gold, a Cheddar-type cheese with non-bitter taste after extensive aging. The objective of the present study was to clone genes encoding for selected peptidases from *Lb. helveticus* WSU19 and to characterize the activities of these peptidases on chymosin-derived peptides, β-CN f193-209 and α_{s1}-CN f1-23.

The *pepN, pepE, pepO, pepO2,* and *pepO3* genes from *Lb. helveticus* WSU19 were successfully cloned in *Escherichia coli* DH5α using the corresponding genes from *Lb. helveticus* CNRZ32 as probes. Primer walking of 5 genomic inserts (2.7-5.8 kb) revealed open reading frames encoding for the PepN, PepE, PepO, PepO2, and PepO3 enzymes. The deduced amino acid sequences of the cloned genes share 97-99% identities with the corresponding sequences from *Lb. helveticus* CNRZ32.

PepN cleaves the bitter peptide, β-CN f193-209, at Tyr_{193}-Gln_{194} and Gln_{194}-Gln_{195} bonds. Degradation of α_{s1}-CN f1-23 by PepN occurs in the presence of PepO, PepO2, or PepO3. PepE cleaves β-CN f193-209 in the presence of PepN or PepO-like endopeptidases.

The Lys_3-His_4 bond is the preferred cleavage site of PepE in α_{s1}-CN f1-23. PepO, PepO2, and PepO3 possess post-proline activities on β-CN f193-209. The Pro_{196}-Val_{197} and Pro_{206}-Ile_{207} bonds are the preferred cleavage sites of PepO, PepO2, and PepO3 in β-CN f193-209. In addition, PepO and PepO3 cleave at the Pro_{200}-Val_{201} bond. In contrast to PepO3, PepO hydrolyzed Leu_{198}-Gly_{199} and Val_{201}-Arg_{202} upon prolonged incubation. The Gln_{13}-Glu_{14} and Glu_{14}-Val_{15} bonds are the preferred cleavage sites of PepO, PepO2, and PepO3 in α_{s1}-CN f1-23.

Hydrolysis of β-CN f193-209 by the combination of PepN and PepE produced a peptide with a MW of 898 Da, corresponding to β-CN f202-209. This peptide, with a bitterness threshold of 0.004 mM, is one of the most bitter peptides reported. Combinations of PepN-PepO or PepN-PepO3 degrade β-CN f193-209 into peptides with MW less than 1000 Da. In contrast to the PepN-PepE combination, none of the peptides formed by PepN-PepO or PepN-PepO3 combinations was previously identified as bitter. Based on these results, construction of double-peptidase mutants of *Lb. helveticus* WSU19 (Δ*pepN*Δ*pepO*, Δ*pepN*Δ*pepO3*, Δ*pepE*Δ*pepO*, and Δ*pepN*Δ*pepE*) is recommended to determine the role(s) of these enzymes in cheese ripening.

TABLE OF CONTENTS

Page

ACKNOWLEDGMENTS..……... iii

ABSTRACT…….. iv

LIST OF TABLES…….… xii

LIST OF FIGURES……... xvi

CHAPTER

I. GENERAL INTRODUCTION……... 1

II. LITERATURE REVIEW…… 6

1. Chemistry of caseins……... 7

1.1. Phosphorylation…… 7

1.2. Hydrophobicity…….… 8

1.3. Casein micelles…….… 8

1.4. Secondary structure of caseins…….… 10

2. Bitterness in cheese…….… 10

2.1. Relationship between structure of bitter peptides and bitterness intensity…… 13

2.2. Development and control of bitterness in cheese…….… 16

3. Proteolysis of caseins in cheese…….. 20

3.1. Proteolysis by chymosin……... 21

3.2. Proteolysis by plasmin…….. 23

3.3. Proteolysis by lactic acid bacteria…… 25

3.3.1. Proteinases of LAB…….. 26

3.3.2. Peptidases of LAB……... 31

III. MATERIALS AND METHODS…… 36

1. Bacterial strains, growth media, and culture conditions…...…… 37

2. Molecular biology techniques…… 38

3. Isolation of genomic DNAs from *Lb. helveticus* WSU19 and CNRZ32…… 38

4. Cloning of the complete *pepE*, *pepO*, *pepO2*, and *pepO3* genes…… 40

4.1. Isolation of plasmid DNAs from the recombinant *E. coli* cells carrying peptidase gene from *Lb. helveticus* CNRZ32…….. 40

4.2. Probe syntheses…… 42

4.2.1. DNA amplification via PCR…… 42

4.2.2. Gel extraction of probes…….. 44

4.2.3. Dot blot estimation of probe concentrations……... 45

4.3. Southern hybridization…… 47

4.3.1. Digestion of genomic DNA from *Lb. helveticus* WSU19 with single restriction enzyme…… 47

4.3.2. Gel electrophoresis of the digested genomic DNAs…… 47

4.3.3. Southern transfer……. 48

4.3.4. Prehybridization and hybridization……. 49

4.3.5. Detection……. 49

4.3.6. Digestion of genomic DNA from *Lb. helveticus* WSU19 with two restriction enzymes and the second Southern blot……... 50

4.4. Preparation of insert DNAs……. 52

4.4.1. Digestion of genomic DNA from *Lb. helveticus* WSU19 with cloning enzyme(s)……... 52

4.4.2. Gel extraction of hybridization-positive DNA fragments…….... 52

4.5. Preparation of pJDC9 vector DNA……... 54

4.5.1. Digestion of pJDC9 plasmid DNA with cloning enzyme(s)….... 54

4.5.2. Purification of the digested pJDC9 plasmid DNAs……..… 54

4.5.3. Dephosphorylation of digested pJDC9 vector DNA (for single cloning enzyme)…….. 55

4.6. Ligation of insert genomic DNAs into pJDC9 vector DNA…… 56

4.7. Electroporation of ligated DNAs into electrocompetent *E. coli* DH5α cells……... 56

4.8. Colony hybridization…… 57

4.8.1. Replica plating……..… 57

4.8.2. Colony lifts…….. 57

4.8.3. Prehybridization and hybridization……. 58

4.8.4. Detection…….. 59

4.9. Confirmation of peptidase-positive clone(s)…… 60

4.9.1. Small-scale plasmid DNA preparation from hybridization-positive colonies…….. 60

4.9.2. Restriction enzyme analysis…… 61

4.9.3. Chloramphenicol-permeabilized cells / cell-free extract (CFE) assay for confirmation of PepE activity…….. 62

4.9.4. Medium-scale plasmid DNA preparation from hybridization- 62

positive colonies……..

4.9.5. 5’ and 3’ end DNA sequencing……... 64

4.9.6. Large-scale plasmid DNA preparation from peptidase-positive clones……... 64

4.9.7. Primer walking DNA sequencing…… 65

5. Cloning of the *pepN* structural gene from *Lb. helveticus* WSU19…….. 65

5.1. Design of degenerate primers……... 65

5.2. PCR amplification of the *pepN* structural gene from *Lb. helveticus* WSU19…… 66

5.3. Preparation of insert and vector DNA…….. 69

5.4. Ligation of insert into pJDC9 vector DNA…….. 69

5.5. Electroporation of the ligated DNA into electrocompetent *E. coli* DH5α cells..... 70

5.6. Screening for PepN-positive clone(s)……... 70

6. Cloning of the complete *pepN* gene from *Lb. helveticus* WSU19…….. 71

6.1. Probe synthesis……. 71

6.2. Restriction enzyme analysis of pES3……... 71

6.3. Southern hybridization…… 72

6.4. Cloning of the *pepN* gene……. 72

7. Preparation of CFEs from *E. coli* DH5α derivatives expressing selected peptidase genes from *Lb. helveticus* WSU19…….. 72

8. Degradation of β-CN f193-209 and α_{s1}-CN f1-23 by CFE(s)…… 74

9. MALDI-TOF mass spectrometry analyses…… 75

IV. RESULTS AND DISCUSSION…….… 76

1. Cloning strategies…… 78

1.1. One-step cloning…….. 78

1.2. Two-step cloning……. 79

1.3. Screening and confirmation of the peptidase-positive clone(s)……... 80

2. Cloning of the *pepE*, *pepO*, *pepO2*, *pepO3*, and *pepN* genes……..… 81

3. DNA sequence analysis of the 2.7-kb *Pst*I genomic insert containing the *pepE* gene.…… 96

4. DNA sequence analysis of the 4.3-kb *Hind*III-*Sal*I genomic insert containing the *pepO* gene…….. 98

5. DNA sequence analysis of the 5.8-kb *Xba*I-*Sph*I genomic insert containing the *pepO2* gene…… 101

6. DNA sequence analysis of the 3.4-kb *Kpn*I genomic insert containing the *pepO3* gene…….. 103

7. DNA sequence analysis of the 5-kb *Sac*I-*Sph*I genomic insert containing the *pepN* gene…… 105

8. Degradation of β-CN f193-209 by PepO, PepO2, and PepO3……...……. 139

9. Degradation of β-CN f193-209 by PepN.……... 144

10. Degradation of β-CN f193-209 by PepE……..……. 151

11. Degradation of α_{s1}-CN f1-23 by PepO, PepO2, and PepO3……...…….. 177

12. Degradation of α_{s1}-CN f1-23 by PepE……..……...…….. 188

13. Degradation of α_{s1}-CN f1-23 by PepN-an endopeptidase activities……. 193

V. SUMMARY AND FUTURE RESEARCH…… 216

1. Summary……. 217

2. Future research…… 220

VI. REFERENCES…… 222

LIST OF TABLES

Page

Table 1. Bitter peptides isolated from cheese…… 12

Table 2. Relationship between bitterness of a peptide and its average hydrophobicity... 13

Table 3. Peptides produced by the lactococcal proteinase (P_I or P_{III}-type) within 1-h incubation with caseins…….. 28

Table 4. Specificities of lactobacilli PrtP on α_{s1}-CN f1-23……... 30

Table 5. Peptidases from LAB……... 32

Table 6. Forward and reverse primers for endopeptidase probe syntheses……... 43

Table 7. Forward and reverse primers for synthesis of the *pepN* gene probe…… 71

Table 8. Plasmids used or generated in the cloning of the peptidase genes from *Lb. helveticus* WSU19…….. 95

Table 9. Amino acid BLAST analyses for the deduced PepE sequence from *Lb. helveticus* WSU19…….. 114

Table 10. Peptide fragments formed during hydrolysis of β-CN f193-209 by PepO from *Lb. helveticus* WSU19 at 37°C under simulated cheese conditions (4% salt, w/v; 50 mM citrate buffer pH 5.2)……. 156

Table 11. Peptide fragments formed during hydrolysis of β-CN f193-209 by PepO2 from *Lb. helveticus* WSU19 at 37°C under simulated cheese conditions (4% salt, w/v; 50 mM citrate buffer pH 5.2)……. 158

Table 12. Peptide fragments formed during hydrolysis of β-CN f193-209 by PepO3 from *Lb. helveticus* WSU19 at 37°C under simulated cheese conditions (4% salt, w/v; 50 mM citrate buffer pH 5.2)……. 159

Table 13. Peptide fragments formed during hydrolysis of β-CN f193-209 by PepN from *Lb. helveticus* WSU19 at 37°C under simulated cheese conditions (4% salt, w/v; 50 mM citrate buffer pH 5.2)……. 163

Table 14. Peptide fragments formed during hydrolysis of β-CN f193-209 by PepN and PepO from *Lb. helveticus* WSU19 at 37°C under simulated cheese conditions (4% salt, w/v; 50 mM citrate buffer pH 5.2)…… 165

Table 15. Peptide fragments formed during hydrolysis of β-CN f193-209 by PepN and PepO2 from *Lb. helveticus* WSU19 at 37°C under simulated cheese conditions (4% salt, w/v; 50 mM citrate buffer pH 5.2)……. 166

Table 16. Peptide fragments formed during hydrolysis of β-CN f193-209 by PepN and PepO3 from *Lb. helveticus* WSU19 at 37°C under simulated cheese conditions (4% salt, w/v; 50 mM citrate buffer pH 5.2)……. 167

Table 17. Peptide fragments formed during hydrolysis of β-CN f193-209 by PepE and PepN from *Lb. helveticus* WSU19 at 37°C under simulated cheese conditions (4% salt, w/v; 50 mM citrate buffer pH 5.2)……. 170

Table 18. Peptide fragments formed during hydrolysis of β-CN f193-209 by PepE and PepO from *Lb. helveticus* WSU19 at 37°C under simulated cheese conditions (4% salt, w/v; 50 mM citrate buffer pH 5.2)……. 172

Table 19. Peptide fragments formed during hydrolysis of β-CN f193-209 by PepE and PepO2 from *Lb. helveticus* WSU19 at 37°C under simulated cheese conditions (4% salt, w/v; 50 mM citrate buffer pH 5.2)……. 173

Table 20. Peptide fragments formed during hydrolysis of β-CN f193-209 by PepE and PepO3 from *Lb. helveticus* WSU19 at 37°C under simulated cheese conditions (4% salt, w/v; 50 mM citrate buffer pH 5.2)……. 174

Table 21. Peptide fragments formed during hydrolysis of α_{s1}-CN f1-23 by PepO from *Lb. helveticus* WSU19 at 37°C under simulated cheese conditions (4% salt, w/v; 50 mM citrate buffer pH 5.2)…….. 197

Table 22. Peptide fragments formed during hydrolysis of α_{s1}-CN f1-23 by PepO2 from *Lb. helveticus* WSU19 at 37°C under simulated cheese conditions (4% salt, w/v; 50 mM citrate buffer pH 5.2)…….. 199

Table 23. Peptide fragments formed during hydrolysis of α_{s1}-CN f1-23 by PepO3 from *Lb. helveticus* WSU19 at 37°C under simulated cheese conditions (4% salt, w/v; 50 mM citrate buffer pH 5.2)…….. 201

Table 24. Peptide fragments formed during hydrolysis of α_{s1}-CN f1-23 by PepE from *Lb. helveticus* WSU19 at 37°C under simulated cheese conditions (4% salt, w/v; 50 mM citrate buffer pH 5.2)…….. 206

Table 25. Peptide fragments formed during hydrolysis of α_{s1}-CN f1-23 by PepE and PepO from *Lb. helveticus* WSU19 at 37°C under simulated cheese conditions (4% salt, w/v; 50 mM citrate buffer pH 5.2)……. 208

Table 26. Peptide fragments formed during hydrolysis of α_{s1}-CN f1-23 by PepE and PepO2 from *Lb. helveticus* WSU19 at 37°C under simulated cheese conditions (4% salt, w/v; 50 mM citrate buffer pH 5.2)……. 209

Table 27. Peptide fragments formed during hydrolysis of α_{s1}-CN f1-23 by PepE and PepO3 from *Lb. helveticus* WSU19 at 37^{o}C under simulated cheese conditions (4% salt, w/v; 50 mM citrate buffer pH 5.2)……. 210

Table 28. Peptide fragments formed during hydrolysis of α_{s1}-CN f1-23 by a combination of PepN and endopeptidase from *Lb. helveticus* WSU19 at 37^{o}C under simulated cheese conditions (4% salt, w/v; 50 mM citrate buffer pH 5.2)…… 213

Table 29. Peptide fragments formed during hydrolysis of α_{s1}-CN f1-23 by PepN and PepE from *Lb. helveticus* WSU19 at 37^{o}C under simulated cheese conditions (4% salt, w/v; 50 mM citrate buffer pH 5.2)……. 214

LIST OF FIGURES

Page

Figure 1. 'Hairy' model of casein micelle……. 9

Figure 2. Casein micelle proposed by Holt…… 9

Figure 3. Model of the binding of bitter peptide to bitter taste receptor…… 16

Figure 4. Hydrolysis of caseins to amino acids……. 21

Figure 5. Proteolytic system of *Lactococcus* sp.……... 26

Figure 6. Classification of strains of *Lc. lactis* according to PrtP specificities on α_{s1}-CN f1-23…….. 29

Figure 7. Protein alignment of PepN enzymes for designing the forward degenerate primer…….…… 67

Figure 8. Protein alignment of PepN enzymes for designing the reverse degenerate primer……. 67

Figure 9. Nucleotide alignment of the *pepN* genes for designing the forward degenerate primer……. 68

Figure 10. Nucleotide alignment of the *pepN* genes for designing the reverse degenerate primer……... 68

Figure 11. Phylogenetic tree of *Lb. helveticus* WSU19 based on the 16S rRNA gene sequence and alignment……. 77

Figure 12. Map of plasmid pJDC9……. 79

Figure 13. High stringency Southern hybridization of genomic DNA from *Lb. helveticus* WSU19 using DIG-labeled probes synthesized based on DNA sequence information available for *Lb. helveticus* CNRZ32: *pepE*, *pepO*, *pepO2*, and *pepO3* genes (Single digest)…….. 84

Figure 14. High stringency Southern hybridization of genomic DNA from *Lb. helveticus* WSU19 using a DIG-labeled probe synthesized based on the *Lb. helveticus* CNRZ32 *pepE* gene (Double digest)……. 85

Figure 15. High stringency Southern hybridization of genomic DNA from *Lb. helveticus* WSU19 using a DIG-labeled probe synthesized based on the *Lb. helveticus* CNRZ32 *pepO* gene (Double digest)…… 86

Figure 16. High stringency Southern hybridization of genomic DNA from *Lb. helveticus* WSU19 using a DIG-labeled probe synthesized based on the *Lb. helveticus* CNRZ32 *pepO2* gene (Double digest)…….. 87

Figure 17. High stringency Southern hybridization of genomic DNA from *Lb. helveticus* WSU19 using a DIG-labeled probe synthesized based on the *Lb. helveticus* CNRZ32 *pepO3* gene (Double digest)……... 88

Figure 18. High stringency Southern hybridization of plasmid DNA samples from the hybridization-positive colonies in the cloning of the *pepO* gene from *Lb. helveticus* WSU19 using a DIG-labeled probe synthesized based on the *Lb. helveticus* CNRZ32 *pepO* gene…….. 89

Figure 19. Nucleic acid sequences of plasmid pES3 carrying the *pepN* structural gene from *Lb. helveticus* WSU19. The pES3 plasmid was extracted from *E. coli* DH5α(pES3) colony #3-5…….. 90

Figure 20. Nucleic acid sequences of plasmid pES3 carrying the *pepN* structural gene from *Lb. helveticus* WSU19. The pES3 plasmid was extracted from *E. coli* DH5α(pES3) colony #7-2……. 91

Figure 21. Nucleic acid sequences of plasmid pES3 carrying the *pepN* structural gene from *Lb. helveticus* WSU19. The pES3 plasmid was extracted from *E. coli* DH5α(pES3) colony #7-5…….. 92

Figure 22. Restriction enzyme analysis of the plasmid pES3 from *E. coli* DH5α(pES3) colony #7-5, expressing the *pepN* structural gene from *Lb. helveticus* WSU19……... 93

Figure 23. High stringency Southern hybridization of genomic DNA from *Lb. helveticus* WSU19 using a DIG-labeled probe synthesized based on the *Lb. helveticus* WSU19 *pepN* structural gene…… 94

Figure 24. Open reading frame (ORF) and restriction enzyme analyses of the 2.7-kb *Pst*I genomic insert containing the *pepE* gene from *Lb. helveticus* WSU19……. 108

Figure 25. Nucleic acid sequence of the 2.7-kb *Pst*I genomic insert and the deduced amino acid sequence of the PepE enzyme from *Lb. helveticus* WSU19……... 109

Figure 26. Alignment of the deduced amino acid sequence of PepE from *Lb. helveticus* WSU19 and the published amino acid sequences of thiol proteases from lactobacilli…. 111

Figure 27. Open reading frame (ORF) and restriction enzyme analyses of the 4.3-kb *Hind*III-*Sal*I genomic insert containing the *pepO* gene from *Lb. helveticus* WSU19….. 115

Figure 28. Nucleic acid sequence of the 4.3-kb *Hind*III-*Sal*I genomic insert and the deduced amino acid sequence of the PepO enzyme from *Lb. helveticus* WSU19…… 116

Figure 29. Alignment of the deduced amino acid sequence of PepO from *Lb. helveticus* WSU19 and the published amino acid sequences of PepO from lactobacilli…… 119

Figure 30. Open reading frame (ORF) and restriction enzyme analyses of the 5.8-kb *Xba*I-*Sph*I genomic insert containing the *pepO2* gene from *Lb. helveticus* WSU19……. 121

Figure 31. Nucleic acid sequence of the 5.8-kb *Xba*I-*Sph*I genomic insert and the deduced amino acid sequence of the PepO2 enzyme from *Lb. helveticus* WSU19…….. 122

Figure 32. Open reading frame (ORF) and restriction enzyme analyses of the 3.4-kb *Kpn*I genomic insert containing the *pepO3* gene from *Lb. helveticus* WSU19……. 125

Figure 33. Nucleic acid sequence of the 3.4-kb *Kpn*I genomic insert and the deduced amino acid sequence of the PepO3 enzyme from *Lb. helveticus* WSU19……. 127

Figure 34. Alignment of the deduced and published amino acid sequences of PepO, PepO2, and PepO3……. 129

Figure 35. Open reading frame (ORF) and restriction enzyme analyses of the 5-kb *Sac*I-*Sph*I genomic insert containing the *pepN* gene from *Lb. helveticus* WSU19…….. 131

Figure 36. Nucleic acid sequence of the 5-kb *Sac*I-*Sph*I genomic insert and the deduced amino acid sequence of the PepN enzyme from *Lb. helveticus* WSU19…… 132

Figure 37. Alignment of the deduced amino acid sequence of PepN from *Lb. helveticus* WSU19 and the published amino acid sequences of PepN from lactobacilli…… 135

Figure 38. Cleavage sites of PepO from *Lb. helveticus* WSU19 in β-CN f193-209 as a function of incubation time…… 161

Figure 39. Cleavage sites of PepO2 from *Lb. helveticus* WSU19 in β-CN f193-209 as a function of incubation time…… 161

Figure 40. Cleavage sites of PepO3 from *Lb. helveticus* WSU19 in β-CN f193-209 as a function of incubation time…… 162

Figure 41. Cleavage sites of PepN from *Lb. helveticus* WSU19 in β-CN f193-209 as a function of incubation time…… 164

Figure 42. Cleavage sites of PepN and PepO from *Lb. helveticus* WSU19 in β-CN f193-209 as a function of incubation time……. 168

Figure 43. Cleavage sites of PepN and PepO2 from *Lb. helveticus* WSU19 in β-CN f193-209 as a function of incubation time……. 168

Figure 44. Cleavage sites of PepN and PepO3 from *Lb. helveticus* WSU19 in β-CN f193-209 as a function of incubation time……. 169

Figure 45. Cleavage sites of PepE and PepN from *Lb. helveticus* WSU19 in β-CN f193-209 as a function of incubation time……. 171

Figure 46. Cleavage sites of PepE and PepO from *Lb. helveticus* WSU19 in β-CN f193-209 as a function of incubation time……. 175

Figure 47. Cleavage sites of PepE and PepO2 from *Lb. helveticus* WSU19 in β-CN f193-209 as a function of incubation time……. 175

Figure 48. Cleavage sites of PepE and PepO3 from *Lb. helveticus* WSU19 in β-CN f193-209 as a function of incubation time……. 176

Figure 49. Cleavage sites of PepO from *Lb. helveticus* WSU19 in α_{s1}-CN f1-23 as a function of incubation time…… 203

Figure 50. Cleavage sites of PepO2 from *Lb. helveticus* WSU19 in α_{s1}-CN f1-23 as a function of incubation time…… 204

Figure 51. Cleavage sites of PepO3 from *Lb. helveticus* WSU19 in α_{s1}-CN f1-23 as a function of incubation time…… 205

Figure 52. Cleavage sites of PepE from *Lb. helveticus* WSU19 in α_{s1}-CN f1-23 as a function of incubation time…… 207

Figure 53. Cleavage sites of PepE and PepO from *Lb. helveticus* WSU19 in α_{s1}-CN f1-23 as a function of incubation time……... 211

Figure 54. Cleavage sites of PepE and PepO2 from *Lb. helveticus* WSU19 in α_{s1}-CN f1-23 as a function of incubation time……... 211

Figure 55. Cleavage sites of PepE and PepO3 from *Lb. helveticus* WSU19 in α_{s1}-CN f1-23 as a function of incubation time……... 212

Figure 56. Cleavage sites of PepN and endopeptidases O, O2, or O3 from *Lb. helveticus* WSU19 in α_{s1}-CN f1-23 at 12-h incubation…….. 215

Figure 57. Cleavage sites of PepN and PepE from *Lb. helveticus* WSU19 in α_{s1}-CN f1-23 as a function of incubation time……... 215

CHAPTER I:

General Introduction

Proteolysis of caseins contributes to the flavor development of aged Cheddar-type cheeses via production of peptides and amino acids (Lemieux and Simard, 1992; Steele, 1995; Fox et al., 1996; McSweeney, 1997; Sousa et al., 2001). Casein-degrading enzymes that influence cheese ripening include proteinase from coagulant, indigenous proteinase of milk, and proteinases and peptidases from starter and non-starter lactic acid bacteria. Despite the development of desirable flavor, the actions of proteinases from coagulant and starter lactic acid bacteria on caseins produce bitter peptides, low molecular weight peptides that are high in hydrophobicity. Overproduction or inadequate degradation of the bitter-tasting peptides is responsible for the accumulation of bitter peptides, resulting in bitterness of cheese. Although bitter notes may contribute to the desirable flavor of ripened cheese, excessive bitterness limits the acceptance of the cheese (Shinoda et al., 1985a; Lemieux and Simard, 1991; Sousa et al., 2001). Bitterness is recognized as a major taste defect in Gouda and Cheddar cheeses (Lemieux and Simard, 1991).

Utilization of adjunct cultures in cheesemaking in addition to the starter culture is an approach to reduce bitterness (Bartels et al., 1987; El Abboudi et al., 1991; Drake et al., 1997; Fox et al., 1998; Fajarrini, 1999; El Soda et al., 2000). Adjunct cultures consist mainly of lactobacilli possessing high proteolytic and peptidolytic activities to enhance degradation of bitter peptides. Besides degradation of bitter peptides, adjunct cultures contribute to the improvement of flavor of aged cheese (El Soda et al., 2000).

To date at least 16 peptidases from lactobacilli have been characterized at the molecular level (Christensen et al., 1999; Christensson et al., 2002; Chen et al., 2003; Sridhar, 2003). However, the key peptidases that play important roles in the ripening of cheese are still under debate. Using recombinant lactococcus starters, Guinec et al. (2000)

reported the importance of PepN, PepT, and PepX for cheese ripening, while Guldfeldt et al. (2001) indicated the important roles of PepN and PepC in flavor development and reduction of bitterness. Courtin et al. (2002) reported that proline-specific peptidases PepW, PepX, and PepQ were the most efficient peptidases in increasing the amounts of amino acids during cheese ripening. Conversion of amino acids into aroma compounds is important for the development of cheese flavor. Understanding the key peptidases during ripening of cheese will be useful for screening of adjunct cultures as well as for improving starter cultures via enzyme over-expression technology.

Lactobacillus helveticus WSU19 is used as an adjunct culture in the manufacture of Cougar Gold cheese, a white Cheddar-type cheese with a sharp, nutty flavor. The cheese is ripened for at least one year prior to sale. Despite the long ripening time, Cougar Gold cheese develops little bitterness, which makes the cheese unique. The addition of *Lb. helveticus* WSU19 as an adjunct culture is believed to play roles in the prevention of bitterness and the development of flavor in Cougar Gold cheese.

Studies have been conducted by our research group to reveal the role of *Lb. helveticus* WSU19 in the prevention of bitterness in cheese. Olson (1998) demonstrated the debittering activity of cell-free extract (CFE) from *Lb. helveticus* WSU19 on bitter cheese made with coagulant only. Fajarrini (1999) reported the debittering activity of *Lb. helveticus* WSU19 as an adjunct culture in Cheddar cheese made with a starter culture known as a bitter-cheese producer. Matrix-assisted laser desorption/ionization time-of-flight (MALDI-TOF) mass spectrometry spectra of water-soluble extract (WSE) of the bitter cheeses identified a major peak with mass-to-charge (m/z) ratio of 1881 Da, which corresponds to the mass of bitter peptide β-casein (β-CN) f193-209 (Soeryapranata et al., 2002a). The debittering activity of

Lb. helveticus WSU19 was accompanied by a marked decrease of the 1881-Da peak intensity. Soeryapranata et al. (2002b) successfully correlated the concentration of β-CN f193-209 in the WSE of Cheddar cheese with bitterness intensity of the cheese after 6-month aging. Soeryapranata et al. (2004) indicated the importance of general aminopeptidase (AP) and endopeptidase activities of *Lb. helveticus* WSU19 in hydrolyzing the bitter peptide β-CN f193-209. The hydrolysis rate of β-CN f193-209 by CFE from *Lb. helveticus* WSU19 was 10 times more rapid than the hydrolysis rate by CFE from *Lb. helveticus* W900R, a poor debittering adjunct culture (Soeryapranata et al., 2004).

The role of *Lb. helveticus* WSU19 in the debittering of Cougar Gold cheese underlies our studies to elucidate the contribution of peptidases from *Lb. helveticus* WSU19 to the production of high quality, non-bitter cheese. Despite detailed characterization of peptidases from *Lb. helveticus* strains CNRZ32 and 53/7, the specificities of peptidases from *Lb. helveticus* WSU19 in degrading casein fragments are unknown. *Lb. helveticus* strains are known to possess wide variability in proteolytic and peptidase activities (Fortina et al., 1998).

Our long-range goal is to completely characterize the biochemistry and genetics of the peptidases from *Lb. helveticus* WSU19 and to determine their contribution to the prevention of bitterness and the development of cheese flavor. Understanding the enzymology of *Lb. helveticus* WSU19 will allow a systematic development of improved adjunct cultures for the dairy industries. Specifically, the objectives of the current study are:

1. To clone the genes of selected peptidases from *Lb. helveticus* WSU19 that are potentially important in debittering of cheese, namely endopeptidase E (*pepE*), endopeptidase O (*pepO*), endopeptidase O2 (*pepO2*), endopeptidase O3 (*pepO3*), and general aminopeptidase N (*pepN*) genes,

2. To determine the specificities of these peptidases on chymosin-derived peptides, β-CN f193-209 and α_{s1}-casein (α_{s1}-CN) f1-23.

In addition to the specific objectives, the current study has initiated the development of a gene transfer system for *Lb. helveticus* WSU19 and the construction of isogenic strains of *Lb. helveticus* WSU19 that are deficient in PepE or PepO2 activity. The isogenic strains of *Lb. helveticus* WSU19 will be used to determine the role(s) of the peptidase(s) in the ripening of cheese and the growth of the bacterium.

CHAPTER II:

Literature Review

1. Chemistry of caseins

Milk proteins consist of caseins and whey proteins (Swaisgood, 1992; Fox et al., 2000). Caseins comprise approximately 80% of the total protein in bovine, ovine, caprine, and buffalo milk. Unlike whey proteins, caseins are insoluble at pH 4.6 and 20^{o}C (Fox and McSweeney, 1997). In rennet-coagulated cheese, most of the whey proteins are lost in the whey. Therefore, studies on milk protein in cheese are usually focused on caseins.

The predominant proteins in bovine caseins, i.e., α_{s1}-, α_{s2}-, β-, and κ-caseins, comprise approximately 40%, 10%, 35%, and 12% of the total casein, respectively (Fox and McSweeney, 1997). Bovine caseins contain minor proteins as a result of limited proteolysis by plasmin. The action of plasmin on α_{s1}-CN and β-CN produces λ-caseins and γ-caseins and proteose peptones, respectively (Swaisgood, 1992; Fox and Mc Sweeney, 1997).

1.1. Phosphorylation

Phosphorylation occurs in all caseins as a result of post-translational modification (Swaisgood, 1992). The phosphate groups are esterified predominantly at serine residues, in a cluster of SerP-X-SerP-SerP-SerP where X is leucine or isoleucine (Swaisgood, 1992; Dalgleish, 1997; Fox et al., 2000). The α_{s1}-, α_{s2}-, and β-caseins contain 8-9, 10-13, and 4-5 moles of phosphate groups per mole of protein, respectively (Fox et al., 2000).

Strong affinity of the phosphate groups for polyvalent cations, such as calcium, causes precipitation of the α_{s1}-, α_{s2}-, and β-caseins at calcium concentrations above 6 mM. Since most κ-casein (κ-CN) molecules contain only 1 mole of phosphate group per mole, the protein binds calcium weakly and therefore, is not sensitive to high calcium concentration. The κ-CN can stabilize the calcium-sensitive caseins by forming micelles (Fox et al., 2000).

1.2. Hydrophobicity

The hydrophobicity of caseins is due to the presence of many non-polar amino acid residues (Swaisgood, 1992; Dalgleish, 1997). Among the caseins, β-CN is the most hydrophobic, while α_{s2}-casein (α_{s2}-CN) is the least. The hydrophilicity of α_{s2}-CN is due to the presence of three clusters of anionic phosphorseryl and glutamyl residues (Swaisgood, 1992). The hydrophobicity of caseins is responsible for the high propensity of casein hydrolysates to be bitter (Fox et al., 2000).

The hydrophobic, polar, and charged amino acid residues in caseins occur as hydrophobic or hydrophilic patches (Swasigood, 1992; Dalgleish, 1997). Most of the charged and polar amino acids in β-CN are located at the N-terminus (residues 1-40), while the remaining molecule is strongly hydrophobic. The N-terminus of κ-CN (residues 1-105) is hydrophobic, while the C-terminal region (residues 106-169) is hydrophilic. Glycosylation of κ-CN enhances the hydrophilicity of the C-terminal region (Swaisgood, 1992). The distribution of hydrophilic and hydrophobic residues in the α_{s1}-CN and α_{s2}-CN is more uniform than in the β-CN and κ-CN, but still exhibits the hydrophobic patch phenomenon.

1.3. Casein micelles

Two models describing the internal structure of casein micelles were proposed by Walstra (1990) and Holt (1992), respectively. The 'hairy' model by Walstra (1990) assumes that casein micelles are roughly spherical. The micelles are composed of smaller units of about 14 nm diameter, called submicelles. Aggregation of the submicelles occurs via calcium phosphate bridges, hydrophobic interaction, and hydrogen bonds. The hydrophobic core of the submicelles is composed of the calcium-sensitive caseins and the N terminus of κ-CN.

The hydrophilic C-terminus of κ-CN protrudes from the micelle surface, forming a hairy layer that prevents further aggregation of the submicelles (Figure 1).

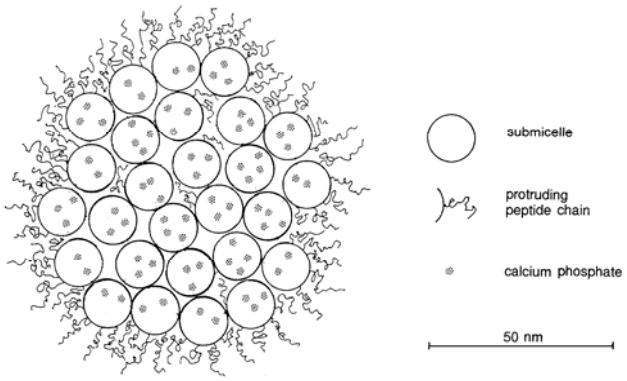

Figure 1. 'Hairy' model of casein micelle (Walstra, 1999)

In contrast to Walstra (1990), Holt (1992) suggests that calcium phosphate nanoclusters are the centers from which casein micelles grow. Caseins bind to the calcium phosphate via phosphoserine residues to form submicelles, which coalesce gradually due to hydrophobic interaction. The κ-CN has a tendency to be on the outside, while the minerals tend to be associated with the phosphoserine residues of the caseins. In this model, calcium acts as a negative-charge neutralizer instead of a cross-linker. The resulting micelles have discontinuous distribution of caseins and calcium phosphate.

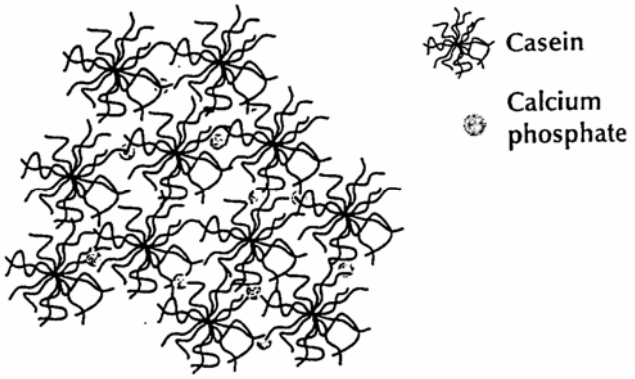

Figure 2. Casein micelle proposed by Holt (Creamer and MacGibbon, 1996)

1.4. Secondary structure of caseins

Caseins possess low levels of secondary and tertiary structures (Dalgleish, 1997; Fox et al., 2000). The presence of large amounts of proline in caseins, particularly β-casein, prevents the formation of α-helical and β-sheet structures. Furthermore, the α_{s1}-CN and β-CN do not contain cysteine residues, and consequently are unable to form inter- and intramolecular disulfide bonds. The lack of stable secondary structure increases caseins susceptibility to proteolysis, which is important in cheese ripening (Fox et al., 2000).

Despite lack of stable secondary structure, caseins do not exhibit random coil or unordered structures (Swasigood, 1992). Approximately 50% of the amino acid residues in caseins are present in α-helix, β-strand, or β-turn structures. Holt and Sawyer (1993) described the flexible structure of caseins as rheomorphic (meaning formed under flow). This concept hypothesized that the regular casein structures do not occur without the formation of aggregates. Farrell et al. (2002) proposed the concept of tensegrity to describe the structural properties of caseins. In this concept, stabilization of caseins structure is obtained through a balance between rigidity and flexibility. The sheet-turn-sheet motifs centered on proline residues in caseins provide rigid rod-like structure, while loops and helices contribute to flexibility.

2. Bitterness in cheese

Human tongues recognize at least four basic tastes, which are most commonly recognized sweet, salty, sour, and bitter. Bitter taste is perceived most acutely by the taste buds at the back of the tongue (Lemieux and Simard, 1992; McSweeney, 1997). Response to

bitter taste is slow, but the taste tends to linger, suggesting long duration binding of bitter compounds by the bitter taste receptor.

While bitter notes may contribute to the desirable flavor of aged cheese, excessive bitterness will limit the acceptability of cheese (Shinoda et al., 1985a; Lemieux and Simard, 1991; McSweeney, 1997; Sousa et al., 2001). Besides Gouda and Cheddar cheeses, the bitter taste defect has been reported in Camembert, French Camembert, Swiss mountain, Butterkäse, Gorgonzola, and Ragusano cheeses (Lemieux and Simard, 1991; Fallico et al., 2005).

During aging of cheese, glycolysis and lipolysis are important for the production of aroma compounds, while proteolysis influences the taste of cheese via the production of peptides and amino acids (McSweeney, 1997). Bitterness in cheese usually results from the imbalance in the formation and degradation of hydrophobic peptides originating from α_{s1}- and β-caseins (Sullivan and Jago, 1972; Richardson and Creamer, 1973; Visser et al., 1983a; Lee et al., 1996; Gomez et al., 1997; Broadbent et al., 1998; Frister et al., 2000; Sousa et al., 2001; Soeryapranata et al., 2002b).

Table 1 summarizes bitter peptides isolated from various cheeses. Sullivan and Jago (1972) indicated cheese peptides with the strongest bitterness intensity were composed of 2 to 23 amino acids. This indication was in agreement with Lee et al. (1996) findings that the strongest bitterness intensity was exhibited by cheese peptides with molecular weight (MW) between 500 and 3000 Da.

Bitter compounds must be at least slightly soluble in water (Lemieux and Simard, 1992; McSweeney, 1997). In full fat cheeses, the hydrophobic peptides might partition into the fat phase, which reduces the bitter perception (Fox et al., 1996). Consequently, bitterness

can be more problematic in low fat than full fat cheeses due to the reduction in partitioning of the hydrophobic peptides into the fat phase.

Table 1. Bitter peptides isolated from cheese

Cheese	Origin	Peptide Sequence	Reference
Cheddar	α_{s1}-CN f1-7	Arg-Pro-Lys-His-Pro-Ile-Lys	Lee et al. (1996)
	α_{s1}-CN f1-9	Arg-Pro-Lys-His-Pro-Ile-Lys-His-Gln	Broadbent et al. (1998)
	α_{s1}-CN f1-13	Arg-Pro-Lys-His-Pro-Ile-Lys-His-Gln-Gly-Leu-Pro-Gln	Lee et al. (1996)
	α_{s1}-CN f11-14	Leu-Pro-Gln-Glu	Lee et al. (1996)
	α_{s1}-CN f14-17	Glu-Val-Leu-Asn	Richardson and Creamer (1973)
	α_{s1}-CN f17-21	Asn-Glu-Asn-Leu-Leu	Hamilton et al. (1974)
	α_{s1}-CN f26-32	Ala-Pro-Phe-Pro-Glu-Val-Phe	Richardson and Creamer (1973)
	α_{s1}-CN f26-33	Ala-Pro-Phe-Pro-Glu-Val-Phe-Gly	Hamilton et al. (1974)
	β-CN f8-16	Val-Pro-Gly-Glu-Ile-Val-Glu-Ser-Leu	Lee et al. (1996)
	β-CN f46-67	Gln-Asp-Lys-Ile-His-Pro-Phe-Ala-Gln-Thr-Gln-Ser-Leu-Val-Tyr-Pro-Phe-Pro-Gly-Pro-Ile-Pro	Richardson and Creamer (1973)
	β-CN f46-84	Gln-Asp-Lys-Ile-His-Pro-Phe-Ala-Gln-Thr-Gln-Ser-Leu-Val-Tyr-Pro-Phe-Pro-Gly-Pro-Ile-Pro-Asn-Ser-Leu-Pro-Gln-Asn-Ile-Pro-Pro-Leu-Thr-Gln-Thr-Pro-Val-Val-Val	Hamilton et al. (1974)
	β-CN f193-209	Tyr-Gln-Gln-Pro-Val-Leu-Gly-Pro-Val-Arg-Gly-Pro-Phe-Pro-Ile-Ile-Val	Fox et al. (1995)
Gouda	β-CN f84-89	Val-Pro-Pro-Phe-Leu-Gln	Visser et al. (1983a)
	β-CN f193-207	Tyr-Gln-Gln-Pro-Val-Leu-Gly-Pro-Val-Arg-Gly-Pro-Phe-Pro-Ile	Visser et al. (1983a)
	β-CN f193-208	Tyr-Gln-Gln-Pro-Val-Leu-Gly-Pro-Val-Arg-Gly-Pro-Phe-Pro-Ile-Ile	Visser et al. (1983a)
	β-CN f193-209	Tyr-Gln-Gln-Pro-Val-Leu-Gly-Pro-Val-Arg-Gly-Pro-Phe-Pro-Ile-Ile-Val	Visser et al. (1983a)
Alpkase	α_{s1}-CN f198-199	Leu-Trp	Guigoz and Solms (1974)
Butterkase	β-CN f61-69	Pro-Phe-Pro-Gly-Pro-Ile-Pro-Asn-Ser	Huber and Klostermeyer (1974)

2.1. Relationship between structure of bitter peptides and bitterness intensity

According to Ney (1979), bitterness of a peptide does not relate to specific amino acid or peptide sequence. The average hydrophobicity (Q) of a peptide is the important factor determining its bitterness intensity. Bitterness threshold decreases with the number of hydrophobic amino acid residues and increases with the number of hydrophilic residues (McSweeney, 1997). The Q value is the sum of hydrophobicity of amino acid residues ($\Sigma\Delta f$) divided by the number of amino acid residues in the sequence (n). Bitterness occurs only when the Q value is above 1400 cal/residue for peptides with MW between 100 and 6000 Da (Table 2). When the Q value is between 1300 and 1400 cal/residue, the bitterness of a peptide is not predictable. Peptides with MW above 6000 Da are not bitter, although the Q value may be higher than 1400 cal/residue.

Table 2. Relationship between bitterness of a peptide and its average hydrophobicity (Ney, 1979)

Non-bitter taste
Q < 1300 cal/res Molecular weight (MW): 100-10,000 Da
Q > 1400 cal/res Molecular weight (MW): 6,000-10,000Da
Bitter taste
Q > 1400 cal/res, Molecular weight (MW): 100-6,000 Da

Ney's hypothesis on the importance of hydrophobicity in bitterness of a peptide concurred with the studies reported by Matoba et al. (1970), Minamiura et al. (1972), Hashimoto et al. (1980), and Ishibashi et al. (1988a). Matoba et al. (1970) isolated 3 bitter peptides rich in hydrophobic amino acids, particularly proline and phenylalanine, which were

bitter in their free forms. Similar to Matoba et al. (1970), Minamiura et al. (1972) reported a bitter peptide with the sequence of bitter core of Gly-Pro-Pro-Phe, while Hashimoto et al. (1980) synthesized a bitter-tasting peptide with the sequence of H-Gly-Pro-Phe-Pro-Ile-Ile-Val-OH. Ishibashi et al. (1988a) reported bitter peptides composed of valine and some hydrophobic amino acid residues, such as leucine, isoleucine, and phenylalanine. The latter study indicated the side chains of a peptide should consist of at least three carbon atoms to exhibit bitterness. Otherwise the peptide was either sweet or tasteless.

In contrast to the above results, Lee et al. (1996) isolated 3 bitter peptides with relatively low hydrophobicity from Cheddar cheese. The isolated peptides were α_{s1}-CN f1-13 (MW = 1538 Da), α_{s1}-CN f11-14 (MW = 484.4 Da), and β-CN f8-16 (MW = 939.7 Da), with Q values of 1363, 1367, and 1390 cal/residue, respectively. Similar to Lee et al. (1996), an earlier study by Matoba et al. (1970) reported stronger bitterness intensities of peptides than were expected from the hydrophobicity of amino acids composing the peptides. These findings suggested no direct correlation between the average hydrophobicity and bitterness intensity. Furthermore, the findings by Matoba et al. (1970) and Lee et al. (1996) suggested the importance of peptide structure and the position of amino acids in the peptide in developing and enhancing bitterness intensity.

Besides the average hydrophobicity, distribution of hydrophobic amino acids along a peptide chain affects bitterness intensity of the peptide (Lemieux and Simard, 1992; Habibi-Najafi and Lee, 1996). Shinoda et al. (1985b) reported an increase in bitterness intensity of the peptides through the introduction of hydrophobic amino acids, however the number of hydrophobic amino acids alone did not control the bitterness intensity of the peptides. Otagiri et al. (1983), Kanehisa et al. (1984), Kato et al. (1985), and Shinoda et al. (1985a) suggested

the presence of a hydrophobic amino acid at the C-terminus and a basic amino acid, such as arginine residue, at the N-terminus of a peptide increased bitterness of the peptide. Ishibashi et al. (1988b) confirmed the increase of bitterness intensity when arginine was at the N-terminus. Ishibashi et al. (1987) reported bitterness of a peptide was more pronounced when leucine was at the C-terminus than at the N-terminus or in the middle.

The importance of amino acid distribution in determining bitterness intensity of a peptide relates to the mechanism of the bitter taste sensation. Ishibashi et al. (1988c) hypothesized the participation of two determinant sites in the perception of bitter taste of a peptide. The primary site was a hydrophobic group composed of at least 3 carbon atoms, while the secondary site was another hydrophobic group or a bulky basic group, such as a guanidino group or an α-amino group. This hypothesis coincided with Belitz et al. (1979) description on the structure of bitter compounds, which consisted of a combination of one polar group and one hydrophobic group or a combination of two hydrophobic groups. The primary and secondary sites bound to the bitter taste receptor via a binding unit (BU) and a stimulating unit (SU), respectively (Figure 3). The distance between the two sites in the steric conformation of the peptide was essential and was estimated to be 4.1Å. Ishibashi et al. (1988b) demonstrated the role of the imino ring of a proline residue in peptide bitterness by altering the conformational folding of a peptide to position the BU and SU adjacently, suitable for the bitter taste receptor. Miyake et al. (1983) and Otagiri et al. (1983) confirmed the importance of spatial structure in peptide bitterness.

Based on these studies, bitterness intensity of a peptide is determined not only by the hydrophobicity of the amino acids making up the peptide, but also by: (i) the number of

carbon atoms composing the amino acid side chain; (ii) the features of the BU and SU; and (iii) the distance between the two units.

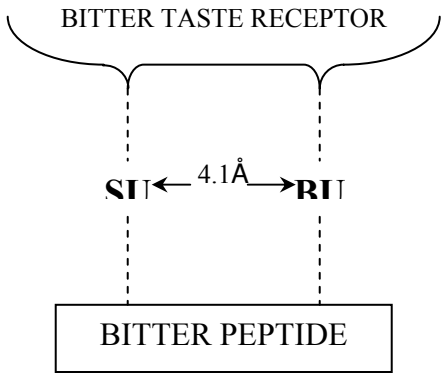

Where BU: binding unit (hydrophobic group)
SU: stimulating unit (hydrophobic or basic group)

Figure 3. Model of the binding of bitter peptide to bitter taste receptor (Redrawn from Ishibashi et al., 1988c)

2.2. Development and control of bitterness in cheese

Accumulation of hydrophobic peptides in cheese is believed to be responsible for the development of bitter cheese. Studies have been done to elucidate the roles of enzymes that are essential for the formation and degradation of the bitter-tasting peptides, and consequently prevent the accumulation of the bitter peptides in cheese.

Czulak (1959) proposed that rennet was responsible for the degradation of caseins to bitter peptides. According to Czulak (1959), production of lactic acid by starter culture decreased cheese pH, which reduced the ability of the starter culture to degrade peptides produced by rennet. In contrast to the starter culture, the decrease in cheese pH increased rennet activity, and resulted in the accumulation of bitter peptides. Olson (1998) reported bitter cheese made with rennet only, without the addition of starter culture. Bitterness of the

cheese made by Olson (1998) was due to the accumulation of C-terminal fragment of β-CN produced by rennet (Soeryapranata et al., 2002a). Singh et al. (2005) confirmed the bitterness of the peptide from the C-terminal of β-CN in water, milk, and cheese matrices.

In contrast to Czulak (1959), Lowrie and Lawrence (1972) hypothesized that starter culture was important in developing bitter flavor in Cheddar cheese. According to Lowrie and Lawrence (1972), rennet degraded caseins to produce high MW peptides, which were mostly non-bitter. These peptides were subsequently degraded to smaller MW bitter peptides by the starter proteinases. Peptidases from the starter cultures could further degrade the bitter peptides to non-bitter peptides and amino acids. According to this model, starter cultures were responsible for both developing and reducing bitterness. Studies by Richardson and Creamer (1973), Broadbent et al. (1998), and Soeryapranata et al. (2002b) supported the role of starter cultures in developing bitterness in cheese.

Lowrie and Lawrence (1972) proposed that all starters had the potential to be bitter and non-bitter starters. Population of the starter culture reached during cheesemaking, in response to the selected manufacturing conditions, such as cooking temperature, determined the presence or absence of bitterness in cheese (Lowrie et al., 1972). In contrast, Stadhouders et al. (1983) reported that only certain starter bacteria form bitter peptides in cheese. The degrading enzymes were present in all strains, but location of the enzymes was probably more or less restricted in bitter and non-bitter starters, respectively. Martley and Lawrence (1972) indicated that non-bitter starters exhibited less proteolytic activity in cheese than bitter starters and degraded the high MW peptides at a slower rate. The peptidolytic activity, on the other hand, was expected to be higher in non-bitter than bitter strains.

Visser et al. (1983b) reported the formation of bitter peptides from β-CN by independent action of rennet and proteinases from the cell wall of certain starter cultures. The bitter peptides were further hydrolyzed by the peptidase system in the cytoplasmic membrane or in the cytoplasm. Addition of salt decreased permeability of the cell wall and promoted a strong hydrophobic association of the bitter β-CN fragments, which rendered the latter resistant to the peptidase system.

Sorensen et al. (1996) and Broadbent et al. (2002) confirmed the role of starter proteinase in the formation of bitter Danbo cheese and reduced fat Cheddar cheese, respectively. Bitterness of Danbo cheese decreased when the cheese was made with proteinase-negative starter culture (Sorensen et al., 1996). Similarly, reduced fat Cheddar cheese made with proteinase-positive starter culture was more bitter than the cheese made with a proteinase-negative isogen (Broadbent et al., 2002). Pillidge et al. (2003) reported an increase in bitterness of dry-salted Gouda cheese made with starter strain containing plasmid-encoded cell wall proteinase type I (lactocepin P_I-type).

The ability of the peptidase system to hydrolyze bitter peptides was confirmed by several studies. Cliffe and Law (1990) reported the use of intracellular peptidase extract from *Streptococcus lactis* NCDO 712 to reduce bitterness in Cheddar cheese slurries, prepared using proteinase from *Bacillus subtilis.* Aminopeptidase from *Pseudomonas fluorescens* was reported by Gobbetti et al. (1995) to hydrolyze synthetic bitter pentapeptide H-Leu-Trp-Met-Arg-Phe-OH and bitter tetrapeptide H-Val-Pro-Leu-Leu-OH. The aminopeptidase from *Ps. fluorescens* was reported to play a role in the debittering of aged Italian Caciotta type cheese. Tan et al. (1993a) reported debittering activity of aminopeptidase N from *Lactococcus lactis* subsp. *cremoris* Wg2 on tryptic digest of β-CN. Lee et al. (1996) utilized the intracellular

peptidases from *Lc. lactis* subsp. *cremoris* SK11 to hydrolyze bitter peptides from Cheddar cheese, and consequently decreased the bitterness of the cheese. Baankreis et al. (1995), Smit et al. (1996), Koka and Weimer (2000), Chen et al. (2003), and Soeryapranata et al. (2004) used peptidases from starter and adjunct cultures to hydrolyze synthetic bitter peptides from α_{s1}-CN and β-CN.

The importance of peptidases in the reduction of bitterness in cheese underlies the use of lactobacilli as debittering starter adjuncts in cheesemaking. Gomez et al. (1996) reported debittering effects of peptidases from adjuncts *Lb. plantarum* ESI144 and *Lb. paracasei* subsp. *paracasei* ESI207 in bitter cheese prepared using Neutrase®. Drake et al. (1997) used a *Lb. helveticus* adjunct to reduce bitterness in reduced fat Cheddar cheese. Soeryapranata et al. (2002b) reported that adjunct *Lb. helveticus* WSU19 reduced bitterness in Cheddar-type cheese made with bitter starter. Benech et al. (2003) reported that incorporation of *Lb. casei-casei* L2A adjunct culture decreased bitterness of cheese made with nisin-producing starter *Lc. lactis* subsp. *lactis* biovar. *diacetylactis* UL719.

Besides peptidase activities, bitterness in cheese is also affected by lytic ability of the starter culture (Boutrou et al., 1998). Cell lysis was reported to release the intracellular peptidase debittering enzymes (Kunji et al., 1998). Cheeses made with high lytic strain *Lc. lactis* subsp. *cremoris* RD251 that was low in peptidase activities were bitter (Boutrou et al., 1998). The same result was reported for cheeses made with low lytic strain *Lc. lactis* subsp. *lactis* RD232 that possessed high proteolytic activity (Boutrou et al., 1998). Lepeuple et al. (1998) confirmed that lysis of the starter strains resulted in increased free amino acid production rate and a decrease of bitterness in Saint-Paulin pressed-type cheese. Crow et al. (1995) reported that bitter flavor was prominent in Cheddar cheese made with high rennet

concentration in the absence of high lytic starter culture. In agreement with the hypothesis of Boutrou et al. (1998) on cell lysis and debittering of cheese, Meijer et al. (1998) and Benech et al. (2003) reported that cheeses made with nisin-producing starters, *Lc. lactis* subsp. *cremoris* SK110::Tn*5276*-NI and *Lc. lactis* subsp. *lactis* biovar. *diacetylactis* UL719, respectively, were bitter due to the decrease of the susceptibility of cells to lysis. Morgan et al. (2002) developed a three-strain starter system to increase starter lysis. This starter combination consisted of a bacteriocin-producing (lactococcin A, B, and M) starter, which lysed a second starter sensitive to bacteriocin, and a third starter resistant to bacteriocin activity for acid production in cheesemaking. Cheese made with bacteriocin-producing starter exhibited a decrease in bitterness over cheeses made without the bacteriocin-producing starter.

3. Proteolysis of caseins in cheese

Enzymes involved in the hydrolysis of caseins in cheese include: (i) milk coagulating enzyme (e.g. chymosin, pepsin, microbial or plant acid proteinase); (ii) indigenous milk proteinase (e.g. plasmin and perhaps cathepsin D); (iii) proteinases and peptidases from starter and non-starter lactic acid bacteria; (iv) enzymes from secondary cultures (e.g. *Penicillium camemberti* in Camembert and Brie-type cheeses, *P. roqueforti* in blue cheese, *Propionibacterium freudenreichii* in Swiss-type cheese); (v) exogenous proteinases or peptidases or both, added to accelerate ripening (Sousa et al., 2001; Stepaniak, 2004; McSweeney et al., 2004).

Figure 4 illustrates hydrolysis of caseins to free amino acids during ripening of Cheddar-type cheeses (Steele, 1995). Proteolysis contributes to the softening of cheese

texture during ripening due to the hydrolysis of the casein matrix of the curd and a decrease in the water activity of the curd (McSweeney, 2004). Furthermore, proteolysis affects cheese flavor through the production of free amino acids, which serve as precursors for a series of catabolic reactions. Low molecular weight peptides produced during proteolysis of caseins may contribute to bitterness of cheese.

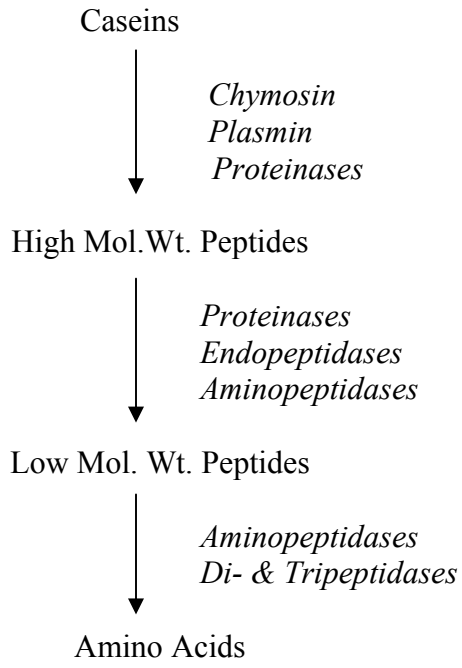

Figure 4. Hydrolysis of caseins to amino acids (Redrawn from Steele, 1995)

3.1. Proteolysis by chymosin

Bovine rennet consists of two proteolytic enzymes, i.e. chymosin (EC 3.4.23.4; 88-94% of milk clotting activity, MCA) and bovine pepsin (EC 3.4.23.1; 6-12% MCA), used for coagulating milk in cheesemaking (Fox et al., 2000; Sousa et al., 2001). Chymosin and pepsin are aspartyl proteinases containing two aspartyl residues (Asp_{32} and Asp_{215}) at their active sites (Chitpinityol and Crabbe, 1998; Stepaniak, 2004). About 0-15% of the rennet

activity added to milk is retained in the cheese curd, depending on cooking temperature and pH at whey drainage (Sousa et al., 2001; McSweeney, 2004). The retained rennet activity is important for the initial proteolysis of caseins during cheese ripening (Fox et al., 1996). Bovine pepsin is more sensitive to denaturation by pH than chymosin, therefore pepsin activity retained in the curd depends on the pH of milk at setting (Sousa et al., 2001). Chymosin loses its activity at pH 3-4, a pH not attained in cheese, due to autodegradation (Chitpinityol and Crabbe, 1998).

Chymosin hydrolyzes κ-CN at Phe_{105}-Met_{106}, which destabilizes casein micelles and initiates the coagulation of milk (Farkye, 1995; Fox et al., 2000; McSweeney, 2004; Stepaniak, 2004). The cleavage of κ-CN results in the formation of para-κ-CN (κ-CN f1-105), which remains in the casein micelle, and glycomacropeptide (κ-CN f106-169), which is lost in the whey. The para-κ-CN is resistant to chymosin, reflecting the relatively high level of secondary structure in κ-CN compared to other caseins (McSweeney, 2004).

Hydrolysis of α_{s1}-, α_{s2}-, and β-caseins occurs in cheese ripening, not in the milk coagulation step (Fox et al., 1996). The action of chymosin on β-CN during ripening of cheese is primarily at Leu_{192}-Tyr_{193} (Fox et al., 2000; McSweeney, 2004). The peptide fraction β-CN f193-209 formed by this cleavage is very bitter (Visser et al., 1983a; Singh et al., 2005). Awad et al. (1998) reported that hydrolysis of the Leu_{192}-Tyr_{193} bond by chymosin is strongly inhibited by 5-10% NaCl, a level not generally found in most cheeses.

The primary cleavage site of chymosin in α_{s1}-CN during cheese ripening is at Phe_{23}-Phe_{24} (McSweeney, 2004). Cleavage at this site is responsible for the softening of cheese texture and the production of α_{s1}-CN f1-23, which is further hydrolyzed by cell envelope proteinases. In addition to the Phe_{23}-Phe_{24} bond, chymosin cleaves α_{s1}-CN at Leu_{101}-Lys_{102}

during cheese ripening (McSweeney, 2004). In contrast to β-CN, NaCl concentration does not have a marked effect on the proteolysis of α_{s1}-CN (Awad et al., 1998).

Compared to α_{s1}-CN, α_{s2}-CN is more resistant to hydrolysis by chymosin. Cleavage of α_{s2}-CN by chymosin is limited to the hydrophobic regions, i.e. sequences 90-120 and 160-207 (McSweeney, 2004).

3.2. Proteolysis by plasmin

Plasmin (EC 3.4.21.7), the principal indigenous milk proteinase, is a serine proteinase with an optimum pH of 7.5-8.0 and optimum temperature of 37^{o}C (Fox et al., 2000; Forde and Fitzgerald, 2000; Nielsen, 2002). Although plasmin has an alkaline optimum pH, the enzyme is stable over a broad pH range. The enzyme is a glycoprotein and exists as a dimer with monomers linked by disulfide bonds (Nielsen, 2002; Stepaniak, 2004). Cleavage by plasmin activity is restricted to the carboxyl end of L-lysine, and to a lesser extent the L-arginine residues (Nielsen, 2002; McSweeney, 2004).

Plasmin exists in milk primarily in the inactive form, plasminogen (Nielsen, 2002; Stepaniak, 2004). The presence of plasminogen activators (PAs) is essential to convert the inactive plasminogen to active plasmin for milk protein degradation (Nielsen, 2002). Plasmin, plasminogen, and PAs are extremely heat stable, while plasmin inhibitor and PA inhibitors are heat labile (Bastian and Brown, 1996; Broome and Limsowtin, 1998, Nielsen, 2002). Plasmin, plasminogen, and PAs can survive pasteurization and UHT processes (Bastian and Brown, 1996; Broome and Limsowtin, 1998).

Somers and Kelly (2002) reported that increasing cooking temperature from 38^{o}C to 55^{o}C during cheesemaking increased plasmin activity and plasminogen activation during

ripening of cheese, but decreased chymosin activity. Inactivation of PA inhibitor during heat treatment contributes to the increase of plasmin proteolytic activity (Nielsen, 2002). The increase of plasmin activity in late lactation milk increases the clotting time of milk and reduces the firmness of cheese curd (Farkye, 1995).

Plasmin, plasminogen, and PAs are associated with the casein micelles in the pH range 4.6-6.6 and consequently are retained in the cheese curd (Broome and Limsowtin, 1998, Nielsen, 2002; Stepaniak, 2004). Plasmin inhibitor and PA inhibitor are lost in the whey fraction (Stepaniak, 2004). Lysine residues in plasmin play a role in the association between plasmin and the protein in casein micelles.

Plasmin activities in various cheeses are as follows: Romano > Emmental (Swiss) > Gouda > Cheddar > Cheshire, depending on the cooking temperature during cheesemaking and the pH during ripening (Farkye, 1995; Nielsen, 2002). Proteolysis in high-cooked and washed-curd cheeses primarily results from the action of plasmin (Farkye, 1995; Fox et al., 2000). The importance of plasmin in these types of cheese is due to the inactivation of chymosin by high-cooking temperatures and the removal of inhibitors of PA (Bastian and Brown, 1996; McSweeney, 2004). However, the importance of plasmin in cheese ripening is still under debate since the optimum pH of plasmin is far from the pH of cheese (Farkye, 1995; Bastian and Brown, 1996; Nielsen, 2002).

Plasmin is active on most caseins, especially β-CN and α_{s2}-CN (Fox and McSweeney, 1997; Stepaniak, 2004). In contrast, κ-CN is quite resistant to plasmin activity (Sousa et al., 2001; McSweeney, 2004). Creamer (1975) suggested that hydrolysis of β-CN in cheese is mainly due to plasmin. The primary plasmin cleavage sites on β-CN are Lys_{28}-Lys_{29}, Lys_{105}-His_{106}, and Lys_{107}-Glu_{108} to produce γ-caseins and proteose peptones (Sousa et

al., 2001). The γ-caseins, released in the hydrolysis of β-CN by plasmin, are used as an indicator of plasmin activity during cheese ripening (Fox and McSweeney, 1997; Stepaniak, 2004). However, the γ-caseins are not found in the aqueous extract of cheese, which implies little contribution of plasmin to the formation of water-soluble nitrogen in cheese (Farkye, 1995).

3.3. Proteolysis by lactic acid bacteria

Lactic acid bacteria (LAB) require external nitrogen sources for growth to high numbers (10^9-10^{10} cfu/mL) because of a limited ability to synthesize amino acids (Sousa et al., 2001; McSweeney, 2004). In a medium containing large concentrations of protein but small amounts of free amino acids such as milk, LAB depend on a proteolytic system to degrade caseins as the major source of amino acids.

The proteolytic system of LAB (Fig. 5) consists of: (i) cell-envelope proteinase (CEP or lactocepin or PrtP) for breaking down casein into oligopeptides; (ii) intracellular proteinases; and (iii) intracellular peptidases for hydrolyzing the oligopeptides to amino acids (Pritchard and Coolbear, 1993; Mulholland, 1997; Sousa et al., 2001; McSweeney, 2004). Proteinases and peptidases of LAB are essential in cheese ripening since most of the peptides produced by chymosin and plasmin are too large to contribute to cheese flavor (Fox et al., 1995; Mulholland, 1997; McSweeney, 2004).

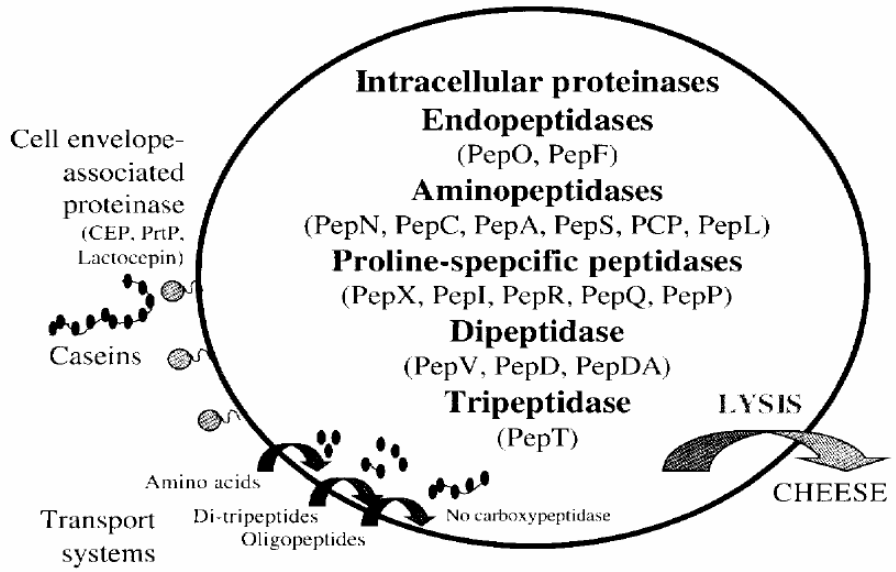

Figure 5. Proteolytic system of *Lactococcus* sp. (McSweeney, 2004)

3.3.1. Proteinases of LAB

Lactocepin (PrtP), the principal lactococcal proteinase, is expressed as a preproteinase with a MW of >200 kDa (Hutkins, 2001). A leader sequence directs the inactive proteinase across the cytoplasmic membrane. After removal of the leader sequence, the remaining protein is loosely attached to the cell envelope via Ca^{2+} (Hutkins, 2001; McSweeney, 2004). Activation of the preproteinase occurs through the action of maturation protein (PrtM) that induces autolytic cleavage at the proline region of the enzyme. The mature PrtP possesses a MW of 180-190 kDa (Pritchard and Coolbear, 1993; Hutkins, 2001).

PrtP is a serine-type proteinase with acidic pH optimum (pH 5.5-6.5) (Tan et al., 1993b; McSweeney, 2004). The active site of PrtP is a triad consisting of Asp_{30}, His_{94}, and Ser_{443} (Law and Haandrikman, 1997; Mulholland, 1997). Small concentrations of Ca^{2+} can either activate or stabilize PrtP (Mayo, 1993).

The primary role of PrtP in cheese ripening is to hydrolyze casein-derived peptides produced by chymosin or plasmin into small fragments suitable as substrates for intracellular peptidases (Fox et al., 1995; Law and Mulholland, 1995; McSweeney, 2004). McSweeney et al. (1993) reported the inability of PrtP from *Lc. lactis* subsp. *cremoris* HP and *Lc. lactis* subsp. *lactis* JL3601 and JL521 to readily hydrolyze β-CN in 6-month old Cheddar cheese. The failure of PrtP to hydrolyze β-CN in cheese was likely due to the hydrophobic interaction of β-CN in cheese causing the susceptible bonds to be inaccessible. In contrast to McSweeney et al. (1993), Juillard et al. (1995) reported the ability of P_I-type proteinase from *Lc. lactis* subsp. *cremoris* Wg2 to hydrolyze β-CN in solution into more than 100 oligopeptides.

Originally, PrtP was classified into 3 groups based on the specificity on casein degradation, i.e., P_I-type (HP-type), P_{III}-type (AM1-type), and intermediate P_I /P_{III}-type (U-type) (Pritchard and Coolbear, 1993; Tan et al., 1993b; Hutkins, 2001; Pillidge, et al., 2003; McSweeney, 2004; Stepaniak, 2004). P_I-type PrtP degrades β-CN rapidly, but acts slowly on α_{s1}-CN and κ-CN. P_{III}-type PrtP attacks β-CN at different sites from the P_I-type in addition to κ-CN and α_{s1}-CN (Law and Haandrikman, 1997; Broome and Limsowtin, 1998; Hutkins, 2001; Stepaniak, 2004). Two regions in the PrtP protein contribute to the differentiation in substrate specificity of P_I-type and P_{III}-type PrtP (Tan et al., 1993b). The first region is around the center of the active site and is homologous with the substrate-binding site of subtilisin. The second region is the amino acid residues at 747-748.

The β-CN cleavage site of P_I-type PrtP is characterized by glutamine and serine residues and is usually located in the region having low charge, high hydrophobicity, and high proline content (Tan et al., 1993b; Mayo, 1993; Fox et al., 1995). P_{III}-type PrtP cleaves

β-CN at Glx-X or X-Glx peptide bonds, where X is generally a hydrophobic residue such as methionine, phenylalanine, leucine, or tyrosine. The broader specificity of P_{III}-type PrtP than the P_I-type towards β-CN causes the production of fewer bitter peptides from casein by P_{III}-producing strains. Table 3 summarizes the peptides formed during 1 h in-vitro incubations of casein fractions with PrtP.

Table 3. Peptides produced by the lactococcal proteinase (P_I- or P_{III}-type) within 1-h incubation with caseins (Law and Mulholland, 1995)

Casein peptide	**Amino acid sequence**
β-CN f176-182	Lys-Ala-Val-Pro-Tyr-Pro-Gln
β-CN f183-193	Arg-Asp-Met-Pro-Ile-Gln-Ala-Phe-Leu-Leu-Tyr
β-CN f194-207	Gln-Gln-Pro-Val-Leu-Gly-Pro-Val-Arg-Gly-Pro-Phe-Pro-Ile
β-CN f194-209	Gln-Gln-Pro-Val-Leu-Gly-Pro-Val-Arg-Gly-Pro-Phe-Pro-Ile-Ile-Val
κ-CN f96-106	Ala-Arg-His-Pro-His-Pro-His-Leu-Ser-Phe-Met
κ-CN f161-169	Thr-Val-Gln-Val-Thr-Ser-Thr-Ala-Val
α-CN f143-148	Ala-Tyr-Phe-Tyr-Pro-Glu
α-CN f162-169	Gly-Ala-Trp-Tyr-Tyr-Val-Pro-Leu
α-CN f170-199	Gly-Thr-Gln-Tyr-Thr-Asp-Ala-Pro-Ser-Phe-Ser-Asp-Ile-Pro-Asn-Pro-Ile-Gly-Ser-Glu-Asn-Ser-Glu-Lys-Thr-Thr-Met-Pro-Leu-Trp

Exterkate et al. (1993) proposed another scheme to classify lactococcal PrtP based on specificity of hydrolysis of α_{s1}-CN f1-23. The scheme classified PrtP into 7 groups, i.e. group a to group g (Figure 6). Group a in this classification was formerly reported as P_{III}-type PrtP, while group e was formerly P_I-type PrtP. Broadbent et al. (1998) added group h PrtP to the Exterkate et al. (1993) classification. The latter PrtP was reported to produce α_{s1}-CN f1-9 that was responsible for bitterness in Cheddar cheese (Broadbent et al., 1998; Broadbent et al., 2002).

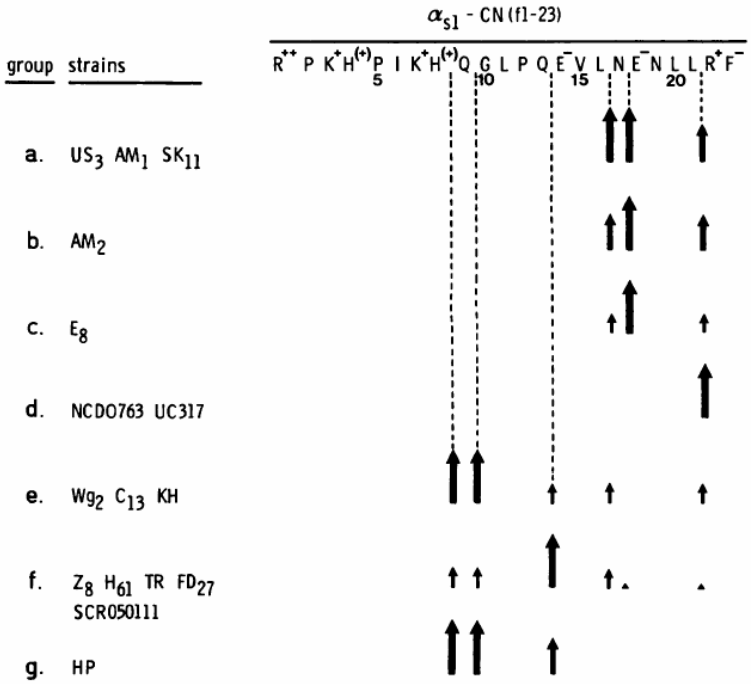

Figure 6. Classification of strains of *Lc. Lactis* according to PrtP specificities on α_{s1}-CN f1-23 (Exterkate et al., 1993)

In addition to the lactococcal PrtP, different specificites of PrtP were reported in lactobacilli (Bockelmann, 1995; Hebert et al., 2002; Oberg et al., 2002). Tsakalidou et al. (1999) isolated a PrtP from *Lb. delbrueckii* subsp. *lactis* ACA-DC178, which is similar to P_I-type lactococcal PrtP. Hebert et al. (2002) reported the activities of cell-surface proteinases from *Lactobacillus* on α-CN and β-CN and their inhibition by peptides in the peptide-rich medium and chemically defined medium supplemented with Casitone, a pancreatic digest of casein. Oberg et al. (2002) reported the specificities of PrtP from 14 strains of *Lb. delbrueckii* subsp. *bulgaricus* and 8 strains of *Lb. helveticus* on α_{s1}-CN f1-23. The results indicated 6

groups of lactobacilli PrtP specificities based on the primary and secondary products of α_{s1}-CN f1-23 hydrolysis (Table 4).

Table 4. Specificities of lactobacilli PrtP on α_{s1}-CN f1-23 (Oberg et al., 2002)

Group	Species	Strains	Primary products	Secondary products
I	Ldb	1,2,26	f 1-13 + f 14-23	f 1-9 + f 10-13
	Lh	29	f 1-16 + f 17-23	f 1-6 + f 7-13
II	Lh	10,12,36	f 1-9 + f 10-23	f 1-6 + f 7-13
			f 1-13 + f 14-23	
III	Ldb	4,5,6,8	f 1-9 + f 10-23	f 1-6 + f 7-13
			f 1-13 + f 14-23	f 1-9 + f 10-13
			f 1-17	
IV	Ldb	7	f 1-13 + f 14-23	f 1-9 + f 10-13
				f 1-6 + f 7-13
				f 1-7
V	Ldb	13	f 1-9 + f 10-23	f 1-6 + f 7-13
	Lh	9,11	f 1-16 + f 17-23	
VI	Lh	3,37,41	f 1-8 + f 9-23	f 1-6 + f 7-13
	Ldb	38	f 1-9 + f 10-23	
			f 1-13 + f 14-23	
			f 1-16 + f 17-23	

Ldb – *Lb. delbrueckii* subsp. *bulgaricus;* Lh – *Lb. helveticus.*

Besides proteinases attached to the cell-surface, LAB also possess intracellular proteinases (Zevaco and Desmazeaud, 1980; Shin et al., 2004). However, the importance of intracellular proteinase in cheese ripening is not clear (McSweeney, 2004). Zevaco and Desmazeaud (1980) isolated intracellular neutral proteinase from *Lc. lactis* subsp. *lactis* biovar *diacetylactis*. The enzyme degraded β-CN slowly at Pro_{186}-Ile_{187} and Ala_{189}-Phe_{190}. The enzyme was also reported to be active on β-CN f193-209, with cleavage site at Pro_{206}-Ile_{207}, and β-CN f165-189, with cleavage sites at Lys_{169}-Val_{170} and Lys_{176}-Ala_{177}. Shin et al. (2004) purified an intracellular proteinase from *Lb. casei* subsp. *casei* LLG. The latter

proteinase was reported to be more active on β-CN than on α_{s1}-CN and κ-CN (Shin et al., 2004).

3.3.2. Peptidases of LAB

Intracellular peptidases are important in the degradation of casein fragments and the release of free amino acids as precursors for flavor formation during cheese ripening (McSweeney, 2004). Location of the peptidases in the cytoplasm indicates the importance of cell lysis for the development of flavor of ripened cheese (Pritchard and Coolbear, 1993). The intracellular peptidases in LAB are classified as aminopeptidases, proline-specific peptidases, dipeptidases, tripeptidases, and endopeptidases (Christensen et al., 1999; Hutkins, 2001; McSweeney, 2004). Table 5 summarizes the intracellular peptidases purified and characterized from LAB.

Most of the intracellular peptidases isolated from lactococci, such as PepN, PepC, PepO, PepO2, PepF, PepV, PepX, and PepQ, were detected in lactobacilli (Bockelmann, 1995; Christensen et al., 1999; Chen et al., 2003). To date, PepA and PepP were reported only in *Lactococcus* sp., while PepD, PepR, PepL, PepE, PepO3, and PepG were reported only in *Lactobacillus* sp. (Christensen et al., 1999; Sridhar et al., 2003). Dako et al. (1995) and Sasaki et al. (1995) reported higher peptidase activity in lactobacilli compared to lactococci. Takafuji et al. (1995) showed significant difference of R_m values on polyacrylamide gel between the corresponding peptidases from lactobacilli and lactococci, suggesting lactobacilli might have proteolytic enzymes different from lactococci.

Table 5. Peptidases from LAB (Hutkins, 2001)

Peptidase	**Abbreviation**	**Substrate of Specificity**[a]
Aminopeptidase A	PepA	Glu/Asp↓(X)n
Aminopeptidase C	PepC	X↓(X)n
Aminopeptidase L	PepL	Leu↓X or Leu↓X–X
Aminopeptidase N	PepN	X↓(X)n
Aminopeptidase P	PepP	X↓Pro–(X)n
Aminopeptidase X	PepX	X–Pro↓(X)n
Pyrrolidone carboxylyl peptidase	PCP	Glu↓(X)n
Dipeptidase V	PepV	X↓X
Dipeptidase D	PepD	X↓X
Tripeptidase T	PepT	X↓X–X
Proiminopeptidase	PepI	Pro↓X–(X)n
Prolidase	PepQ	X↓Pro
Prolinase	PepR	Pro↓X
Endopeptidase F	PepF	(X)n–X–X↓X–(X)n
Endopeptidase O	PepO	(X)n–X ↓ X–(X)n
Endopeptidase E	PepE	(X)n–X ↓ X–(X)n
Endopeptidase G	PepG	(X)n–X ↓ X–(X)n

[a] The position of the hydrolyzed peptide bonds are shown by arrows.

Aminopeptidase N (PepN) is a general aminopeptidase with specificities for peptides containing residues that are basic (Lys- and Arg-) or hydrophobic (Leu-) at the N terminus (Pritchard and Coolbear, 1993; Law and Haandrikman, 1997; Christensen et al., 1999). PepN activity is negligible when Gly-, Pro-, Asp-, and Glx- residues are at the N-terminus. The ability of PepN to release hydrophobic amino acids from peptides suggests the possibility to

use PepN as a debittering enzyme. Tan et al. (1993a) reported the ability of PepN to debitter a tryptic digest of β-CN. Baankreis (1992) showed an increase of bitterness in Gouda cheese manufactured with a *pepN* negative strain starter culture. Guldfeldt et al. (2001) reported flavor improvement and low bitterness in cheeses made with strains overexpressing *pepN* gene from *Lc. lactis* subsp. *cremoris* Wg2. Courtin et al. (2002) reported the increase of aromatic amino acids, proline, and glutamic acid in cheese made with *Lc. lactis* MG1363 expressing *pepN* gene from *Lb. helveticus* 53/7. Guinec et al. (2002) reported reduction in the total amino acid from cheeses made in the absence of PepN. In contrast to these studies, McGarry et al. (1994) reported no significant changes between control and experimental cheeses made using strains overexpressing *pepN* gene from *Lc. lactis* subsp. *lactis* MG1363 with respect to the body, flavor, and texture characteristics. Christensen et al. (1995) reported similar results for cheeses made with strains overexpressing the *pepN* gene from *Lb. helveticus* CNRZ32. Joutsjoki et al. (2002) reported a decrease of recombinant PepN activity to an undetectable level at pH and salt concentration resembling cheese ripening.

Aminopeptidase C (PepC) is a general aminopeptidase having broader specificity than PepN. The enzyme is active on peptides with N-terminus containing residues that are basic (Lys-, His-, and Arg-), acidic (Glu- and Asp-), hydrophobic/uncharged (Ala- and Leu-), or aromatic (Phe-) (Law and Mulholland, 1995; Law and Haandrikman, 1997; Christensen et al., 1999). Guldfeldt et al. (2001) reported that overexpression of *pepC* gene produced cheese with low bitterness and improved flavor. However, Guinec et al. (2002) reported no significant changes in the level of amino acids in cheeses made in the absence of PepC.

Both PepN and PepC are not able to hydrolyze N-terminal or penultimate proline residues, which causes LAB to depend on the proline-specific peptidases (Mayo, 1993; Tan

et al., 1993b; Fox et al., 1995; Law and Haandrikman, 1997; Christensen et al., 1999). X-prolyl dipeptidyl aminopeptidase (PepX) is essential for casein hydrolysis due to the large amounts of proline in β-CN (Law and Mulholland, 1995). PepX cleaves the N-terminal X-Pro from X-Pro-Y… oligopeptides containing 3-7 amino acids (Tan et al., 1993b; Christensen et al., 1999). PepX exhibits highest activity when the N-terminus is uncharged or basic (Christensen et al., 1999). The action of PepX on oligopeptides results in the release of dipeptides containing C-terminal proline, mainly Glx-Pro, Leu-Pro, Val-Pro, Phe-Pro, Gly-Pro, and Tyr-Pro (Tan et al., 1993b; Pritchard and Coolbear, 1993). The X-Pro dipeptides are hydrolyzed by prolidase (PepQ), a dipeptidase specific for dipeptides with C-terminal proline (Law and Haandrikman, 1997; Christensen et al., 1999). Baankreis (1992) showed that Gouda cheese manufactured with a *pepX* negative strain starter culture developed poor organoleptic quality but did not develop bitterness.

Aminopeptidase A (PepA), often referred to as glutamyl aminopeptidase, specifically cleaves peptides with acidic amino acid residues (Glu- or Asp-) at the N-terminus (Fox et al., 1995; Christensen et al., 1999). PepA might have a significant effect in the development of cheese flavor during ripening since glutamate is well known as a flavor enhancer (Fox et al., 1995). Glutamic acid/glutamine was found as the major free amino acid in the water-soluble fraction of Cheddar cheese aged 10-27 months (Lee and Warthesen, 1996).

Besides removal by PepA, the N-terminal glutamyl residues can undergo spontaneous intramolecular cyclization, forming an N-terminal 2-pyrrolidone 5-carboxylic acid (PCA; pyroglutamate) residue (Fox et al., 1995; Law and Haandrikman, 1997). Pyrollidone carboxylyl peptidase (PCP) is a specific aminopeptidase for hydrolyzing the pyroglutamic acid residue, which may be formed in cheese due to the large amounts of glutamate in casein

hydrolysates. Mucchetti et al. (2002) reported in-vitro synthesis of pyroglutamate from Gln-Gln dipeptide by cyclotransferase (cyclase) activity of *Lb. helveticus* strains.

Dipeptidase D (PepD) and dipeptidase V (PepV) are dipeptidases with broad substrate specificities (Christensen et al., 1999). PepD hydrolyzes dipeptides containing hydrophobic/uncharged residue at the N-terminus, except for Val-X (X is -Arg, -Gly, -Leu) or Ile-X (X is -Gln, -Val). PepV is active on dipeptides containing basic (Arg-, Lys-, His-), hydrophobic/uncharged (Ala-, Ile-, Leu-, Val-), aromatic (Phe-, Tyr-), and methionine residues at the N-terminus. Both PepD and PepV do not hydrolyze peptides containing Gly-, Gln-, or Pro- residue at the N-terminus. Tripeptidase T (PepT) hydrolyzes the N-terminal residue of tripeptides without proline at the penultimate position (Tan et al., 1993b; Law and Haandrikman, 1997). The tripeptidase is not active on dipeptides, tetrapeptides, or oligopeptides.

Oligopeptidase F (PepF) and neutral endopeptidase O (PepO) are both intracellular endopeptidases (Mulholland, 1997). PepF is active on peptides containing 7-17 amino acids, while PepO is active on peptides containing more than 5 amino acids (Mulholland, 1997). PepO, isolated from *Lc. lactis* subsp. *cremoris* Wg2, seems to be closely related to the neutral oligopeptidase (NOP) from *Lc. lactis* subsp. *cremoris* C13 (Baankreis et al., 1995; Stepaniak and Fox, 1995). Under cheese-like conditions, NOP was essential to degrade α_{s1}-CN f1-23 and β-CN f193-209 (Baankreis et al., 1995). Stepaniak and Fox (1995) isolated a 70kDa endopeptidase from proteinase negative *Lc. lactis* subsp. *lactis* MG1363, which is immunologically identical with PepO. This endopeptidase from MG1363 hydrolyzed the Leu_{198}-Trp_{199} bond from α_{s1}-CN f165-199. The dipeptide Leu_{198}-Trp_{199} is known to be a bitter peptide in Alpkase cheese (Guigoz and Solms, 1974).

CHAPTER III:

Materials and Methods

1. Bacterial strains, growth media, and culture conditions

Lb. helveticus WSU19 (WSU Creamery, Pullman, WA) and *Lb. helveticus* CNRZ32 (Dr. James L. Steele, University of Wisconsin, Madison, WI) were grown in Lactobacilli MRS Broth (Becton, Dickinson and Company, Sparks, MD) at 37°C without shaking. *Escherichia coli* DH5α was grown at 37°C with vigorous shaking in Luria Bertani (LB) Broth Base (Invitrogen, Carlsbad, CA), while the recombinant *E. coli* DH5α and *E. coli* SURE cells were grown in the same media in the presence of 1 mg/mL of erythromycin (Em) (Fisher Scientific, Fairlawn, NJ). Bacteria were maintained as frozen stocks at –80°C. The frozen stocks of *Lactobacillus* sp. were prepared by mixing 0.3 mL of cultures with 0.3 mL of sterile 50% glycerol (Sigma-Aldrich Co., St. Louis, MO) and 1 mL of sterile 11% non-fat dry milk in cryovials. The frozen stocks of wild type and recombinant *E. coli* were prepared by mixing 0.7 mL of cultures with 0.3 mL of sterile 50% glycerol in cryovials.

Screening for peptidase-positive clones, using blue/white screening and colony hybridization, was conducted on LB agar plates containing 1 mg/mL of Em. The plates were prepared by adding 1.5% of Granulated Agar (Becton, Dickinson and Company, Sparks, MD) to the liquid medium. For blue/white screening (α-complementation) experiments, 5-bromo-4-chloro-3-indolyl-β-D-galactopyranoside (X-Gal) and isopropyl-β-D-thiogalactoside (IPTG) (Fisher Scientific, Fairlawn, NJ) were added at concentrations of 40 μg/mL and 120 μg/mL, respectively, to the liquid medium. The LB agar plates with and without X-Gal/IPTG were incubated aerobically at 37°C.

The Em stock solution (50 mg/mL) was prepared in 95% ethanol (Sigma-Aldrich Co., St. Louis, MO) and stored at –20°C. The X-Gal stock solution was freshly prepared at a concentration of 20 mg/mL in N, N-dimethylformamide (Sigma-Aldrich Co., St. Louis, MO).

The IPTG stock solution was prepared at a concentration of 0.1 M in deionized water, sterilized using 0.45 μm Sterile Acrodisc® Syringe Filter (Pall Life Sciences, Ann Arbor, MI), and stored at –20°C.

2. Molecular biology techniques

DNA manipulation and cloning essentially followed procedures described by Sambrook et al. (1989). Genomic DNA was isolated from *Lactobacillus* sp. using QIAGEN® Genomic-Tip 500/G, QIAGEN® Genomic DNA Buffer Set, QIAGEN® Protease, and RNaseA (Qiagen, Valencia, CA), lysozyme, and mutanolysin (Sigma-Aldrich Co., St. Louis, MO). DNA fragments for cloning experiments were extracted from agarose gels using QIAEX-II® Gel Extraction Kit or QIAquick® Gel Extraction Kit (Qiagen, Valencia, CA). DNA fragments after restriction digestions, ligations, and PCR reactions were purified using QIAprep® Spin Column or QIAquick® PCR Purification Kit (Qiagen, Valencia, CA). Plasmid DNA was extracted from recombinant *E. coli* cells using QIAprep® Spin Miniprep Kit (small-scale), QIAGEN® Plasmid Midi Kit (medium-scale), or QIAGEN® Maxi Kit (large-scale) (Qiagen, Valencia, CA). Plasmid and genomic DNAs were dissolved in elution buffer EB (10 mM Tris-HCl, pH 8.5) (Qiagen, Valencia, CA). Restriction enzyme digestions were performed according to the enzyme manufacturers' instructions (Invitrogen, Carlsbad, CA; New England Biolabs Inc., Beverly, MA; Promega Corp., Madison, WI).

3. Isolation of genomic DNAs from *Lb. helveticus* WSU19 and CNRZ32

Frozen stocks of *Lb. helveticus* strains (100 μL) were inoculated into 10 mL of Lactobacilli MRS broth and incubated at 37°C for 24 h without shaking. The cultures (300

μL) were transferred into 30 mL of MRS broth and grown at 37°C for 16 h without shaking. The cells were harvested by centrifuging for 10 min (5,000 x *g* at 4°C) using an Avanti™ J-25 centrifuge (Beckman Coulter, Fullerton, CA). The supernatants were discarded and the pellets were used for genomic DNA isolations following the QIAGEN Genomic DNA Handbook.

The bacterial pellets were resuspended in 11 mL of bacterial lysis buffer B1 (50 mM Tris-HCl, pH 8.0; 50 mM EDTA, pH 8.0; 0.5% Tween®-20; 0.5% Triton® X-100) by vortexing at maximum speed. The resuspended pellets were mixed with 22 μL of 100 mg/mL RNase A, 300 μL of 100 mg/mL lysozyme, and 500 μL of 20 mg/mL QIAGEN® protease. To facilitate lysis of *Lb. helveticus* CNRZ32 cells, 250 μL of 10,000 U/mL mutanolysin (Sigma-Aldrich Co., St. Louis, MO) was used. The addition of mutanolysin was not needed for the isolation of genomic DNA from *Lb. helveticus* WSU19. The cell suspensions were incubated at 37°C for 16-17 h. After incubation at 37°C, the lysates were mixed with 4 mL of bacterial lysis buffer B2 (3 M guanidine HCl; 20% Tween®-20) and incubated at 50°C for 30 min or until the lysates became clear.

The cleared lysates were vortexed at maximum speed for 10 s and applied to the QIAGEN® Genomic-tips 500/G, pre-equilibrated with 10 mL of equilibration buffer QBT (750 mM NaCl; 50 mM MOPS, pH 7.0; 15% isopropanol, 0.15% Triton® X-100). The lysates moved through the Genomic-tips by gravity. The tips were washed twice with 15 mL of wash buffer QC (1.0 M NaCl; 50 mM MOPS, pH 7.0; 15% isopropanol). The genomic DNAs were eluted with 15 mL of elution buffer QF (1.25 M NaCl; 50 mM Tris-HCl, pH 8.5; 15% isopropanol), and precipitated by adding 10.5 mL (0.7 volumes) of room temperature isopropanol (JT Baker Inc., Phillipsburg, NJ).

The precipitated DNAs were recovered by centrifuging for 30 min (7,500 x *g* at 4°C). The supernatants were carefully decanted. The DNA pellets were washed with 4 mL of cold 70% ethanol, mixed, and centrifuged for 10 min (7,500 x *g* at 4°C). The supernatants were carefully decanted. The DNA pellets were air-dried and re-dissolved in 500 μL of elution buffer EB overnight on an orbital shaker VWR DS-500 at 60 rpm (VWR International, West Chester, PA). The concentrations and purities of DNAs were measured at 260 nm and 280 nm using a Lambda 35 spectrophotometer (PerkinElmer, Boston, MA).

4. Cloning of the complete *pepE*, *pepO*, *pepO2*, and *pepO3* genes

4.1. Isolation of plasmid DNAs from the recombinant *E. coli* cells carrying peptidase genes from *Lb. helveticus* CNRZ32

The following *E. coli* clones expressing the peptidase genes from *Lb. helveticus* CNRZ32 (Dr. James L. Steele, University of Wisconsin, Madison, WI) were the sources of plasmids to be used as DNA templates for the *pepE*, *pepO*, and *pepO2* gene probe syntheses: *E. coli* SURE(pTRKL2::*pepE*), *E. coli* DH5α(pTRKL2::*pepO*), and *E. coli* DH5α(pJDC9::*pepO2*), respectively.

Frozen stocks of the *E. coli* clones (100 μL) were inoculated into 10 mL of LB broth containing 1 mg/mL of Em and incubated at 37°C for 16 h with vigorous shaking. The cultures (5 mL) were transferred into 500 mL of LB broth containing 1 mg/mL Em and incubated at 37°C for 16 h (A_{600} ~ 4.0) with vigorous shaking. Cell densities were measured at 600 nm using a Lambda 35 spectrophotometer (PerkinElmer, Boston, MA). The cells were harvested by centrifuging for 15 min (6,000 x *g* at 4°C) using an Avanti™ J-25 centrifuge (Beckman Coulter, Fullerton, CA). The supernatants were discarded. The pellets were used

for large-scale plasmid DNA preparation following the QIAGEN® Plasmid Purification Handbook protocols.

The bacterial pellets were resuspended in 10 mL of resuspension buffer P1 (50 mM Tris-HCl, pH 8.0; 10 mM EDTA; 100 μg/mL RNase A) by vortexing at maximum speed. The suspensions were transferred into 50 mL sterile centrifuge tubes. Ten mL of lysis buffer P2 (200 mM NaOH, 1% SDS) was added to the suspensions and mixed gently by inverting the tubes 4-6 times. The lysates were incubated at room temperature for 5 min. After incubation, 10 mL of chilled neutralization buffer P3 (3.0 M potassium acetate, pH 5.5) was added to the lysates and mixed gently by inverting the tubes 4-6 times. The mixtures were incubated on ice for 20 min, and then centrifuged for 30 min (22,000 x *g* at 4°C) using an Avanti™ J-25 centrifuge (Beckman Coulter, Fullerton, CA). The supernatants containing plasmid DNAs were transferred to clean, sterile 50 mL centrifuge tubes and re-centrifuged for 15 min (22,000 x *g* at 4°C).

The supernatants containing plasmid DNAs from the second centrifugation were applied promptly to the QIAGEN®-tips 500, pre-equilibrated with 10 mL of equilibration buffer QBT (750 mM NaCl; 50 mM MOPS, pH 7.0; 15% isopropanol, 0.15% Triton® X-100). The supernatants flowed through the tip by gravity. The columns were washed twice with 30 mL of wash buffer QC (1.0 M NaCl; 50 mM MOPS, pH 7.0; 15% isopropanol). Plasmid DNAs were eluted with 15 mL of elution buffer QF (1.25 M NaCl; 50 mM Tris-HCl, pH 8.5; 15% isopropanol) and precipitated with 10.5 mL (0.7 volumes) of room temperature isopropanol. The precipitated DNAs were recovered by centrifuging for 30 min (22,000 x *g* at 4°C).

After carefully decanting the supernatants, the plasmid DNA pellets were washed with 5 mL of room temperature 70% ethanol, and then centrifuged for 10 min (22,000 x *g* at 4^{o}C). The supernatants were decanted carefully. The plasmid DNA pellets were air-dried and re-dissolved in 500 μL of elution buffer EB overnight on an orbital shaker VWR DS-500 at 60 rpm (VWR International, West Chester, PA). DNA concentrations were estimated by restriction enzyme digestions of the plasmid DNAs, followed by gel electrophoresis in 0.8% agarose (Invitrogen, Carlsbad, CA). The High DNA Mass Ladder was used as the standard (Invitrogen, Carlsbad, CA).

4.2. Probe syntheses

4.2.1. DNA amplification via PCR

Four sets of oligonucleotide primers (Table 6) were designed to synthesize the *pepE* (1.3kb), *pepO* (1.9 kb), *pepO2* (1.9 kb), and *pepO3* (1.9 kb) gene probes using the coding sequence of the corresponding peptidase genes from *Lb. helveticus* CNRZ32. GenBank accession numbers for the *pepE*, *pepO*, *pepO2*, and *pepO3* genes from *Lb. helveticus* CNRZ32 are U77050, AF019410, AF321539, and AY365128, respectively. Primers for DNA amplification were designed using Vector NTI® Suite 2 Version 7 (Invitrogen, Carlsbad, CA) and were synthesized by Invitrogen Life Technologies (Carlsbad, CA). The primers (approximately 50 nmoles each) were dissolved in elution buffer EB to final concentrations of 150 pmoles/μL.

The following plasmids, containing the previously cloned peptidase genes from *Lb. helveticus* CNRZ32, were used as DNA templates for the *pepE*, *pepO*, and *pepO2* gene probes: pTRKL2::*pepE*, pTRKL2::*pepO*, and pJDC9::*pepO2* (Dr. James L. Steele,

University of Wisconsin, Madison, WI). Genomic DNA from *Lb. helveticus* CNRZ32 was used as the template for the *pepO3* gene probe. Plasmid and genomic DNA templates were diluted in elution buffer EB to 2 ng/μL and 60 ng/μL, respectively.

Table 6. Forward and reverse primers for endopeptidase probe syntheses

Primers	Sequence
PepE forward	5'-ATGGCTCATGAATTAACTGTG-3'
PepE reverse	5'-TTAAGCAAGTGAATCCCATG-3'
PepO forward	5'-AGAAGATATTTAGCTGTACG-3'
PepO reverse	5'-TAATTCTATCTTCAGGATCA-3'
PepO2 forward	5'-TGAATTTAGCAAAAATCCGC-3'
PepO2 reverse	5'-ACCAAATGACTACGCGCTTA-3'
PepO3 forward	5'-ATAAAATGACTGTACGCGGC-3'
PepO3 reverse	5'-ACACGTTTTTCAGGATCGAG-3'

The probes were labeled with nonradioactive digoxigenin-dUTP (DIG) using PCR DIG Probe Synthesis Kit (Roche Diagnostics Corp., Indianapolis, IN). For PCR reactions, the following reagents were mixed in a PCR tube: 10 μL of 10X PCR buffer containing $MgCl_2$; 5 μL of 10X PCR DIG probe synthesis mix; 5 μL of 10X dNTP stock solution, 2 μL of 150 pmoles/μL forward primer, 2 μL of 150 pmoles/μL reverse primer, 1.5 μL of enzyme mix Expand High Fidelity, 1 μL of template DNA, and sterile deionized water to make the volume to 100 μL. For synthesis of the *pepE* gene probe, 10 μL of 10X PCR DIG probe synthesis mix was used, without the addition of 10X dNTP stock solution. The PCR mixtures were scaled up to 800 μL to prepare the probes for both Southern and colony hybridizations. DNA amplifications were performed using a GeneAmp® PCR System 2700 (Applied

Biosystems, Foster City, CA) at the following thermal cycle: a single cycle of 95°C for 2 min (initial denaturation); 30 cycles of 95°C for 30 s (denaturation), 60°C for 30 s (annealing), 72°C for 15 min (elongation); and a single cycle of 72°C for 7 min (final elongation).

4.2.2. Gel extraction of probes

The synthesized probes were purified using QIAquick® Gel Extraction Kit. Probe DNAs were electrophoresed in 1% agarose gel at 75 V for 55 min. Gel electrophoresis was performed using a Bio-Rad Power Pac 300 (Bio-Rad Laboratories, Hercules, CA). The gels were stained for 10 min with 0.5 μg/mL of ethidium bromide (Sigma-Aldrich Co., St. Louis, MO) and DNA fragments were visualized on a VWR Benchtop Ultraviolet Transilluminator (VWR International, West Chester, PA). The DNA fragments of interest were cut out of the gels and excised in 350-400 mg gel slices. The gel slices were placed in sterile 1.5 mL microcentrifuge tubes.

Solubilization and binding buffer QG was added to the tubes at a ratio of 3 volumes to 1 volume of gel slice (100 mg ~ 100 μL). The tubes were incubated at 50°C for 10 min or until the gel slices dissolved completely. During incubation, the tubes were vortexed every 2-3 min to facilitate the dissolution of the gel slices. After the gel slices completely dissolved, color of the solutions should have remained yellow; otherwise 10 μL of 3 M sodium acetate (pH 5.0) was added to turn the color to yellow.

The dissolved gel solutions were applied to QIAquick® columns (750 μL at a time). To increase probe concentrations, solutions of 2 gel slices were applied to a single column. The columns were centrifuged for 1 min (16,100 x *g* at room temperature) using an Eppendorf® Microcentrifuge 5415D (Brinkmann Instruments, Westbury, NY). The flow-

through fractions were discarded. Buffer QG (500 μL) was added to the columns for removal of traces of agarose. The columns were centrifuged for 1 min (16,100 x *g* at room temperature). After discarding the flow-through fractions, 750 μL of wash buffer PE was added to the columns to wash out the remaining salt. The columns were centrifuged for 1 min (16,100 x *g* at room temperature). The flow-through fractions were discarded and the columns were re-centrifuged for an additional 1 min (16,100 x *g* at room temperature).

The columns were placed in sterile 1.5 mL microcentrifuge tubes. The probe DNAs were eluted with 50 μL of elution buffer EB, added to the center of the QIAquick® membranes. The columns were centrifuged for 1 min (16,100 x *g* at room temperature). The flow-through fractions containing probe DNAs were stored at –20°C until used.

4.2.3. Dot blot estimation of probe concentrations

Dot blot was performed using DIG Nucleic Acid Detection Kit (Roche Diagnostics Corp., Indianapolis, IN), following the manufacturer's instructions, with modifications. All chemicals for the dot blot experiments were purchased from Sigma Aldrich Co. (St. Louis, MO). Serial dilutions of DIG-labeled control DNA (pBR328 DNA/BamHI; 5 μg/mL) were prepared in DNA dilution buffer to obtain concentrations of 1 ng/μL; 100 pg/μL; 10 pg/μL; 1 pg/μL; and 0.1 pg/μL. Dilution factors to attain these concentrations were 1/5; 1/50; 1/500; 1/5,000; and 1/50,000, respectively. Serial dilutions of DIG-labeled probe DNAs were prepared using the same dilution factors as the DIG-labeled control DNA.

The diluted DIG-labeled control DNA (1μL) was spotted alongside the DIG-labeled probe DNA (1μL) of the same dilution factor on a positively charged nylon membrane (Roche Diagnostics Corp., Indianapolis, IN). After air-drying, DNA samples were fixed to

the membrane using a Stratalinker® 2400 UV Crosslinker (Stratagene, La Jolla, CA). The membrane was equilibrated with 10 mL of washing buffer (0.1 M maleic acid; 0.15 M NaCl; 0.3% Tween®-20; pH 7.5) for 5 min at room temperature with shaking.

The equilibrated membrane was incubated in 10 mL of blocking solution for 5 min at room temperature with shaking, followed by incubation in 10 mL of antibody solution for 5 min. The blocking solution was freshly prepared by mixing 1 part of 10% blocking reagent (Roche Diagnostics Corp., Indianapolis, IN) in maleic acid buffer with 9 parts of maleic acid buffer (0.1 M maleic acid; 0.15 M NaCl; pH 7.5). The antibody solution was freshly prepared by diluting 2 μL of Anti-DIG-alkaline phosphatase (AP) conjugate (Roche Diagnostics Corp., Indianapolis, IN) in 10 mL of blocking solution.

Following incubation with the antibody solution, the membrane was transferred to a clean container and washed twice, 5 min each, in 10 mL of washing buffer at room temperature with shaking. After the second wash, the membrane was incubated in 10 mL of color substrate solution in the dark to allow for color development. The color substrate solution was prepared by diluting 100 μL of nitroblue tetrazolium chloride /5-bromo-4-chloro-3-indolyl-phosphate (NBT/BCIP) stock solution (Roche Diagnostics Corp., Indianapolis, IN) in 5 mL of detection buffer (0.1 M Tris-HCl; 0.1 M NaCl; pH 9.5). Once the desired spots were detected, the membrane was rinsed with deionized water to prevent over-development of the color. The diluted DIG-labeled control DNA with the closest color intensity to the diluted DIG-labeled probe DNA was used as the reference for calculating the probe DNA concentration.

4.3. Southern hybridization

Southern hybridization was conducted essentially as described by Southern (1975) and Sambrook et al. (1989). All chemicals for Southern and colony hybridizations were purchased from Sigma-Aldrich Co. (St. Louis, MO).

4.3.1. Digestion of genomic DNA from *Lb. helveticus* WSU19 with single restriction enzyme

Genomic DNA from *Lb. helveticus* WSU19 was digested with 17 restriction enzymes, including *Bam*HI, *Cla*I, *Dra*I, *Eco*RI, *Eco*RV, *Hind*III, *Kpn*I, *Nru*I, *Pst*I, *Pvu*II, *Sac*I, *Sac*II, *Sal*I, *Sma*I, *Spe*I, *Sph*I, and *Xba*I. The concentration of genomic DNA from *Lb. helveticus* WSU19 in each digestion mixture was approximately 0.1 μg/μL. Digestion was performed for 20 h at 37^{o}C, except for *Sma*I at 30^{o}C.

4.3.2. Gel electrophoresis of the digested genomic DNAs

Agarose gels (0.8%) were prepared using 15x7 cm tray and 20-well comb (Bio-Rad Laboratories, Hercules, CA) by dissolving 0.56 g agarose in 70 mL of 1X TAE buffer (40 mM Tris, pH 8.0; 20 mM acetic acid; 1 mM EDTA) (Bio-Rad Laboratories, Hercules, CA). Gel electrophoresis was performed at 75V for 55 min. The ladder used was the DIG-labeled DNA MW Marker VII (Roche Diagnostics Corp., Indianapolis, IN). After staining for 10 min with 0.5 μg/mL of ethidium bromide (Sigma-Aldrich Co., St. Louis, MO), the DNA samples were visualized under UV light in a MultiImage™ Light Cabinet (Alpha Innotech Corp., San Leandro, CA). Pictures of the gels were taken using an Alpha Imager® Imaging System Version 5.5 (Alpha Innotech Corp., San Leandro, CA). The gels were soaked in

sterile, deionized water for 10 min at room temperature on an orbital shaker VWR DS-500 at 60 rpm (VWR International, West Chester, PA).

4.3.3. Southern transfer

The agarose gels were submerged in depurination solution (250 mM HCl) for 10 min at room temperature on an orbital shaker at 60 rpm to improve the transfer of DNA fragments larger than 10 kb. The DNAs were denatured by soaking the gels in denaturation solution (0.5 N NaOH; 1.5 M HCl) for 60 min at room temperature on an orbital shaker at 60 rpm. After the denaturing step, the gels were submerged in neutralization solution (1.0 M Tris-HCl; 1.5 M NaCl; pH 8.0) for 60 min at room temperature on an orbital shaker at 60 rpm.

Southern transfer was facilitated by applying pressure to the gels using PosiBlot® 30-30 Pressure Blotter and Pressure Control Station (Stratagene, La Jolla, CA). Two pieces of Whatman 3 MM Chr paper (Whatman Inc., Florham Park, NJ) were cut to the gel size, saturated with 10X SSC solution (diluted from 20X SSC solution: 3 M NaCl; 0.3 M sodium citrate; pH 7.0), and placed on top of the membrane support pad of the Pressure Blotter. Positively charged nylon membrane was saturated with 10X SSC solution and placed on top of the Whatman 3 MM Chr paper. The membrane was smoothed out so that no wrinkles or air bubbles were present. A mask with a windowed area was placed over the membrane such that the membrane was located within the windowed area. The gel was placed over the mask, within the windowed area. Two pieces of Whatman 3 MM Chr paper were saturated with 10X SSC solution and placed on top of the gel, followed by a sponge saturated with 10X SSC. The DNA was blotted from the gel for 2 h at 70 mmHg pressure.

After blotting, the membrane was soaked in 5X SSC solution and placed on a filter paper to air-dry. The DNA was fixed to the membrane using Stratalinker® 2400 UV Crosslinker (Stratagene, La Jolla, CA). The crosslinking was performed twice using Autocross-link program. The gel was stained with ethidium bromide for 10 min and the gel picture after Southern transfer was documented.

4.3.4. Prehybridization and hybridization

The membranes were placed in 150 x 35 mm hybridization tubes containing 15 mL of prehybridization solution (5X SSC; 1% blocking reagent; 0.1% N-lauroylsarcosine; 0.02% SDS; 50% formamide). Prehybridization steps were conducted under a high stringency condition at 42°C for 6 h, using a PersonalHyb® Hybridization Oven (Stratagene, La Jolla, CA). The prehybridization solution for the *pepO3* gene did not contain 50% formamide, and therefore the high stringency condition was achieved at 68°C. The used prehybridization solutions were discarded. Probes were heated at 65°C for 10 min to denature the DNAs, and then added to 15 mL of fresh prehybridization solutions to provide final probe concentrations of 25 ng/mL (hybridization solutions). After mixing, the hybridization solutions were added to the membranes in the hybridization tubes. Hybridization steps were conducted under a high stringency condition for 12 h. The used hybridization solutions were stored at –20°C for later use.

4.3.5. Detection

The membranes were washed twice with 15 mL of 2X wash solution (2X SSC; 0.1% SDS), 5 min per wash, at room temperature in the hybridization tubes. The membranes were

washed twice with 15 mL of 0.5X wash solution (0.5X SSC; 0.1% SDS), 15 min per wash at 68^{o}C in the hybridization tubes. After the stringency washes, the membranes were equilibrated with 15 mL of washing buffer for 5 min at room temperature in the hybridization tubes. After equilibration, the membranes were incubated at room temperature in 20 mL of blocking solution for 60 min, followed by incubation in 20 mL of antibody solution for 60 min. Compositions of the washing buffer, blocking solution, and antibody solution are described in Section 4.2.3.

After incubation with the antibody solution, the membranes were transferred to clean containers. The membranes were washed twice with 100 mL of washing buffer, 15 min per wash at room temperature on an orbital shaker at 60 rpm. After the washing steps, the membranes were equilibrated in detection buffer at room temperature for 5 min on an orbital shaker at 60 rpm. After equilibration, the membranes were incubated in 10 mL of color substrate solution in the dark to allow for color development. Preparations of the detection buffer and color substrate solution are described in Section 4.2.3. When the desired bands were detected, the membranes were rinsed with deionized water to prevent over-development of the color.

4.3.6. Digestion of genomic DNA from *Lb. helveticus* WSU19 with two restriction enzymes and the second Southern hybridization

Restriction enzymes that produced a single band in the first Southern hybridization were used in combination to digest the genomic DNA from *Lb. helveticus* WSU19 for the second Southern hybridization. Simultaneous digestions were used for *pepE*, *pepO*, and *pepO2*, while sequential digestion was done for *pepO3*. All digestions were performed for 20

h. In the simultaneous digestion, genomic DNA was digested in the buffer that provided the highest activities for both restriction enzymes. No DNA purification was necessary at the end of the digestion.

In the sequential digestion, genomic DNA after the first digestion was purified using QIAprep® Spin column prior to the second digestion. Purification of the DNA followed the QIAprep® Miniprep Handbook protocols. Binding buffer PB was added at a ratio of 5 volumes to 1 volume of the DNA solution. After mixing, the mixture was applied to the QIAprep® Spin column and centrifuged for 1 min (16,100 x *g* at room temperature) using an Eppendorf® Microcentrifuge 5415D (Brinkmann Instruments, Westbury, NY) to draw the DNA to the QIAprep® membrane. After discarding the flow-through fraction, the column was washed with 750 μL of wash buffer PE and centrifuged for 1 min (16,100 x *g* at room temperature). The flow-through fraction was discarded and the column was re-centrifuged to remove residual wash buffer. The column was placed in a sterile 1.5 mL microcentrifuge tube. The DNA was eluted with 30 μL of elution buffer EB and incubated at room temperature for 1 min before centrifugation (1 min; 16,100 x *g* at room temperature). To increase the DNA yield, the elution buffer EB was warmed to 70^{o}C before being added to the column. The flow-through fraction containing DNA was digested with the second restriction enzyme.

The second Southern hybridization was conducted as described in Sections 4.3.1 to 4.3.5. The ladder used in the second Southern was DIG-labeled DNA MW Marker II instead of VII (Roche Diagnostics Corp., Indianapolis, IN).

4.4. Preparation of insert DNAs

4.4.1. Digestion of genomic DNA from *Lb.helveticus* WSU19 with cloning enzyme(s)

The restriction enzyme(s) used for cloning of the endopeptidase genes based on the results of the first and second Southern hybridizations were *Pst*I for *pepE*; *Hind*III and *Sal*I for *pepO*; *Sph*I and *Xba*I for *pepO2*; and *Kpn*I for *pepO3*. The genomic DNA from *Lb. helveticus* WSU19 was digested with these restriction enzymes according to the enzyme manufacturers' instructions. Simultaneous digestion was used for cloning with 2 restriction enzymes. The amounts of genomic DNA used in each digestion were approximately 27 μg per 300 μL digestion mixture for *pepE* and 24 μg per 150 μL digestion mixtures for *pepO*, *pepO2*, and *pepO3*. Digestions were performed at 37^{o}C for 20 h.

4.4.2. Gel extraction of hybridization-positive DNA fragments

The sizes of DNA fragments to be extracted were determined based on the hybridization-positive fragments from Southern hybridizations. The digested genomic DNAs from *Lb. helveticus* WSU19 were gel electrophoresed in 0.8% agarose. The ladder was the non DIG-labeled DNA MW Marker II (Roche Diagnostics Corp., Indianapolis, IN). The DNA marker was heated at 65^{o}C for 10 min and chilled quickly on ice for 1 min prior to use.

Gel extraction of the hybridization-positive DNA fragment containing the *pepE* gene was conducted following the QIAquick® Gel Extraction Kit Protocol described in Section 4.2.2. Extraction of genomic DNA using the QIAquick® column caused smearing of the DNA. Therefore, QIAEX-II® Gel Extraction Kit, as described below, was used for extracting DNA fragments containing the *pepO*, *pepO2*, *pepO3*, and *pepN* genes.

The DNA fragments were gel electrophoresed in 0.8% agarose, stained with ethidium bromide for 10 min, and visualized on a VWR Benchtop Ultraviolet Transilluminator (VWR International, West Chester, PA). The DNA fragments containing the genes of interest were cut out of the gels in 300-350 mg gel slices. The gel slices were placed in sterile 1.5 mL microcentrifuge tubes. For DNA fragments larger than 4 kb, solubilization and binding buffer QX1 (3 volumes) and sterile deionized water (2 volumes) were added to the gel slices (100 mg ~ 100 μL). For DNA fragments smaller than 4 kb, buffer QX1 (3 volumes) were added per volume of gel slices. The QIAEX-II suspension was vortexed for 30 sec and then 30 μL of the suspension was added to each tube. The mixtures were incubated at 50^{o}C for 10 min or until the agarose solubilized. The tubes were inverted and flicked every 2 min to keep the QIAEX-II in suspension. Color of the mixtures should have remained yellow at the end of incubation; otherwise 10 μL of 3 M sodium acetate (pH 5.0) was added to turn the color to yellow. The mixtures were centrifuged for 30 sec (16,100 x *g* at room temperature) using an Eppendorf® Microcentrifuge 5415D (Brinkmann Instruments, Westbury, NY).

After decanting the supernatants, buffer QX1 (500 μL) was added to the pellets for removal of residual agarose contaminants. The pellets were resuspended by vortexing. The suspensions were centrifuged for 30 sec (16,100 x *g* at room temperature). The supernatants were discarded and the pellets were washed twice with 500 μL of wash buffer PE to remove residual salt contaminants. The pellet suspensions were centrifuged for 30 sec (16,100 x *g* at room temperature) in each washing step.

After air-drying for 30 min, the pellets were re-suspended in 20 μL of elution buffer EB. The suspensions were incubated at 50^{o}C for 5 min for DNA fragments between 4 and 10 kb. For DNA fragments smaller than 4 kb, incubation was conducted at room temperature for

5 min. The suspensions were centrifuged for 30 sec (16,100 x *g* at room temperature) after incubation. The supernatants containing DNA were pipetted into a sterile 1.5 mL microcentrifuge tube. The elution step was repeated twice. The insert DNAs were stored at –20^{o}C until used.

4.5. Preparation of pJDC9 vector DNA

4.5.1. Digestions of pJDC9 plasmid DNA with cloning enzyme(s)

The pJDC9 plasmid DNA (Dr. Donald A. Morrison, University of Illinois, Chicago) was the vector used for cloning of the endopeptidase genes from *Lb. helveticus* WSU19. The plasmid was isolated from *E. coli* DH5α(pJDC9) following the procedure described in Section 4.1. For isolation of pJDC9 plasmid DNA, the recombinant *E. coli* DH5α was grown in 100 mL of LB broth containing 1 mg/mL Em and the DNA was dissolved in 250 μL of elution buffer EB.

For each gene of interest, the pJDC9 plasmid DNA was digested with the same restriction enzyme(s) used for the digestion of the insert genomic DNA from *Lb. helveticus* WSU19 (Section 4.4.1). The amount of pJDC9 vector DNA used in each digestion was approximately 1.5 μg per 100 μL digestion mixture. The digestions were performed at 37^{o}C for 5 h.

4.5.2. Purification of the digested pJDC9 plasmid DNAs

The digested pJDC9 plasmid DNAs were purified following the QIAquick® PCR Purification Kit Protocol. The digested plasmid DNAs (1 volume) were mixed with 5 volumes of binding buffer PB. The mixtures were applied to the QIAquick® columns and

centrifuged for 1 min (16,100 x *g* at room temperature) using an Eppendorf® Microcentrifuge 5415D (Brinkmann Instruments, Westbury, NY). After discarding the flow-through fractions, the columns were washed with 750 µL of wash buffer PB and centrifuged for 1 min (16,100 x *g* at room temperature). The flow-through fractions were discarded and the columns were re-centrifuged for 1 min. After centrifuging, the QIAquick® columns were placed in sterile 1.5 mL microcentrifuge tubes. The plasmid DNAs were eluted with 50 µL of elution buffer EB, applied to the center of the QIAquick® membranes. The columns were centrifuged for 1 min (16,100 x *g* at room temperature). The flow-through fractions containing digested vector DNAs were stored at –20°C until used. Concentrations of the digested vector DNAs were estimated by agarose gel electrophoresis, using High DNA Mass Ladder as the standard.

4.5.3. Dephosphorylation of digested pJDC9 vector DNA (for single cloning enzyme)

The pJDC9 vector DNA digested with single cloning enzyme was dephosphorylated using Shrimp Alkaline Phosphatase (SAP; 1U/µL) (Promega Corp., Madison, WI). Three units (3U) of SAP were added per µg of the digested vector DNA. SAP buffer (10X) was added to a final concentration of 1X. Sterile deionized water was added to make the volume to 50 µL. The dephosphorylation mixture was incubated at 37°C for 30 min, followed by heat inactivation of SAP at 65°C for 15 min. The mixture was immediately chilled on ice after heat inactivation. The dephosphorylated vector DNA was purified following the QIAquick® PCR Purification Kit Protocol described in Section 4.5.2. The vector DNA was eluted in 40 µL of elution buffer EB.

4.6. Ligation of insert genomic DNAs into pJDC9 vector DNA

Ligations of the insert genomic DNA into the pJDC9 vector DNA were facilitated by T4 DNA ligase (1U/μL; Invitrogen, Carlsbad, CA). Six ligation mixtures were prepared by varying the volume ratio of insert and vector DNA. The volumes of vector DNA (15 ng/μL) ranged from 2.5 μL to 10.0 μL, while the volumes of insert DNA ranged from 15.0 μL to 22.5 μL. The ligation mixtures were prepared in total volumes of 50 μL. The T4 DNA ligase and DNA ligase buffer (5X) were added at 12.5 and 10 μL, respectively. Ligations were performed at 16^{o}C for 20-24 h. The ligated DNAs were purified using QIAprep® Spin column described in Section 4.3.6. The DNAs were eluted in 40 μL of elution buffer EB.

4.7. Electroporation of ligated DNAs into electrocompetent *E. coli* DH5α cells

Sterile electroporation cuvettes (0.2 cm gap; Bio-Rad Laboratories, Hercules, CA) and sterile microcentrifuge tubes were chilled on ice. Frozen cells of electrocompetent *E. coli* DH5α (ElectroMAX™ DH5α-E™; Invitrogen, Carlsbad, CA) were thawed on ice. After thawing, 20 μL of the electrocompetents *E. coli* DH5α were mixed with 20 μL of the ligated DNAs in the chilled microcentrifuge tubes, and then transferred to the chilled electroporation cuvettes. The cuvettes were placed in the cuvette holder of the MicroPulser (Bio-Rad Laboratories, Hercules, CA) and zapped using Ec2 program (2.5 kV; 10 μF; 600 ohms). One mL of S.O.C medium (2% tryptone, 0.5% yeast extract, 10 mM NaCl, 2.5 mM KCl, 10 mM $MgCl_2$, 10 mM $MgSO_4$, and 20 mM glucose; Invitrogen, Carlsbad, CA) was added to the cuvettes at room temperature. The cells in S.O.C medium were transferred into sterile 5 mL tubes and incubated at 37^{o}C for 1 h with shaking at 250 rpm. The cell suspensions were diluted to 10^{-1} and 10^{-2}. The diluted and undiluted suspensions were plated in triplicate, 100

μL each, on LB agar containing X-Gal/IPTG and 1 mg/mL Em as described in Section 1. A total of 9 plates were prepared for each ligated DNA sample. The plates were incubated aerobically at 37^{o}C for 48-72 h.

4.8. Colony hybridization

4.8.1. Replica plating

White colonies on LB agar containing X-Gal/IPTG plates were further screened for hybridization-positive clone(s) using colony hybridization. Approximately 1000 white colonies were screened for each gene of interest. Each white colony was inoculated on 3 LB agar plates containing 1 mg/mL Em. Each plate could hold 50 colonies. A total of 20-22 sets of triplicate plates were prepared in each cloning. The plates were incubated aerobically at 37^{o}C for 16 h. Except for *pepO3* cloning, the *E. coli*(pJDC9) and *E. coli* clone expressing the corresponding endopeptidase gene from *Lb. helveticus* CNRZ32 served as the negative and positive controls, respectively.

4.8.2. Colony lifts

Colony lifts were performed according to the Nylon Membranes for Colony and Plaque Hybridization Instruction with modifications (Roche Diagnostics Corp., Indianapolis, IN). One of the triplicate plates were pre-cooled at 4^{o}C for 1 h. Nylon membranes for colony and plaque hybridization (82 mm diameter; Roche Diagnostics Corp., Indianapolis, IN) were carefully placed on the surface of the pre-cooled plates. The membrane discs were left on the plates for 5 min at room temperature, then removed carefully with sterile filter tweezers, and briefly blotted on Whatman 3 MM Chr paper.

The membrane discs were placed side up for 15 min at room temperature on 2 pieces of Whatman 3 MM Chr paper, saturated with denaturation solution (0.5 M NaOH; 1.5 M NaCl). The discs were air-dried on Whatman 3 MM Chr paper, then placed upside for 15 min at room temperature on 2 pieces of Whatman 3 MM Chr paper, saturated with neutralization solution (1.5 M NaCl; 1.0 Tris-HCl; pH 8.0). The discs were air-dried on Whatman 3 MM Chr paper, and then placed upside for 10 min at room temperature on 2 pieces of Whatman 3 MM Chr paper, saturated with 2X SSC solution. The 2X SSC solution was diluted from 20X SSC solution (3 M NaCl; 0.3 M sodium citrate; pH 7.0). The transferred DNAs were subsequently crosslinked to the membranes using a Stratalinker® 2400 UV Crosslinker. The crosslinking was conducted twice using Autocross-link program.

The colony lifts were treated with proteinase K (Roche Diagnostics Corp., Indianapolis, IN) for removal of cell debris. The proteinase K (>600 units/mL, 14-22 mg/mL) was diluted 1:10 in 2X SSC solution. The diluted enzyme (500 μL) was added to each membrane disc, which was placed on a foil, and distributed evenly. The discs were incubated at 37^{o}C for 1 h. After incubation, the discs were placed between 2 pieces of Whatman 3 MM Chr paper pre-soaked in sterile deionized water. The paper was pressed firmly onto the discs using a ruler or test tube. The debris was removed by gently pulling off the paper. This step was repeated if visible debris was still on the membrane disc.

4.8.3. Prehybridization and hybridization

Prehybridization and hybridization steps were carried out in a 2.7 L round Rubbermaid container on an orbital shaker at 50 rpm. Prehybridization steps were performed in 600 mL of prehybridization solution (5X SSC; 1% blocking reagent; 0.1% N-

lauroylsarcosine; 0.02% SDS) under a high stringency condition at 68°C for 6-12 h. The used prehybridization solutions were discarded. Probes, after being denatured at 65°C for 10 min, were added to 600 mL of fresh prehybridization solutions to obtain final concentrations of 25 ng/mL. Probe syntheses and determination of probe concentrations are described in Section 4.2. When frozen hybridization solutions were utilized, the solutions were heated in boiling water for 10 min before adding to the membrane discs. Hybridization steps were conducted under a high stringency condition at 68°C for 12 h. The used hybridization solutions were stored at –20°C for later use.

4.8.4. Detection

The membrane discs were washed twice with 600 mL of 2X wash solution (2X SSC; 0.1% SDS), 15 min per wash, at room temperature. The discs were washed twice with 600 mL of 0.5X wash solution (0.5X SSC; 0.1% SDS), 30 min per wash at 68°C. After the stringency washes, the membranes were equilibrated with 600 mL of washing buffer for 5 min at room temperature. After equilibration, the membranes were incubated at room temperature in 600 mL of blocking solution for 60 min, followed by incubation in 600 mL of antibody solution for 30 min. All incubations were performed on an orbital shaker at 50 rpm. Preparations of the washing buffer, blocking solution, and antibody solution are described in Section 4.2.3.

After incubation with the antibody solution, the membranes were transferred to a clean container. The membranes were washed twice with 600 mL of washing buffer, 15 min per wash at room temperature on an orbital shaker at 50 rpm. After the washing steps, the membranes were equilibrated in 100 mL of detection buffer at room temperature for 5 min

on an orbital shaker at 50 rpm. After equilibration, the membranes were incubated in 5 mL of color substrate solution in the dark to allow for color development. Preparations of the detection buffer and color substrate solution are described in Section 4.2.3. When the desired spots were detected, the membranes were rinsed with deionized water to prevent over-development of the color.

4.9. Confirmation of peptidase-positive clone(s)

4.9.1. Small-scale plasmid DNA preparation from hybridization-positive colonies

If the colony hybridization screening resulted in less than 3 hybridization-positive colonies, plasmids from these colonies were prepared in medium-scale for restriction enzyme analyses and 5', 3' end DNA sequencing. Otherwise, plasmids were prepared in small-scale for restriction enzyme analyses before proceeding to medium- and large-scale for further confirmations.

Hybridization-positive colonies were inoculated in 10 mL of LB broth containing 1 mg/mL Em and incubated at 37^{o}C for 16 h with vigorous shaking. The cultures (1.5 mL) were harvested by centrifuging for 1 min (16,100 x *g* at room temperature) using an Eppendorf® Microcentrifuge 5415D (Brinkmann Instruments, Westbury, NY). The supernatants were decanted. The pellets were used for small-scale plasmid preparation following the QIAprep® Miniprep Handbook protocols.

The bacterial pellets were re-suspended in 250 μL of resuspension buffer P1 containing 100 μg/mL RNaseA by vortexing at maximum speed. The cells were lysed in 250 μL of lysis buffer P2 for 5 min. The tubes were inverted gently 4-6 times to mix. Addition of 350 μL of neutralization buffer N3 stopped the lysis reaction. After the addition of buffer N3,

the tubes were immediately, gently inverted 4-6 times to avoid localized precipitation. The solutions were centrifuged for 10 min (16,100 x *g* at room temperature).

Supernatants were decanted to the QIAprep® Spin columns and centrifuged for 1 min (16,100 x *g* at room temperature). The flow-through fractions were discarded and the columns were washed with 500 μL of binding buffer PB, followed by centrifugation for 1 min (16,100 x *g* at room temperature). The flow-through fractions were discarded. The columns were washed with 750 μL of wash buffer PE and centrifuged for 1 min (16,100 x *g* at room temperature). After discarding the flow-through fractions, the columns were re-centrifuged for an additional 1 min to remove residual wash buffer.

The QIAprep® columns were placed in sterile 1.5 mL microcentrifuge tubes. The plasmid DNAs were eluted with 50 μL of elution buffer EB, centrifuged for 1 min (16,100 x *g* at room temperature). The flow-through fractions containing plasmid DNAs were used for restriction enzyme analysis for confirmation of the positive clone(s).

4.9.2. Restriction enzyme analyses

Plasmid DNAs were digested with the cloning enzymes to confirm the presence of the endopeptidase genes of interest. The pJDC9 vector DNA digested with the same restriction enzymes served as the control. Digestion mixtures were prepared in a total volume of 20 μL by mixing 10 μL of plasmid DNA with 2 μL of 10X buffer, 1 μL of restriction enzyme, and sterile deionized water to make up the volume. Digestions were performed at 37^{o}C for 5 h, followed by gel electrophoresis in 0.8% agarose.

4.9.3. Chloramphenicol-permeabilized cells / cell-free extract (CFE) assay for confirmation of PepE activity

The chloramphenicol-permeabilized cells / CFE assay for peptidase activity followed the procedure developed by Bhowmik and Marth (1988), with some modifications. A single hybridization-positive colony was inoculated in 10 mL of LB broth containing 1 mg/mL Em and incubated at 37°C for 16 h with vigorous shaking. The culture (0.2 mL) was mixed with 2.8 mL of 50 mM Hepes buffer (pH 7.0; Sigma-Aldrich Co., St. Louis, MO). Chloramphenicol (4-5 drops; JT Baker Inc., Phillipsburg, NJ) was added to the mixture and vortexed well. Substrate N-Benzoyl-Phenylalanine-Valine-Arginine-p-Nitroanilide.HCl (Sigma-Aldrich Co., St. Louis, MO) was dissolved in methanol to a concentration of 3 mM and added to the mixture (100 μL). After vortexing, the mixture was incubated at 37°C with shaking (~250 rpm). The *E. coli* SURE(pTRKL2::*pepE*) and *E. coli* DH5α(pJDC9) served as positive and negative controls, respectively. Peptidase-positive clones carrying the *pepE* gene developed yellow color after approximately 2 h incubation.

4.9.4. Medium-scale plasmid DNA preparation from hybridization-positive colonies

Frozen stocks of the hybridization-positive *E. coli* DH5α (100 μL) were inoculated in 10 mL of LB broth containing Em and incubated at 37°C for 16 h with vigorous shaking. One mL of the cultures were transferred into 100 mL of LB broth containing 1 mg/mL Em and incubated at 37°C for 16 h with vigorous shaking. The cells were harvested by centrifuging for 15 min (6,000 x *g* at 4°C) using an Avanti™ J-25 centrifuge (Beckman Coulter, Fullerton, CA). The supernatants were discarded. The pellets were used for medium-scale plasmid preparation following the QIAGEN® Plasmid Purification Handbook protocols.

The bacterial pellets were resuspended in 4 mL of resuspension buffer P1 (50 mM Tris-HCl, pH 8.0; 10 mM EDTA; 100 μg/mL RNase A) by vortexing at maximum speed. The suspensions were transferred to sterile 50 mL centrifuge tubes. Four mL of lysis buffer P2 (200 mM NaOH, 1% SDS) was added to the suspensions and mixed gently by inverting the tubes 4-6 times. The lysates were incubated at room temperature for 5 min. After incubation, 4 mL of chilled neutralization buffer P3 (3.0 M potassium acetate, pH 5.5) was added to the lysates and mixed gently by inverting the tubes 4-6 times. The mixtures were incubated on ice for 15 min, and then centrifuged for 30 min (22,000 x *g* at 4°C) using an Avanti™ J-25 centrifuge (Beckman Coulter, Fullerton, CA). The supernatants containing plasmid DNAs were transferred to clean, sterile 50 mL centrifuge tubes and re-centrifuged for 15 min (22,000 x *g* at 4°C).

Supernatants containing plasmid DNAs from the second centrifugation were applied promptly to the QIAGEN®-tips 100, pre-equilibrated with 4 mL of equilibration buffer QBT (750 mM NaCl; 50 mM MOPS, pH 7.0; 15% isopropanol, 0.15% Triton® X-100). The supernatants flowed through the tips by gravity flow. The columns were washed twice 10 mL of wash buffer QC (1.0 M NaCl; 50 mM MOPS, pH 7.0; 15% isopropanol). Plasmid DNAs were eluted with 5 mL of elution buffer QF (1.25 M NaCl; 50 mM Tris-HCl, pH 8.5; 15% isopropanol) and precipitated with 3.5 mL (0.7 volumes) of room temperature isopropanol. The precipitated DNAs were recovered by centrifuging for 30 min (22,000 x *g* at 4°C).

After carefully decanting the supernatants, the plasmid DNA pellets were washed with 2 mL of room temperature 70% ethanol, and centrifuged for 10 min (22,000 x *g* at 4°C). The supernatants were decanted carefully. The plasmid DNA pellets were air-dried and re-dissolved in 150 μL of elution buffer EB overnight on an orbital shaker at 60 rpm. DNA

concentrations were estimated by restriction enzyme digestions of the DNAs followed by gel electrophoresis in 0.8% agarose. The High DNA Mass Ladder was used as the standard.

4.9.5. 5' and 3' end DNA sequencing

The Laboratory for Biotechnology and Bioanalysis I (LLB 1) at Washington State University (Pullman, WA) performed the 5' and 3' end DNA sequencing using M13 forward and reverse universal primers. The plasmid DNAs prepared from hybridization-positive colonies, as described in Section 4.9.4., were used as the sequencing templates. For confirmation of the *pepO* clone(s), additional sequencing was performed using the PepO forward and reverse primers from *Lb. helveticus* CNRZ32 (Table 6). Nucleic acid and protein identities searches were performed using Basic Local Alignment Search Tool (BLAST) through the National Center for Biotechnology Information (NCBI) website. Positive insert DNAs confirmed by the 5' and 3' end DNA sequencing were subjected to primer walking for complete sequencing of the genomic inserts.

4.9.6. Large-scale plasmid DNA preparation from peptidase-positive clones

Plasmid DNAs were prepared in a large-scale from peptidase-positive clones that were confirmed by the 5' and 3' end DNA sequencing. The large-scale plasmid DNAs were used as the templates for complete sequencing of the genomic inserts. The large-scale plasmid preparation is described in Section 4.1. If cloning of a particular endopeptidase gene resulted in more than one positive clone, one of the positive clones was selected for complete sequencing.

4.9.7. Primer walking DNA sequencing

The Nucleic Acid and Protein Facility at the University of Wisconsin Biotechnology Center (Madison, WI) conducted the primer walking for complete sequencing of the genomic inserts. Primer walking was performed using universal (M13 forward and reverse) and custom primers. The DNA sequences were analyzed using Vector NTI Advance™ 9.0 (Invitrogen, Carlsbad, CA). Nucleic acid and protein identities searches were performed using BLAST through the NCBI website.

5. Cloning of the *pepN* structural gene from *Lb. helveticus* WSU19

5.1. Design of degenerate primers

A set of degenerate primers was designed based on the sequence of the *pepN* genes and PepN enzymes from *Lb. helveticus* CNRZ32, *Lb. helveticus* 53/7, *Lb. gasseri*, *Lb. plantarum* WCFS1, and *Lb. delbrueckii* ssp. *lactis* DSM7290. GenBank accession numbers for the *pepN* genes from these bacteria are U08224, Z30323, AJ506050, AL935254, and Z21701, respectively. Figures 7 and 8 illustrate protein alignments of PepN enzymes from these bacteria for the forward and reverse degenerate primers, respectively. Figures 9 and 10 illustrate nucleotide alignments of the coding sequences of the *pepN* genes.

Based on these alignments, the sequences of the forward and reverse degenerate primers were 5'-CGAGCTCACWTTYCAHCCAGAWCAYTAYRATHTN-3' and 5'-GCTCTAGARTCCATCTTRATYTCMCGVBTHAR-3', respectively. The *Sac*I and *Xba*I sites, indicated by the underlined nucleotides, were added to the forward and reverse degenerate primers, respectively. To increase the efficiency of digestion, additional 1-2

nucleotides were added to flank the restriction sites. The size of PCR product was expected to be 2.4 kb.

5.2. PCR amplification of the *pepN* structural gene from *Lb. helveticus* WSU19

Amplification of the *pepN* structural gene utilized genomic DNA from *Lb. helveticus* WSU19 as the template. The DNA was diluted in elution buffer EB to a final concentration of approximately 150 ng/μL. The degenerate primers were dissolved in elution buffer EB to a final concentrations of 100 pmoles/μL. DNA polymerase used in the amplification reaction was Cloned *Pfu* DNA polymerase (2.5 U/μL; Stratagene, La Jolla, CA).

For the PCR reaction, the following reagents were mixed in a PCR tube: 10 μL of 10X Cloned *Pfu* buffer containing $MgCl_2$; 8 μL of 10 mM dNTP mix (Stratagene, La Jolla, CA), 1 μL of forward degenerate primer, 1 μL of reverse degenerate primer, 2 μL of cloned Pfu DNA polymerase, 2 μL of template DNA, and sterile deionized water to make the volume to 100 μL. The PCR reaction was performed using the following thermal cycle: a single cycle of 95^{o}C for 45 s (initial denaturation); 30 cycles of 95^{o}C for 45 s (denaturation), 55^{o}C for 45 s (annealing), 72^{o}C for 5 min (elongation); and a single cycle of 72^{o}C for 10 min (final elongation). The PCR product was purified following the QIAquick® PCR Purification Kit Protocol described in Section 4.5.2.

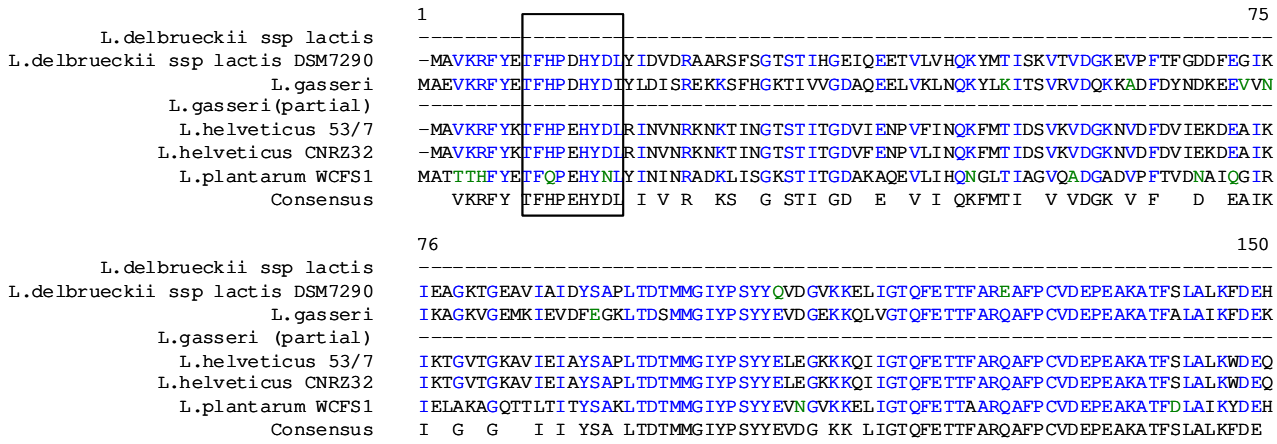

Figure 7. Protein alignment of PepN enzymes for designing the forward degenerate primer.

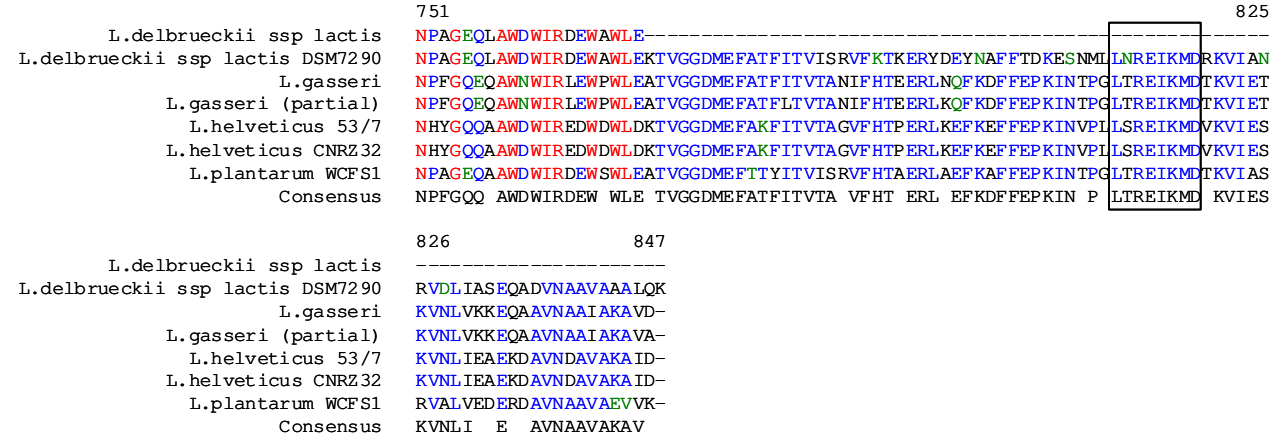

Figure 8. Protein alignment of PepN enzymes for designing the reverse degenerate primer.

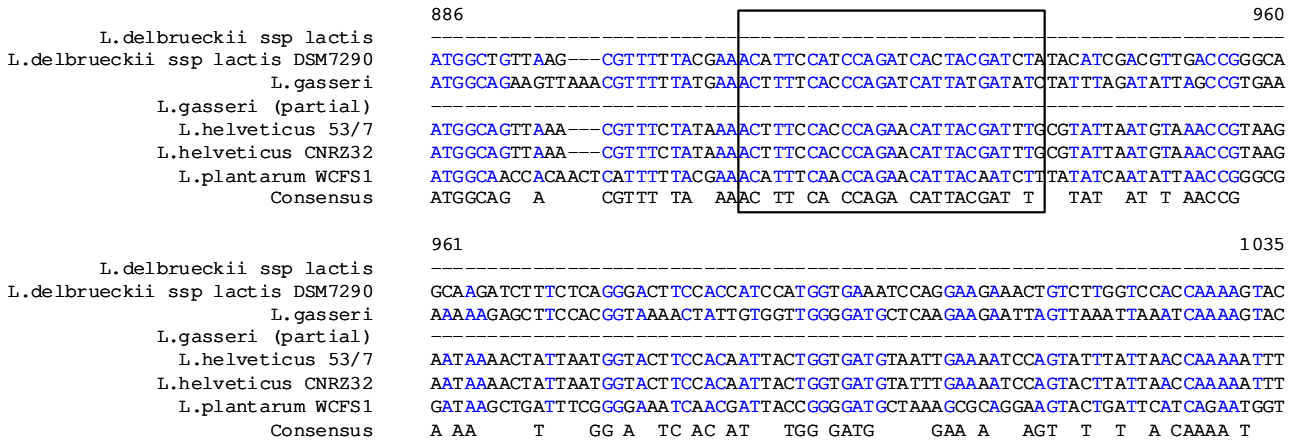

Figure 9. Nucleotide alignment of the *pepN* genes for designing the forward degenerate primer.

Figure 10. Nucleotide alignment of the *pepN* genes for designing the reverse degenerate primer.

5.3. Preparation of insert and vector DNA

The pJDC9 plasmid DNA was the vector used for cloning of the *pepN* structural gene from *Lb. helveticus* WSU19. The plasmid was isolated from *E. coli* DH5α(pJDC9) following the procedure described in Section 4.1.

The PCR product and pJDC9 plasmid DNAs were digested with *Sst*I (isoschizomer of *Sac*I) and *Xba*I (Invitrogen, Carlsbad, CA) at 37°C for 16 and 5 h, respectively. Digestion with both enzymes was conducted simultaneously following the enzyme manufacturer's instructions. The amount of pJDC9 vector DNA used in the digestion was approximately 1.5 μg per 100 μL of digestion mixture. The digested insert and vector DNAs were purified following the QIAquick® PCR Purification Kit Protocol described in Section 4.5.2. Concentrations of the insert and vector DNA were estimated by gel electrophoresis in 0.8% agarose using High DNA Mass Ladder as the standard.

5.4. Ligation of insert into pJDC9 vector DNA

Two ligation mixtures were prepared to provide molar ratios of vector to insert of approximately 1:3 and 1:7. The mass ratio of vector (~6.95 kb) to insert (~2.4 kb) is approximately 3:1. The ligation mixture (1:3 molar ratio) consisted of 1 μL of vector DNA (12 ng/μL); 5 μL of insert DNA (3 ng/μL); 5 μL of 1 U/μL T4 DNA ligase; 8 μL of 5X T4 DNA ligase buffer; and sterile deionized water to make the volume to 40 μL. To obtain a vector to insert molar ratio of 1:7, the amount of insert DNA was increased to 10 μL. Ligations were performed at 16°C for 2 h. The ligation mixtures were purified using the QIAquick® PCR Purification Kit Protocol described in Section 4.5.2. Elution was performed

in 40 μL of elution buffer EB.

5.5. Electroporation of the ligated DNA into electrocompetent *E. coli* DH5α cells

Electroporation of the ligated DNA into *E. coli* DH5α cells followed the procedure described in Section 4.7. The electroporated cells were plated on LB agar plates containing X-Gal/IPTG, described in Section 1. A total of 4 plates were prepared per ligated DNA sample.

5.6. Screening for PepN-positive clone(s)

White colonies on the LB agar plate containing X-Gal/IPTG were screened for PepN-positive clone(s). Six colonies were randomly selected from each ligation and used for small-scale plasmid DNA preparation described in Section 4.9.1. The plasmid DNA was digested simultaneously with *Sst*I and *Xba*I (Invitrogen, Carlsbad, CA) at 37^{o}C for 5 h. Preparation of digestion mixture is described in Section 4.9.2. PCR product digested with the same restriction enzymes served as the positive control. The digested DNA was electrophoresed in 0.8% agarose. Plasmid DNA(s) carrying insert of the same size as the PCR product were subjected to 5' and 3' end DNA sequencing for further confirmation. Medium-scale plasmid preparation for the sequencing template is described in Section 4.9.4. The 5' and 3' end DNA sequencing and sequence analysis are described in Section 4.9.5.

6. Cloning of the complete *pepN* gene from *Lb. helveticus* WSU19

6.1. Probe synthesis

A set of primers (Table 7) was designed using the sequence of insert DNA obtained from the 5' and 3' DNA sequencing and the sequences of formerly-designed degenerate primers. The *Sac*I and *Xba*I restriction sites were removed from these primers. Plasmid pJDC9 carrying the *pepN* structural gene, designated as pES3 (Table 8), was used as the template for probe synthesis, described in Section 4.2.

Table 7. Forward and reverse primers for synthesis of the *pepN* gene probe

Primers	Sequence
19PepN forward	5'-ACATTTCACCCAGATCATTACGATTTG-3'
19PepN reverse	5'-ATCCATCTTGATTTCCCGACTAAG-3'

6.2. Restriction enzyme analysis of pES3

Plasmid pES3 from large-scale preparation was subjected to restriction enzyme analysis to determine the enzyme(s) that had only one restriction site on the plasmid. The large-scale plasmid preparation is described in Section 4.1. Restriction enzymes used in this analysis were those found in the multiple cloning site (MCS) of pJDC9 vector DNA, i.e., *Bam*HI, *Eco*RI, *Hind*III, *Kpn*I, *Pst*I, *Sal*I, *Sma*I, *Sph*I, *Sst*I (isoschizomer of *Sac*I), and *Xba*I (Invitrogen, Carlsbad, CA).

The digestion mixture was prepared in a total volume of 20 μL by mixing 5 μL of plasmid DNA with 2 μL of 10X buffer, 2 μL of restriction enzyme, and sterile deionized water to make to the volume. Digestion was performed at 37^{o}C for 5 h, except for *Sma*I at 30^{o}C, followed by gel electrophoresis in 0.8% agarose.

6.3. Southern hybridization

Based on the results of restriction enzyme analyses, the following enzymes were determined to cleave the plasmid pES3 at a single site, i.e., *Bam*HI, *Kpn*I, *Sal*I, *Sph*I, *Sst*I, and *Xba*I. These enzymes were used in combination (a total of 15 combinations) to digest the genomic DNA from *Lb. helveticus* WSU19, followed by Southern hybridization as described in Section 4.3. Prehybridization and hybridization steps were performed under high stringency conditions at 68^{o}C in the absence of 50% formamide. The Southern hybridization result determined *Sac*I and *Sph*I to be used as the cloning enzymes for the *pepN* gene from *Lb. helveticus* WSU19.

6.4. Cloning of the *pepN* gene

The steps in cloning of the *pepN* gene, from preparation of insert and vector DNA to confirmation of the *pepN* clone(s) from *Lb. helveticus* WSU19 followed the same procedures described previously for the endopeptidase genes. The *E. coli* DH5α(pJDC9) and *E. coli* DH5α(pES3) were used as negative and positive controls, respectively, in colony hybridization. The chloroform / CFE assay for confirmation of PepN activity utilized L-lysine-paranitroanilide.HCl (Sigma-Aldrich, Co., St. Louis, MO) as the substrate at a concentration of 25 mM in methanol.

7. Preparation of CFEs from *E. coli* DH5α derivatives expressing selected peptidase genes from *Lb. helveticus* WSU19

Frozen stocks of *E. coli* DH5α clones (50 μL) were inoculated into 5 mL of LB broth containing 1 mg/mL of Em and incubated at 37^{o}C for 16 h with vigorous shaking. The

cultures (100 μL) were transferred into 10 mL of LB broth containing 1 mg/mL of Em and incubated at 37°C for 16 h with vigorous shaking. The cultures were transferred into 150 mL of LB broth at 0.005-1% inoculation level depending on desired harvest time. The cultures were incubated at 37°C with vigorous shaking until A_{600} of 4.0, and transferred into 250 mL centrifuge bottles. The cells were harvested by centrifuging for 15 min (6,000 x *g* at 4°C) using an Avanti™ J-25 centrifuge (Beckman Coulter, Fullerton, CA).

After decanting the supernatants, the cells were washed with 75 mL of 50 mM Pipes buffer (pH 7.0; ice-cold; Sigma-Aldrich, Co., St. Louis, MO) and centrifuged for 15 min (7,500 x *g* at 4°C) using an Avanti™ J-25 centrifuge (Beckman Coulter, Fullerton, CA). The supernatants were discarded. The cells were washed again with 75 mL of 50 mM Pipes buffer (pH 7.0; ice-cold) and centrifuged for 15 min (7,500 x *g* at 4°C). The supernatants were discarded and the cells were re-suspended in 7.5 mL of 50 mM Pipes buffer (pH 7.0; ice-cold).

The cell suspensions were transferred to 50 mL centrifuge tube. Glass beads (106 microns; 7.5 g) (Sigma-Aldrich, Co., St. Louis, MO) were added to the suspensions. The mixtures were incubated on ice for 15 min, and homogenized for 5 min using the Red Devil Paint Mixer (Red Devil Equipment Co., Plymouth, MN). The mixtures were incubated on ice for another 15 min followed by homogenization for 5 min using the Red Devil Paint Mixer. The mixtures were centrifuged for 30 min (20,000 x *g* at 4°C) using an Avanti™ J-25 centrifuge (Beckman Coulter, Fullerton, CA). The supernatants were removed carefully and stored at –80°C until used.

Protein contents of CFEs were estimated by the Bradford method (1976). Coomassie Brilliant Blue G-250 (Bio-Rad Laboratories, Hercules, CA) was diluted with deionized water

(1:4) and filtered through Whatman #1 filter paper. CFEs (50 μL) were mixed with 5 ml of the diluted dye reagent and incubated for 20 min at room temperature. The amounts of protein present in CFEs were derived from the absorbance at 595 nm. A standard curve was prepared using bovine serum albumin (BSA; Sigma-Aldrich, Co., St. Louis, MO) at concentrations of 0.2, 0.4, 0.6, and 0.8 mg/mL.

8. Degradation of β-CN f193-209 and α_{s1}-CN f1-23 by CFE(s)

The β-CN f193-209 and α_{s1}-CN f1-23 peptides, synthesized by the Laboratory for Biotechnology and Bioanalysis I (LLB 1) at Washington State University (Pullman, WA), were dissolved to final concentrations of 4 mg/mL in 50 mM citrate buffer (pH 5.2) containing 4% (w/v) sodium chloride (JT Baker Chemical Co., Phillipsburg, NJ). Reaction mixtures were prepared by mixing 400 μL of each casein fragment solution with CFEs, added as an individual CFE or a combination of two CFEs. Each CFE contained 1-1.5 mg/mL of protein and was added to obtain a total protein of approximately 50 μg. The mixtures were incubated at 37°C. Aliquots were withdrawn from the incubation mixtures at 0, 2, 4, 8, 12, 24, 48, and 72 h, followed by heat treatment at 70°C for 20 min to terminate the reaction. The aliquots were immediately cooled in an ice-bath and stored at –80°C. Degradation patterns of the CFEs on the casein fragments were determined using matrix-assisted laser desorption/ionization time-of-flight mass spectrometry (MALDI-TOF MS).

9. MALDI-TOF mass spectrometry analyses

Aliquots from the CFE-casein digest by CFE were desalted using ZipTip C18 (Millipore, Bedford, MA) according to manufacturer's instructions. The ZipTip C18 minicolumns were washed twice with 10 μL of 50% acetonitrile in Milli-Q grade water, and then equilibrated twice with 10 μL of 0.1% TFA in Milli-Q grade water. Samples were bound to the tips by aspirating and dispensing 10 μL of aliquots in 3 to 5 cycles. The bound samples were desalted 6 to 10 cycles with 10 μL of 0.1% TFA in Milli-Q grade water. The analytes were eluted with 10 μL of matrix solution. One μL of the eluates were deposited on MALDI spot and air-dried prior to loading into TOF. Matrix for MALDI analysis was α-cyano-4-hydroxycinnamic acid (CHCA; Sigma-Aldrich Co., St. Louis, MO). The matrix solution was prepared by mixing approximately 20 mg of CHCA in 750 μL of solvent (60% acetonitrile in Milli-Q grade water containing 0.1% of trifluoroacetic acid; TFA).

MALDI analyses were performed using a PerSeptive Biosystems (Framingham, MA) DE-RP time-of-flight mass spectrometer. Samples were ionized by a 337-nm nitrogen laser pulse and accelerated under 25,000 V before entering the TOF mass analyzer. The instrument was set in the positive reflector mode with delayed extraction. The mass to charge ratio (m/z) was acquired between 500 and 4,000 Da. Each spectrum generated in the analysis was the result of 32 laser shots. A total of 8 spectra (a sum of 256 laser pulses) were collected for each sample.

CHAPTER IV:

Results and Discussion

Species designation for *Lb. helveticus* WSU19 was confirmed using a 16S rRNA analysis (MIDI Labs, Newark, DE). Figure 11 illustrates the phylogenetic tree of *Lb. helveticus* WSU19 based on the 16S rRNA gene sequence and alignment. The 0.09% difference between the 16S rRNA gene sequence of the strain WSU19 and its closest relative, *Lb. helveticus*, suggests that the strain WSU19 is a *Lb. helveticus*.

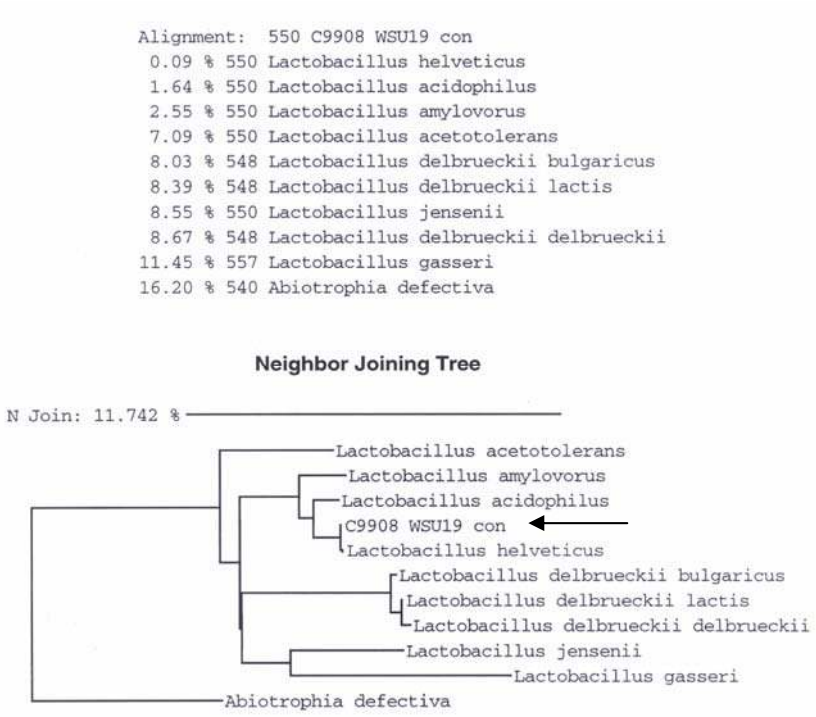

Figure 11. Phylogenetic tree of *Lb. helveticus* WSU19 based on the 16S rRNA gene sequence and alignment. The horizontal arrow indicates the strain WSU19.

1. Cloning strategies

The goal of cloning the selected peptidase genes from *Lb. helveticus* WSU19 was to obtain an insert DNA containing the complete peptidase gene of interest so that the gene expresses peptidase activity. A complete gene consists of the coding sequence of the gene of interest as well as the gene expression signals, including promoter, terminator, and ribosomal binding site (RBS). Cloning of the peptidase genes used a one-step or a two-step approach. The two-step strategy was applied when the one-step approach failed to obtain peptidase-positive clone(s).

1.1. One-step cloning

A genomic DNA fragment containing the peptidase gene of interest from *Lb. helveticus* WSU19 was cloned into the pJDC9 vector DNA. The insert DNA was ligated to the pJDC9 plasmid at the MCS of the vector DNA. Figure 12 illustrates the map of plasmid pJDC9. There are 10 restriction enzymes in the MCS of plasmid pJDC9 to facilitate ligation of an insert DNA: *Sst*I (isoschizomer of SacI), *Kpn*I, *Sma*I, *Bam*HI, *Xba*I, *Sal*I, *Pst*I, *Sph*I, *Hind*III, and *Eco*RI (Figure 12).

Southern hybridization was used to determine the cloning enzyme(s) and the size of the DNA fragment containing the target gene. In one-step cloning, coding sequence of the corresponding peptidase gene from *Lb. helveticus* CNRZ32 was used as the probe for Southern hybridization to identify the complete target gene from *Lb. helveticus* WSU19. The selected cloning enzyme(s) were: (i) the restriction enzyme(s) in the MCS of plasmid pJDC9, (ii) able to produce a single hybridization-positive fragment in the Southern hybridization,

and (iii) able to generate a hybridization-positive fragment of 1.5X to 2X the size of the corresponding gene from *Lb. helveticus* CNRZ32.

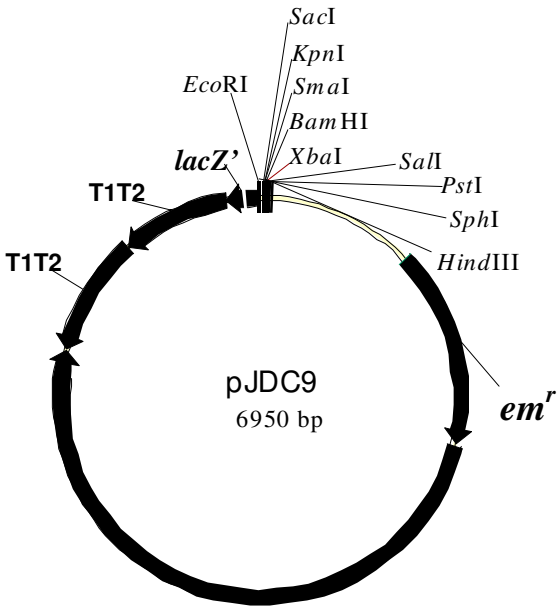

Figure 12. Map of plasmid pJDC9

1.2. <u>Two-step cloning</u>

In two-step cloning, the structural gene of interest from *Lb. helveticus* WSU19 was initially cloned into the pJDC9 vector DNA. A structural gene contains only the coding sequence of the target gene. The structural gene of the target peptidase from *Lb. helveticus* WSU19 was amplified using degenerate primers. Genomic DNA from *Lb. helveticus* WSU19 was the template in the amplification. The degenerate primers were designed based on the published amino acid sequences of the target peptidase from *Lactobacillus* species and the corresponding nucleic acid sequences.

To facilitate ligation of the blunt end PCR product to the vector DNA, recognition site(s) of the cloning enzyme(s) were added to the 5' end of the degenerate primers.

Digestion of the PCR product with the selected cloning enzyme(s) produced protruding ends, known as cohesive or sticky ends, at the 5' and 3' ends of the DNA. In addition to generating sticky ends, the selected cloning enzyme(s): (i) should be the restriction enzyme(s) in the MCS of pJDC9 plasmid and (ii) should not have recognition site(s) inside the coding sequences used for designing the degenerate primers.

The second cloning to obtain the complete peptidase gene used the same approach as the one-step cloning. Southern hybridization was performed to determine the cloning enzyme(s) and the size of DNA fragment containing the peptidase gene of interest. The sequence of the structural gene of interest from *Lb. helveticus* WSU19 was used as the probe for Southern hybridization.

1.3. <u>Screening and confirmation of the peptidase-positive clone(s)</u>

Peptidase-positive clones from one-step and two-step cloning were screened by antibiotic resistance, blue/white screening, and colony hybridization. The plasmid pJDC9 carries a gene encoding for erythromycin resistance (*em*^{r}; Figure 12). Antibiotic-resistant transformants, i.e., *E. coli* DH5α carrying the pJDC9 vector DNA with or without an insert, are able to grow in the medium containing Em. Blue/white screening was performed to identify the recombinant plasmid(s), i.e., the vector DNA with an insert. Colony hybridization, using the same probe as Southern hybridization, was conducted to determine recombinant plasmid(s) carrying the gene of interest.

Blue/white screening involves an insertional inactivation of β-galactosidase gene (*lacZ*). The plasmid pJDC9 carries a gene encoding for the N-terminal α-peptide of β-galactosidase (*lacZ'*; Figure 12), which is a shortened derivative of the *lacZ* gene. The host *E.*

coli DH5α, on the other hand, carries a gene that expresses only the C-terminal of β-galactosidase (*lacZΔM15*). IPTG is an inducer for expression of the latter gene in the presence of *lac* repressor. Although the two parts of β-galactosidase are not active enzymatically, they can associate to form an active β-galactosidase (α-complementation), which utilizes X-gal to produce a blue product. In a recombinant plasmid, the presence of insert DNA in the MCS interrupts expression of the α-peptide and consequently the development of blue color. Thus, the white colonies do not express β-galactosidase and are likely to contain the inserted DNA fragments, while the blue colonies are likely to contain the religated vectors or the supercoiled DNA that did not get digested (Sambrook et al., 1989).

Confirmation of the peptidase-positive clone(s) was conducted by restriction enzyme analyses followed by 5' and 3' end DNA sequencing of insert DNA and nucleic acid BLAST analysis of the DNA sequence. Primer walking determined the nucleic acid sequence of the insert genomic DNA from the peptidase-positive clone(s).

2. Cloning of the *pepE*, *pepO*, *pepO2*, *pepO3*, and *pepN* genes

Figures 13-17 exhibit high stringency Southern hybridization analyses for the *pepE*, *pepO*, *pepO2*, and *pepO3* genes using single and double restriction enzyme digest(s). Based on the Southern hybridization results, the cloning enzyme(s) for the *pepE*, *pepO*, *pepO2*, and *pepO3* genes were *Pst*I, *Hind*III-*Sal*I, *Sph*I-*Xba*I, and *Kpn*I, respectively.

Cloning of the putative *pepE*, *pepO*, *pepO2*, and *pepO3* genes resulted in 2, 14, 1, and 26 hybridization-positive colonies, respectively. Restriction enzyme analyses of the plasmids from all hybridization-positive colonies in the *pepE* and *pepO2* cloning and from 20 hybridization-positive colonies in the *pepO3* cloning revealed the expected restriction

patterns (data not shown). CFEs from both hybridization-positive colonies in the *pepE* cloning exhibited yellow color upon incubation with N-Benzoyl-Phenylalanine-Valine-Arginine-p-Nitroanilide substrate. The yellow color indicated expression of PepE activity in both colonies.

Figure 18 shows the result of high stringency Southern hybridization using plasmids extracted from the hybridization-positive colonies in *pepO* cloning and digested with *Eco*RI. Plasmids extracted from 7 hybridization-positive colonies in the *pepO* cloning hybridized to the *pepO* probe in Southern hybridization. Restriction enzyme analysis of the 7 Southern hybridization-positive plasmids using *Hind*III revealed the expected restriction patterns (data not shown). However, the 7 plasmids were not digested by *Sal*I, suggesting the ligated *Sal*I site could not be recut. *Sal*I was one of the cloning enzymes used in the *pepO* cloning.

E. coli DH5α clones confirmed by 5' and 3' end DNA sequencing, as well as primer walking, to carry the *pepE*, *pepO*, *pepO2*, and *pepO3* genes from *Lb. helveticus* WSU19 were #12-31, #4-6, #15-17, and #1-4, respectively. The pJDC9 derivatives containing the *pepE*, *pepO*, *pepO2*, and *pepO3* genes from *Lb. helveticus* WSU19 were designated pES1, pES5, pES2, and pES6, respectively (Table 8).

Three clones carrying the *pepN* structural gene from *Lb. helveticus* WSU19 were obtained and designated as #3-5, #7-2, and #7-5, respectively. Figures 19-21 show the nucleic acid sequences of these clones confirmed by 5' and 3' end DNA sequencing. Nucleic acid BLAST analyses revealed 98% identities with the nucleotide regions 161-975 and 1791-2587 of the *pepN* gene from *Lb. helveticus* 53/7. Additionally, the *pepN* structural gene from *Lb. helveticus* WSU19 was determined to share 98% identitities with the nucleotide regions 905-1719 and 2535-3331 of the *pepN* gene from *Lb. helveticus* CNRZ32. The pJDC9

derivatives containing the *pepN* structural gene from *Lb. helveticus* WSU19 were designated pES3 (Table 8). The plasmid pES3 from colony #7-5 was the template for synthesizing the probe for Southern and colony hybridizations.

Figure 22 demonstrates the results of restriction enzyme analysis of the plasmid pES3. The restriction enzymes used in this analysis are present in the MCS of the plasmid pJDC9 (Figure 12). Based on this analysis, *Bam*HI, *Kpn*I, *Sal*I, *Sph*I, *Sst*I (isoschizomer of *Sac*I), and *Xba*I cleaved the plasmid pES3 at a single site. Figure 23 displays the results of high stringency Southern hybridization analysis for the *pepN* gene from *Lb. helveticus* WSU19 using a combination of these enzymes. Based on the Southern hybridization result, cloning enzymes for the *pepN* gene were *Sac*I (isoschizomer of *Sst*I) and *Sph*I.

Cloning of the putative *pepN* gene resulted in 7 hybridization-positive colonies. Restriction enzyme analysis of the plasmids from all hybridization-positive colonies revealed the expected restriction patterns (data not shown). CFEs from all hybridization-positive colonies in the *pepN* cloning exhibited yellow color upon incubation with L-Lysine-p-Nitroanilide substrate. The production of yellow color indicated expression of PepN enzyme activity. *E. coli* DH5α clone #3-38 was confirmed by 5' and 3' end DNA sequencing as well as primer walking to carry the *pepN* gene from *Lb. helveticus* WSU19. The derivative of the plasmid pJDC9 containing the complete *pepN* gene from *Lb. helveticus* WSU19 was designated as pES4 (Table 8).

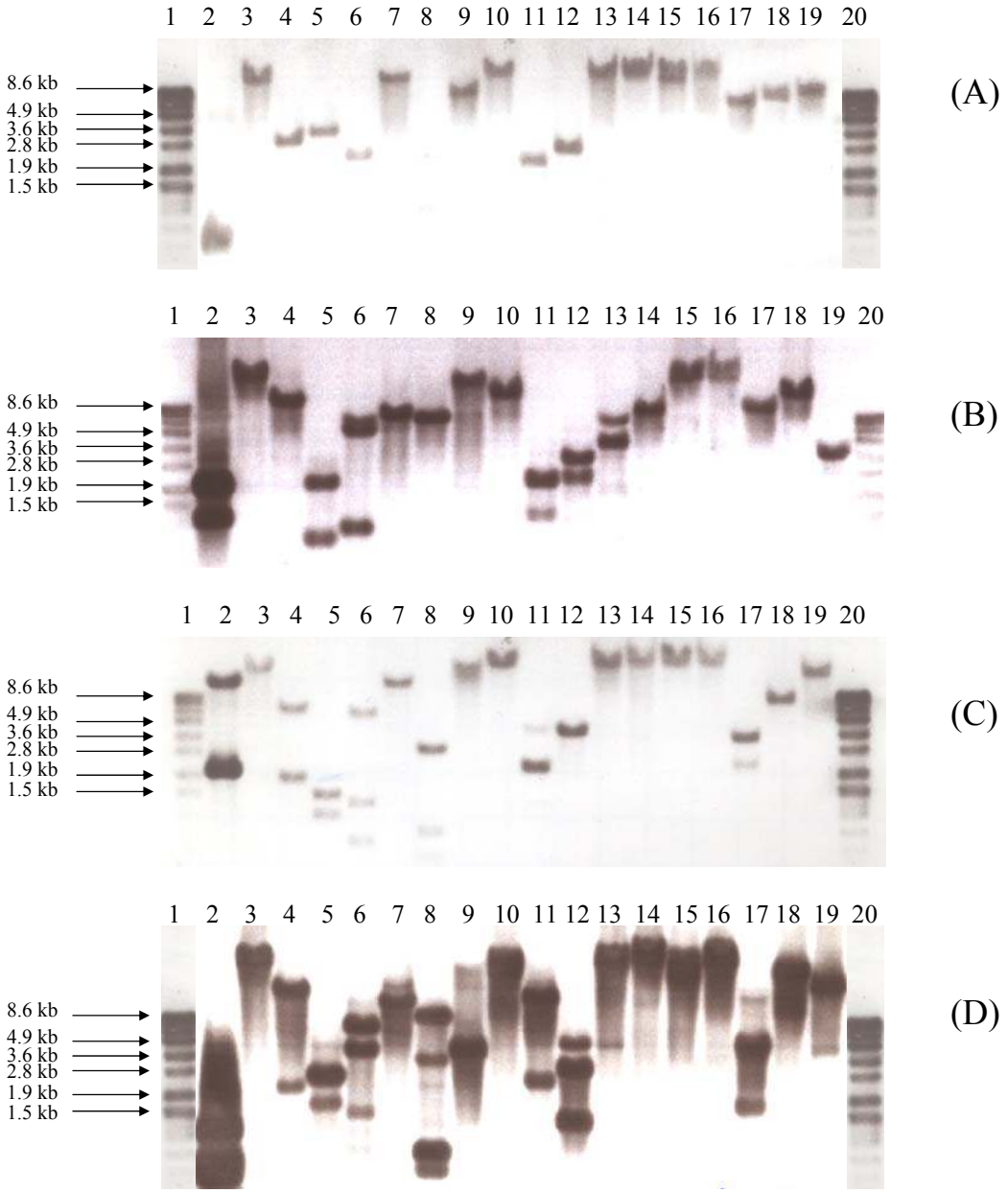

Figure 13. High stringency Southern hybridization of genomic DNA from *Lb. helveticus* WSU19 using DIG-labeled probes synthesized based on DNA sequence information available for *Lb. helveticus* CNRZ32: (A) *pepE*, (B) *pepO*, (C) *pepO2*, (D) *pepO3*. Lane 1. DIG-labeled DNA MW Marker VII; lane 2A. pTRKL2::*pepE* (CNRZ32) digested with *Eco*RI; lane 2B. pTRKL2::*pepO* (CNRZ32) digested with *Pst*I; lane 2C. pJDC9::*pepO2* (CNRZ32) digested with *Xba*I and *Pst*I; lane 2D. *pepO3* (CNRZ32) PCR product digested with *Hind*III; lanes 3-19. genomic DNA from *Lb. helveticus* WSU19 digested with: *Bam*HI (lane 3); *Cla*I (lane 4); *Dra*I (lane 5); *Eco*RI (lane 6); *Eco*RV (lane 7); *Hind*III (lane 8); *Kpn*I (lane 9); *Nru*I (lane 10); *Pst*I (lane 11); *Pvu*II (lane 12); *Sac*I (lane 13); *Sac*II (lane 14); *Sal*I (lane 15); *Sma*I (lane 16); *Spe*I (lane 17); *Sph*I (lane 18); *Xba*I (lane 19); lane 20. DIG-labeled DNA MW VII.

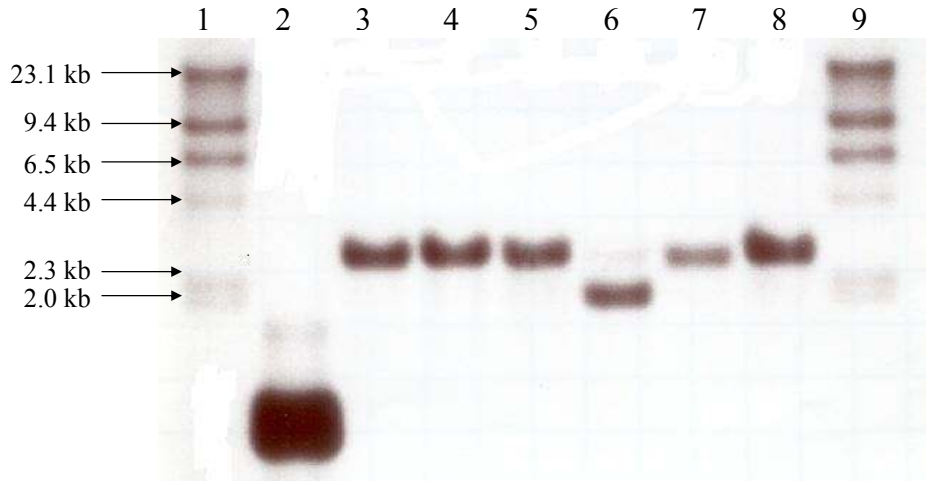

Figure 14. High stringency Southern hybridization of genomic DNA from *Lb. helveticus* WSU19 using a DIG-labeled probe synthesized based on the *Lb. helveticus* CNRZ32 *pepE* gene. Lane 1. DIG-labeled DNA MW Marker II; lane 2. pTRKL2::*pepE* (CNRZ32) digested with *Eco*RI; lanes 3-8. genomic DNA from *Lb. helveticus* WSU19 digested with: *Pst*I (lane 3); *Pst*I and *Xba*I (lane 4); *Pst*I and *Kpn*I (lane 5); *Pst*I and *Bam*HI (lane 6); *Pst*I and *Sph*I (lane 7); *Pst*I (lane 8); lane 9. DIG-labeled DNA MW Marker II.

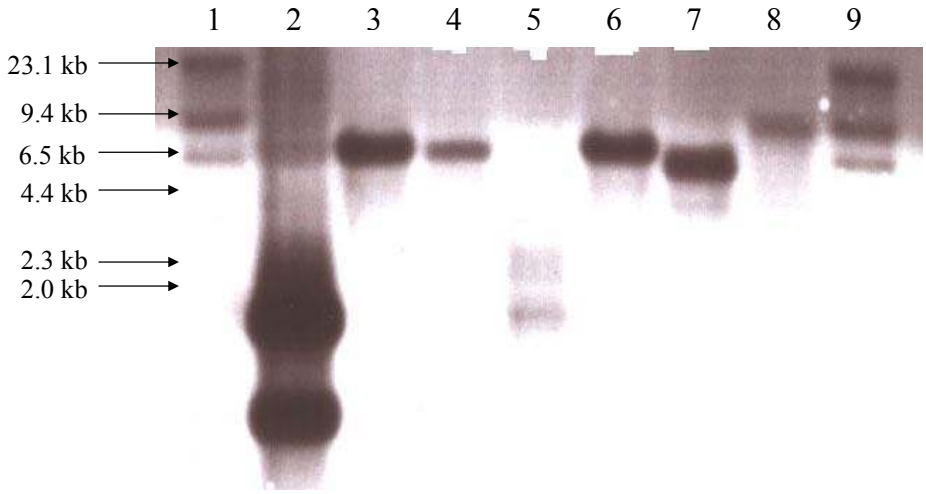

Figure 15. High stringency Southern hybridization of genomic DNA from *Lb. helveticus* WSU19 using a DIG-labeled probe synthesized based on the *Lb. helveticus* CNRZ32 *pepO* gene. Lane 1. DIG-labeled DNA MW Marker II; lane 2. pTRKL2::*pepO* (CNRZ32) digested with *Pst*I; lanes 3-8. genomic DNA from *Lb. helveticus* WSU19 digested with: *Hind*III (lane 3); *Hind*III and *Sph*I (lane 4); *Hind*III and *Bam*HI (lane 5); *Hind*III and *Sal*I (lane 6); *Hind*III and *Kpn*I (lane 7); *Kpn*I and *Sph*I (lane 8); lane 9. DIG-labeled DNA MW Marker II.

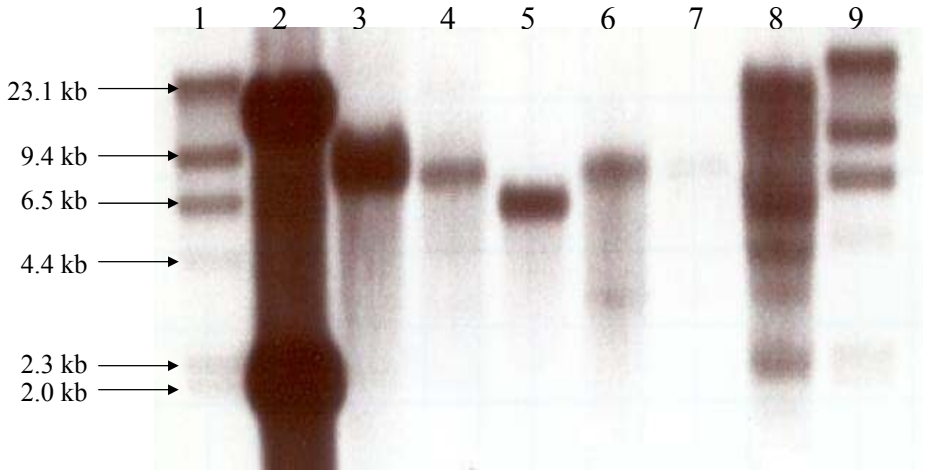

Figure 16. High stringency Southern hybridization of genomic DNA from *Lb. helveticus* WSU19 using a DIG-labeled probe synthesized based on the *Lb. helveticus* CNRZ32 *pepO2* gene. Lane 1. DIG-labeled DNA MW Marker II; lane 2. pJDC9::*pepO2* (CNRZ32) digested with *Pst*I and *Xba*I; lanes 3-8. genomic DNA from *Lb. helveticus* WSU19 digested with: *Sph*I (lane 3); *Sph*I and *Bam*HI (lane 4); *Sph*I and *Xba*I (lane 5); *Sph*I and *Kpn*I (lane 6); *Sph*I and *Sal*I (lane 7); *Bam*HI and *Kpn*I (lane 8); lane 9. DIG-labeled DNA MW Marker II.

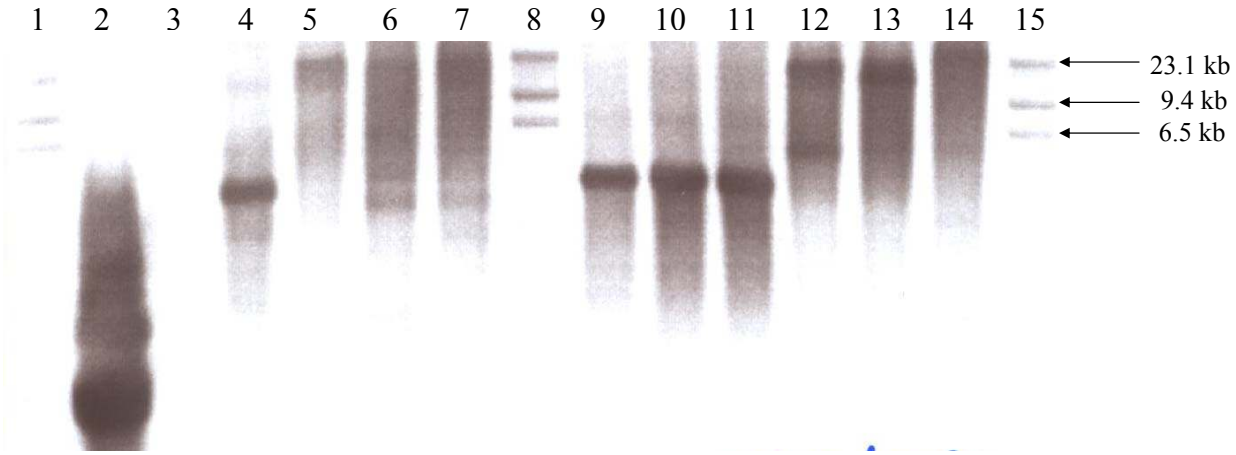

Figure 17. High stringency Southern hybridization of genomic DNA from *Lb. helveticus* WSU19 using a DIG-labeled probe synthesized based on the *Lb. helveticus* CNRZ32 *pepO3* gene. Lane 1. DIG-labeled DNA MW Marker II; lane 2. the *pepO3* (CNRZ32) PCR product digested with *Hind*III; lane 3. pJDC9 digested with *Hind*III; lanes 4-7. genomic DNA from *Lb. helveticus* WSU19 digested with: *Bam*HI and *Kpn*I (lane 4); *Bam*HI and *Sal*I (lane 5); *Bam*HI and *Sst*I (lane 6); *Bam*HI and *Sma*I (lane 7); lane 8. DIG-labeled DNA MW Marker II; lanes 9-14. genomic DNA from *Lb. helveticus* WSU19 digested with: *Kpn*I and *Sal*I (lane 9); *Kpn*I and *Sst*I (lane 10); *Kpn*I and *Sma*I (lane 11); *Sal*I and *Sma*I (lane 12); *Sal*I and *Sst*I (lane 13); *Sst*I and I (lane 14); lane 15. DIG-labeled DNA MW Marker II.

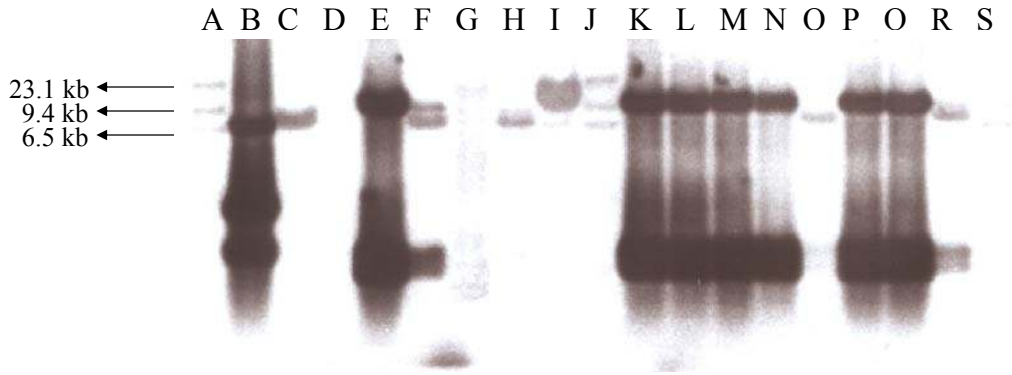

Figure 18. High stringency Southern hybridization of plasmid DNA samples from the hybridization-positive colonies in the cloning of the *pepO* gene from *Lb. helveticus* WSU19 using a DIG-labeled probe synthesized based on the *Lb. helveticus* CNRZ32 *pepO* gene. Lane A. DIG-labeled DNA MW Marker II; lane B. pTRKL2::*pepO* (CNRZ32) digested with *Pst*I; lane C. pJDC9 digested with *Hind*III; lanes D-I. plasmid DNA samples digested with *Eco*RI: #3-8 (lane D); #4-6 (lane E); #4-20 (lane F); #6-12 (lane G); #7-8 (laneH); #8-15 (lane I); lane J. DIG-labeled DNA MW Marker II; lane K-R. plasmid pJDC9 derivatives digested with *Eco*RI: #9-2 (lane K); #10-44 (lane L); #13-33 (lane M); #17-50 (lane N); #19-28 (lane O); #19-30 (lane P); #19-36 (lane Q); #21-20 (lane R); lane S. DIG-labeled DNA MW Marker II.

(a) File name: 02ellyFN3-5_03[1].ab1 Colony #3-5

GTGTAACGCCGGCCAGNGGAATTCGANTCCTTTTTCNAGNANAACACTACGATTTGNTCTCTAATGTAAACCGT
AAGAATAAAACTATTAATGGTACTTCCACAATTACTGGTGATGTAATTGAAAATCCAGTATTTATTAACCAAAA
ATTTATGACCATTGATAGCGTTAAGGTTGATGGTAAAAATGTTGATTTTGATGTAATCGAAAAAGATGAAGCAA
TCAAAATTAAAACAGGAGTAACTGGCAAAGCTGTAATCGAAATTGCTTATAGCGCACCACTTACTGATACTATG
ATGGGTATTTATCCTTCATATTACGAATTAGAAGGTAAGAAGAAGCAAATCATCGGTACGCAATTCGAAACTAC
TTTTGCTCGCCAAGCATTCCCATGTGTGGACGAACCTGAAGCTAAAGCTACATTCTCACTTGCTCTTAAGTGGG
ATGAACAAGATGGTGAAGTTGCACTTGCTAACATGCCAGAAGTAGAAGTTGACAAGGATGGCTACCACCACTTT
GAAGAAACTGTCCGCATGTCTAGTTACTTAGTTGCCTTTGCCTTTGGTGAATTACAATCTAAGACTACTCATAC
TAAGGATGGCGTATTAATTGGCGTTTACGCAACTAAGGCACACAAGCCTAAGGAATTAGACTTCGCTTTGGACA
TTGCTAAGCGCGCAATTGAATTTTACGAAGAATTCTACCAAACCAAATACCCACTTCCACAGNCATGGCAACTN
GCATTGGCAGACTTCTCAGCTGGGGGCATGGAAAACTGGGGGCTTGGAACTTACNGGGNAGCANANTGGCTCCT
GNCCCANAAANACTAGCTGGGAANGAAAANNTNGGTGCCCAGNTATACCNTGAATGGCNCNCAAGGGTCGGGNA
NTGGAACAGGAGGGGGGACACTTA

(b) File name: 05ellyRN3-5_09[1].ab1 Colony #3-5

GCCAGCTTGCATGCCTGCAGGTCGACTCNAGAATCCATCATTGAATCTCCCGACTAAGAAGTGGAACATTAATC
TTTGGTTCAAAGAATTCCTTGAATTCCTTAAGTCTTTCTGGGGTATGGAAGACGCCTGCAGTAACAGTGATAAA
TTTAGCAAATTCCATGTCACCACCAATAGTCTTGTCAAGCCAATCCCAGTCTTCTCTGATCCAGTCCCAAGCTG
CTTGTTGACCATAATGGTTAGCAAGTAAACCACGGTACCAATCACATAAATCTTGTGGCTTAACTACGTCAGCA
TTTTCAAAGTCGCCAACAATAGCCTTGATAGCTGCAAGATCCTTGGTGCTGGTTACAGCGCTGCGTAAGTCAAC
CTTGTATGATGGGTCAGCTGTTCTTTGGTATTCCTTAATTAACTTATCAACTAATTCAGCATTGCCAAAGTTCT
TAACTTCATTGATTAAAACGTATGGACGAATATCTGCATTCAATGCTTCCAAGTTATCTTCATTTTCAGTAAAG
ATTTGGTGAGCTGCCTTAATTGAGTCCGCATTTTCAGCGTAAAGACTTGCGCTCAACTCGTATGGACGAATTTG
AACATCTTCATCGCTTTCGCCTGGCTTTACTTCCCAGCCTAAACGTGCAACTTGATCCTTTGATAAGAGATCAT
AAAGCTTCTTCAAGTTCTTTTCTTCATTTGATTCTGGGTCAACGAATTGACGAAGCTTAGCTGCAGTAGTGTAA
AGTGCGTTAATTACCAAGCTGGACTTAGAATCAGCGAATTTAACCAAAGNGGAACANTGAAGCGTAAGAAATTG
CTNCCTTCTGCTANANACGTAGGTCTGGAGCANTGNACTTATCANTGGANCANTCTTTACACTGAAAAATTCTC
AGCAAGTCTGNCTATCACGAGAAGGGNGT

Figure 19. Nucleic acid sequences of plasmid pES3 carrying the *pepN* structural gene from *Lb. helveticus* WSU19. The pES3 plasmid was extracted from *E. coli* DH5α(pES3) colony #3-5. The sequences were obtained from 5' and 3' end DNA sequencing using: (a) M13 forward primer and (b) M13 reverse primer.

(a) File name: 03ellyFN7-2_05[1].ab1 Colony #7-2

GTNGTAACGACGGCCAGTGAATTCGAGCTCACTTTTCAACCAGATCATTATGATTTGCGTATTAATGTAAACCG
TAAGAATAAAACTATTAATGGTACTTCCACAATTACTGGTGATGTAATTGAAAATCCAGTACTTATTAACCAAA
AATTTATGACCATTGATAGCGTTAAGGTTGATGGTAAAAATGTTGATTTTGATGTAATCGAAAAAGATGAAGCA
ATCAAAATTAAAACAGGAGTAACTGGCAAAGCTGTAATCGAAATTGCTTATAGCGCACCACTTACTGATACTAT
GATGGGTATTTATCCTTCATATTACGAATTAGAAGGTAAGAAGAAGCAAATCATCGGTACGCAATTCGAAACTA
CTTTTGCTCGCCAAGCATTCCCATGTGTGGACGAACCTGAAGCTAAAGCTACATTCTCACTTGCTCTTAAGTGG
GATGAACAAGATGGTGAAGTTGCACTTGCTAATATGCCAGAAGTAGAAGTTGACAAGGATGGCTACCACCACTT
TGAAGAAACTGTCCGCATGTCTAGTTACTTAGTTGCCTTTGCCTTTGGTGAATTACAATCTAAGACTACTCATA
CTAAGGATGGCGTATTAATTGGCGTTTACGCAACTAAGGCACACAAGCCTAAGGAATTAGACTTCGCTTTGGAC
ATTGCTAAGCGCGCAATTGAATTTTACGAAGAATTCTACCAAACCAAATACCCCCTTCCACAGTCATTGCAACT
GGCATGCCAGACTTCTCAGCTGGTGCCNTGGAAAACTGGGGTCTTGTACTTACNGNGNAGCATACTTGCTCCTG
ACCCAACAATACTAGCTGGGAATGAAAAGTNGNTGCCCNGTTNTNCCCTGAATGGCTCCCCANGGTCGGGACTG
GGAACCTGANGGGGGGCACTTTGNNTACGAN

(b) File name: 06ellyRN7-2_11[1].ab1 Colony #7-2

CGCCAGCTTGCATGCCTGCAGGTCGACTCTAGAGTCCATCTTGATTTCACGACTAAGAAGTGGAACATTAATCT
TTGGTTCAAAGAATTCTTTGAATTCCTTAAGTCTTTCTGGGGTATGGAAGACGCCTGCAGTAACAGTGATAAAT
TTAGCAAATTCCATGTCACCACCAACAGTCTTGTCAAGCCAATCCCAGTCTTCTCTGATCCAGTCCCAAGCTGC
TTGTTGACCATAATGGTTAGCAAGTAAACCACGGTACCAATCACATAAATCTTGTGGCTTAACTACGTCAGCAT
TTTCAAAGTCGCCAACAATAGCCTTGATAGCTGCAAGATCCTTGGTGCTGGTTACAGCGCTGCGTAAGTCAACC
TTGTATGATGGGTCAGCTGTTCTTTGGTATTCCTTAATTAACTTATCAACTAATTCAGCATTGCCAAAGTTCTT
AACTTCATTGATTAAAACGTATGGACGAATATCTGCATTCAATGCTTCCAAGTTATCTTCATTTTCAGTAAAGA
TTTGGTGAGCTGCCTTAATTGAGTCCGCATTTTCAGCGTAAAGACTTGCACTCAACTCGTATGGACGAATTTGA
ACATCTTCATCGCTTTCGCCTGGCTTTACTTCCCAGCCTAAACGTGCAACTTGATCCTTTGATAAGAGATCATA
AAGCTTCTTCAAGTTCTTTTCTTCATTTGATTCTGGTTCANCGAATTGACGAAGCTTAGCTGCAGTAGTGTAAA
GTGCGTTAATTACCANGCTGGACTNGAATCAGCGAATTTANCCAAAGNGGAACAATTGAAGCGTAAGAAATTGC
TNACCTCTGCTAAANACGTAGNCNTGANGCANTGNAACTTATCAATNGGATCCATTCNTTACCTCTGAAAANTT
CCTCAAGCAAAGCCTGNCNNATTCAACGAAGAANGGGGNGTGGTGCCAAATN

Figure 20. Nucleic acid sequences of plasmid pES3 carrying the *pepN* structural gene from *Lb. helveticus* WSU19. The pES3 plasmid was extracted from *E. coli* DH5α(pES3) colony colony #7-2. The sequences were obtained from 5' and 3' end DNA sequencing using: (a) M13 forward primer and (b) M13 reverse primer.

(a) File name: 04ellyFN7-5_07[1].ab1 Colony #7-5

GTGTACGCGGCCAGTGAATTCGAGCTCACATTTCACCCAGATCATTACGATTTGCGTATTAATGTAAACCGTAA
GAATAAAACTATTAATGGTACTTCCACAATTACTGGTGATGTAATTGAAAATCCAGTATTTATTAACCAAAAAT
TTATGACCATTGATAGCGTTAAGGTTGATGGTAAAAATGTTGATTTTGATGTAATCGAAAAAGATGAAGCAATC
AAAATTAAAACAGGAGTAACTGGCAAAGCTGTAATCGAAATTGCTTATAGCGCACCACTTACTGATACTATGAT
GGGTATTTATCCTTCATATTACGAATTAGAAGGTAAGAAGAAGCAAATCATCGGTACGCAATTCGAAACTACTT
TTGCTCGCCAAGCATTCCCATGTGTGGACGAACCTGAAGCTAAAGCTACATTCTCACTTGCTCTTAAGTGGGAT
GAACAAGATGGTGAAGTTGCACTTGCTAACATGCCAGAAGTAGAAGTTGACAAGGATGGCTACCACCACTTTGA
AGAAACTGTCCGCATGTCTAGTTACTTAGTTGCCTTTGCCTTTGGTGAATTACAATCTAAGACTACTCATACTA
AGGATGGCGTATTAATTGGCGTTTACGCAACTAAGGCACACAAGCCTAAGGAATTAGACTTCGCTTTGGACATT
GCTAAGCGCGCAATTGAAATTTTACGAAGAATTCTACCNAACCAAATACCCACTTCCACAGTCATTGCAACTTG
CATTGCCAGACTTTCTCAGCTGGTGCCATGGAAAACTGGGGTCTTGTAACTTACCGNGGAGCATACTTGCTCCT
TGNNCCNGACAATACTAGCTTGGAAATGAANANNTNGTTGCCCNGTTNTTNCCCTGAATGGGCTCCCANNGGTC
GGGNCNTGGTACCTGANGGGGGGACACTTNGNTTA

(b) File name: 07ellyRN7-5_13[1].ab1 Colony #7-5

CCAGCTTGCATGCCTGCAGGTCGACTCTAGAATCCATCTTNATTTCCCGACTAAGAAGTGGAACATTAATCTTT
GGTTCAAAGAATTCCTTGAATTCCTTAAGTCTTTCTGGGGTATGGAAGACGCCTGCAGTAACAGTGATAAATTT
AGCAAATTCCATGTCACCACCAATAGTCTTGTCAAGCCAATCCCAGTCTTCTCTGATCCAGTCCCAAGCTGCTT
GTTGACCATAATGGTTAGCAAGTAAACCACGGTACCAATCACATAAATCTTGTGGCTTAACTACGTCAGCATTT
TCAAAGTCGCCAACAATAGCCTTGATAGCTGCAAGATCCTTGGTGCTGGTTACAGCGCTGCGTAAGTCAACCTT
GTATGATGGGTCAGCTGTTCTTTGGTATTCCTTAATTAACTTATCAACTAATTCAGCATTGCCAAAGTTCTTAA
CTTCATTGATTAAAACGTATGGACGAATATCTGCATTCAATGCTTCCAAGTTATCTTCATTTTCAGTAAAGATT
TGGTGAGCTGCCTTAATTGAGTCCGCATTTTCAGCGTAAAGACTTGCGCTCAACTCGTATGGACGAATTTGAAC
ATCTTCATCGCTTTCGCCTGGCTTTACTTCCCAGCCTAAACGTGCAACTTGATCCTTTGATAAGAGATCATAAA
GCTTCTTCAAGTTCTTTTCTTCATTTGATTCTGGTTCACGAATTGACGAAGCTTAGCTGCAGTAGTGTAAAGTG
CGTTAATTACNAGCTGGACTTAGAATCAGCGAANTTANCCAAAGNGGAACAATTGAAGCGTAAGAAANTTGCTN
ACCTTCTGCTANANACGTAGTCTGGAGCATTGTACTTATCATTGGATCNATTCNTTACCTCTGAAAAATTCCTC
AGCAAGTCTGTNTNTCACGAGAAGGGGGGTGTGCC

Figure 21. Nucleic acid sequences of plasmid pES3 carrying the *pepN* structural gene from *Lb. helveticus* WSU19. The pES3 plasmid was extracted from *E. coli* DH5α(pES3) colony colony #7-5. The sequences were obtained from 5' and 3' end DNA sequencing using: (a) M13 forward primer and (b) M13 reverse primer.

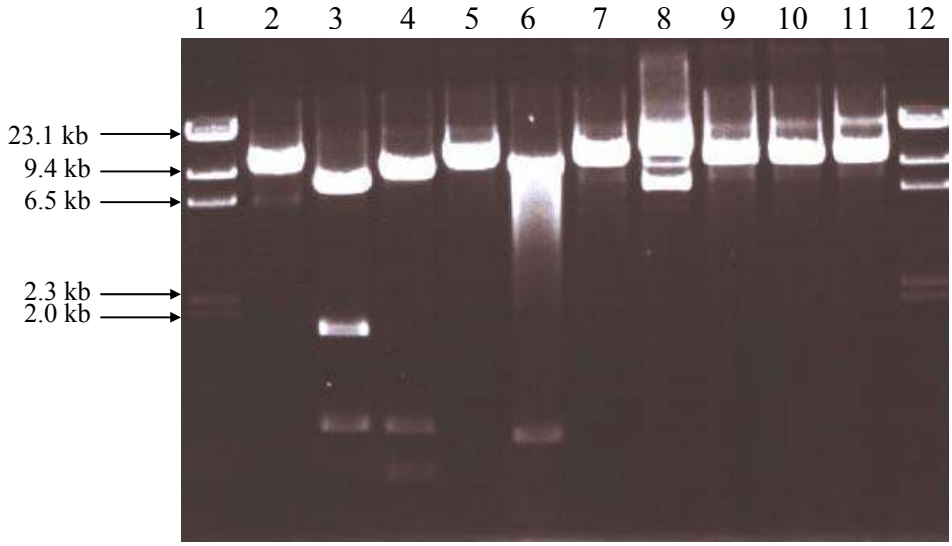

Figure 22. Restriction enzyme analysis of the plasmid pES3 from *E. coli* DH5α(pES3) colony #7-5, expressing the *pepN* structural gene from *Lb. helveticus* WSU19. Lane 1. λ DNA/*Hind*III ladder (molecular mass indicated on the left in kilobase pairs); lanes 2-11. Plasmid pES3 digested with: *Bam*HI (lane 2); *Eco*RI (lane 3); *Hind*III (lane 4); *Kpn*I (lane 5); *PstI* (lane 6); *Sal*I (lane 7); *Sma*I (lane 8); *Sph*I (lane 9); *Sst*I (lane 10); *Xba*I (lane 11); lane 12. λ DNA/*Hind*III ladder.

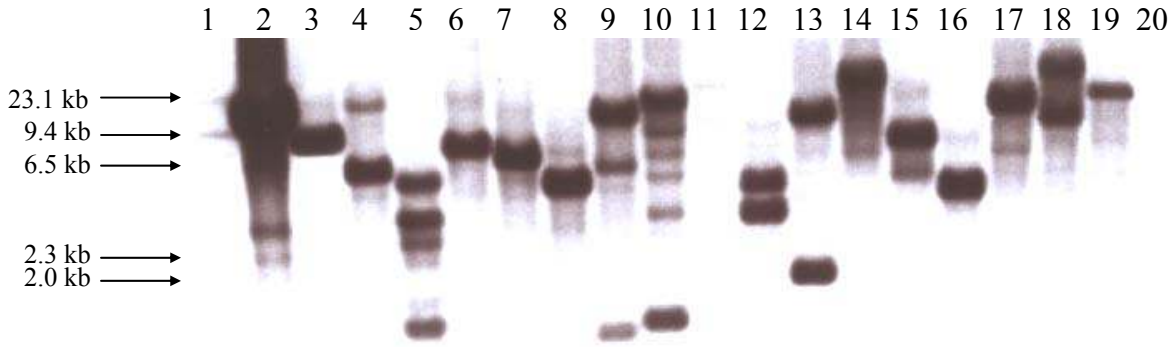

Figure 23. High stringency Southern hybridization of genomic DNA from *Lb. helveticus* WSU19 using a DIG-labeled probe synthesized based on the *Lb. helveticus* WSU19 *pepN* structural gene. Lane 1. DIG-labeled DNA MW Marker II; lane 2. pES3 digested with *Sst*I; lane 3. pJDC9 digested with *Sst*I; lanes 4-10. genomic DNA from *Lb. helveticus* WSU19 digested with: *Sst*I and *Kpn*I (lane 4); *Sst*I and *Bam*HI (lane 5); *Sst*I and *Xba*I (lane 6); *Sst*I and *Sph*I (lane 7); *Xba*I and *Sph*I (lane 8); *Sph*I and *Kpn*I (lane 9); *Bam*HI and *Kpn*I (lane 10); lane 11. DIG-labeled DNA MW Marker II; lanes 12-19. genomic DNA from *Lb. helveticus* WSU19 digested with: *Xba*I and *Bam*HI (lane 12); *Sph*I and *Bam*HI (lane 13); *Sst*I and *Sal*I (lane 14); *Xba*I and *Sal*I (lane 15); *Kpn*I and *Xba*I (lane 16); *Sph*I and *Sal*I (lane 17); *Bam*HI and *Sal*I (lane 18); *Kpn*I and *Sal*I (lane 19); lane 20. DIG-labeled DNA MW Marker II.

Table 8. Plasmids used or generated in the cloning of the peptidase genes from *Lb. helveticus* WSU19

Plasmid	Relevant characteristics	Reference
pJDC9	Em^r *lacZ'*	Chen and Morrison, 1987
pES1	Em^r, pJDC9 with a 2.7-kb *Pst*I insert genomic DNA from the strain WSU19 (*pepE* clone)	Present study
pES2	Em^r, pJDC9 with a 5.8-kb *Sph*I-*Xba*I insert genomic DNA from the strain WSU19 (*pepO2* clone)	Present study
pES3	Em^r, pJDC9 with a 2.4-kb *Sac*I-*Xba*I fragment from the strain WSU19 (*pepN* structural gene clone)	Present study
pES4	Em^r, pJDC9 with a 5-kb *Sac*I-*Sph*I insert genomic DNA from the strain WSU19 (*pepN* clone)	Present study
pES5	Em^r, pJDC9 with a 4.3-kb *Hind*III-*Sal*I insert genomic DNA from the strain WSU19 (*pepO* clone)	Present study
pES6	Em^r, pJDC9 with a 3.4-kb *Kpn*I insert genomic DNA from the strain WSU19 (*pepO3* clone)	Present study

3. DNA sequence analysis of the 2.7-kb *Pst*I genomic insert containing the *pepE* gene

Figure 24 illustrates the open reading frame (ORF) and restriction enzyme analyses of the 2.7-kb *Pst*I genomic insert. The nucleic acid sequence of the 2.7-kb *Pst*I genomic insert is shown in Figure 25. Six ORFs were identified, three of which contain conserved domains: ORF1 (nt. 334 to 777; 444 bp), ORF2 (nt. 921 to 2234; 1314 bp), and ORF3 (nt. 2293 to 2682; 390 bp). The amino acid residues 19 to 135 in the ORF1 align with the amino acid residues 19 to 132 in the IbpA domain (146 residues). The amino acid residues 4 to 438 in the ORF2 align with the amino acid residues 1 to 438 in the PepC domain (438 residues). The amino acid residues 1 to 118 in the ORF3 align with amino acid residues 354 to 468 in the IMP dehydrogenase / GMP reductase (IMPDH) domain (468 residues, 25% aligned). The deduced amino acid sequences of the ORF1 and ORF2 were determined to contain conserved domains of small heat shock protein (IbpA) and aminopeptidase C (PepC), respectively.

Amino acid BLAST analyses revealed that the deduced amino acid sequence of the ORF2 shares 99% and 89% identities with endopeptidase E (PepE) from *Lb. helveticus* CNRZ32 (Fenster et al., 1997) and *Lb. acidophilus* NCFM (Altermann et al., 2005), respectively. The BLAST analyses also revealed that the deduced amino acid sequence of the ORF1 shares 82% identity with amino acids 18-141 of the 141-Da heat shock protein low MW from *Lb. acidophilus* NCFM. The deduced amino acid sequence of the ORF3 shares 97% identity with amino acids 251-380 of the 380-Da inosine-5'-monophosphate dehydrogenase from *Lb. acidophilus* NCFM.

Based on the amino acid BLAST analyses, the ORF2 was determined to encode for PepE, a protein of 438 amino acids with a calculated molecular weight of 50 kDa. Nucleic acid BLAST analysis revealed that the *pepE* gene from *Lb. helveticus* WSU19 shares 95%

and 83% identities with the *pepE* gene from *Lb. helveticus* CNRZ32 and *Lb. acidophilus* NCFM, respectively.

Figure 25 shows the nucleic acid sequence and the deduced amino acid sequence of the *pepE* gene from *Lb. helveticus* WSU19. The start codon (ATG) of the ORF2 is preceded by a putative RBS (AAGGAG; nt. 906-911) and putative promoters –10 (TAAAAT; nt. 867-872) and –35 (TTGAAC; nt. 844-849). The putative promoters and RBS were assigned based on the published consensus sequences for lactobacilli (Pouwels and Leer, 1993; Pouwels and Chaillou, 2003; Chen and Steele, 2005). An inverted repeat (nt. 2253 to 2264 and 2273 to 2284) observed in the 3' non-coding region may function as a putative rho-independent transcriptional terminator. The presence of the putative transcriptional promoters and terminator suggests that the *pepE* gene from *Lb. helveticus* WSU19 is transcribed monocistronically and is not part of an operon, which is in agreement with Fenster et al. (1997).

PROSITE database searches with the deduced PepE sequence from *Lb. helveticus* WSU19 identified 2 domains involved in the substrate binding and catalysis: amino acids 64-75 (QkhsGrCWlfAT; thiol protease cysteine motif) and 360-370 (VsHAMtLVGvD; thiol protease histidine motif). Figure 26 shows alignment of the deduced amino acid sequence of PepE from *Lb. helveticus* WSU19 and the published amino acid sequences of thiol proteases, including PepE, PepE2, PepG, PepW, and PepC, from other lactobacilli. Among the amino acids involved in the substrate binding and catalysis of thiol proteases, the residues Gln_{64}, Ser_{67}, Gly_{68}, Arg_{69}, Cys_{70}, Trp_{71}, Phe_{73}, His_{362}, Met_{364}, Val_{369}, and Asp_{370} are conserved among PepE, PepE2, PepG, PepW, and PepC from lactobacilli, indicating the importance of these amino acids for thiol protease activity. In contrast, the amino acid residues His_{66}, Thr_{75},

Val_{360}, Ser_{361}, Ala_{363}, Thr_{365}, Leu_{366}, Val_{367}, and Gly_{368} are conserved in PepE only. The highly conserved thiol protease motif in PepE from *Lb. helveticus* WSU19 suggests that this enzyme has the same catalytic mechanism as the thiol protease family.

Homology between the deduced PepE sequence from *Lb. helveticus* WSU19 and the published amino acid sequences of thiol proteases is listed in Table 9. In addition to the high identities with PepE from *Lb. helveticus* CNRZ32 and *Lb. acidophilus* NCFM, PepE from *Lb. helveticus* WSU19 shares 40-69% identities with PepE2 from *Lb. helveticus* CNRZ32 (Sridhar, 2003); PepG from *Lb. delbrueckii* subsp. *lactis* DSM7290 (Klein et al., 1997) and *Lb. acidophilus* NCFM (Altermann et al., 2005); PepW from *Lb. delbrueckii* subsp. *lactis* DSM7290 (Klein et al., 1997); and PepC from *Lb. gasseri*, *Lb. johnsonii* NCC533 (Pridmore et al., 2004), *Lb. delbrueckii* subsp. *bulgaricus* ATCC BAA-365, *Lb. casei* ATCC334, *Lb. plantarum* WCFS1 (Kleerebezem et al., 2004), *Lb. helveticus* CNRZ32 (Fernandez et al., 1994), *Lb. acidophilus* NCFM (Altermann et al., 2005), *Lb. delbrueckii* subsp. *lactis* DSM7290 (Klein et al., 1994), and *Lb. helveticus* 53/7 (Vesanto et al., 1994). The high amino acid identities between PepE from *Lb. helveticus* WSU19 and the thiol proteases suggest that these enzymes are evolutionally related and may have evolved from the same ancestral proteolytic enzyme.

4. DNA sequence analysis of the 4.3-kb *Hind*III-*Sal*I genomic insert containing the *pepO* gene

Figure 27 illustrates the ORF and restriction enzyme analyses of the 4.3-kb *Hind*III-*Sal*I genomic insert. The nucleic acid sequence of the 4.3-kb *Hind*III-*Sal*I genomic insert is shown in Figure 28. Twelve ORFs were identified, three of which contain conserved

domains: ORF1 (nt. 321 to 2261; 1941 bp), ORF2 (nt. 2325 to 3545; 1221 bp), and ORF3 (nt. 3593 to 4231; 639 bp). The amino acid residues 13 to 647 in the ORF1 align with residues 10 to 654 in the PepO domain (654 residues). Ninety-seven percents of the 283 amino acid residues in the Cfa domain (aa. 11 to 283) align with residues 117 to 389 in the ORF2. The amino acid residues 1 to 205 in the ORF3 align with residues 23 to 255 in the PlsC domain (255 residues). The deduced amino acid sequences of the ORF1, ORF2, and ORF3 were determined to contain conserved domains of predicted metalloendopeptidase (PepO), cyclopropane fatty acid synthase and related methyltransferases (Cfa), and 1-acyl-sn-glycerol-3-phosphate acyltransferase (PlsC), respectively.

Amino acid BLAST analyses revealed that the deduced amino acid sequence of the ORF1 shares 99% and 60-85% identities with endopeptidase O (PepO) from *Lb. helveticus* CNRZ32 (Chen and Steele, 1998) and neutral endopeptidases from *Lb. acidophilus* NCFM (Altermann et al., 2005), respectively. In addition, the deduced amino acid sequence of the ORF1 shares 48-63% and 42% identities with PepO from *Lb. johnsonii* NCC533 (Pridmore et al., 2004) and *Lb. plantarum* WCFS1 (Kleerebezem et al., 2005), respectively; 56% and 62% identities with PepO2 and PepO3 from *Lb. helveticus* CNRZ32, respectively (Chen et al., 2003; Sridhar, 2003). The BLAST analyses also revealed that the deduced amino acid sequence of the ORF2 shares 89% identity with 393-Da cyclopropane-phospholipid-fatty-acyl-synthase from *Lb. acidophilus* NCFM. The deduced amino acid sequence of the ORF3 shares 91% identity with 240-Da acyltransferase family protein from *Lb. acidophilus* NCFM.

Based on the amino acid BLAST analyses, the ORF1 was determined to encode for PepO, a protein of 647 amino acids with a calculated molecular weight of 73.6 kDa. Nucleic

acid BLAST analysis revealed that the *pepO* gene from *Lb. helveticus* WSU19 shares 99% identity with the *pepO* gene from *Lb. helveticus* CNRZ32.

Figure 28 shows the nucleic acid sequence and the deduced amino acid sequence of the *pepO* gene from *Lb. helveticus* WSU19. The start codon (ATG) of the ORF2 is preceded by a putative RBS (AAGGAG; nt. 310- 315) and putative promoters –10 (TATAAT; nt. 268-273) and –35 (TTGGCT; nt. 240-245). The putative promoters and RBS were assigned based on the published consensus sequences for lactobacilli (Pouwels and Leer, 1993; Pouwels and Chaillou, 2003; Chen and Steele, 2005). An inverted repeat (nt. 2279 to 2292 and 2297 to 2310) observed in the 3' non-coding region may function as a putative rho-independent transcriptional terminator. The presence of the putative transcriptional promoters and terminator suggests that the *pepO* gene from *Lb. helveticus* WSU19 is transcribed monocistronically and is not part of an operon, which is in agreement with Chen and Steele (1998).

In contrast to the *pepO* gene from *Lb. helveticus*, the lactococcal *pepO* gene was reported to be associated with an oligopeptide transport system (Tan et al., 1991; Mierau et al., 1993; and Tynkkynen et al., 1993). The lactococcal *opp* operon was arranged in the order of *oppDFBCA*, i.e., the ATP-binding proteins (*oppD* and o*ppF*), the integral membrane proteins (*oppB* and *oppC*), and the substrate-binding protein (*oppA*). The lactococcal *pepO* gene was reported to be located downstream of *oppA* (Mierau et al., 1993).

PROSITE database searches with the deduced PepO sequence from *Lb. helveticus* WSU19 identified a neutral zinc metallopeptidase motif in amino acid residues 493-502 (TigHEVSHaF). Figure 29 shows an alignment of the deduced amino acid sequence of PepO from *Lb. helveticus* WSU19 and the published amino acid sequences of PepO from other

lactobacilli, including *Lb. helveticus* CNRZ32, *Lb. acidophilus* NCFM, *Lb. johnsonii* NCC533, and *Lb. plantarum* WFCS1. The residues Ile_{494}, His_{496}, Glu_{497}, His_{500}, Ala_{501}, and Phe_{502} are conserved in PepO from lactobacilli. The presence of zinc metallopeptidase motif in PepO from *Lb. helveticus* WSU19 indicates the presence of the same mechanism of catalytic action for PepO and the metalloprotease family.

5. DNA sequence analysis of the 5.8-kb *Xba*I-*Sph*I genomic insert containing the *pepO2* gene

Figure 30 illustrates the ORF and restriction enzyme analyses of the 5.8-kb *Xba*I-*Sph*I genomic insert. The nucleic acid sequence of the 5.8-kb *Xba*I-*Sph*I genomic insert is shown in Figure 31. Fifteen ORFs were identified. Conserved domains were identified in two of the ORFs: ORF1 (nt. 748 to 1689; 942 bp) and ORF2 (nt. 3070 to 5013; 1944 bp). The ORF1 was determined to contain a conserved domain of amino acid permease (AA_permease). The amino acid residues 5 to 278 in the ORF1 align with the residues 116 to 421 in the AA_permease domain (473 residues). The ORF2 was determined to contain a conserved domain of predicted metalloendopeptidase (PepO). The amino acid residues 12 to 648 in the ORF2 align with the residues 10 to 654 in the PepO domain (654 residues).

Amino acid BLAST analyses revealed that the deduced amino acid sequence of the ORF2 shares 98% and 41% identities with endopeptidase O2 (PepO2) from *Lb. helveticus* CNRZ32 (Chen et al., 2003) and *Lc. lactis* MG1363, respectively. Furthermore, the deduced amino acid sequence of the ORF2 shares 62% and 56% identities with PepO3 and PepO from *Lb. helveticus* CNRZ32, respectively (Chen and Steele, 1998; Sridhar, 2003); a 41% identity with neutral endopeptidase O from *Lactococcus lactis* subsp. *lactis* IL1403 (Bolotin et al.,

2001) and *Lc. lactis* subsp. *cremoris* P8-2-47 (Mierau et al., 1993), respectively. The BLAST analyses also revealed that the deduced amino acid sequence of the ORF1 shares 83% identity with residues 141-441 of 441-Da amino acid permease from *Lb. acidophilus* NCFM. Based on the amino acid BLAST analyses, the ORF2 was determined to encode for PepO2, a protein of 648 amino acids with a calculated molecular weight of 73.8 kDa. Nucleic acid BLAST analysis revealed that the *pepO2* gene from *Lb. helveticus* WSU19 shares 96% identity with the *pepO2* gene from *Lb. helveticus* CNRZ32.

Figure 31 shows the nucleic acid sequence and the deduced amino acid sequence of the *pepO2* gene from *Lb. helveticus* WSU19. The start codon (ATG) of the ORF2 is preceded by a putative RBS (AAGGAG; nt. 3057-3062) and putative promoters –10 (TATGAT; nt. 3033-3038) and –35 (TTTTCA; nt. 3009-3014). The putative promoters and RBS were assigned based on the published consensus sequences for lactobacilli (Pouwels and Leer, 1993; Pouwels and Chaillou, 2003; Chen and Steele, 2005). An inverted repeat (nt. 5036 to 5048 and 5069 to 5081) observed in the 3' non-coding region may function as a putative rho-independent transcriptional terminator. The presence of the putative transcriptional promoters and terminator suggests that the *pepO2* gene from *Lb. helveticus* WSU19 is transcribed monocistronically and is not part of an operon, which is in agreement with Chen et al. (2003).

PROSITE database searches with the deduced PepO2 sequence from *Lb. helveticus* WSU19 identified a neutral zinc metallopeptidase motif in amino acid residues 494-503 (ViaHEISHaF). The presence of zinc metallopeptidase motif indicates the presence of the same catalytic mechanism for the PepO2 enzyme from *Lb. helveticus* WSU19 and the zinc-dependent proteases.

6. DNA sequence analysis of the 3.4-kb *Kpn*I genomic insert containing the *pepO3* gene

Figure 32 illustrates the ORF and restriction enzyme analyses of the 3.4-kb *Kpn*I genomic insert. The nucleic acid sequence of the 3.4-kb *Kpn*I genomic insert is shown in Figure 33. Eight ORFs were identified. Conserved domain of a predicted metalloendopeptidase (PepO) was identified in ORF2 (nucleotides 841 to 2781; 1941 bp). The deduced amino acid residues 13 to 647 of the ORF2 align with the residues 10 to 654 in the PepO domain (654 residues). No conserved domains were identified in ORF1 (nucleotides 23 to 760; 738bp) and ORF3 (nucleotides 3009 to 3392; 384 bp).

Amino acid BLAST analyses revealed that the deduced amino acid sequence of the ORF2 shares a 99% identity with endopeptidase O3 (PepO3) from *Lb. helveticus* CNRZ32 (Sridhar, 2003). In addition, the deduced amino acid sequence of the ORF2 shares 77% and 71% identities with the predicted metalloendopeptidases from *Lb. gasseri* and *Lb. delbrueckii* subsp. *bulgaricus* ATCC BAA-365, respectively; 62% identities with PepO and PepO2 from *Lb. helveticus* CNRZ32, respectively (Chen and Steele, 1998; Chen et al., 2003).

The BLAST analyses also revealed that the deduced amino acid sequence of the ORF1 shares 62%, 70%, 71%, and 89% identities with amino acid residues 151-335 of a 339-Da permease major facilitator superfamily (MFS) protein from *Lb. delbrueckii* subsp. *bulgaricus* ATCC BAA-365; residues 160-376 of a 405-Da permease MFS protein from *Lb. johnsonii* NCC533; residues 181-397 of a 426-Da permease MFS protein from *Lb. gasseri*; and residues 160-377 of a 405-Da multidrug resistance protein from *Lb. acidophilus* NCFM, respectively. PROSITE database searches with the deduced amino acid sequence of the ORF1 identified an MFS motif in amino acid residues 1 to 209. The deduced amino acid sequence of the ORF3 shares 99% and 80% identities with potassium uptake (Kup) protein

from *Lb. acidophilus* NCFM and *Lb. delbrueckii* subsp. *bulgaricus* ATCC BAA-365, respectively.

Based on the amino acid BLAST analyses, the ORF2 was determined to encode for PepO3, a protein of 643 amino acids with a calculated molecular weight of 72.6 kDa. Nucleic acid BLAST analysis revealed that the *pepO3* gene from *Lb. helveticus* WSU19 shares a 96% identity with the *pepO3* gene from *Lb. helveticus* CNRZ32.

Figure 33 shows the nucleic acid sequence and the deduced amino acid sequence of the *pepO3* gene from *Lb. helveticus* WSU19. The start codon (ATG) of the ORF2 is preceded by a putative RBS (AGGGGG; nt. 827-833) and putative promoters –10 (TATATT; nt. 774-779) and –35 (TTGTAT; nt. 752-757). The putative promoters and RBS were assigned based on the published consensus sequences for lactobacilli (Pouwels and Leer, 1993; Pouwels and Chaillou, 2003; Sridhar, 2003). An inverted repeat (nt. 2793 to 2806 and 2808 to 2821) observed in the 3' non-coding region may function as a putative rho-independent transcriptional terminator. The presence of the putative transcriptional promoters and terminator suggests that the *pepO3* gene from *Lb. helveticus* WSU19 is transcribed monocistronically and is not part of an operon, which is in agreement with Sridhar (2003).

PROSITE database searches with the deduced PepO3 sequence from *Lb. helveticus* WSU19 identified a neutral zinc metallopeptidase motif in amino acid residues 489-498 (ViaHEISHaF). The existence of zinc metallopeptidase motif suggests that PepO3 from *Lb. helveticus* WSU19 possesses a similar mechanism of catalytic action to the metalloprotease family.

Figure 34 demonstrates an alignment of the deduced and published amino acid sequences of PepO, PepO2, and PepO3 from *Lb. helveticus* WSU19, *Lb. helveticus* CNRZ32,

and *Lc. lactis* MG1363. The amino acid sequences involved in substrate binding and enzymatic catalysis (positions 499 to 508; Figure 34) are conserved in PepO, PepO2, and PepO3 from lactobacilli as well as in PepO2 from *Lactococcus.* To date, only 2 copies of PepO enzymes, namely PepO and PepO2, were reported in *Lactococcus* (Hellendoorn, et al., 1996; Christensen et al., 1999). The presence of 3 copies of PepO enzymes in *Lb. helveticus* CNRZ32 and WSU19 indicates the importance of these proteins in the physiology of the bacteria.

7. DNA sequence analysis of the 5-kb *Sac*I-*Sph*I genomic insert containing the *pepN* gene

Figure 35 illustrates the ORF and restriction enzyme analyses of the 5-kb *Sac*I-*Sph*I genomic insert. The nucleic acid sequence of the 5-kb *Sac*I-*Sph*I genomic insert is shown in Figure 36. Two large ORFs, ORF1 and ORF2, and twelve small ORFs were identified. ORF2 (nt. 2291 to 4822; 2532 bp) was determined to contain a conserved domain of aminopeptidase N (PepN). The deduced amino acid residues 10 to 833 in the ORF2 align with 97% of the 859 amino acid residues in the PepN domain (aa. 22 to 858). A conserved domain was not identified in the ORF1 (nt. 467 to 1639; 1173 bp).

Amino acid BLAST analyses revealed the deduced amino acid sequence of the ORF2 shares 99%, 98%, 90%, 70%, 65%, 67%, and 62% identities with PepN from *Lb. helveticus* 53/7 (Varmanen, et al., 1994), *Lb. helveticus* CNRZ32 (Christensen et al., 1995), *Lb. acidophilus* NCFM (Altermann et al., 2005), *Lb. delbrueckii* subsp. *bulgaricus* ATCC BAA-365, *Lb. johnsonii* NCC533 (Pridmore et al., 2004), *Lb. gasseri*, and *Lb. casei* ATCC334, respectively. The BLAST analyses also revealed the deduced amino acid sequence of the

ORF1 shares a 74% identity with a 372-Da putative d-ala-d-ala-ligase from *Lb. acidophilus* NCFM. Based on the amino acid BLAST analyses, the ORF2 was determined to encode for PepN, a protein of 844 amino acids with a calculated molecular weight of 95.8 kDa. Nucleic acid BLAST analysis revealed that the *pepN* gene from *Lb. helveticus* WSU19 shares 99% and 98% identities with the *pepN* genes from *Lb. helveticus* 53/7 and *Lb. helveticus* CNRZ32, respectively.

Figure 36 shows the nucleic acid sequence and the deduced amino acid sequence of the *pepN* gene from *Lb. helveticus* WSU19. The start codon (ATG) of the ORF2 is preceded by a putative RBS (AGGAGG; nt. 2278- 2283) and putative promoters –10 (TAAAAT; nt. 2251-2256) and –35 (TTAAGC; nt. 2226-2231). The putative promoters and RBS were assigned based on the published consensus sequences for lactobacilli (Pouwels and Leer, 1993; Pouwels and Chaillou, 2003; Chen and Steele, 2005). An inverted repeat (nt. 4841 to 4857 and 4867 to 4883) observed in the 3' non-coding region may function as a putative rho-independent transcriptional terminator. The presence of the putative transcriptional promoters and terminator suggests the *pepN* gene from *Lb. helveticus* WSU19 is transcribed monocistronically and is not part of an operon, which is in agreement with Varmanen et al. (1994) and Christensen et al. (1995).

PROSITE database searches with the deduced PepN sequence from *Lb. helveticus* WSU19 identified a neutral zinc metallopeptidase motif in amino acid residues 286-295 (VitHELAHqW). The presence of the zinc metallopeptidase motif in PepN from *Lb. helveticus* WSU19 suggests the presence of the same catalytic mechanism for PepN and the metalloprotease family.

Figure 37 shows an alignment of the deduced amino acid sequence of PepN from *Lb. helveticus* WSU19 and the published amino acid sequences of PepN from other lactobacilli, including *Lb. helveticus, Lb. acidophilus, Lb. johnsonii, Lb. plantarum, Lb. gasseri,* and *Lb. casei*. The amino acid sequences involved in substrate binding and enzymatic catalysis (positions 298 to 307; Figure 37) are highly conserved in PepN from lactobacilli. In addition, highly conserved amino acid sequences also occur outside the catalytic region of PepN from lactobacilli (positions 105 to 117; 128 to 152; 258 to 271; 281 to 297; and 308 to 332; Figure 37). However, the function of these regions in PepN activity is not clear.

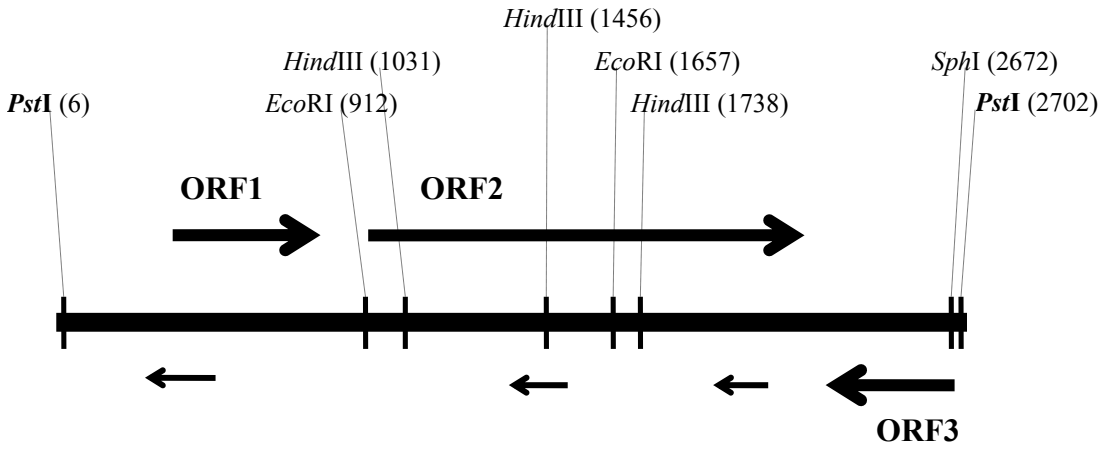

Figure 24. Open reading frame (ORF) and restriction enzyme analyses of the 2.7-kb *Pst*I genomic insert containing the *pepE* gene from *Lb. helveticus* WSU19. The vertical lines represent restriction enzyme sites. The numbers in parentheses refer to nucleotide positions. The horizontal line represents genomic insert. The horizontal arrows represent ORFs; the arrows above the horizontal line correspond to the direct DNA strand; the arrows below the horizontal line correspond to the complementary DNA strand.

Figure 25. Nucleic acid sequence of the 2.7-kb *Pst*I genomic insert and the deduced amino acid sequence of the PepE enzyme (in single-letter code) from *Lb. helveticus* WSU19. The numbers to the left refer to nucleic acids (bottom lines) and amino acid residues (top lines). The putative –10 and –35 promoter sequences are underlined and labeled. The putative ribosomal binding site is indicated in bold letters, underlined, and labeled rbs. The putative transcriptional terminator is indicated by the dotted horizontal arrows. Stop codon is indicated by asterisk. The thiol protease motifs are double-underlined and labeled.

```
   1 CTGCAGAATCTTTATTCTACGAGGACGATCCTTTTTTAATCGTGCAATTTCATCTTCAAT
  61 TTGTTTGTAGCCTTCCGGCGTCATTTTTTGAAAATATACCATAATTTAACACCTGATTAA
 121 CAGTTCATTCATTTTTTCTTTCTAATTATACAAAAGTTATCCACAGGTGTTAAGCATTGA
 181 TCTAGCAAAGTTTTTTTACAAAAATTAGCACTATATGCTTTTGAATGCTAAATAATTTAA
 241 CTTATTTAAAAAACGACTATAATAATCAGTGTAAGGAAAAAGAACGAGACCTTACAGATT
 301 AAACAAGCAAAAAATTGAAAGGAAGTTTTCAATATGGCAAACGATATGATGAATCGTCGT
 361 AATGATATGATGGATGCAATGAACGACTGGTTTGGTTTTCCAAGAAACTTCTTGGGTTTT
 421 CCAAGAAACTTCTTTGATGACACTGAAATTGAAAACATCATGCAATCAGATGTTGCTGAA
 481 ACCGATAAAGACTATACTGTTAAGATTGATATGCCTGGTATGAATAAAGAAGACATCAAT
 541 GTAAATTACAAAGATGGTTTTTTAACAGTTGTAGGTAGCAGAAAATCATTCAAGGATACA
 601 AGCGACAAGGATAAGAATATTATCCACAAAGAAAGAAGCGAAGGTCGCATTTCAAGAAGC
 661 TATAGATTGCCAAATATAGTTGCAAGTGAGATCCATGCAAAGTATGATAATGGTGTATTG
 721 ACTATCACCTTGCCAAAGCAAAACGCTGGCGATGATAGCAATTCTATCCATATTGATTAA
 781 TTTATTAGATTAAGCAAGAAGTCTAATAAGTGACGGATATAATTCTCTGAAGCGAGTTCA
 841 TTATTGAACCCGCTTTTATTTTGGTTTAAAATAGAATTAATTTAAGAAAAAATTAAAAAT
       -35                    -10

   1                    M  A  H  E  L  T  V  Q  E  L  E  K  F  S
 901 TATAAAAGGAGAATTCTTAAATGGCTCATGAATTAACTGTGCAGGAACTTGAAAAGTTTT
         rbs

  15   A  D  F  N  K  N  P  K  N  K  V  V  A  R  A  A  Q  R  S  G
 961 CTGCTGATTTTAATAAAAATCCTAAAAATAAAGTCGTTGCTCGTGCTGCCCAACGTAGCG
  35   V  L  E  A  S  Y  N  D  R  V  Q  S  E  L  T  R  V  F  S  T
1021 GTGTACTTGAAGCTTCTTATAATGACCGCGTTCAAAGCGAATTAACCCGTGTCTTTTCAA

                                          (thiol_protease_cys motif)
  55   E  L  D  T  D  N  V  T  N  Q  K  H  S  G  R  C  W  L  F  A
1081 CTGAACTTGATACTGACAACGTTACTAACCAAAAACACTCAGGTCGTTGCTGGTTATTTG
  75   T  L  N  V  L  R  H  E  F  G  K  K  Y  K  A  K  D  F  T  F
1141 CCACATTAAACGTTTTGCGTCATGAATTTGGCAAGAAATACAAGGCAAAAGACTTTACTT
  95   S  Q  A  Y  N  F  F  W  D  K  I  E  R  A  N  M  F  Y  N  R
1201 TCTCACAAGCATACAACTTCTTCTGGGACAAGATTGAACGTGCTAACATGTTCTACAACC
 115   I  L  D  S  A  D  M  P  L  D  S  R  Q  V  K  T  D  L  D  F
1261 GTATCTTAGACAGCGCTGATATGCCACTTGATTCTCGTCAAGTTAAGACTGACTTAGACT
```

Figure 25 (continued)

```
 135   A  G  T  D  G  G  Q  F  Q  M  A  A  A  L  V  E  K  Y  G  V
1321 TTGCAGGTACAGATGGTGGTCAATTCCAAATGGCTGCTGCCTTAGTTGAAAAATATGGTG
 155   V  P  S  Y  A  M  P  E  T  F  N  T  N  N  T  T  G  F  A  T
1381 TCGTACCTTCATATGCTATGCCTGAAACCTTTAACACTAACAACACTACTGGTTTTGCCA
 175   A  L  G  D  K  L  K  K  D  A  L  V  L  R  K  L  K  Q  E  G
1441 CTGCATTAGGCGACAAGCTTAAGAAGGATGCTTTGGTTCTTAGAAAATTAAAGCAAGAAG
 195   K  D  D  E  I  K  K  T  R  E  K  F  L  S  E  V  Y  Q  M  T
1501 GCAAAGATGACGAAATCAAGAAGACTCGTGAAAAATTCTTGAGCGAAGTTTACCAAATGA
 215   A  I  A  V  G  E  P  P  K  K  F  D  L  E  Y  R  D  D  D  K
1561 CTGCTATTGCTGTTGGTGAACCACCTAAGAAGTTCGATCTTGAATACCGTGATGACGATA
 235   K  Y  H  L  E  K  D  L  T  P  L  E  F  L  H  K  Y  L  G  G
1621 AGAAGTACCACTTAGAAAAAGACCTTACTCCACTTGAATTCTTGCACAAGTACTTAGGTG
 255   V  D  F  D  D  Y  V  V  L  T  N  A  P  D  H  E  Y  D  K  L
1681 GCGTTGACTTTGATGACTACGTTGTTTTGACCAACGCACCAGACCACGAATATGACAAGC
 275   Y  G  L  P  A  E  D  N  V  S  G  S  I  R  I  K  L  L  N  V
1741 TTTATGGTTTACCAGCAGAAGACAACGTCTCTGGTTCAATCAGAATTAAACTTTTGAATG
 295   P  M  E  Y  L  T  A  A  S  I  A  Q  L  K  D  G  E  A  V  W
1801 TTCCTATGGAATACTTAACCGCTGCTTCTATTGCTCAATTAAAAGACGGTGAAGCTGTTT
 315   F  G  N  D  V  L  R  Q  M  D  R  K  T  G  Y  L  D  T  N  L
1861 GGTTCGGTAATGATGTGCTTCGTCAAATGGACCGTAAGACTGGCTACCTTGACACTAACC
 335   Y  K  L  D  D  L  F  G  V  D  L  K  M  S  K  A  D  R  L  K
1921 TTTACAAGTTGGATGACTTATTTGGCGTTGACCTTAAGATGTCAAAGGCTGACAGATTAA

                        (thiol_protease_his motif)
 355   T  G  V  G  E  V  S  H  A  M  T  L  V  G  V  D  E  D  N  G
1981 AGACTGGTGTCGGCGAAGTTTCTCACGCCATGACCTTAGTCGGTGTTGATGAAGACAACG
 375   E  V  R  Q  W  K  V  E  N  S  W  G  D  K  S  G  A  K  G  Y
2041 GTGAAGTTCGTCAATGGAAAGTTGAAAACTCATGGGGCGACAAGTCCGGTGCAAAGGGTT
 395   Y  V  M  N  N  E  W  F  N  D  Y  V  Y  E  V  V  V  H  K  K
2101 ATTACGTAATGAACAATGAATGGTTCAACGATTACGTTTATGAAGTTGTCGTTCACAAGA
 415   Y  L  T  D  K  Q  K  K  L  A  E  G  P  I  T  D  L  P  A  W
2161 AGTATTTGACTGATAAGCAAAAGAAACTTGCAGAAGGCCCAATTACTGATCTTCCTGCAT
 435   D  S  L  A  *
2221 GGGATTCACTTGCTTAATTATTAGAGCAATAGAAAAGGATTAAGCCGATCGACTTAATCC

2281 TTTTTTAGTTTACTTGTAATTAGGTGCTGCCTTGGTCATTTGTACATCATGTGGGTGAGA

2341 TTCACGCAAACCGGCATTAGTAATTTGTACAAATTGAGCTTTCTCAATCAATTCAGGAAT
2401 ATTAGCTGCACCACAGTATCCCATACCTGAACGCAGACCACCATCAATTTGGAAAACAAC
2461 ATCGCTAACATCGCCCTTGTATTCTACACGAGCTTCAACACCTTCTGGCACTAACTTGTT
2521 AGCTTCGTTAACTCCACCTTGGAAGTAGCGATCGCTTGAGCCGTGAGCTTGAGCCATAGC
2581 GCCCATAGAACCCATACCACGGTAACGCTTATACTTCTTACCATTATCTTCAAAAATATC
2641 GCCAGGAGCTTCTGTAGTACCGCTAAGCATGCTTCCGAGCATTACAGCATTGCCACCTGC
2701 AG
```

Figure 26. Alignment of the deduced amino acid sequence of PepE from *Lb. helveticus* WSU19 and the published amino acid sequences of thiol proteases from lactobacilli. Letter colors: black, dissimilar sequence; blue with turquoise background, conservative sequence; black with green background, similar sequence; red with yellow background, identical sequence; green, weakly similar sequence. Abbreviations: Lhel19-E, PepE from *Lb. helveticus* WSU19; Lhel32-E, PepE from *Lb. helveticus* CNRZ32; Laci-E, PepE from *Lb. acidophilus* NCFM; Lhel32-E2, PepE2 from *Lb. helveticus* CNRZ32; Ldla-W, PepW from *Lb. delbrueckii* subsp. *lactis* DSM7290; Ldla-G, PepG from *Lb. delbrueckii* susbp. *lactis* DSM7290; Laci-G, PepG from *Lb. acidophilus* NCFM; Lgas-C, PepC from *Lb. gasseri*; Ljoh-C, PepC from *Lb. johnsonii* NCC533; Ldbu-C, PepC from *Lb. delbruckeii* subsp. *bulgaricus* ATCC BAA-365; Lhel32-C, PepC from *Lb. helveticus* CNRZ32; Lhel53/7, PepC from *Lb. helveticus* 53/7; Laci-C, PepC from *Lb. acidophilus* NCFM; Lcas-C, PepC from *Lb. casei* ATCC 334; Ldla-C, PepC from *Lb. delbrueckii* subsp. *lactis* DSM7290; Lpla-C, PepC from *Lb. plantarum* WCFS1.

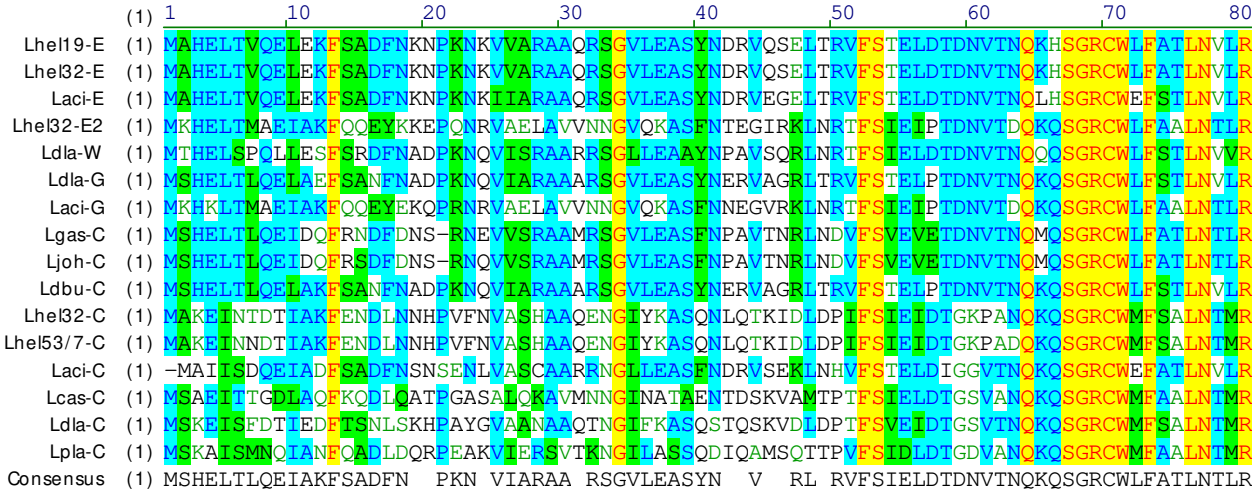

Figure 26 (continued)

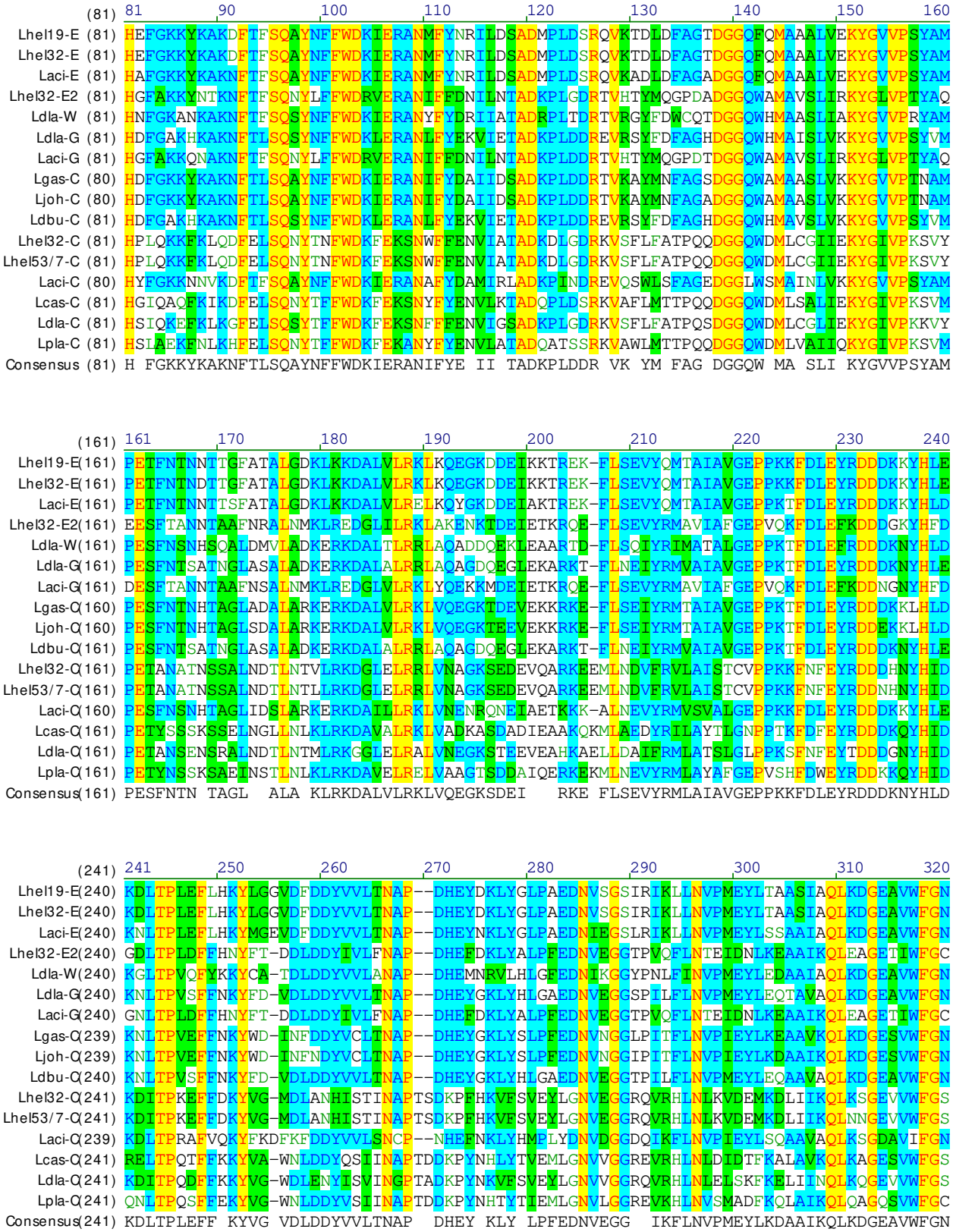

Figure 26 (continued)

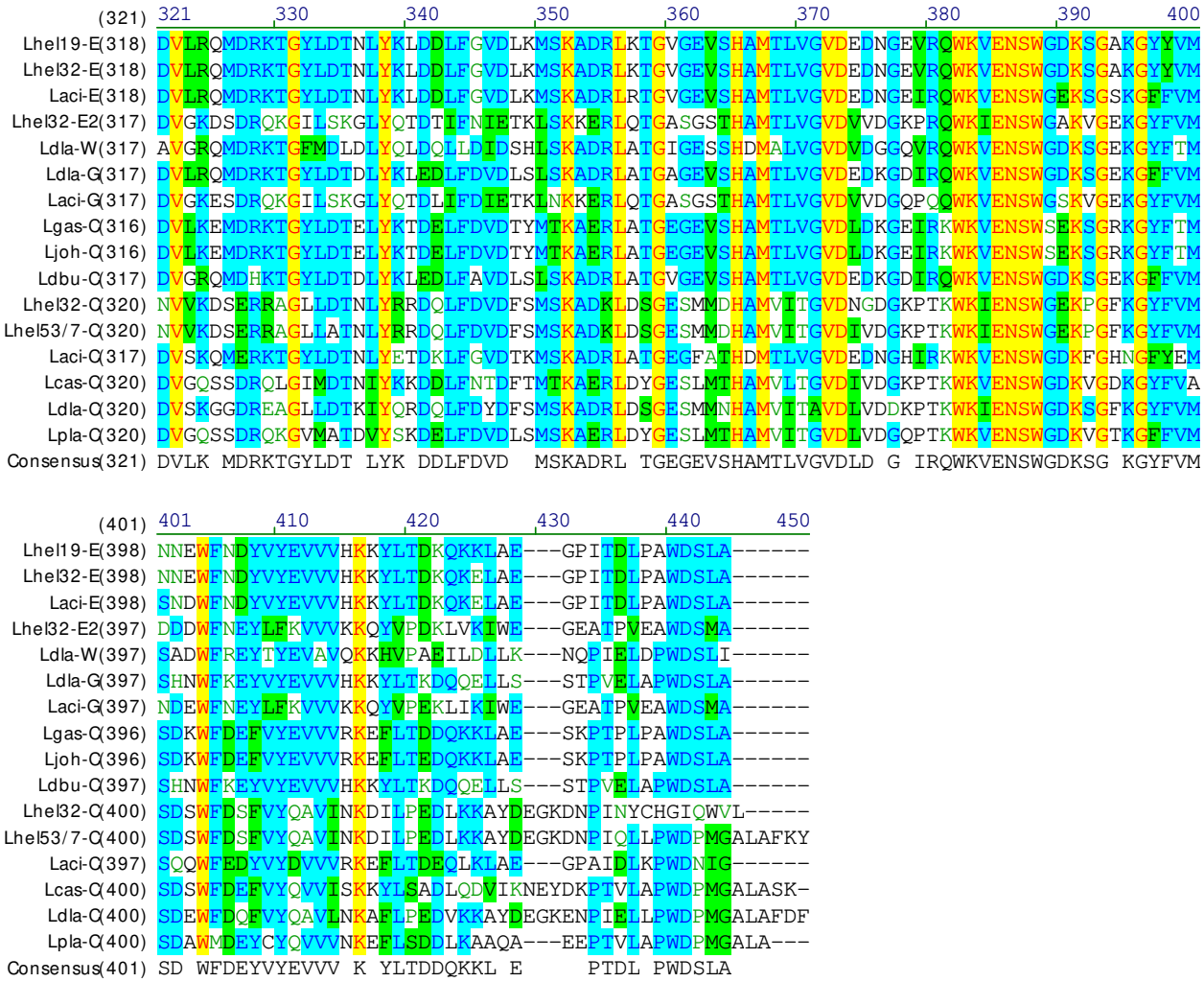

Table 9. Amino acid BLAST analyses for the deduced PepE sequence from *Lb. helveticus* WSU19

Thiol proteases	Bacteria	Identity (%)
PepE	*Lb. helveticus* CNRZ32	99
	Lb. acidophilus NCFM	89
PepE2	*Lb. helveticus* CNRZ32	52
PepG	*Lb. acidophilus* NCFM	63
	Lb. delbrueckii subsp. *lactis* DSM7290	52-69
PepW	*Lb. delbrueckii* subsp. *lactis* DSM7290	59
PepC	*Lb. gasseri*	43-68
	Lb. johnsonii NCC533	43-67
	Lb. delbruckeii subsp. *bulgaricus* ATCC BAA-365	59-69
	Lb. casei ATCC334	44-45
	Lb. plantarum WCFS1	44-49
	Lb. helveticus CNRZ32	42
	Lb. acidophilus NCFM	41
	Lb. delbrueckii subsp. *lactis* DSM7290	41
	Lb. helveticus 53/7	40

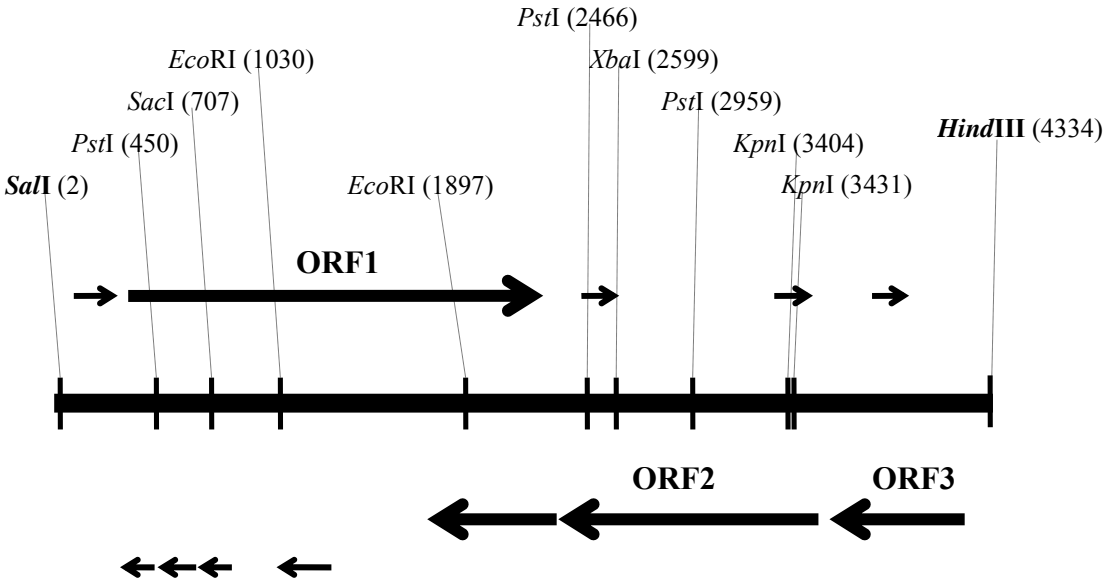

Figure 27. Open reading frame (ORF) and restriction enzyme analyses of the 4.3-kb *Hind*III-*Sal*I genomic insert containing the *pepO* gene from *Lb. helveticus* WSU19. The vertical lines represent restriction enzyme sites. The numbers in parentheses refer to nucleotide positions. The horizontal line represents genomic insert. The horizontal arrows represent ORFs; the arrows above the horizontal line correspond to the direct DNA strand; the arrows below the horizontal line correspond to the complementary DNA strand.

Figure 28. Nucleic acid sequence of the 4.3-kb *Hind*III-*Sal*I genomic insert and the deduced amino acid sequence of the PepO enzyme (in single-letter code) from *Lb. helveticus* WSU19. The numbers to the left refer to nucleic acids (bottom lines) and amino acid residues (top lines). The putative –10 and –35 promoter sequences are underlined and labeled. The putative ribosomal binding site is indicated in bold letters, underlined, and labeled rbs. The putative transcriptional terminator is indicated by the dotted horizontal arrows. Stop codon is indicated by asterisk. The zinc metallopeptidase motif is double-underlined and labeled.

```
   1 GTCGACACAGAAACGGAAACTTTAATTCAGGAAGGGTTAAAGAGACTCCGTAAAGGTCGT
  61 ACACTTTGGCAATTGCACACCGGCTTTCGACATCGCAGATGCTGATCAAATTATTGTGCT
 121 TGATCAAGTTCGAATTGTTGAAAGAGGTAATCACAAAGAACTGCTTGCCAAGAAAGGCTA
 181 TTATTACAATTTATATACCTTGCAAAAAAATGAAGGCGAAAATTAATGCGGAAGAACATT

 241 TGGCTAATCCTCAGACGTTCTTTTTGCTATAATGAATTTAAATGATTAAATAGTTATGAA
      -35                          -10

   1                    M  R  R  Y  L  A  V  R  G  G  A  G  D  V
 301 TATTTCTATAAGGAGCAAATATGAGAAGATATTTAGCTGTACGTGGCGGTGCAGGGGATG
               rbs

  15   A  E  P  D  L  N  A  K  P  Q  D  N  L  Y  L  A  V  N  S  E
 361 TTGCTGAACCTGATTTAAACGCTAAGCCACAAGATAATTTATATTTAGCCGTCAATTCCG
  35   W  L  S  K  A  E  I  P  A  D  Q  T  S  A  G  V  N  T  E  L
 421 AATGGTTGTCTAAAGCAGAAATTCCTGCAGATCAAACTTCTGCCGGAGTAAATACTGAAT
  55   D  I  K  I  E  K  R  M  M  K  D  F  A  D  I  A  S  G  K  E
 481 TAGATATTAAAATTGAAAAACGCATGATGAAAGATTTTGCGGATATTGCGTCTGGTAAGG
  75   K  M  P  D  I  R  D  F  D  K  A  I  A  L  Y  K  I  A  K  N
 541 AAAAGATGCCAGATATTCGTGACTTCGATAAGGCGATTGCCTTGTATAAGATTGCGAAGA
  95   F  D  K  R  D  A  E  K  A  N  P  I  Q  N  D  L  Q  K  I  L
 601 ATTTTGATAAAAGGGATGCTGAAAAGGCAAACCCAATTCAAAATGATTTACAAAAGATCC
 115   D  L  I  N  F  D  K  F  K  D  N  A  T  E  L  F  M  G  P  Y
 661 TTGATTTAATTAACTTTGATAAATTTAAGGATAATGCAACAGAGCTCTTCATGGGTCCAT
 135   A  L  P  F  V  F  D  I  D  A  D  M  K  N  T  D  F  N  V  L
 721 ATGCCTTGCCTTTTGTATTTGATATAGATGCTGACATGAAAAATACAGATTTTAATGTCT
 155   H  F  G  G  P  S  T  F  L  P  D  T  T  T  Y  K  T  P  E  A
 781 TGCATTTTGGTGGTCCAAGCACATTTTTACCAGATACAACTACTTATAAGACACCTGAAG
 175   K  K  L  L  D  I  L  E  K  Q  S  I  N  L  L  E  M  A  G  I
 841 CCAAAAAATTACTTGATATTTTAGAAAAACAAAGTATCAACTTGTTAGAGATGGCAGGTA
 195   G  K  E  E  A  R  V  Y  V  Q  D  A  L  A  F  D  Q  K  L  S
 901 TTGGTAAAGAAGAAGCACGTGTTTATGTTCAAGATGCTTTAGCCTTTGATCAAAAATTAT
 215   K  V  V  K  S  T  E  E  W  S  D  Y  A  A  I  Y  N  P  V  S
 961 CCAAGGTCGTCAAGTCTACTGAAGAATGGTCAGATTATGCTGCAATCTATAATCCGGTTT
 235   L  T  E  F  L  A  K  F  K  S  F  D  M  A  D  F  L  K  T  I
1021 CTTTGACTGAATTCTTAGCTAAGTTTAAGTCATTTGATATGGCTGACTTTTTAAAGACAA
 255   L  P  E  K  V  E  R  V  I  V  M  E  P  R  F  L  D  H  A  D
1081 TTTTGCCTGAAAAAGTTGAACGAGTAATTGTAATGGAACCACGTTTCCTTGACCATGCTG
```

Figure 28 (continued)

```
 275   E  L  I  N  P  A  N  F  D  E  I  K  G  W  M  L  V  K  Y  I
1141 ATGAATTAATTAATCCGGCAAACTTTGATGAAATTAAAGGCTGGATGCTGGTTAAATATA
 295   N  S  V  A  K  Y  L  S  Q  D  F  R  A  A  A  F  P  F  N  Q
1201 TTAATAGCGTAGCTAAGTACTTGTCACAAGATTTCCGTGCCGCTGCATTTCCATTTAACC
 315   A  I  S  G  T  P  E  L  P  S  Q  I  K  Q  A  Y  R  L  A  N
1261 AAGCAATTTCAGGTACGCCAGAATTGCCTTCTCAAATTAAGCAAGCCTATCGTTTAGCTA
 335   G  A  F  D  E  V  V  G  I  F  Y  G  K  K  Y  F  G  E  E  A
1321 ATGGTGCTTTTGATGAAGTTGTTGGTATTTTTTATGGTAAGAAATACTTTGGTGAAGAAG
 355   K  H  D  V  E  D  M  I  H  N  M  L  K  V  Y  E  Q  R  I  N
1381 CTAAACACGATGTCGAAGATATGATTCACAATATGCTTAAAGTATATGAGCAAAGAATCA
 375   D  N  N  W  L  S  E  D  T  K  K  K  A  I  I  K  L  R  A  L
1441 ATGATAATAATTGGTTATCTGAAGATACTAAGAAAAAGGCAATTATTAAATTAAGAGCTT
 395   V  L  K  I  G  Y  P  E  K  I  E  K  I  Y  D  L  L  Q  I  D
1501 TAGTACTTAAGATTGGTTATCCAGAAAAAATCGAAAAGATTTATGATCTTTTGCAAATTG
 415   P  E  R  S  L  Y  E  N  E  A  Q  M  A  T  V  R  T  K  Y  M
1561 ACCCAGAAAGGAGTCTTTATGAAAATGAAGCTCAAATGGCAACGGTACGCACCAAGTATA
 435   L  D  K  L  T  Q  P  V  D  R  S  V  W  L  M  P  G  N  L  N
1621 TGCTCGATAAATTAACTCAGCCAGTAGATCGCTCAGTATGGCTCATGCCAGGAAACTTGA
 455   N  A  C  Y  D  P  Q  R  N  D  L  T  F  P  A  G  I  L  Q  A
1681 ACAATGCTTGTTATGATCCACAAAGAAATGATTTAACTTTCCCAGCTGGTATTTTGCAAG

                                                                (zinc
 475   P  F  Y  D  I  H  Q  S  R  G  A  N  Y  G  G  I  G  A  T  I
1741 CGCCATTTTATGATATTCATCAATCCCGTGGTGCAAATTACGGTGGTATCGGTGCAACTA

      metallopeptidase motif)
 495   G  H  E  V  S  H  A  F  D  N  S  G  A  K  F  D  E  H  G  N
1801 TTGGTCATGAAGTTTCTCATGCCTTTGATAATAGTGGTGCTAAATTTGATGAACACGGAA
 515   M  N  N  W  W  T  D  E  D  F  A  E  F  N  K  R  V  G  Q  M
1861 ATATGAATAACTGGTGGACTGATGAAGACTTCGCTGAATTCAATAAGCGGGTTGGCCAAA
 535   V  D  I  F  D  G  L  Q  Y  G  P  A  K  I  N  G  K  Q  V  V
1921 TGGTTGATATTTTTGATGGCTTGCAATACGGTCCAGCTAAGATTAACGGTAAGCAAGTAG
 555   G  E  N  I  A  D  L  A  G  L  A  C  A  V  Q  A  G  K  N  D
1981 TAGGAGAAAATATTGCTGACTTGGCAGGGCTTGCTTGTGCTGTTCAAGCTGGTAAGAACG
 575   N  V  D  L  K  D  L  F  E  N  Y  A  R  S  W  M  Q  K  Q  R
2041 ACAATGTTGATTTGAAAGACTTGTTTGAAAATTATGCAAGAAGCTGGATGCAAAAGCAAC
 595   P  E  A  I  K  T  E  V  Q  V  D  V  H  A  P  Q  P  T  R  V
2101 GTCCAGAAGCAATTAAAACTGAAGTGCAAGTTGACGTTCATGCACCACAACCAACTCGTG
 615   N  I  P  V  Q  C  Q  D  D  F  Y  T  A  F  D  V  K  P  D  D
2161 TAAATATCCCAGTTCAATGTCAAGACGATTTCTACACTGCATTTGATGTTAAGCCTGATG
 635   G  M  W  L  D  P  E  D  R  I  T  I  W  *
2221 ATGGCATGTGGCTTGATCCTGAAGATAGAATTACTATTTGGTAATTTAGACAAAATAAAA

2281 ATGACTACTGGATTTTTCCAGTAGTCATTTTTGGTTTGCACTTATTTATTATTAAGCATG

2341 TAATCACGGGTCATTGGCAAGTTCTTACCAGATAGGCCCTTAGTTAAAAGATATTGTACA
2401 ACATCAATGTTGCCTGATTCAAAGCTGGCAGCACATGCTTGAAGGTACATATCCCACATT
2461 CTGCAGAATCTTTCGCCCATCTTCTTTTCAATTTCAGGACGAGCATTGTTAAAGTTCTTG
2521 TCCCAAATTTCCAAAGTCCTTTGGTAGTGACGACGGAGCATTTCAACGTCACTAATTTGC
2581 AAGTGAGCTTCTTCAATTCTAGAAATAATTTCAACTAAACCTGGAATGTAACCACCTGGG
2641 AAGATGTATTTATTAATCCAAGCATTAGTGGCACCGCCTTGTTGACGAGTAATACCATGG
2701 ATTAATGCTACACCATCGGTCTTTAAGTATTTAGCTACATCATTGAAGTATTCACTCAAG
2761 TTTTCAGAACCAACGTGTTCAAACATACCAACTGAAGTGACGTAATCCCATTGTTGATCA
2821 CCTAATTTACGATAATCTGCAAGTTTAACTTCGGCAACATCTTGCAAGTTTTCGGCATAA
2881 ATCTTCTTTTGAACTAACTTGTATTGTTCTTCACTCAAAGTAACACCGGTAACTTTAAGA
```

Figure 28 (continued)

```
2941 CCATATTCTTTAGCTGCAGTGAGCATCAAAGTACCCCAGCCACAACCGATATCAAGTAAA
3001 GTCTTTCCTTTTTGTGGGTGTAACTTGTTTAAAATGTGATGTACTTTGGCGATCTGAGCT
3061 TGTTCAAGATCATCTTTATTATCGTCCGTAAAGTAAGCACATGAATAAGTCAAGGTTGGG
3121 TCAAGCCATTGTTCGTAGAAATCATTACCGATATCATAGTGACTTTGAACGTCCTCTTCA
3181 CTTTGCTTTTCAGTATGTTTAGTTTTAGGCAAGAATTTACGGAATTTGGATGAACGCATG
3241 AAACTGTCGGCACTTTCGTATACGCCGTCAATTAATTTTTGAATGCTGCCATGGATTTCA
3301 ATTTTCTTGTCCATGTATGCTTCACCAAGTGCTAGGGATGCATTTCTTGTAATGTCGCCC
3361 ATTGGAATTTTTTCATTGAAAACTATTTCAATTTCTGGGGTACCGTTACCATATACTTCT
3421 TCTGGGGTACCGTTACCATATACTTCGCTTTTACCATCCCAATAAGTTACTTTAACGGGA
3481 AAAGGGAAGGACTTACTGAGCATCATTTTGTAAAAGGCTTTTTCTAACAATGTAATTTCC
3541 TCCACTAATTATTAAACCTAATTAGTTACGTATTTTAACGCTAAAATTTTTACTTGGCAA
3601 CATAGTGAAAATTAGGATCAAGTTCATCATCTAATTTCTTCCAAGCGTCTTCTAATTGCT
3661 GATAAATGATTTTTTCATTTTCATGGGTTAATTTAGTTTTGCGATCAATAGTGATTGGAT
3721 CACCAAAATTAACCTCTAATCCTTTTCGTTTTAATAAACCCTTGAAGGATAAAGGCCCTT
3781 GATAAACCACCGGAACCATTGGCTTTTGTGACATTTTAGAAATTAAAAGCGCACCACCTT
3841 TTAATTCAGCTGAATGTCTTGTGCCAGATGGAAAAATGATGAGTGATAGTTCACCTTTTC
3901 TTAACCCTTTAACTGGAATCTTCAATGCAGATGGACCAGGTTTTTTCCGGTCAACAGGGA
3961 AGGCATGGACATGATCTAAAATAAAACGTAAAACCGGATTTTTAAACAGTTCTATTTTCG
4021 CCATGGACATAAATTCCATTGGACTGGCACCTAAAGCAAATAAAATAGGTTCCCACCAAG
4081 TACGGTGAGGTGCAACTAAGATATAGCTGCCTTTAGGCAAACGATTCTTATGGTGAATGT
4141 GTAAATGTCCATTTAATACCCATACAATAAAGCGGGCAATCGGACGGATTATTTTATAAA
4201 ACATCTTTTTTGTTCCTCCAATTGTTGTAATATTACGCGTGGTGCTAGTTAAATCGTTTT
4261 AGTTAAATAAAAAGTCCAATCTTGTTAAACTCGACTTGTAAATAGTAATAATAGAAAAGA
4321 GTCTGACTAGATTG
```

Figure 29. Alignment of the deduced amino acid sequence of PepO from *Lb. helveticus* WSU19 and the published amino acid sequences of PepO from lactobacilli. Number 2 after species designation indicates multiple amino acid sequences from the same species. Letter colors: black, dissimilar sequence; blue with turquoise background, conservative sequence; black with green background, similar sequence; red with yellow background, identical sequence; green, weakly similar sequence. Abbreviations: Lhel19, *Lb. helveticus* WSU19; Lhel32, *Lb. helveticus* CNRZ32; Laci, *Lb. acidophilus* NCFM; Ljoh, *Lb. johnsonii* NCC533; Lpla, *Lb. plantarum* WCFS1.

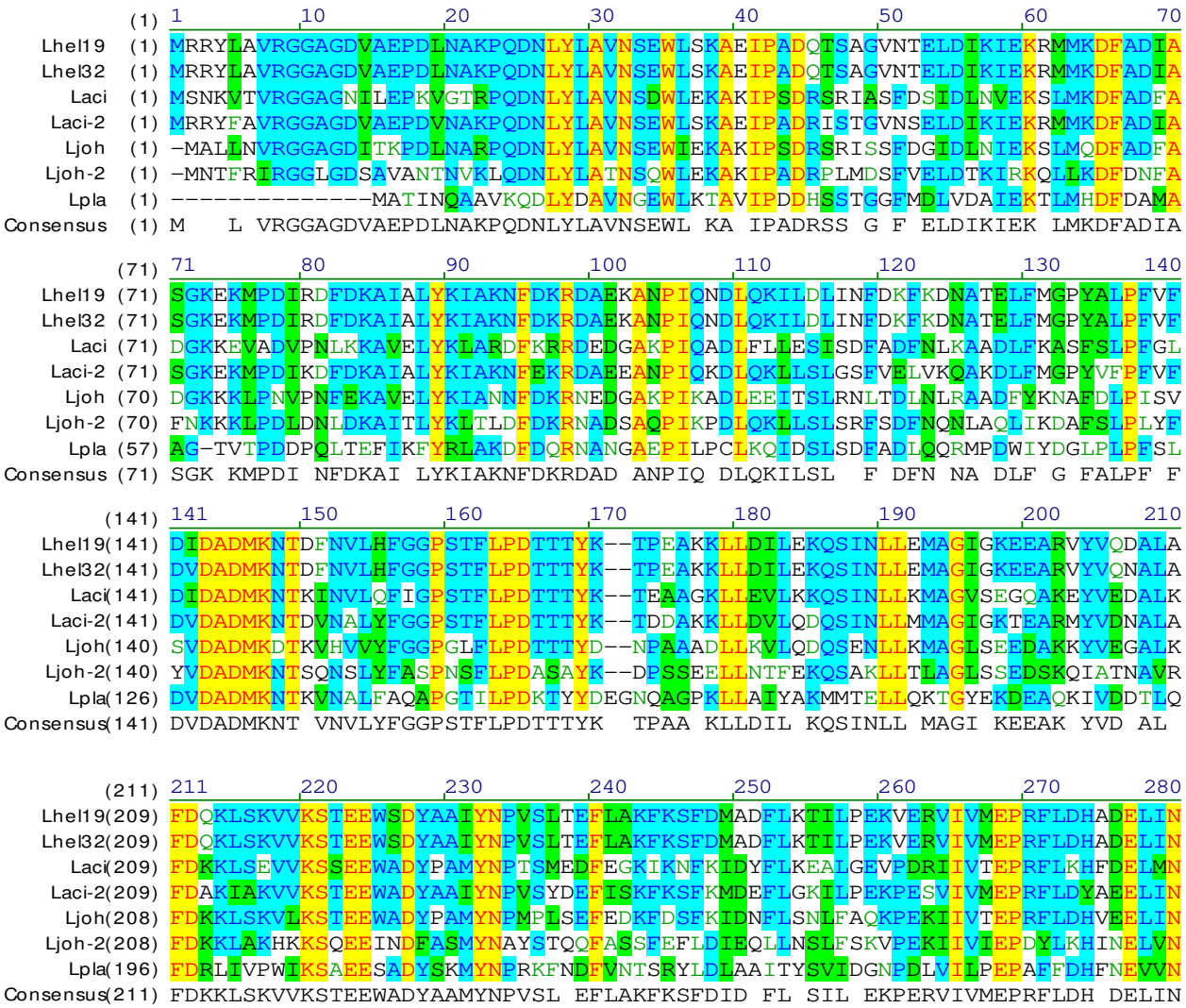

Figure 29 (continued)

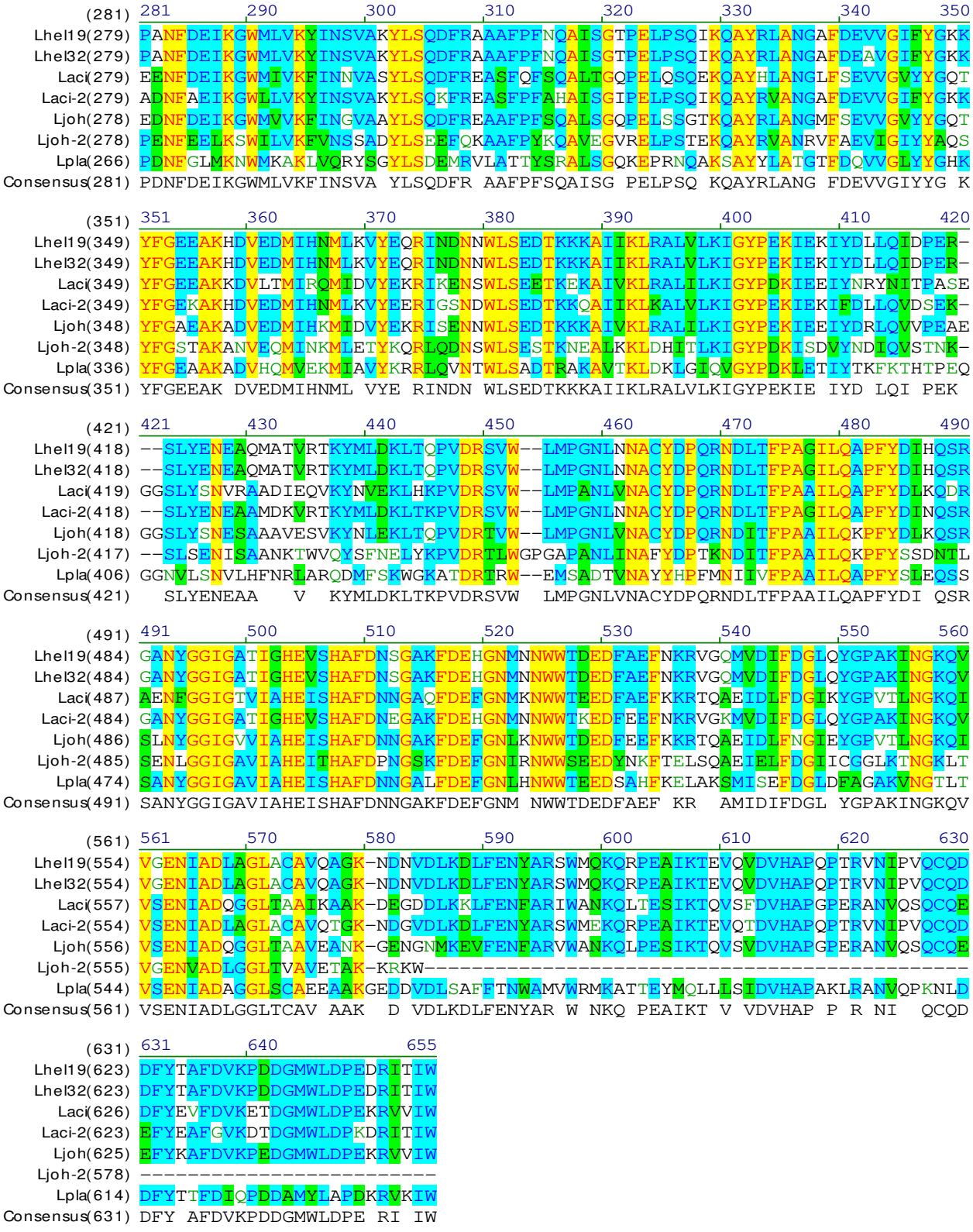

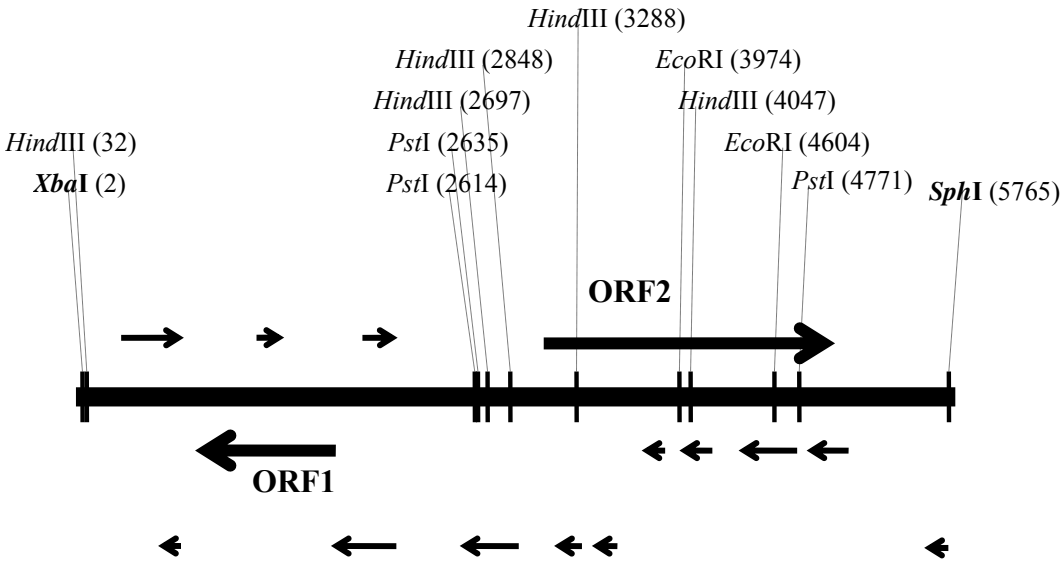

Figure 30. Open reading frame (ORF) and restriction enzyme analyses of the 5.8-kb *Xba*I-*Sph*I genomic insert containing the *pepO2* gene from *Lb. helveticus* WSU19. The vertical lines represent restriction enzyme sites. The numbers in parentheses refer to nucleotide positions. The horizontal line represents genomic insert. The horizontal arrows represent ORFs; the arrows above the horizontal line correspond to the direct DNA strand; the arrows below the horizontal line correspond to the complementary DNA strand.

Figure 31. Nucleic acid sequence of the 5.8-kb *Xba*I-*Sph*I genomic insert and the deduced amino acid sequence of the PepO2 enzyme (in single-letter code) from *Lb. helveticus* WSU19. The numbers to the left refer to nucleic acids (bottom lines) and amino acid residues (top lines). The putative –10 and –35 promoter sequences are underlined and labeled. The putative ribosomal binding site is indicated in bold letters, underlined, and labeled rbs. The putative transcriptional terminator is indicated by the dotted horizontal arrows. Stop codon is indicated by asterisk. The zinc metallopeptidase motif is double-underlined and labeled.

```
   1 TCTAGAACTTTTACTCCATAACGCTCCATTAAGCTTAATACATATCTTAAATTACCAGAA
  61 GTAACATTGTATTCTCTACCTAATTGCTCAACTGATTTACCATAATTTTTCCAGCTATTG
 121 TAAATATCAATTTTGTCTTGTTTAGATAATTTGGACATAACAAAAACCTCGAAATTCTTG
 181 TCCGAATTTCGGGGTTCATATCAAATTTGGACTTGAGCTAAAACAAAAAGACCAGTAGTC
 241 TGATGTTAACCAAAAAAACACATTAGAAGCTGGTCTTTTATGGAATCTATTATAACTGAT
 301 ATCGTGAAAATTATTAAGTCTGAAAATAATGTTATTGCCCGTGAAAAGGCATTAATGTGC
 361 TACTTCTTTGATCTGATTAGAGAATTGATGACAGCAGCACTAGAAGAAGTTGATGCTGGT
 421 CTAGTTGAAGAGACTAAAAAGCAAGGCTATCAGATCGAGAAGAAAAATAAGCGTTCAGTT
 481 GTGACTGCCTTTGGTGAAATCAGCTATTGGCGCAGAAGATATGCTTGTCCAGGCAAGAAG
 541 AAACCGCTGACTCAGCAGGACAGAGAGCTGAGTCAGCGGTTTCTTCAATTCGAATCAAGG
 601 TCGAGCATGTATTTGGCAAGGTCAAAGCATACAAAATATTTTCTACTACGTATCGCAATC
 661 ATCGCCGACGTTTTAATTTAAGAATGAATTTAATCTGCGGGATCATCAGCCAAGAACTGG
 721 CTATCTAGTTTCGCAGTAACTCTATTATTTCAATCTTTTTCTGTCCATTCGTTTTACTAC
 781 ATAAAATATTGGCAAACCTACAATTACGATGCCAATGAATAATAAAACTCCAGCAGGATC
 841 GTTGATCAATTCACTAATAAGTACAAATAAGCCACCTAGGATAGCTACGATTGGAACAAG
 901 TGGATAAAGCGGTGTGCTGAATGGACGCGTTTTGTTTTTCTTACGCAAGATAAAGATGCC
 961 GAAGAATGCTAATAAGTAAAAACAATAGACAGTAAATACGCACAAGTCTGACAAATGATC
1021 TGGTTCAAAGAACATCATCATGATAGTAGCCAATACTATGATGAATAAGGTTGCAACCAC
1081 TGGTGATTTACCTTTAGGAGTGACATATGACAAATATTTTGAAAATGGAAGGTCGCCACG
1141 TCTAGCCATTGCGTAGACAATTCGAGGGAATGTCAGCATCTTGCCATTCAAGGTTCCCAT
1201 CATTGAGATGATAATTCCAGCAGAAAGCAATTTCCCTCCGATTGTGCCGAAGACCTTAGT
1261 TGCTAAATATGCGGTCGTATTTTCACCCAAACGATGGATTAAACCTACTGGCAAAAAGCG
1321 AAAAATCCCGATTGTTACTAGTGTATAGATCACAAGTACAGAACTAATACCCAAAATAAT
1381 AGCTTTAGGCAACAACTTTTGTGGATTCTTAATTTCGCCACCTAGATTGGCAATTAAGAT
1441 CCAGCCATCGTAGGCAAACAAGGTAGCTAAAACAGCAACGCCAAAGCCGCCAGTCGATTG
1501 ATTGACTTGACTAATGGTTTGCCCTAACGCATCTTGATGTCCCCAAAAGATACCGCAAAT
1561 TACAATAGCTGCAATTGGAATCATCTTAACGATGGTAGTAATGACAGAGAAAACCGCACC
1621 AACTTTGTTTTCCAGGAAATTTAATAATCCTATAGCGATAACGGTAACATCGCTAAAGGG
1681 ATGCTCCAATTAGGACCAAGTCCGAAGAAATTAGCCATCAAAATACTCATGAAGCCGGCT
1741 ACTGAAGCAATAATCGCAGGACCATAGACGATGATCTGCATCCATCCTGCCATAAAGCCG
1801 CAAATTCGACCATACAGATTTTCAATATACACATATAAACCACCAGTGTATGGCATCTGA
1861 GCACCGATTTCAGCAATCGTTAATCCACCTGTCAGCGTGATCAATCCACCAAAAATCCAG
1921 GCGATAATTGCCATTGTACTTGAACCGGCACTATCCAATACGGAAACTTGCTTAAAAAAT
1981 ATGCCTGAACCAATGATTGTACCGATTACGATTGAAATGGCTGAACCAAAACCGATTGAA
2041 CGTTTTAGGTTATTGTTGGGGTGTTTATCTACCATAATTATTTCCTCCATGAAAAAAGCC
2101 TGAGCCTACTTAATTATCACCTGAGCCTACTTAATTATCATGAGTAGGTTTAGGCTATGA
2161 ATTATCTGTATGCCAAACCTACTCAAGTTCAACGGGAAGAACTTGAGCTAGATGAAGTTG
```

Figure 31 (continued)

```
2221 AAGCTACATTGGCGTTAAGATAAAACATGATTTTTTCCTCTTTCAATTAATTTTTATTAG
2281 AATATCATGAGCTTTTTAATATGGCAAGATATTTTTAAGGCCGATTGTAAAATTAAGTTG
2341 AACACTTTGTAAAAAATAAAAGTCCATCTGGACCTGTTTGATAGAATGTTAATAACCACA
2401 AAAACATCTATTGGAGGTCACAAATGGACTCTTTACATTCAGCGAGATATTTTTAAACAA
2461 AAAAGCTGGGGAAAATGCCCAGCTTGATTGCTATTTTAATTAAGTTTTTATGCAAATACT
2521 TCTTCGATGTTTAAGTTAACTACGAATGCATTTGGAAATTCAGTCTTAGCTAAAACTTTC
2581 TTTGCGTAGTCATCATCTTCGTGAACTTCTGCAGTAGCAAGTACCCTAACTGCAGTATGT
2641 GATGGAACATCAGCTGCAACAAGAGCAACCTTTGAACCGCGCTTAATGTTTTCGTAAGCT
2701 TCACCCTTGGTCTTTTCAAGGTATTGTAAGTGACTTGGATCTAAGACAGTCATTGAGCCC
2761 TTAGGACCAACTTGTGGGTTGCCGTCAGCATCAACAGTTGCTAAGTAAACTAAGTTATTC
2821 TTGAAAAGATTTACTTGTTCTTCAGTAAGCTTGTTAGTATTTAATTTCTTCATAGACAAT
2881 ACATCCTTTCTGTTTTGTCGATACACTATAAGTATACATCAATTTAATAGCAGGTGTTAG
2941 GGATTTGCTTACATCCTTATTTTTATTTAAAAAAATGCTTTTATTACTATAAAATAAGCA
3001 AAATTAAATTTTCATTTTATTTTAAAAAATGCTATGATTTAACCAACTAAAAAACAAAGG
             -35                      -10                    rbs

   1         M  N  L  A  K  I  R  G  G  A  G  D  I  T  K  P  D
3061 AGAAAACATATGAATTTAGCAAAAATCCGCGGCGGTGCTGGTGATATCACCAAGCCCGAT

  18 L  N  A  R  I  Q  D  N  L  Y  L  A  V  N  S  D  W  I  S  K
3121 CTCAATGCCCGCATTCAAGATAACTTATACTTAGCCGTTAACTCTGACTGGATTTCTAAA
  38 A  K  I  P  A  D  R  P  L  I  S  S  F  S  E  I  D  L  K  I
3181 GCCAAGATCCCTGCCGATCGTCCATTAATCAGTAGTTTCAGTGAAATTGATTTAAAAATC
  58 E  K  E  L  M  N  D  L  A  D  F  A  S  D  K  K  A  L  P  D
3241 GAAAAAGAATTGATGAACGACTTAGCTGATTTTGCTTCTGATAAAAAAGCTTTGCCTGAT
  78 I  P  N  F  D  K  A  I  E  V  Y  K  L  A  K  D  F  A  K  R
3301 ATTCCTAACTTTGACAAGGCAATCGAAGTTTATAAATTAGCTAAAGATTTCGCCAAAAGA
  98 D  A  D  G  F  Q  P  A  Q  A  D  L  E  T  L  I  N  L  K  Y
3361 GATGCCGATGGCTTTCAACCTGCTCAAGCTGATCTTGAAACTTTAATAAACTTAAAATAT
 118 V  D  D  V  K  Q  N  L  A  K  L  L  L  R  F  S  F  P  F  L
3421 GTCGATGACGTCAAGCAAAATCTAGCAAAATTATTATTGCGCTTTAGCTTTCCATTTTTA
 138 F  E  V  E  P  D  R  K  N  T  K  T  N  S  L  S  F  D  R  N
3481 TTCGAAGTTGAACCTGATCGTAAGAATACGAAGACCAATTCTCTTTCCTTTGATCGCAAC
 158 S  L  I  L  P  D  T  T  S  Y  Q  S  P  S  A  K  H  L  L  D
3541 TCATTGATCTTGCCTGACACTACTAGTTACCAATCACCTTCTGCTAAGCATTTGCTCGAT
 178 V  W  Q  K  Q  T  E  N  L  L  K  M  A  G  V  E  E  A  A  A
3601 GTTTGGCAAAAGCAAACCGAAAACTTGTTAAAGATGGCTGGTGTTGAAGAAGCTGCTGCT
 198 K  K  Y  V  T  D  A  I  A  F  D  A  K  I  V  K  V  A  K  S
3661 AAGAAATACGTCACTGATGCGATTGCATTCGATGCTAAAATCGTTAAGGTTGCAAAATCA
 218 A  E  E  R  A  D  D  V  A  L  Y  N  P  I  K  T  N  E  F  E
3721 GCCGAAGAACGTGCCGATGATGTAGCTCTTTACAACCCAATCAAGACTAACGAATTTGAA
 238 E  K  T  S  S  L  N  L  D  Q  L  L  E  Q  L  F  E  K  K  P
3781 GAAAAGACTAGCTCTTTGAACTTGGATCAGTTGCTTGAGCAGCTCTTTGAAAAGAAGCCA
 258 N  Y  V  V  V  R  E  P  K  F  L  D  H  F  N  E  L  F  N  Q
3841 AATTACGTTGTAGTACGTGAACCAAAATTCTTGGACCACTTCAACGAATTATTTAATCAA
 278 E  S  F  D  E  L  K  G  W  L  I  S  T  F  I  N  K  A  A  A
3901 GAGAGCTTCGATGAACTTAAAGGTTGGTTAATCTCTACCTTCATTAATAAAGCTGCCGCG
 298 F  L  S  E  E  F  R  Q  A  A  F  P  F  K  Q  A  T  Y  G  Q
3961 TTTTTATCAGAAGAATTCCGTCAAGCTGCCTTCCCATTTAAGCAAGCTACTTATGGTCAA
 318 K  E  L  P  S  Q  E  K  E  A  Y  Y  K  A  N  N  L  F  D  D
4021 AAAGAATTGCCTAGTCAAGAAAAGGAAGCTTACTACAAAGCTAATAATTTGTTTGATGAT
 338 V  I  G  V  Y  Y  G  R  T  Y  F  G  E  D  A  K  A  D  V  E
4081 GTAATCGGCGTTTATTATGGTCGCACTTACTTCGGCGAAGATGCCAAGGCCGACGTTGAA
 358 D  M  I  H  R  M  I  D  V  Y  E  Q  R  I  T  N  N  E  W  L
4141 GATATGATTCATCGCATGATCGATGTCTACGAACAACGAATTACCAATAATGAATGGCTC
```

Figure 31 (continued)

```
 378 S  P  A  T  K  E  K  A  I  T  K  L  R  A  L  V  L  K  I  G
4201 TCACCTGCTACTAAGGAAAAGGCAATTACTAAGTTGCGCGCCTTGGTTTTAAAGATTGGT
 398 Y  P  N  K  I  D  H  V  Y  D  L  F  Q  V  T  P  A  N  E  G
4261 TATCCTAATAAAATCGATCACGTTTACGATTTATTCCAAGTTACTCCAGCAAATGAAGGT
 418 G  N  L  Y  S  N  Q  A  N  I  R  E  V  S  L  K  H  N  F  D
4321 GGCAACCTCTACAGTAATCAAGCAAATATTCGTGAAGTCAGCTTAAAGCATAATTTCGAT
 438 K  L  Y  K  P  V  D  R  S  E  W  Y  M  P  G  N  L  I  D  A
4381 AAACTGTACAAGCCAGTTGACCGCAGCGAATGGTACATGCCAGGAAACTTGATCGATGCT
 458 C  Y  D  P  Q  R  N  D  I  T  F  P  A  A  I  L  E  A  P  F
4441 TGTTACGATCCACAGAGAAACGATATTACCTTCCCTGCCGCTATCTTGGAAGCACCTTTC

                                                        (zinc metallo-
 478 Y  D  I  N  A  S  R  A  T  N  Y  G  G  I  G  V  V  I  A  H
4501 TACGACATCAATGCTTCTCGTGCTACTAACTATGGCGGTATTGGTGTGGTAATCGCCCAC

     peptidase motif)
 498 E  I  S  H  A  F  D  N  N  G  A  K  Y  D  E  F  G  N  M  K
4561 GAAATTTCTCACGCATTCGACAACAACGGTGCCAAGTACGATGAATTCGGCAACATGAAG
 518 N  W  W  T  K  E  D  F  A  E  F  E  K  R  T  Q  A  E  I  D
4621 AATTGGTGGACCAAGGAAGACTTTGCGGAATTTGAAAAGCGTACTCAAGCTGAAATCGAC
 538 L  F  D  G  I  K  Y  G  P  V  T  L  N  G  K  Q  I  V  S  E
4681 TTGTTCGATGGCATTAAGTATGGTCCTGTAACTCTTAATGGTAAACAAATCGTTAGTGAA
 558 N  I  A  D  Q  G  G  L  T  A  G  I  E  A  N  K  N  E  H  G
4741 AACATCGCCGACCAAGGTGGTTTAACTGCAGGTATTGAAGCTAATAAGAATGAACATGGC
 578 D  M  K  E  L  F  E  N  Y  A  R  I  W  A  S  K  E  S  P  E
4801 GACATGAAAGAACTATTCGAAAACTATGCTCGCATTTGGGCAAGTAAAGAATCTCCTGAA
 598 I  I  K  T  I  A  A  F  D  V  H  A  P  G  P  V  R  V  N  V
4861 ATCATTAAGACAATTGCCGCATTCGATGTTCACGCTCCAGGTCCTGTAAGAGTTAACGTT
 618 Q  V  Q  C  Q  P  E  F  Y  K  A  F  N  V  Q  E  G  D  G  M
4921 CAAGTGCAATGCCAACCTGAATTTTACAAAGCCTTCAATGTTCAAGAAGGAGATGGCATG
 638 W  L  D  P  A  K  R  V  V  I  W  *
4981 TGGCTTGACCCTGCTAAACGCGTAGTCATTTGGTAAATTTTTAATCAATAAATCTAAAAT

5041 CCTATTAAATCTTGGTATTAACCTTGAATTAATAGGATTTTTTGCTTCATTAAGCATCGC

5101 TATTTCCTAGGTACATACAGTTTTCTTGATTTCTAGCTTTCAAGTTCCAGTTATTAACTA
5161 TAATTGATAATTGAAATTAAATTGTTCACATTTTATACTTTACTTAATAAATATTGTTTA
5221 ATTTAATTTGAGGAGTATAAAATGAGATCACGTCATGTAAATGGAATCATTACGAGTTTA
5281 GCTGCAAGTGCCTTAATGGGGCTATTTTTAACAAGTGTCCAAGTTAAAGCAGATACACAA
5341 CAAGTTCAGCAACCAGTTGCTCAAACTACTCAGCAAAATGCTGATTCAACAAAGCAATCT
5401 TCAACTACTGTTTATACTGAAAGCTCGAAAGAAGTACCAGTAGTCAGTTACACTGATCAC
5461 CAGTCAAAGCCGAACAATGATCATTGGTCAAATCCCGCTAAATATAAAGATGCCATTCCT
5521 GTACAAATTTTAGGTATCAATGATGTACACGGAAATATTGATACCACTGGTAAAACTTGG
5581 ATTGGCTATCGTTCCTACCAAAACGCAGGTAATGCTGCCAGATTGGCTGGATATTTGAAC
5641 AATGCCGAATCTGATTTTAAAAAGAAAAATCCAAATGGAACAACTATCAGAGTTGAAGCT
5701 GGTGACATTGTGGGAGCATCTCCAGCAACTTCTTCATTATTGCAAGATGAACCTACAATG
5761 CATGC
```

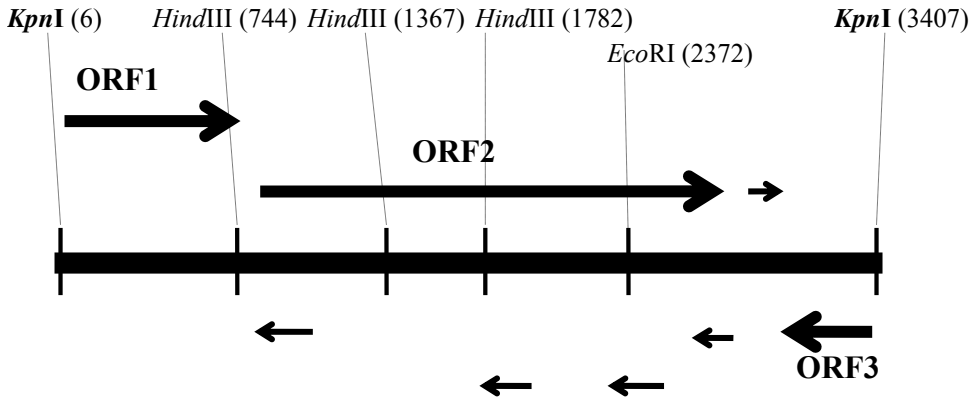

Figure 32. Open reading frame (ORF) and restriction enzyme analyses of the 3.4-kb *Kpn*I genomic insert containing the *pepO3* gene from *Lb. helveticus* WSU19. The vertical lines represent restriction enzyme sites. The numbers in parentheses refer to nucleotide positions. The horizontal line represents genomic insert. The horizontal arrows represent ORFs; the arrows above the horizontal line correspond to the direct DNA strand; the arrows below the horizontal line correspond to the complementary DNA strand.

Figure 33. Nucleic acid sequence of the 3.4-kb *Kpn*I genomic insert and the deduced amino acid sequence of the PepO3 enzyme (in single-letter code) from *Lb. helveticus* WSU19. The numbers to the left refer to nucleic acids (bottom lines) and amino acid residues (top lines). The putative –10 and –35 promoter sequences are underlined and labeled. The putative ribosomal binding site is indicated in bold letters, underlined, and labeled rbs. The putative transcriptional terminator is indicated by the dotted horizontal arrows. Stop codon is indicated by asterisk. The zinc metallopeptidase motif is double-underlined and labeled.

```
   1 GGTACCTTGGATCGTTGGATATTTGTATGATTACTCAGTTACTTTGCTGTTCGTGATTGC
  61 GGCACTGCTCTTTGTCATTGCCTTCATCAATGCGTTGTTTAATTATCGACCAATCATTGG
 121 CTTTCATAAGGAGAGAGTTGCTAAGGGCCAGAGTGGGGATACACAAAAAGCGGTTCCTAT
 181 GCCTAAGCGCAACTTCATTATGACGATGGCCTTCTTCACAACGCTAGGCGTAACTTGGCT
 241 AATGTACATGAACTGGGAATCTAACTTGTCTGTTTATATGGTGTCATTAGGCATCCCATT
 301 CCACTTGTACAGTTTGCTTTGGACTTTAAATGCCAGTGTGATTGTAATTATGCAGGGAAT
 361 TTTGGCTAGATTTCCAAATATGTTCAAAAATCTTTTCCATCAGATCATCTTTGGAATTTG
 421 CATGTTCTCACTGTCTTTCATTACATTAGTCTTTGCCAAAGATTTTGCTCACTTTGCACT
 481 ATCAATGTTTATTTTGACTTTGGGTGAATCTACCGCCTTTCCAGCTATTCCAGCCTACGT
 541 GAATGATTTATCACCTAAAACAAGTAAGGGTAAATATCAAGGAGCAACGATGGCTGCCAG
 601 CGGTATTGGCCGTGCCTTTGGCCCGCTATTTGGTGGTCTAGTAATTGATCAAGCAGGCTA
 661 TATTCCTTTCTTCTGGGTAGCTGCGATTGTAATTGCCTTGATGATCGTCATGATGATTCC
 721 AATTTATTTAAAGTTAGCCAAAAAGCTTACTTTGTATAAGTAAAAAAGCAGACTATATTA
                                   -35                   -10
 781 AATCAAAATGATATACTTAGAATGATTTAATATTAATTTGATAATAAGGGGGATTTCTCT
                                                  rbs

   1             M  T  V  R  G  G  A  G  D  I  T  E  A  D  L  S
 841 TTGAACAATAAAATGACTGTACGCGGCGGTGCTGGCGACATTACTGAAGCCGATTTATCA
  17 A  R  P  Q  D  N  L  Y  L  A  V  N  S  E  W  L  K  N  A  K
 901 GCTCGTCCACAAGATAATTTATACTTAGCCGTTAACTCAGAATGGTTAAAGAATGCCAAG
  37 I  P  S  D  R  S  R  T  S  S  F  D  G  I  D  L  N  I  E  K
 961 ATTCCATCAGATCGTTCCAGAACTAGTAGTTTTGATGGTATTGACTTAAACATTGAAAAA
  57 E  L  M  Q  D  F  A  D  F  A  D  G  K  K  D  L  P  D  V  P
1021 GAATTGATGCAAGACTTTGCAGATTTCGCAGATGGCAAAAAAGATTTGCCAGATGTACCT
  77 N  F  E  K  A  V  A  L  Y  K  I  A  K  D  F  D  R  R  N  A
1081 AACTTTGAAAAGGCAGTAGCACTTTACAAGATCGCTAAAGACTTTGATAGAAGAAATGCG
  97 D  G  A  D  P  I  Q  A  D  L  H  E  I  L  G  L  R  N  F  A
1141 GATGGCGCAGATCCAATTCAAGCAGATTTACATGAAATCTTAGGCTTGCGCAACTTCGCC
 117 D  F  T  F  K  A  A  D  F  F  K  N  G  F  P  M  P  F  D  F
1201 GACTTTACTTTTAAGGCTGCCGACTTCTTCAAGAATGGTTTTCCTATGCCATTTGATTTT
 137 S  V  E  A  D  M  K  N  T  K  I  H  S  L  Q  F  G  G  P  G
1261 TCAGTTGAAGCAGATATGAAGAATACTAAGATTCATTCACTTCAATTTGGTGGTCCAGGC
 157 T  F  L  P  D  T  T  T  Y  K  T  P  A  A  E  K  L  L  A  V
1321 ACATTCTTGCCAGATACTACTACTTACAAGACTCCCGCTGCTGAAAAGCTTTTGGCTGTT
 177 L  K  E  Q  S  I  N  L  L  T  M  S  G  I  S  K  S  E  A  E
1381 TTGAAGGAGCAATCAATCAACTTGTTAACAATGAGCGGCATTAGCAAGTCTGAAGCTGAA
```

Figure 33 (continued)

```
 197 D  Y  A  E  K  A  L  A  Y  D  A  K  I  A  K  V  V  K  S  A
1441 GACTATGCTGAAAAGGCTCTGGCATATGATGCTAAGATTGCCAAGGTAGTTAAGTCTGCC
 217 E  E  W  A  D  Y  P  A  T  Y  N  P  I  S  R  D  D  F  A  D
1501 GAAGAATGGGCTGACTATCCTGCTACATATAATCCAATTTCTCGTGATGATTTTGCCGAT
 237 K  F  K  S  F  K  M  D  Y  F  L  G  E  L  F  A  K  K  P  E
1561 AAGTTCAAGTCATTCAAGATGGATTACTTCTTAGGTGAACTTTTTGCTAAGAAGCCAGAA
 257 R  V  I  N  T  E  P  R  Y  L  D  Y  A  E  E  L  L  N  E  D
1621 AGAGTAATTAATACTGAACCTCGTTATTTAGATTACGCTGAAGAACTCTTGAATGAAGAT
 277 V  F  A  E  I  K  A  W  M  L  V  K  F  V  N  G  V  A  S  S
1681 GTTTTTGCAGAAATTAAGGCTTGGATGCTAGTTAAGTTCGTCAATGGCGTAGCTAGTTCA
 297 L  S  Q  E  F  R  E  A  A  F  P  F  S  Q  A  L  S  G  Q  P
1741 TTGTCACAAGAATTTCGTGAAGCTGCCTTTCCATTTAGCCAAGCTTTGTCTGGTCAACCT
 317 E  L  P  S  G  V  K  Q  A  Y  H  I  A  N  S  D  F  S  E  V
1801 GAACTTCCAAGCGGTGTTAAGCAAGCATATCACATTGCTAACAGCGACTTTAGCGAAGTA
 337 V  G  V  Y  Y  G  Q  T  Y  F  G  A  E  A  K  A  D  V  T  D
1861 GTTGGTGTTTACTATGGTCAAACATACTTTGGTGCAGAAGCTAAGGCTGATGTGACTGAC
 357 M  I  H  K  M  L  D  V  Y  E  K  R  I  R  E  N  S  W  L  S
1921 ATGATTCATAAGATGCTTGACGTTTATGAAAAGAGAATCCGTGAAAATTCATGGCTTTCA
 377 Q  A  T  K  D  K  A  I  V  K  L  R  A  L  I  L  K  I  G  Y
1981 CAAGCAACTAAGGATAAGGCAATTGTTAAGTTGCGTGCTTTGATCTTGAAGATTGGTTAC
 397 P  D  K  I  E  E  I  Y  D  R  L  T  V  D  P  E  A  S  L  Y
2041 CCAGATAAGATTGAAGAAATCTATGATCGTTTAACTGTTGATCCAGAAGCTAGTCTTTAT
 417 A  N  E  A  Q  F  G  R  E  Q  I  K  Y  N  L  E  K  L  D  Q
2101 GCTAATGAAGCTCAATTTGGCAGAGAACAAATTAAGTACAATTTGGAAAAGTTAGATCAA
 437 D  V  D  R  S  V  W  L  M  P  G  N  L  V  N  A  C  Y  D  P
2161 GATGTTGACCGCAGCGTATGGCTTATGCCAGGTAACCTCGTTAACGCATGTTACGATCCT
 457 Q  R  N  D  L  T  F  P  A  A  I  L  Q  K  P  F  Y  D  L  K
2221 CAAAGAAACGATTTGACTTTCCCAGCTGCTATTTTGCAAAAGCCTTTCTACGACTTGAAG

                                                  (zinc metallopeptidase
 477 Q  S  R  S  L  N  Y  G  G  I  G  V  V  I  A  H  E  I  S  H
2281 CAATCACGTAGCTTGAACTACGGTGGTATCGGTGTTGTAATTGCCCACGAAATTTCTCAC

     motif)
 497 A  F  D  N  N  G  A  Q  F  D  E  F  G  N  M  K  N  W  W  T
2341 GCCTTTGACAACAACGGTGCTCAATTTGATGAATTCGGTAATATGAAGAATTGGTGGACT
 517 E  K  D  F  A  E  F  K  K  R  T  Q  A  E  I  D  L  F  D  G
2401 GAAAAGGACTTCGCTGAATTTAAGAAGCGGACTCAAGCTGAAATCGACTTGTTTGACGGT
 537 I  K  Y  G  P  V  T  L  N  G  K  Q  I  V  S  E  N  I  A  D
2461 ATTAAGTACGGCCCTGTAACTCTTAACGGTAAACAAATCGTATCCGAAAATATTGCCGAT
 557 Q  G  G  L  T  A  A  V  E  A  N  K  G  E  D  G  N  M  K  E
2521 CAAGGTGGTTTAACAGCCGCTGTTGAAGCCAACAAGGGCGAAGATGGCAACATGAAGGAA
 577 L  F  E  N  F  A  R  V  W  A  T  K  Q  L  P  E  S  I  K  T
2581 TTATTTGAAAACTTTGCTCGTGTCTGGGCAACCAAGCAATTGCCAGAGAGTATTAAGACG
 597 Q  V  S  V  D  V  H  A  P  G  P  V  R  A  N  V  Q  S  Q  C
2641 CAAGTATCAGTTGATGTTCACGCACCAGGTCCAGTACGTGCCAATGTTCAATCACAATGC
 617 Q  E  E  F  Y  K  A  F  D  V  T  E  H  D  G  M  W  L  D  P
2701 CAAGAAGAATTTTACAAGGCATTTGATGTAACTGAACATGATGGCATGTGGCTCGATCCT
 637 E  K  R  V  V  I  W  *
2761 GAAAAACGTGTTGTAATTTGGTAATAATCAATAAAATAACCTTGCTGAGCAAGGTTATTT

2821 TTTTGCCATTTTAGCTAATTTGTTATTTTTAAATGCTAAAGAGTAGCTTTTTTTTGCATT

2881 GACTCCTATAATGAAGATGACTACAGTGCTTGCTACTACACTGTGGCCTTTATAACTTAT
2941 ACCCATATAAATTTATGCACTAAAAAAGGCTCCCATTTGGGAGCTTTTTTTAGTTGTTAT
```

Figure 33 (continued)

```
  3001 TTTAACTATTTTGTTTTTGCATGGGAATAATCTTTAGGCTTAATCCTCTTGATGTAAGAT
  3061 GGATTTGGTTTACCTAAAATTAATGGTACACGCTCAATGACGGTATCTGCATATTCCAAG
  3121 CCGAACCATGAAGCAGGGTTAGAAGACAAGTTTTGTAAACGAACACGAGCTTCAACTAAC
  3181 CACTTCTCGTAACCAACTAATTGGGTTTGAGGACTGATGACATCGTTGACAATAACGAAT
  3241 GAGAAGTCACCAACGTCACGCCCTGGTGTAGTGGTGTATTCCTGTGGTTGTGGTTCAATT
  3301 GTACCGTCAGCGATCAAATCATGTACGATTTGACGGATGTAAACATTTACGCTTGTTTGC
  3361 TTCTTGAAACCTAGGTACAGCTGAATGTTAATTACGTTCTTGGTACC
```

Figure 34. Alignment of the deduced and published amino acid sequences of PepO, PepO2, and PepO3. Letter colors: black, dissimilar sequence; blue with turquoise background, conservative sequence; black with green background, similar sequence; red with yellow background, identical sequence; green, weakly similar sequence. Abbreviations: Lhel19-O2, PepO2 from *Lb. helveticus* WSU19; Lhel32-O2, PepO2 from *Lb. helveticus* CNRZ32; Lcla-O2, PepO2 from *Lc. lactis* MG1363; Lhel19-O, PepO from *Lb. helveticus* WSU19; Lhel32-O, PepO from *Lb. helveticus* CNRZ32; Lhel19-O3, PepO3 from *Lb. helveticus* WSU19; Lhel32-O3, PepO3 from *Lb. helveticus* CNRZ32.

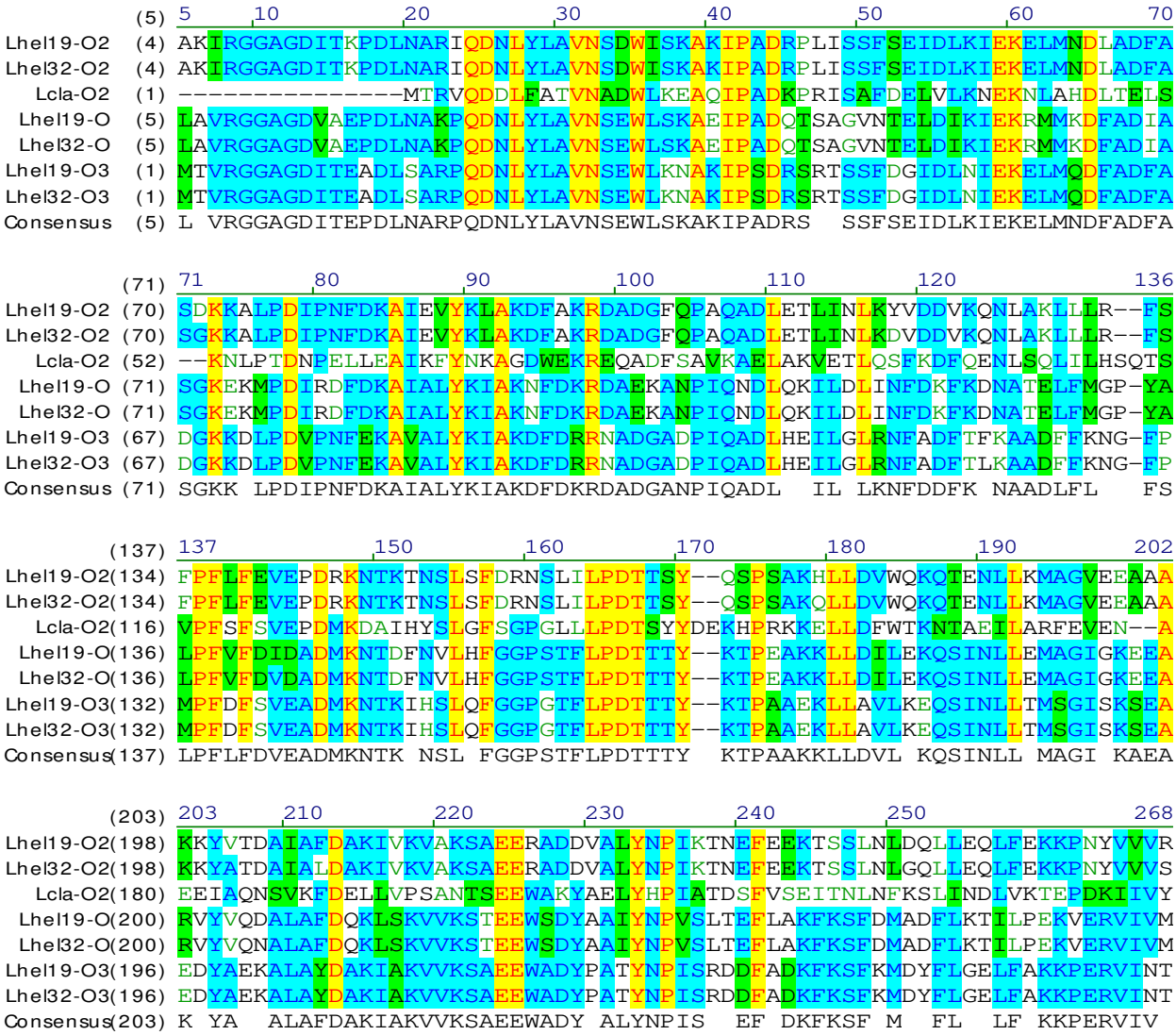

Figure 34 (continued)

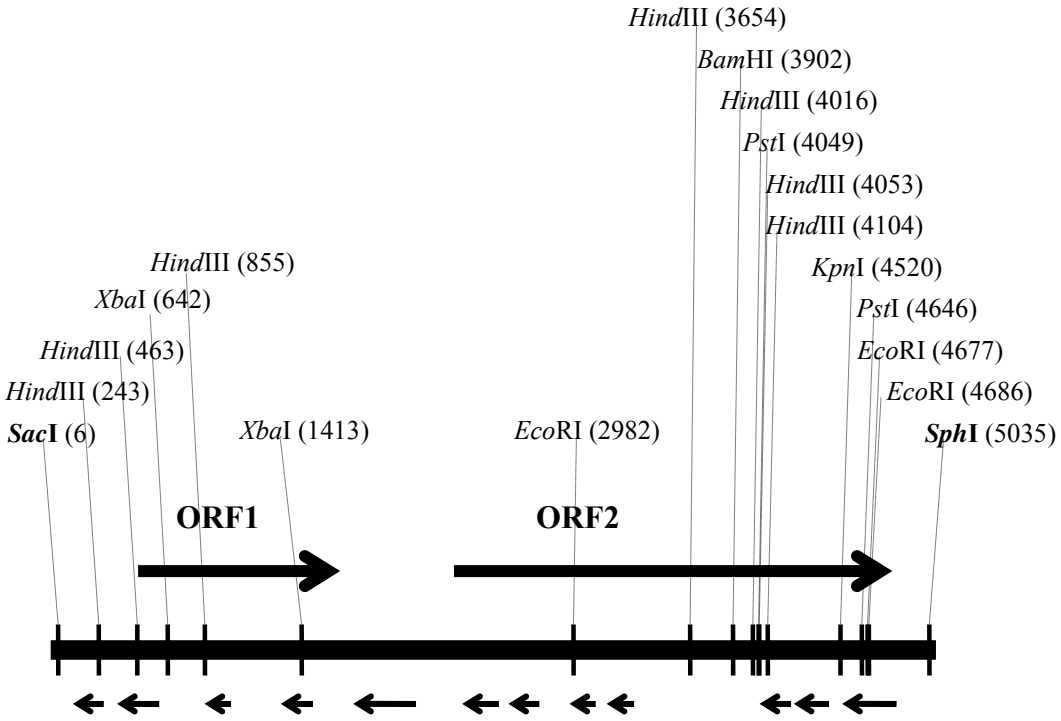

Figure 35. Open reading frame (ORF) and restriction enzyme analyses of the 5-kb *Sac*I-*Sph*I genomic insert containing the *pepN* gene from *Lb. helveticus* WSU19. The vertical lines represent restriction enzyme sites. The numbers in parentheses refer to nucleotide positions. The horizontal line represents genomic insert. The horizontal arrows represent ORFs; the arrows above the horizontal line correspond to the direct DNA strand; the arrows below the horizontal line correspond to the complementary DNA strand.

Figure 36. Nucleic acid sequence of the 5-kb *Sac*I-*Sph*I genomic insert and the deduced amino acid sequence of the PepN enzyme (in single-letter code) from *Lb. helveticus* WSU19. The numbers to the left refer to nucleic acids (bottom lines) and amino acid residues (top lines). The putative –10 and –35 promoter sequences are underlined and labeled. The putative ribosomal binding site is indicated in bold letters, underlined, and labeled rbs. The putative transcriptional terminator is indicated by the dotted horizontal arrows. Stop codon is indicated by asterisk. The zinc metallopeptidase motif is double-underlined and labeled.

```
   1 GAGCTCGGCGATTAAATCGGGAATGGGATAATCCTACAAAGAACCTGCAAAATCTTCTTT
  61 GTGATTCAATCCCTAATTCCGCTTGCTAGATAAGCATAGCTAAGATGGAACTATCAGATA
 121 GCTTGATCTGATCTGTATTTCTGCGATGCTTAAGGGAGTTCGGAGCATACAGCTTATACC
 181 AAGAACGACAAATATTGTTTAAACGAGTAAAACTAACTTGTAAATGATGAGAAAAATGCT
 241 TAAGCTTAAGATAGTTCAATCTAGTCAGACTCTTTTCTATTATTACTATTTACAAGTCGA
 301 GTTTAACAAGATTGGACTTTTTATTTAACTAAAACGATTTAACTAGCACCACGCGTGTAA
 361 TTTAGAATAATTACCCAAATCAGAAATAAACAGTGAGATAAAGGGCATTGTCATTGAGAA
 421 GCCCATCCCGGTAATGAAACAACCTAGCCACAGGGTATAAAAAGCTTTGTGCCACCCCGC
 481 AGGCAGATTGCGTGATTTAATAGCAGTCAAATTGTCATCTCTTTCAAAAAAAATAAGAAT
 541 GGTTTTTAACATCCATTTTAGCACATACAAAAAACTAAATATTTTTCCAATTTTTTACAA
 601 TAGAAAAACTATTAACCAAAAAATGTGCTACGATAATGGTTCTAGAAGGGAGTTATTCTT
 661 TATGGCACATATGTCACGGCGAGAATATCGCATGAAGAAGGAACATGGACAAGGCGTTGC
 721 AGATCAATCACGAGTTAATTATGCTAAAAATAAGGCAAATAGTCGTGAAGAATTTAGAAG
 781 CAAAAAAATTAGCAACCCTAAACCTGCTGCTAATACCAAAATTGATCTTTCACGAGAAAA
 841 TTATAATCACGTAAAGCTTAACTTTTGGACAATCTTTTCTGATCGACCATACATCTCAGT
 901 TGCAATTATTGTTCTAGCACTATTTCTTGCCATGATTAAATTATGGTGGGGATTATTAAT
 961 CTTACTGTTAGTAGTAATTGTCGGAATATATGTCATTGGCCACAGTCACCACCCTCATCA
1021 GGTGCTTAGTCTTGAGTTTCATTTAAAGGCCTCAAGAAAATTAAGCATGTTAAGAGCTTT
1081 AGAGTTAGGTGGCTCAGTTACCATGTTTTTGGCTACCTATATGAAACAGGTGGTTATTGT
1141 TGATTTCTCATCAGCAGGTTCAACTGATAGTTTCCAAATTATCCAAGGAGCCTTATCCAA
1201 TAATGGTGGTTACTATGGTCAGCAAGGATCGTATTTCTTGAGTTTGTTAAATACAGTTAC
1261 TGGCGGTCAGCTTTGGAGTTCATATCGTTATGCTACAAATAGTGCGCAAATGATGGATAG
1321 CAACTCAGGGCGCTGGATTATTATGTGGATCATGCTTTTGATGATTGCCCCAGCTTTTTG
1381 TGTATTGGCACAATTCTTTAAAGAACCATATTCTAGAAATGTGACTTTGATTACTTCATT
1441 GATTACCACATTTAGTTTTATCTTAACTCCTGTTTTAATGCGTAAATGGGTAGTTGGTTA
1501 TGCTATGGAAAACCAAATGACGAGAGAAGCAGCGAATAATGCTGTTCACATTGGGACGAT
1561 GGCCTACGTTGGAATGGCTTGCTCGATCCTAGTATTAATAATTGCAACCTATCGGGTAAT
1621 TAAACAAGACAAGTTTGAATAAAGAAAAAACAGCTTAGTCAACTTGACTAGGCTGTTTTT
1681 TTGGAAATTAAGGAATAAATTAATTTTAGTACCAGTTATGTGCTAACCAAAATCTCATAG
1741 CGTTAACCCATGAACCGTAACGACCATAAACGTATCTGTCAGCAGTACGTTCTTGGTTCT
1801 TTGGTGATAAGTCACCGTGTAAGTAACCGATGCTTAATTGGTACTTACCGTAACATGAAC
1861 CGTTTCTAGCGGTGTAGCTACCACCTGATTCACGCATTGCGATCCATCTCTTAGCTGCCT
1921 TTTCTTTATTAGACATCTTCTTAGCAGCTTGAACAGTTTGACTGGTAGAATTGTTAGCAA
1981 AAGTTTGTGCAACTGCGACACACGCAAAGGCAAGTGCTAATGCAGCTACTAATTTAACAA
2041 AAATAGATTTAACTTGTTTACTCATTGATTTCATTCCTTATTAAAACTTACTTTCCTTAT
2101 TAAAACTTACTTTTAAAAAATTTATATAGTTCTTAATGACTATGCTTATATATTACAAGA
2161 TCTATATGACAGCAATGTTACAAAACGGAAACGGCACTCTTACAATCAGAAAGAAATTGC
```

Figure 36 (continued)

```
2221 CTTTTTTAAGCACTTTTACCGATATTTTGGTAAAATTTAGAATGAATTATGCTAATTAGG
           -35                      -10                       rbs

   1          M  A  V  K  R  F  Y  K  T  F  H  P  E  H  Y  D  L
2281 AGGCAAATATATGGCAGTTAAACGTTTCTATAAAACTTTCCACCCAGAACATTACGATTT
     rbs

  18  R  I  N  V  N  R  K  N  K  T  I  N  G  T  S  T  I  T  G  D
2341 GCGTATTAATGTAAACCGTAAGAATAAAACTATTAATGGTACTTCCACAATTACTGGTGA
  38  V  I  E  N  P  V  F  I  N  Q  K  F  M  T  I  D  S  V  K  V
2401 TGTAATTGAAAATCCAGTATTTATTAACCAAAAATTTATGACCATTGATAGCGTTAAGGT
  58  D  G  K  N  V  D  F  D  V  I  E  K  D  E  A  I  K  I  K  T
2461 TGATGGTAAAAATGTTGATTTTGATGTAATCGAAAAAGATGAAGCAATCAAAATTAAAAC
  78  G  V  T  G  K  A  V  I  E  I  A  Y  S  A  P  L  T  D  T  M
2521 AGGAGTAACTGGCAAAGCTGTAATCGAAATTGCTTATAGCGCACCACTTACTGATACTAT
  98  M  G  I  Y  P  S  Y  Y  E  L  E  G  K  K  K  Q  I  I  G  T
2581 GATGGGTATTTATCCTTCATATTACGAATTAGAAGGTAAGAAGAAGCAAATCATCGGTAC
 118  Q  F  E  T  T  F  A  R  Q  A  F  P  C  V  D  E  P  E  A  K
2641 GCAATTCGAAACTACTTTTGCTCGCCAAGCATTCCCATGTGTGGACGAACCTGAAGCTAA
 138  A  T  F  S  L  A  L  K  W  D  E  Q  D  G  E  V  A  L  A  N
2701 AGCTACATTCTCACTTGCTCTTAAGTGGGATGAACAAGATGGTGAAGTTGCACTTGCTAA
 158  M  P  E  V  E  V  D  K  D  G  Y  H  H  F  E  E  T  V  R  M
2761 CATGCCAGAAGTAGAAGTTGACAAGGATGGCTACCACCACTTTGAAGAAACTGTCCGCAT
 178  S  S  Y  L  V  A  F  A  F  G  E  L  Q  S  K  T  T  H  T  K
2821 GTCTAGTTACTTAGTTGCCTTTGCCTTTGGTGAATTACAATCTAAGACTACTCATACTAA
 198  D  G  V  L  I  G  V  Y  A  T  K  A  H  K  P  K  E  L  D  F
2881 GGATGGCGTATTAATTGGCGTTTACGCAACTAAGGCACACAAGCCTAAGGAATTAGACTT
 218  A  L  D  I  A  K  R  A  I  E  F  Y  E  E  F  Y  Q  T  K  Y
2941 CGCTTTGGACATTGCTAAGCGCGCAATTGAATTTTACGAAGAATTCTACCAAACCAAATA
 238  P  L  P  Q  S  L  Q  L  A  L  P  D  F  S  A  G  A  M  E  N
3001 CCCACTTCCACAGTCATTGCAACTTGCATTGCCAGACTTCTCAGCTGGTGCCATGGAAAA
 258  W  G  L  V  T  Y  R  E  A  Y  L  L  L  D  P  D  N  T  S  L
3061 CTGGGGTCTTGTAACTTACCGTGAAGCATACTTGCTCCTTGACCCAGACAATACTAGCTT

                              (zinc metallopeptidase motif)
 278  E  M  K  K  L  V  A  T  V  I  T  H  E  L  A  H  Q  W  F  G
3121 GGAAATGAAGAAGTTAGTTGCCACAGTTATTACCCATGAATTGGCTCACCAATGGTTCGG
 298  D  L  V  T  M  K  W  W  D  N  L  W  L  N  E  S  F  A  N  M
3181 TGACTTGGTAACCATGAAGTGGTGGGACAACTTATGGCTTAACGAAAGTTTTGCCAACAT
 318  M  E  Y  L  S  V  D  G  L  E  P  D  W  H  I  W  E  M  F  Q
3241 GATGGAATACTTATCAGTTGATGGTTTGGAACCTGACTGGCACATCTGGGAAATGTTCCA
 338  T  S  E  A  A  S  A  L  N  R  D  A  T  D  G  V  Q  P  I  Q
3301 AACTAGTGAAGCTGCATCTGCATTGAACAGAGATGCTACTGATGGTGTTCAACCAATTCA
 358  M  E  I  N  D  P  A  D  I  D  S  A  F  D  G  A  I  V  Y  A
3361 AATGGAAATTAATGACCCAGCAGATATTGACTCAGCCTTTGACGGTGCCATTGTTTATGC
 378  K  G  S  R  M  L  V  M  V  R  S  L  L  G  D  D  A  L  R  K
3421 TAAGGGTTCAAGAATGTTAGTCATGGTTCGTTCACTTCTTGGTGACGACGCACTTCGCAA
 398  G  L  K  Y  Y  F  D  H  H  K  F  G  N  A  T  G  D  D  L  W
3481 AGGTCTTAAGTACTACTTCGACCACCACAAGTTTGGCAATGCCACTGGTGATGACCTTTG
 418  D  A  L  S  T  A  T  D  L  D  I  G  K  I  M  H  S  W  L  K
3541 GGATGCACTTTCAACTGCAACTGATCTTGATATTGGTAAAATCATGCACTCATGGCTTAA
 438  Q  P  G  Y  P  V  V  N  A  F  V  A  E  D  G  H  L  K  L  T
3601 GCAACCTGGTTACCCAGTAGTTAATGCCTTCGTTGCTGAAGATGGTCATTTGAAGCTTAC
 458  Q  K  Q  F  F  I  G  E  G  E  D  K  G  R  Q  W  Q  I  P  L
3661 GCAAAAGCAATTCTTCATTGGTGAAGGTGAAGATAAGGGTAGACAATGGCAAATTCCATT
```

Figure 36 (continued)

```
 478  N  A  N  F  D  A  P  K  I  M  S  D  K  E  I  D  L  G  N  Y
3721 GAATGCTAACTTCGACGCACCTAAGATTATGTCTGATAAGGAAATTGACTTAGGCAATTA
 498  K  I  L  R  E  E  A  G  H  P  L  R  L  N  V  G  N  N  S  H
3781 CAAGATACTTCGCGAAGAAGCAGGTCACCCACTTAGACTTAATGTTGGCAACAACTCACA
 518  F  I  V  E  Y  D  K  T  L  L  D  D  I  L  S  D  V  N  E  L
3841 CTTCATCGTTGAATATGACAAGACTTTGCTTGATGATATTTTGTCAGATGTTAATGAATT
 538  D  P  I  D  K  L  Q  L  L  Q  D  L  R  L  L  A  E  G  K  Q
3901 GGATCCAATTGATAAGTTACAATTGCTTCAAGACTTACGTCTCTTAGCAGAAGGTAAGCA
 558  I  S  Y  A  S  I  V  P  L  L  V  K  F  A  D  S  K  S  S  L
3961 AATTTCTTACGCTTCAATTGTTCCACTTTTGGTTAAATTCGCTGATTCTAAGTCAAGCTT
 578  V  I  N  A  L  Y  T  T  A  A  K  L  R  Q  F  V  E  P  E  S
4021 GGTAATTAACGCACTTTACACTACTGCAGCTAAGCTTCGTCAATTCGTTGAACCAGAATC
 598  N  E  E  K  N  L  K  K  L  Y  D  L  L  S  K  D  Q  V  A  R
4081 AAATGAAGAAAAGAACTTGAAGAAGCTTTATGATCTCTTATCAAAGGATCAAGTTGCACG
 618  L  G  W  E  V  K  P  G  E  S  D  E  D  V  Q  I  R  P  Y  E
4141 TTTAGGCTGGGAAGTAAAGCCAGGCGAAAGCGATGAAGATGTTCAAATTCGTCCATACGA
 638  L  S  A  S  L  Y  A  E  N  A  D  S  I  K  A  A  H  Q  I  F
4201 GTTGAGCGCAAGTCTTTACGCTGAAAATGCGGACTCAATTAAGGCAGCTCACCAAATCTT
 658  T  E  N  E  D  N  L  E  A  L  N  A  D  I  R  P  Y  V  L  I
4261 TACTGAAAATGAAGATAACTTGGAAGCATTGAATGCAGATATTCGTCCATACGTTTTAAT
 678  N  E  V  K  N  F  G  N  A  E  L  V  D  K  L  I  K  E  Y  Q
4321 CAATGAAGTTAAGAACTTTGGCAATGCTGAATTAGTTGATAAGTTAATTAAGGAATACCA
 698  R  T  A  D  P  S  Y  K  V  D  L  R  S  A  V  T  S  T  K  D
4381 AAGAACAGCTGACCCATCATACAAGGTTGACTTACGCAGCGCTGTAACCAGCACCAAGGA
 718  L  A  A  I  K  A  I  V  G  D  F  E  N  A  D  V  V  K  P  Q
4441 TCTTGCAGCTATCAAGGCTATTGTTGGCGACTTTGAAAATGCTGACGTAGTTAAGCCACA
 738  D  L  C  D  W  Y  R  G  L  L  A  N  H  Y  G  Q  Q  A  A  W
4501 AGATTTATGTGATTGGTACCGTGGTTTACTTGCTAACCATTATGGTCAACAAGCAGCTTG
 758  D  W  I  R  E  D  W  D  W  L  D  K  T  I  G  G  D  M  E  F
4561 GGACTGGATCAGAGAAGACTGGGATTGGCTTGACAAGACTATTGGTGGTGACATGGAATT
 778  A  K  F  I  T  V  T  A  G  V  F  H  T  P  E  R  L  K  E  F
4621 TGCTAAATTTATCACTGTTACTGCAGGCGTCTTCCATACCCCAGAAAGACTTAAGGAATT
 798  K  E  F  F  E  P  K  I  N  V  P  L  L  S  R  E  I  K  M  D
4681 CAAGGAATTCTTTGAACCAAAGATTAATGTTCCACTTCTTAGTCGTGAAATTAAGATGGA
 818  V  K  V  I  E  S  K  V  N  L  I  E  A  E  K  D  A  V  N  D
4741 CGTTAAGGTCATCGAAAGCAAGGTTAACTTGATCGAAGCTGAAAAAGATGCTGTTAATGA
 838  A  V  A  K  A  I  D  *
4801 TGCAGTTGCTAAAGCAATTGATTAAGTAATATAAAGTAATAAAAATAAGGATCTATCTGT
                                                  >>>>>>>>>>>>>>>>

4861 AAATAGGATAGGTCCTTATTTTTCGTGGTGTAATTGTTTTTATTGCTTACCTTAGATAAG
       <<<<<<<<<<<<<<<<

4921 AAGAGAGTTTTTCTTTGGGTAAACGAGATTCAAATACAGCATTCTTTGGACAGCCAAAGG
4981 GCTTGTCCACTTTATTCTTCACTGAAATGTGGGAGCGTTTCAGTACACAGCATGC
```

Figure 37. Alignment of the deduced amino acid sequence of PepN from *Lb. helveticus* WSU19 and the published amino acid sequences of PepN from lactobacilli. Letter colors: black, dissimilar sequence; blue with turquoise background, conservative sequence; black with green background, similar sequence; red with yellow background, identical sequence; green, weakly similar sequence. Abbreviations: Lhel19, *Lb. helveticus* WSU19; Lhel32, *Lb. helveticus* CNRZ32; Lhel53/7, *Lb. helveticus* 53/7; Laci, *Lb. acidophilus* NCFM; Lcas, *Lb. casei* ATCC334; Ldla, *Lb. delbrueckii* subsp. *lactis* DSM7290; Ldbu, *Lb. delbrueckii* subsp. *bulgaricus* ATCC BAA-365; Lgas, *Lb. gasseri*; Ljoh, *Lb. johnsonii* NCC533.

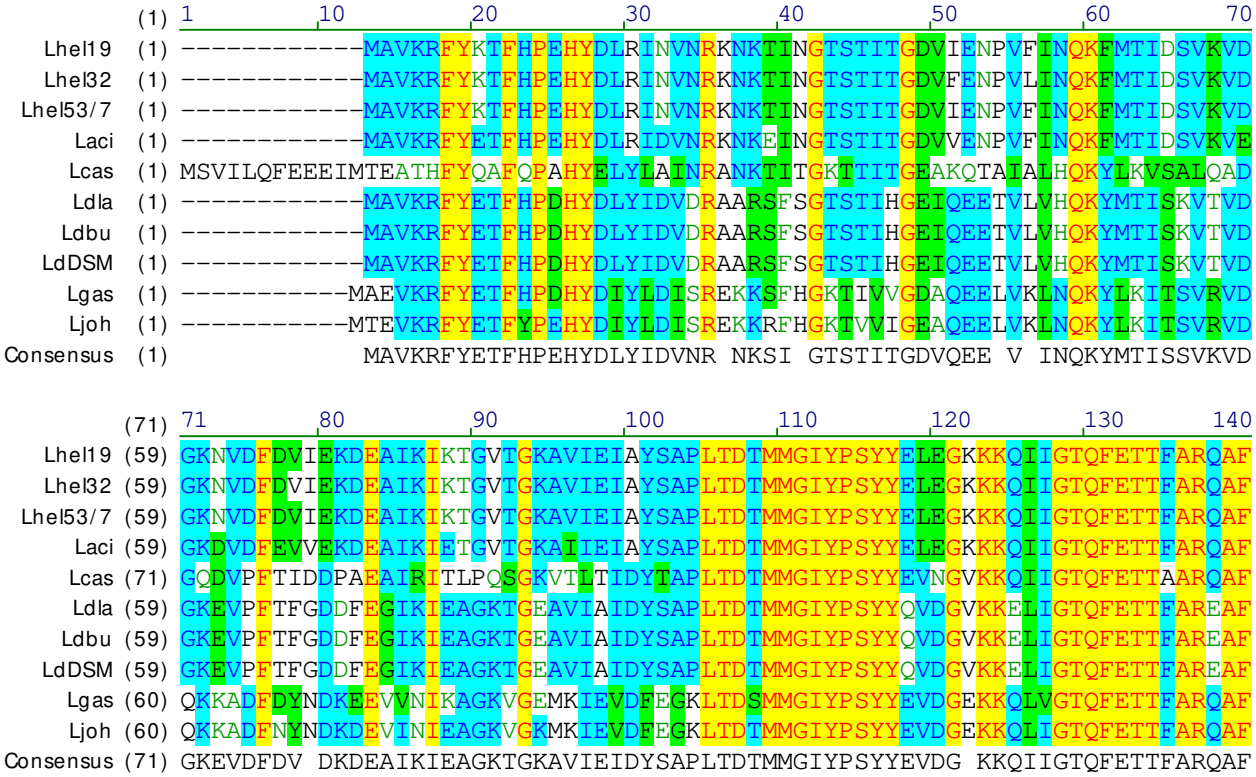

Figure 37 (continued)

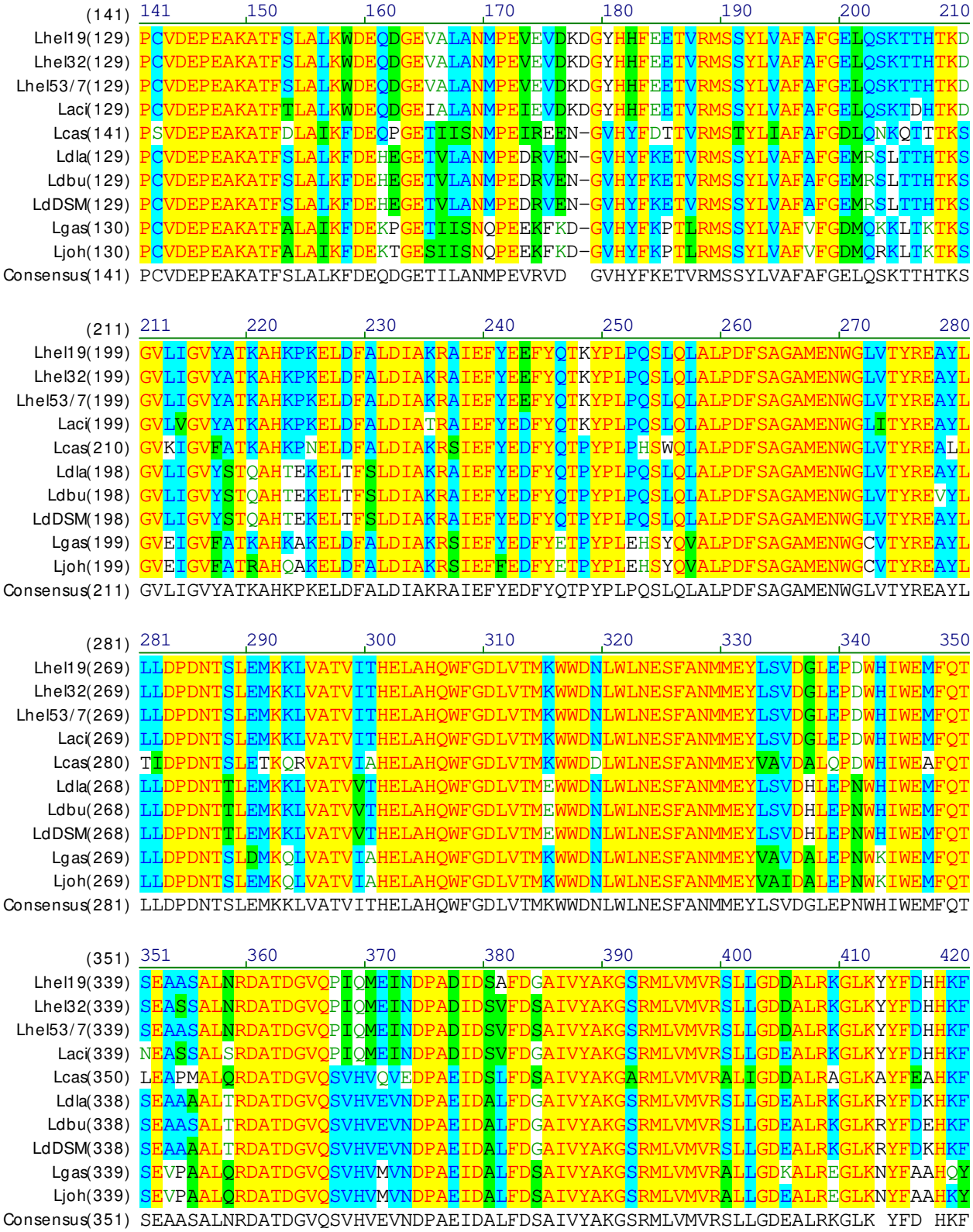

Figure 37 (continued)

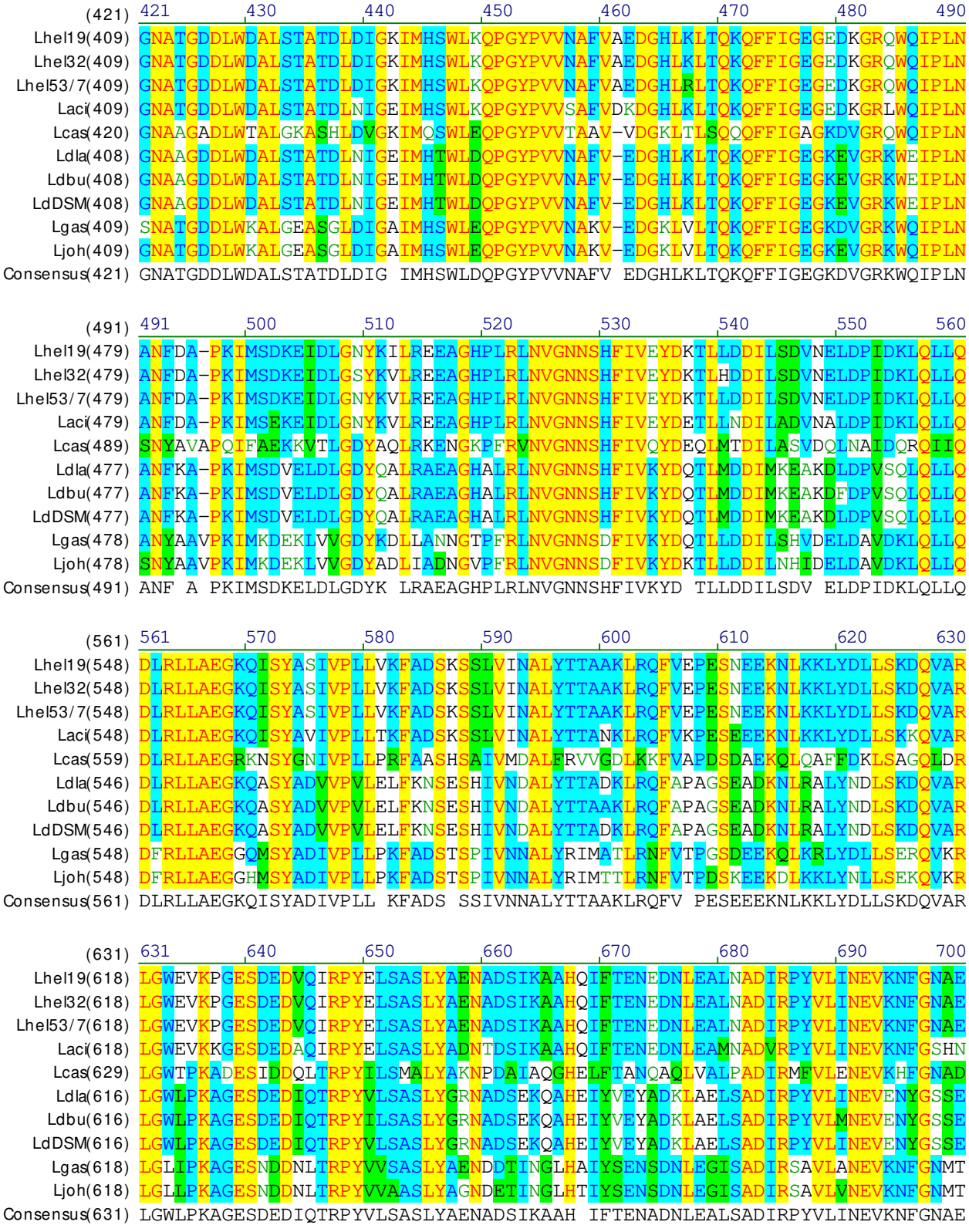

Figure 37 (continued)

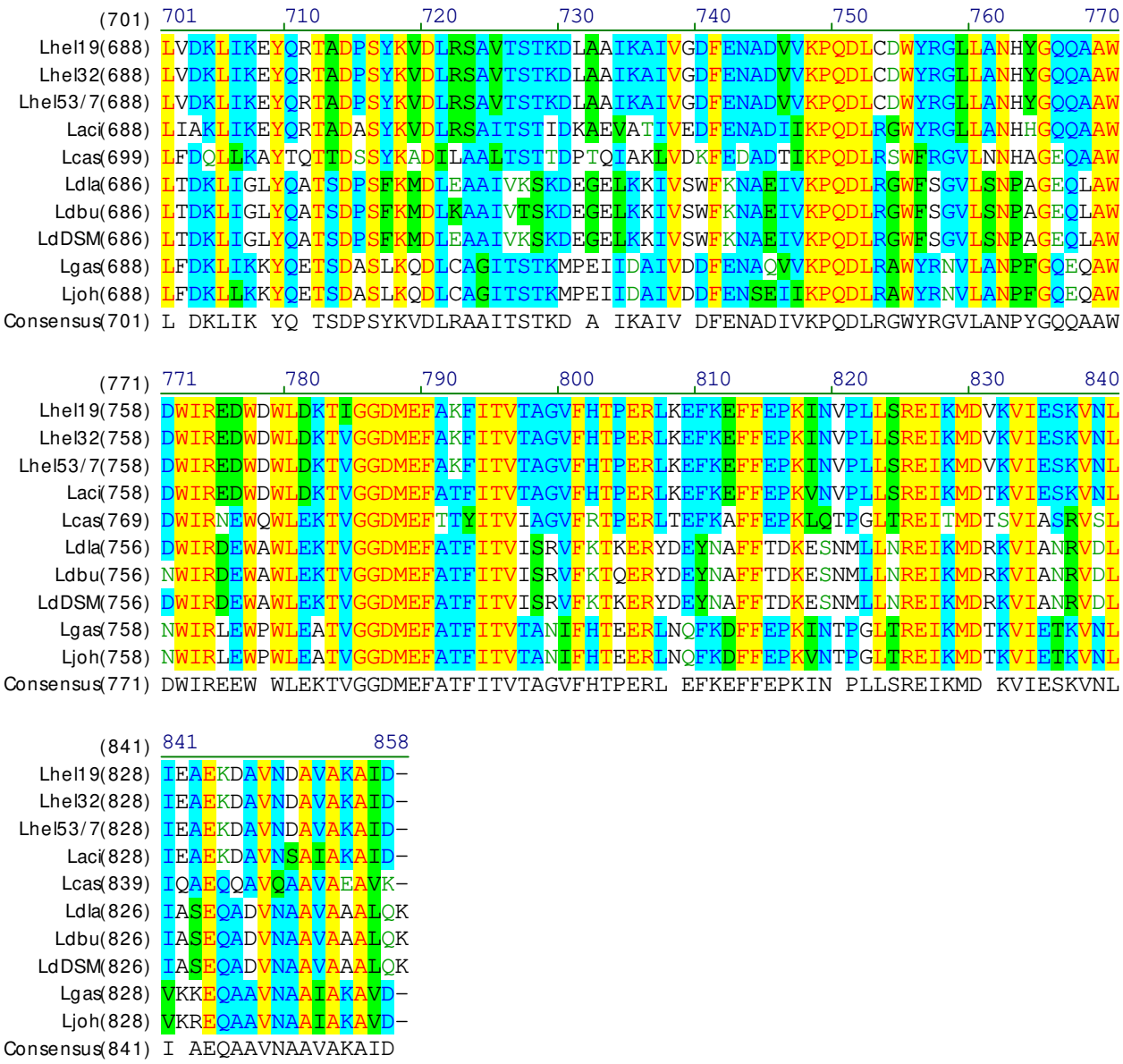

8. Degradation of β-CN f193-209 by PepO, PepO2, and PepO3

Tables 10-12 list the mass-to-charge ratio (m/z) of peaks in the MALDI-TOF spectra and the corresponding peptide fragments formed during hydrolysis of β-CN f193-209 by CFEs from *E. coli* DH5α(pES5), *E. coli* DH5α(pES2), and *E. coli* DH5α(pES6), expressing the *pepO*, *pepO2*, and *pepO3* genes from *Lb. helveticus* WSU19, respectively. Hydrolysis of β-CN f193-209 by CFE from *E. coli* DH5α(pJDC9) served as the control. No peaks corresponding to peptide fragments derived from β-CN f193-209 were observed in the control. The peptide fragments from β-CN f193-209 were determined by matching the sum of average molecular weight of amino acids composing each peptide with the m/z ratio data (Soeryapranata et al., 2004). The primary structure of Bos β-casein A^2-5P reported by Ribadeau-Dumas et al. (1972; Lemieux and Simard, 1992; Whitney, 1999) was the basis for β-CN f193-209 sequence in this study.

The 193-209 fragment of β-CN (m/z 1881 Da) was previously identified as an important bitter peptide in Cheddar and Gouda cheeses (Visser et al., 1983a; Soeryapranata et al., 2002b; Singh et al., 2005). Some of the peptides from the C-terminus of β-CN f193-209 have been determined to be bitter, including β-CN f193-208 (m/z 1781 Da), f193-207 (m/z 1668 Da), f202-209 (m/z 898 Da), f203-208 (m/z 643 Da), and f203-209 (m/z 742 Da) (Lemieux and Simard, 1992). Except for the m/z of 1881 Da, none of these peptide masses were observed in the MALDI-TOF spectra at 0-h to 72-h incubations with PepO, PepO2, or PepO3 enzymes, suggesting the Ile_{208}-Val_{209}, Ile_{207}-Ile_{208}, Val_{201}-Arg_{202}, and Arg_{202}-Gly_{203} bonds are not the preferred cleavage sites of these enzymes (Figures 38-40).

Although the deduced amino acid sequence analysis showed a conserved zinc-binding motif in the active sites of PepO, PepO2, and PepO3, differences in the hydrolysis

rates and the preferred cleavage sites were observed among these enzymes. In general, the pattern of β-CN f193-209 hydrolysis by PepO is more similar to PepO3 than to PepO2. Hydrolysis of the bitter peptide, β-CN f193-209, by PepO or PepO3 appeared to be more rapid than by PepO2 enzyme. The m/z of 1881 Da, corresponding to the mass of β-CN f193-209, was the most intense peak in the MALDI-TOF spectra up to 12-h incubation with PepO or PepO3. In contrast, the 1881-Da peak was the most intense throughout the entire 72-h incubation with PepO2 (Table 11). Incubations of β-CN f193-209 with PepO or PepO3 for 24 and 48 h produced peaks at m/z of 1039 and 673 Da as the major hydrolysis products, respectively (Tables 10, 12). The m/z of 673 Da remained the dominant peak after 72-h incubation.

The lower rate of β-CN f193-209 hydrolysis by PepO2 than PepO or PepO3 was unlikely affected by the expression level, growth phase, or amount of protein added to the digestion mixture. The endopeptidases were cloned in the pJDC9 vector DNA, harvested at the same absorbance level (A_{600} ~4.0), and standardized to the same amount of protein (~50 μg) in the digestion mixture. Moreover, as shown later, the PepO2 enzyme was active on α_{s1}-CN f1-23 substrate. It was likely that the substrate β-CN f193-209 exhibited more inhibitory effect on PepO2 than PepO or PepO3. Stepaniak et al. (1996) reported the inhibitory effects of β-CN f193-209, f69-97, f69-84, and f141-163 on PepO from *Lc. lactis* subsp. *lactis* MG1363.

In addition to the faster hydrolysis of β-CN f193-209 by PepO and PepO3, these enzymes possess more cleavage sites in β-CN f193-209 than PepO2. Incubations of β-CN f193-209 with PepO or PepO3 produced a greater number of peptide fragments than when incubated with PepO2. The first peak produced by PepO2 was observed at m/z of 1365 Da

after 8-h incubation (Table 11). Prolonged incubation with PepO2, up to 72 h, produced an additional peak at m/z of 1556 Da (Table 11). On the other hand, the 8-h incubations with PepO or PepO3 produced peaks at m/z of 1365, 1556, 1039, and 998 Da, corresponding to the masses of β-CN f197-209, f193-206, f197-206, and f201-209, respectively (Tables 10, 12). These peptidolytic patterns indicate that the Pro_{196}-Val_{197} and Pro_{206}-Ile_{207} bonds were the preferred cleavage sites of PepO, PepO2, and PepO3 enzymes (Figures 38-40). In addition, PepO and PepO3 cleave at the Pro_{200}-Val_{201} bond (Figures 38-40).

The β-CN f193-206 and β-CN f197-206 peptides were identified in 1 y old commercial mature Cheddar cheese using MALDI-TOF mass spectrometry (Gouldsworthy et al., 1996). The study reported by Gouldsworthy et al. (1996) suggests that hydrolyses at Pro_{196}-Val_{197} and Pro_{206}-Ile_{207} bonds occur not only in the simulated cheese system, but also in the real cheese system. In addition, the nonappearance of β-CN f197-209 in the MALDI-TOF spectra reported by Gouldsworthy et al. (1996) indicates that β-CN f197-209 may be the precursor for β-CN f197-206. The absence of the β-CN f197-209 peptide might be caused by a complete degradation of the peptide at the Pro_{206}-Ile_{207} bond by intracellular peptidases of the cheese starter cultures.

Differences in cleavage sites were also observed between PepO and PepO3 enzymes. The 48-h and 72-h incubations of β-CN f193-209 with PepO produced additional peaks at m/z of 827 and 574 Da which correspond to the masses of β-CN f199-206 and f202-206, respectively (Table 10). These peaks were not identified in the MALDI-TOF spectra from the corresponding incubation periods with PepO3 enzyme (Table 12). The observed peptidolytic patterns suggest cleavage at Leu_{198}-Gly_{199} and Val_{201}-Arg_{202} bonds by PepO but not PepO3 (Figures 38, 40).

Figures 38-40 illustrate the preferred cleavage sites of PepO, PepO2, and PepO3 from *Lb. helveticus* WSU19 as a function of incubation time with β-CN f193-209 substrate. Cleavage at Pro_{196}-Val_{197} and Pro_{206}-Ile_{207} bonds initiated hydrolysis of β-CN f193-209 by PepO and PepO3 (Figures 38, 40), while cleavage on the Pro_{196}-Val_{197} bond initiated the hydrolysis by PepO2 (Figure 39). The Pro_{196}-Val_{197} bond is likely the first cleavage site of PepO, PepO2, and PepO3 in β-CN f193-209, followed by the Pro_{206}-Ile_{207} bond. Cleavage on the latter bond is important to prevent the formation of bitter peptides β-CN f193-208, f193-207, f202-209, f203-208, and f203-209. The β-CN f202-209 peptide was reported to be extremely bitter, with a threshold value of 0.004 mM (Kanehisa et al., 1972). In addition to the cleavage at Pro_{196}-Val_{197} and Pro_{206}-Ile_{207} bonds, PepO and PepO3 enzymes cleaved at the Pro_{200}-Val_{201} bond. However, the Pro_{204}-Phe_{205} bond was not cleaved by PepO, PepO2, and PepO3, suggesting these endopeptidases from *Lb. helveticus* WSU19 only cleave a peptide bond between Pro and a nonpolar aliphatic amino acid residue (-Pro-X-).

Chen et al. (2003) and Sridhar et al. (2005) reported the post-proline activity of PepO2 and PepO3 enzymes from *Lb. helveticus* CNRZ32. However, the activity of PepO from *Lb. helveticus* WSU19 on β-CN f193-209 observed in this study contrasts the finding reported by Sridhar et al. (2005) on PepO from *Lb. helveticus* CNRZ32. The latter enzyme did not possess activity toward β-CN f193-209 under cheese ripening conditions (pH 5.1, 4% NaCl, and 10^{o}C). However, the incubation temperature, type of buffer, and pH of buffer used for CFE preparations were different between Sridhar et al. (2005) and this study. The former study used 50 mM 2-(N-morpholino)ethanesulfonic acid (MES) buffer (pH 5.0) to prepare the CFE from *E. coli* clones carrying the *pepO* gene from *Lb. helveticus* CNRZ32 and 50 mM Pipes buffer (pH 7.0) was used in the present study.

In contrast to Sridhar et al. (2005), Baankreis et al. (1995) reported the activity of neutral thermolysin-like oligoendopeptidase (NOP) from *Lc*. *lactis* subsp. *cremoris* C13 on β-CN f193-209 and β-CN f193-202. The NOP enzyme is related to PepO from *Lc. lactis* strains Wg2 and P8-2-47 (Tan et al., 1991; Mierau et al., 1993; Baankreis et al., 1995). NOP was reported to have a MW of 70 kDa and was inhibited by EDTA. The enzyme cleaved β-CN f193-209 at Pro_{196}-Val_{197}, Val_{197}-Leu_{198}, Pro_{206}-Ile_{207}, and Ile_{207}-Ile_{208} bonds, while cleavage at Pro_{196}-Val_{197}, Val_{197}-Leu_{198}, Pro_{200}-Val_{201}, and Val_{201}-Arg_{202} bonds were observed on β-CN f193-202. Prolonged incubations of β-CN f193-209 with PepO or PepO3 from *Lb. helveticus* WSU19 revealed additional cleavage sites at Val_{197}-Leu_{198} and Ile_{207}-Ile_{208} bonds (Figures 38, 40). Additionally, PepO from *Lb. helveticus* WSU19 cleaved β-CN f193-209 at Leu_{198}-Gly_{199} and Val_{201}-Arg_{202} after 48-h and 72-h incubations, respectively (Figure 38).

Soeryapranata et al. (2004) reported the importance of endopeptidases in the CFE from *Lb. helveticus* WSU19 in degrading the bitter peptide β-CN f193-209. The fact that PepO, PepO2, and PepO3 endopeptidases from *Lb. helveticus* WSU19 possess post-proline activity on β-CN f193-209 and hydrolyze the bitter peptide without generating additional bitter peptide fragments in the hydrolysates indicates the importance of these endopeptidases in the debittering of Cougar Gold cheese. Considering the small apparent activity of PepO2 from *Lb. helveticus* WSU19 in degrading β-CN f193-209, this enzyme may play a less significant role than PepO and PepO3 during ripening of the Cougar Gold. However, it is possible that PepO2 is expressed more readily or has a longer life in the cheese matrix than does PepO or PepO3.

9. <u>Degradation of β-CN f193-209 by PepN</u>

Table 13 lists the mass-to-charge ratio (m/z) of peaks in the MALDI-TOF spectra and the corresponding peptide fragments formed during hydrolysis of β-CN f193-209 by CFE from *E. coli* DH5α(pES4), expressing the *pepN* gene from *Lb. helveticus* WSU19. Hydrolysis of β-CN f193-209 by CFE from *E. coli* DH5α(pJDC9) was included as the control. No peaks corresponding to the peptide fragments derived from β-CN f193-209 were observed in the control.

Incubations of β-CN f193-209 for 2, 4, and 8 h with PepN from *Lb. helveticus* WSU19 showed the most intense peak at m/z of 1718 Da, corresponding to the mass of β-CN f194-209 (Table 13). The 194-209 fragment of β-CN was not reported as a bitter peptide in cheese (Lemieux and Simard, 1992). Removal of tyrosine from the N-terminus of a bitter peptide was suggested to cause debittering (Matoba et al., 1970). Incubation of β-CN f193-209 with PepN from *Lb. helveticus* WSU19 for 8 h completely hydrolyzed the bitter peptide β-CN f193-209 (Table 13), preventing further formation of β-CN f194-209.

A peak with m/z of 1590 Da, corresponding to β-CN f195-209, showed the same intensity as the 1718-Da peak at 8-h incubation (Table 13). In contrast to the β-CN f194-209 peptide, the 195-209 fragment of β-CN was reported as a bitter peptide isolated from β-CN hydrolysate (Lemieux and Simard, 1992). The 1590-Da peak remained the dominant peak as the incubation with PepN proceeded beyond 8 h. In contrast to the 1590-Da peak, the 1718-Da peak markedly decreased at 12-h incubation and completely disappeared at 48-h incubation, suggesting an increase in bitterness of the hydrolysate. The 1718-Da peak disappeared because hydrolysis of β-CN f194-209 to β-CN f195-209 was not accompanied by the production of β-CN f194-209 from β-CN f193-209.

The glutamine and glutamic acid residues at the N-terminus of a peptide may undergo cyclization under acid condition to form pyrrolidonecarboxylic acid (PCA; Gouldsworthy et al., 1996). Besides the acid condition, the presence of cyclotransferase (cyclase) was reported to be responsible for the synthesis of PCA in Gln-Gln dipeptide (Mucchetti, et al., 2002). Conversion of glutamine to PCA generates a peptide with m/z of 17 Da lower than the parent peptide due to the release of ammonia during cyclization (Gouldsworthy et al., 1996). The MALDI-TOF spectra in the current study showed a peak at m/z of 1701 Da, corresponding to the mass of β-CN f194-209 containing PCA at residue 194 (β-CN PCA-f195-209; Table 13). The formation of β-CN PCA-f195-209 was more likely caused by the acid condition (pH 5.2) used in the β-CN f193-209 hydrolysis than the addition of 0.1% TFA in the MALDI-TOF sample preparation. The 1701-Da peak was observed up to 72-h incubation of β-CN f193-209 with PepN although the β-CN f194-209 peptide with glutamine at residue 194 (m/z 1718 Da) disappeared at 48-h incubation. This observation suggests that the β-CN PCA-f195-209 peptide exists in the hydrolysate and is not hydrolyzed by PepN. If the cyclization of glutamine occurred due to acid condition during MALDI-TOF sample preparation, the 1701-Da peak would not have been observed when the parent peptide, β-CN Gln-f195-209, disappeared. Unlike its parent peptide, β-CN PCA-f195-209 was reported to be a bitter peptide isolated from β-casein hydrolysate (Lemieux and Simard, 1992). Removal of PCA from the N-terminus of a peptide requires pyrrolidone carboxylyl peptidase activity (PCP; Sullivan and Jago, 1972).

Besides the cyclization of glutamine at residue 194, a second cyclization was observed at glutamine residue 195 of β-CN f195-209. The m/z of 1572 Da corresponds to the mass of β-CN f195-209 containing PCA at residue 195 (β-CN PCA-f196-209; Table 13).

This peptide was not reported to be present in the β-casein hydrolysate (Lemieux and Simard, 1992). Thus, its occurrence in the hydrolysate from β-CN f193-209 suggests that the cyclization under acid condition may require a certain amount of peptide containing glutamine/glutamic acid at the N-terminus. The peptide is likely to be bitter, based on the fact that the parent peptide, β-CN f195-209, is bitter and the N-terminus of the peptide is PCA.

Figure 41 illustrates the preferred cleavage sites of PepN from *Lb. helveticus* WSU19 in β-CN f193-209. Hydrolysis of β-CN f193-209 occurred sequentially at Tyr_{193}-Gln_{194} and Gln_{194}-Gln_{195} (Table 13). The absence of hydrolysis on the Tyr_{193}-Gln_{194} bond after 8-h incubation and the Gln_{194}-Gln_{195} bond after 48-h incubation was due to the depletion of β-CN f193-209 and β-CN f194-209, respectively (Table 13). Tan et al. (1993a) reported PepN activity from *Lc. lactis* subsp. *cremoris* Wg2 that degraded β-CN f191-202, producing β-CN f194-202. Parra et al. (1999) reported β-CN f194-209 as the product of β-CN f193-209 hydrolysis by PepN from *Lb. casei* subsp. *casei* IFPL 731. Figure 41 also demonstrates the inability of PepN to hydrolyze peptide bonds containing a proline residue. Hydrolysis of β-CN f193-209 by PepN from *Lb. helveticus* WSU19 was not observed beyond glutamine at residue 195 due to presence of proline at residue 196.

Although β-CN f193-209 completely disappeared after 8-h incubation with PepN from *Lb. helveticus* WSU19 (Table 13), the hydrolysates still contained bitter-tasting peptides that could not be hydrolyzed further due to the presence of proline residues. The peptidolytic pattern of PepN on β-CN f193-209 shown in this study (Table 13; Figure 41) suggests that the presence of large PepN activity actually increases bitterness intensity of the bitter peptide hydrolysate. Wilkinson et al. (1992) utilized FlavourAge-FR, with activities on Leu-pNA and Lys-pNA only, to enhance ripening of Cheddar cheese. The enzyme-treated

cheese was reported to be bitter. On the other hand, the use of DCA50, having post-proline dipeptidylaminopeptidase activity, in combination with the Leu-pNA and Lys-pNA activities, did not result in bitter cheese. Bouchier et al. (2001) reported limited hydrolysis and debittering ability of general aminopeptidase (AP) on tryptic digest β-casein in the absence of proline-specific AP.

Lb. helveticus WSU19 was reported to have large general AP and X-prolyl dipeptidyl AP (PepX) activities on Lys-pNA and Arg-Pro substrates, respectively (Olson, 1998; Fajarrini, 1999). Since peptidases from *Lb. helveticus* WSU19 contributed to the debittering of Cougar Gold, the debittering action must result from balanced general AP and proline-specific AP activities. However, Soeryapranata et al. (2004) reported only the activities of general AP and endopeptidases in hydrolyzing β-CN f193-209. The lack of PepX activity in the study reported by Soeryapranata et al. (2004) might be due to the size of β-CN f193-209, the substrate used in the latter study. PepX is known to hydrolyze peptides containing 3 to 7 amino acid residues (Christensen, et al., 1999), while β-CN f193-209 is composed of 17 amino acids. Therefore, a complete hydrolysis of β-CN f193-209 by peptidases from *Lb. helveticus* WSU19 must be a combined action between PepN and proline-specific endopeptidases, namely PepO, PepO2, and PepO3, as demonstrated below.

Table 14 lists the mass-to-charge ratio (m/z) of peaks in the MALDI-TOF spectra and the corresponding peptide fragments formed during hydrolysis of β-CN f193-209 by CFEs from *E. coli* DH5α(pES4) and *E. coli* DH5α(pES5), expressing the *pepN* and *pepO* genes from *Lb. helveticus* WSU19, respectively. In contrast to the hydrolysis of β-CN f193-209 by PepN alone, the MALDI-TOF spectra showed small intensities of the 1718-Da and 1590-Da peaks after incubation of β-CN f193-209 with PepN-PepO combination (Table 14). At 12-h

incubation, the PepN-derived peptides, namely β-CN f194-209 and β-CN f195-209 and their PCA derivatives, were hydrolyzed into β-CN f194-206 (m/z of 1393 Da), β-CN PCA-f195-206 (m/z of 1376 Da), β-CN f195-206 (m/z of 1265 Da), and β-CN PCA-f196-206 (m/z of 1247 Da). The m/z of 1265 Da was the most intense peak at 12-h incubation (Table 14). The proline residue at the C-terminus of these peptides demonstrates PepO activity on the Pro_{206}-Ile_{207} bond (Figure 42). At 24-h incubation, the hydrolysate was dominated by peptides below 1000 Da, namely β-CN f198-206 (m/z 940 Da), β-CN f199-206 (m/z 827), β-CN f201-206 (m/z 673 Da), and β-CN f202-206 (m/z 574 Da). The m/z of 827 Da was the most intense peak at 24-h incubation (Table 14). Peptides below 500 Da could not be detected in this study due to the setting of MALDI-TOF acquisition between 500-4000 Da. None of the peptides produced by PepN-PepO activities were reported as bitter peptides, confirming the stepwise action of general AP and proline-specific endopeptidase in debittering activity.

Some of the peaks observed after incubation with PepN-PepO combination (Table 14), particularly m/z of 940, 827, and 574 Da, were also observed in the hydrolysate resulting from PepO activity (Table 10). These peaks correspond to β-CN f198-209, f199-206, and f202-206, respectively, resulting from cleaving at Val_{197}-Leu_{198}, Leu_{198}-Gly_{199}, and Val_{201}-Arg_{202} bonds, respectively (Tables 10 and 14; Figures 38 and 42). The formation of these peaks upon 12-h incubation with PepN-PepO combination is more likely due to PepN than PepO activities (Figure 42). This interpretation is based on the fact that PepN activity favors basic or hydrophobic/uncharged amino acid residues at the N-terminus (Christensen et al., 1999). The appearance of these peaks after 12-h incubation (Table 14) indicates hydrolyses on the Val_{197}-Leu_{198}, Leu_{198}-Gly_{199}, and Val_{201}-Arg_{202} bonds were highly preferred. As a

comparison, hydrolyses of these bonds by PepO activity occurred after 24 to 72-h incubations (Table 10).

Although cleavage at Leu_{198}-Gly_{199} (m/z of 827 Da) and Val_{201}-Arg_{202} (m/z of 574 Da) bonds was attributed to PepN activity (Figure 42), the m/z of 827 was the most intense peak after 24-h incubation with PepN-PepO combination (Table 14). This observation relates to the results of PepO activity on β-CN f193-209 (Table 10). The 197-206 fragment of β-CN was the precursor for β-CN f198-206 and f199-206 formation by PepN. On the other hand, the β-CN f201-206 peptide was the substrate for PepN to form β-CN f202-206. The β-CN f197-206 (m/z 1039 Da) and f201-206 (m/z 673 Da) peptides were the major hydrolysis products of β-CN f193-209 by PepO activity after 24-h and 48-h incubations, respectively (Table 10). The accumulation of β-CN f197-206 by PepO activity after 24-h incubation provided more substrate for PepN to cleave at Leu_{198}-Gly_{199} than Val_{201}-Arg_{202} bonds (Figure 42). In addition, PepN did not cleave β-CN f199-206 due to the presence of proline at residue 200. Thus, it is likely the β-CN f199-206 peptide will accumulate in the presence of large activities of PepN and PepO.

Table 15 lists the mass-to-charge ratio (m/z) of peaks in the MALDI-TOF spectra and the corresponding peptide fragments formed during hydrolysis of β-CN f193-209 by CFEs from *E. coli* DH5α(pES4) and *E. coli* DH5α(pES2), expressing the *pepN* and *pepO2* genes from *Lb. helveticus* WSU19, respectively. Although β-CN f195-209 (m/z of 1590 Da) was still the dominant peak up to 48-h incubation, additional peptide fragments were observed in this combined hydrolysis, namely β-CN f199-209 (m/z of 1152 Da) and β-CN f195-206 (m/z of 1264 Da). Due to the low activity of PepO2 on Pro_{206}-Ile_{207} bond (Table 11), most peaks

formed by PepN were not hydrolyzed by PepO2 (Table 15), suggesting the low likelihood of a PepO2 role in the debittering of Cougar Gold.

The m/z of 1152 Da observed in the hydrolysis of β-CN f193-209 by PepN-PepO2 activities (Table 15) did not appear in the hydrolysate formed by PepO2 (Table 11) or PepN (Table 13) alone. The 1152-Da peak is attributed to β-CN f199-209 (Table 15), which is likely formed by PepN activity (Figure 43). This interpretation was based on 3 observations. First, PepO2 showed low activity on the Pro_{206}-Ile_{207} bond and no activity on the Ile_{207}-Ile_{208} bond (Table 11; Figure 39). Therefore, it is unlikely to have a Pro_{206} or Ile_{207} residue at the C-terminus of the peptide associated with the 1152-Da peak. Second, PepN was able to cleave the Leu_{198}-Gly_{199} bond in the presence of an endopeptidase having post-proline activity (Figure 42). Third, PepO2 cleaved at the Pro_{196}-Val_{197} bond, forming β-CN f197-209 (m/z of 1365). However, the enzyme did not cleave at Val_{197}-Leu_{198} and Leu_{198}-Gly_{199} bond to form β-CN f198-209 (m/z of 1266 Da) and f199-209 (m/z of 1152 Da), respectively (Table 11; Figure 39). Therefore, the 1152-Da peak is unlikely formed by PepO2 activity. Although PepO2 preferred to cleave at the Pro_{196}-Val_{197} bond (Table 11; Figure 39), m/z of 1365 Da was not observed in the MALDI-TOF spectra (Table 15). Due to the high PepN activity, it was likely the β-CN f197-209 peptide was hydrolyzed as soon as its formation, and therefore the peak was not observed in the MALDI-TOF spectra. Cleavage on the Pro_{196}-Val_{197} bond must occur, otherwise PepN would not be able to continue cleaving the Leu_{198}-Gly_{199} bond observed here.

Table 16 lists the mass-to-charge ratio (m/z) of peaks in the MALDI-TOF spectra and the corresponding peptide fragments formed during hydrolysis of β-CN f193-209 by CFEs from *E. coli* DH5α(pES4) and *E. coli* DH5α(pES6), expressing the *pepN* and *pepO3* genes

from *Lb. helveticus* WSU19, respectively. The trends observed in the hydrolysis of β-CN f193-209 by the PepN-PepO3 combination was similar to those by the PepN-PepO combination, except the 827-Da peak was dominant at 12-h incubation with PepN-PepO3 combination (Table 16), while m/z of 1265 Da was dominant at the same incubation time with PepN-PepO combination (Table 14). Figure 44 illustrates the cleavage sites of PepN-PepO3 combination on β-CN f193-209, which is similar to the PepN-PepO combination (Figure 42). These results suggest the combined actions of PepN with PepO or PepO3 in debittering of Cougar Gold cheese.

10. <u>Degradation of β-CN f193-209 by PepE</u>

PepE did not show activity on β-CN f193-209, which is in agreement with Sridhar (2003). The m/z of 1881 Da was the only peak observed up to 72-h incubation of β-CN f193-209 with CFE from *E. coli* DH5α(pES1) expressing the *pepE* gene from *Lb. helveticus* WSU19. Incubation of β-CN f193-209 with CFEs from *E. coli* DH5α(pES1) and *E. coli* DH5α(pES4), expressing the *pepE* and *pepN* genes from *Lb. helveticus* WSU19, respectively, exhibited a peak (m/z of 1152 Da) at 4-h incubation in addition to the m/z of 1881 Da (Table 17). Hydrolysis of β-CN f193-209 by PepN (Table 13) or PepE alone did not produce the 1152-Da peak.

Similar to the PepN-PepO2 combination, the 1152-Da peak was attributed to β-CN f199-209. However, the peptide was formed by PepE activity, and not PepN activity, on the Leu_{198}-Gly_{199} bond (Figure 45). This peak was not attributed to PepN activity because hydrolyses at Pro_{196}-Val_{197} and Val_{197}-Leu_{198} bonds were not observed at 2-h and 4-h incubations (Table 17; Figure 45). Moreover, PepE alone did not show post-proline activity,

supported by the fact that none of the peptides formed by PepN were cleaved at Pro_{196}-Val_{197} or Pro_{206}-Ile_{207} bond (Table 17; Figure 45). PepN did not cleave the Val_{197}-Leu_{198} and Leu_{198}-Gly_{199} bonds unless the Pro_{196}-Val_{197} bond was previously hydrolyzed. The β-CN f195-209 peptide (m/z of 1590 Da) was likely the precursor for β-CN f199-209 formation. At 48-h incubation, the 1590-Da and 1152-Da peaks showed equal peak height intensity (Table 17), which was likely due to the termination of β-CN f195-209 formation while hydrolysis of β-CN f195-209 to f199-209 proceeded. The depletion of β-CN f194-209, precursor for β-CN f195-209, was responsible for the termination of β-CN f195-209 production (Table 17).

In addition to the 1152-Da peak, m/z of 898 Da was observed at 48-h incubation. The 898-Da peak corresponds to the mass of β-CN f202-209, which was formed by PepE activity, and not PepN activity, on the Val_{201}-Arg_{202} bond (Figure 45). This interpretation is confirmed by the fact that no cleavage at the Pro_{200}-Val_{201} bond was observed preceeding the cleavage of the Val_{201}-Arg_{202} bond. Although PepE was able to cleave peptides produced by PepN, the β-CN f202-209 peptide formed at prolonged incubation has been reported to be extremely bitter, with a threshold of 0.004 mM (Kanehisa et al., 1972). The lack of PepE activity at the Pro_{206}-Ile_{207} bond enables β-CN f202-209 to accumulate over time and results in bitterness. Therefore, the combined action of PepN-PepE in the debittering of Cougar Gold is less likely than the combination of PepN with PepO or PepO3.

The activity of PepE on Leu_{198}-Gly_{199} and Val_{201}-Arg_{202} bonds were confirmed by hydrolyzing β-CN f193-209 with CFEs from *E. coli* DH5α(pES1) and *E. coli* DH5α(pES5), expressing *pepE* and *pepO* genes from *Lb. helveticus* WSU19, respectively (Tables 8 and 18; Figure 46). At 48-h incubation, m/z of 827 and 574 Da were the most intense peaks observed in the MALDI-TOF spectra. These peaks correspond to β-CN f199-206 and f202-206,

respectively, formed by hydrolysis on Leu_{198}-Gly_{199} and Val_{201}-Arg_{202} bonds, respectively. While present, both peaks did not show large intensities in the β-CN f193-209 hydrolysate by PepO activity (Table 10), indicating that intensities of the 827-Da and 574-Da peaks in the PepE-PepO combination were not contributed predominantly by PepO activity.

In the PepE-PepO combination, the β-CN f197-206 (m/z 1039 Da, Table 18) peptide, formed by PepO activity, was likely the precursor for β-CN f199-206 formation. The m/z of 1039 Da was the most intense peak at 24-h incubation (Table 18). The large amount of PepE substrate, β-CN f197-206, and the occurrence of PepE activity in the PepE-PepO combination allowed the accumulation of β-CN f199-206 (m/z 827 Da) at 48-h incubation. In the case of β-CN f202-206 (m/z 574 Da), the fact that the 574-Da peak was one of the most intense peaks at 48-h incubation (Table 18) indicates formation of this peptide may originate from 2 precursors, β-CN f198-206 and f199-206. This interpretation was based on the following observations. First, in the PepE-PepN combination, hydrolysis of Val_{201}-Arg_{202} bond by PepE did not produce β-CN f202-209 as the most intense peak at 48-h incubation (Table 17). The β-CN f199-209 was more likely than β-CN f195-209 to be the substrate for PepE to form f202-209 in the PepE-PepN combination (Table 17). Thus, PepE activity alone on a single substrate did not produce an intense peak due to cleaving at the Val_{201}-Arg_{202} bond. Second, although PepO cleaved at the Val_{201}-Arg_{202} bond, the hydrolysis did not occur until 72-h incubation (Table 10). Therefore, the large intensity of 574-Da peak in PepE-PepO combination (Table 18) was not likely due to the activities of 2 endopeptidases, i.e., PepE and PepO.

Table 19 and Figure 47 show the peptides derived from β-CN f193-209 when incubated with CFEs from *E. coli* DH5α(pES1) and *E. coli* DH5α (pES2), expressing *pepE*

and the *pepO2* genes from *Lb. helveticus* WSU19, respectively (Table 8). Peaks at m/z of 1152 and 898 Da, corresponding to the β-CN f199-209 and β-CN f202-209 peptides, respectively, were produced by PepE activity (Table 19). The 1152-Da and 898-Da peaks were not the most intense peaks at 48-h incubation (Table 19). In the PepE-PepO2 combination, the 1881-Da was the most intense peak up to 48-h incubation (Table 19). The β-CN f197-209 peptide (m/z of 1364 Da) was likely the precursor for β-CN f199-209 formation, and the latter became the precursor for β-CN f202-209 formation. Therefore, less substrate w as available for PepE in PepE-PepO2 than PepE-PepO combinations.

Table 20 shows the peptides derived from β-CN f193-209 when hydrolyzed by CFEs from *E. coli* DH5α(pES1) and *E. coli* DH5α (pES6), expressing the *pepE* and *pepO3* genes from *Lb. helveticus* WSU19, respectively (Table 8). Figure 48 shows the peptidolytic pattern of the PepE-PepO3 combination on β-CN f193-209. The m/z of 827 and 573 Da peaks were not observed when β-CN f193-209 was digested solely by PepO3 (Table 12, Figure 40). These peaks correspond to the masses of β-CN f199-206 and β-CN 202-206, respectively, indicating PepE activity on Leu_{198}-Gly_{199} and Val_{201}-Arg_{202} bonds (Figure 48). In contrast to the PepE-PepO combination, the PepE-PepO3 mixture did not produce the 827-Da and 573-Da peaks as the most intense peaks at 48-h incubation. At 24-h incubation, m/z of 1039 and 673 Da, corresponding to β-CN f197-206 and f201-206, respectively, were the greatest intensity peaks in the MALDI-TOF spectrum (Table 20), suggesting the possibility of competition for the availability of β-CN f197-206 as the precursor for β-CN f199-206 (PepE activity) and β-CN f201-206 (PepO3 activity). The fact that the 673-Da peak was the most intense peak at 48-h incubation indicates that PepO3 was more active than PepO on the Pro_{200}-Val_{201} bond (Tables 18 and 20).

Since PepE only cleaved β-CN f193-209 when the enzyme was present in combination with PepN or PepO-like endopeptidase, this observation suggests that the number of amino acid residues from the N-terminus of a peptide is important for PepE activity. In the PepE-PepN combination, β-CN f195-209 was the precursor for β-CN f199-209 formation, which became the precursor for β-CN f202-209 formation. Thus, PepE cleaved at the fourth and the third amino acid residue from the N-terminus in each case. With the PepE-PepO combination, β-CN f197-206 was the precursor for β-CN f199-206. In this case, PepE cleaved at the second amino acid residue from the N-terminus. The β-CN f198-206 and f199-206 peptides were possibly the precursors for β-CN f202-206. Thus, PepE cleaved at the fourth and the third amino acid residue from the N-terminus, respectively. Based on these analyses, PepE is likely to possess activity on 2 to 4 amino acid residues from the N-terminus.

Although β-CN f193-209 (m/z of 1881 Da) was still present in the hydrolysate up to 72-h incubation, this bitter peptide was not the most intense peak in the hydrolysis by PepE-PepO or PepE-PepO3 combinations (Tables 18 and 20). The combinations of PepE-PepO or PepE-PepO3 possibly contribute to the debittering of Cougar Gold. None of the peptides produced by PepE-PepO or PepE-PepO3 combinations have been reported to be bitter peptides (Tables 18 and 20). The large PepO or PepO3 activities on the Pro_{206}-Ile_{207} bond may prevent the formation of new bitter peptides from the C-terminus of β-CN f193-209.

Table 10. Peptide fragments formed during hydrolysis of β-CN f193-209 by PepO from *Lb. helveticus* WSU19 at 37°C under simulated cheese conditions (4% salt, w/v; 50mM citrate buffer pH 5.2)

Time (h)	m/z (Da)	193 Y	Q	Q	P	197 V	198 L	199 G	P	201 V	202 R	G	P	F	206 P	207 I	I	209 V	β-casein fragment
0	1881.2																		f193-209
2	1881.3																		f193-209
	1555.8																		f193-206
	1364.6																		f197-209
4	1881.3																		f193-209
	1555.5																		f193-206
	1364.3																		f197-209
	997.9																		f201-209
	1039.3																		f197-206
8	1881.3																		f193-209
	1555.5																		f193-206
	1364.6																		f197-209
	998.0																		f201-209
	1039.4																		f197-206
12	1881.2																		f193-209
	1555.4																		f193-206
	1364.3																		f197-209
	997.9																		f201-209
	1038.8																		f197-206
24	1881.2																		f193-209
	1555.8																		f193-206
	1364.5																		f197-209
	997.6																		f201-209
	1038.7																		f197-206
	1152.2																		f197-207
	939.5																		f198-206
	785.6																		f201-207
	672.4																		f201-206
48	1881.2																		f193-209
	1555.7																		f193-206
	1364.5																		f197-209
	997.6																		f201-209
	1038.7																		f197-206
	1152.8																		f197-207
	939.6																		f198-206
	785.4																		f201-207

Table 10 (continued)

Time (h)	m/z (Da)	193 Y	Q	Q	P	197 V	198 L	199 G	P	201 V	202 R	G	P	F	206 P	207 I	I	209 V	β-casein fragment
	672.3																		f201-206
	826.9																		f199-206
72	1882.8																		f193-209
	1556.6																		f193-206
	1365.4																		f197-209
	998.5																		f201-209
	1039.4																		f197-206
	1152.8																		f197-207
	940.2																		f198-206
	786.0																		f201-207
	672.8																		f201-206
	827.0																		f199-206
	573.7																		f202-206

Bitter peptide

Non-bitter peptide

The highest intensity peak in MALDI-TOF spectrum for each incubation time

Table 11. Peptide fragments formed during hydrolysis of β-CN f193-209 by PepO2 from *Lb. helveticus* WSU19 at 37°C under simulated cheese conditions (4% salt, w/v; 50mM citrate buffer pH 5.2)

Time (h)	m/z (Da)	193 **Y Q Q P V L G P V R G P F P I I V** 209	β-casein fragment
0	1881.3		f193-209
2	1881.3		f193-209
4	1881.3		f193-209
8	1881.3		f193-209
	1364.5		f197-209
12	1881.2		f193-209
	1364.1		f197-209
24	1881.3		f193-209
	1363.5		f197-209
48	1881.3		f193-209
	1364.1		f197-209
72	1881.3		f193-209
	1364.0		f197-209
	1555.1		f193-206

Bitter peptide

Non-bitter peptide

The highest intensity peak in MALDI-TOF spectrum for each incubation time

Table 12. Peptide fragments formed during hydrolysis of β-CN f193-209 by PepO3 from *Lb. helveticus* WSU19 at 37°C under simulated cheese conditions (4% salt, w/v; 50mM citrate buffer pH 5.2)

Time (h)	m/z (Da)	193 Y	Q	Q	P	197 V	198 L	G	P	201 V	R	G	P	F	206 P	207 I	I	209 V	β-casein fragment
0	1881.3																		f193-209
2	1881.3																		f193-209
	1555.8																		f193-206
	1364.6																		f197-209
4	1881.3																		f193-209
	1556.0																		f193-206
	1364.7																		f197-209
8	1881.3																		f193-209
	1555.7																		f193-206
	1364.5																		f197-209
	1038.8																		f197-206
	997.7																		f201-209
12	1881.3																		f193-209
	1555.7																		f193-206
	1364.7																		f197-209
	1038.9																		f197-206
	997.8																		f201-209
24	1881.3																		f193-209
	1555.9																		f193-206
	1364.4																		f197-209
	1039.5																		f197-206
	998.0																		f201-209
	940.0																		f198-206
	785.6																		f201-207
	672.6																		f201-206
48	1881.3																		f193-209
	1555.7																		f193-206
	1364.9																		f197-209
	1039.2																		f197-206
	998.1																		f201-209
	940.0																		f198-206
	785.7																		f201-207
	672.9																		f201-206

Table 12 (continued)

Time (h)	m/z (Da)	193 Y	Q	Q	P	197 V	198 L	G	P	201 V	R	G	P	F	206 P	207 I	I	209 V	β-casein fragment
72	1881.3																		f193-209
	1555.5																		f193-206
	1364.6																		f197-209
	1039.0																		f197-206
	998.0																		f201-209
	939.9																		f198-206
	785.5																		f201-207
	672.5																		f201-206

Bitter peptide

Non-bitter peptide

The highest intensity peak in MALDI-TOF spectrum for each incubation time for each incubation time

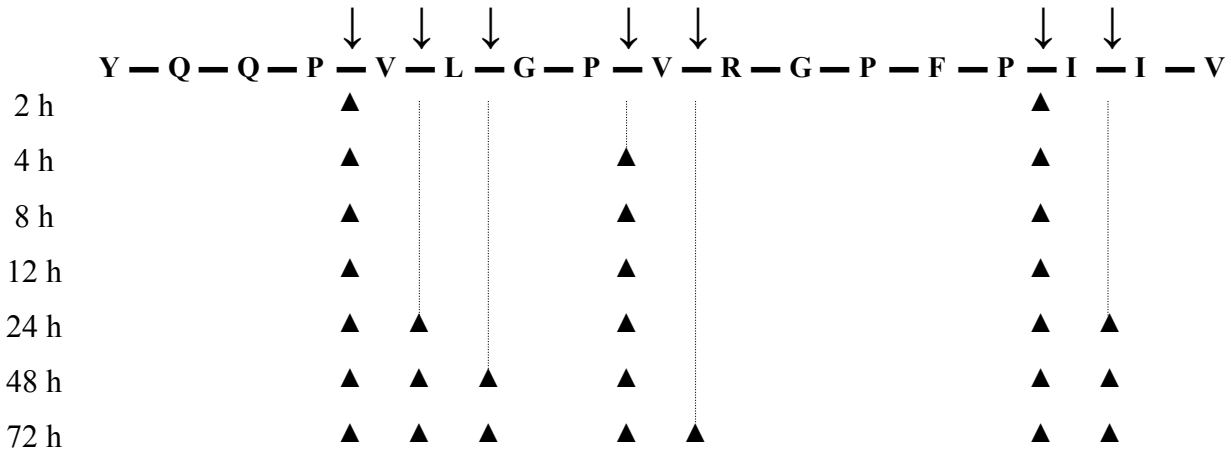

Figure 38. Cleavage sites of PepO from *Lb. helveticus* WSU19 in β-CN f193-209 as a function of incubation time (▲). ↓ indicates the overall peptide bonds in β-CN f193-209 cleaved by PepO from *Lb. helveticus* WSU19.

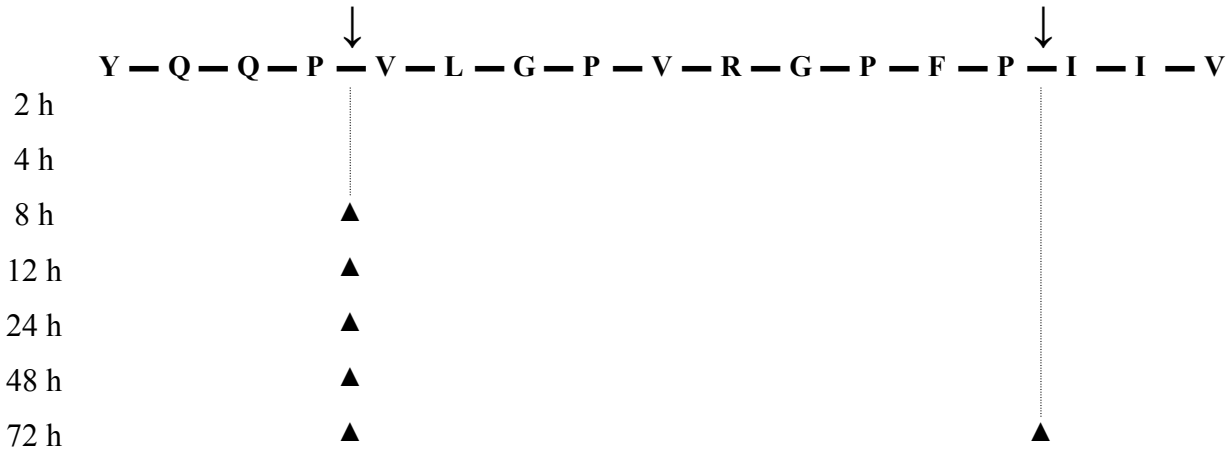

Figure 39. Cleavage sites of PepO2 from *Lb. helveticus* WSU19 in β-CN f193-209 as a function of incubation time (▲). ↓ indicates the overall peptide bonds in β-CN f193-209 cleaved by PepO2 from *Lb. helveticus* WSU19.

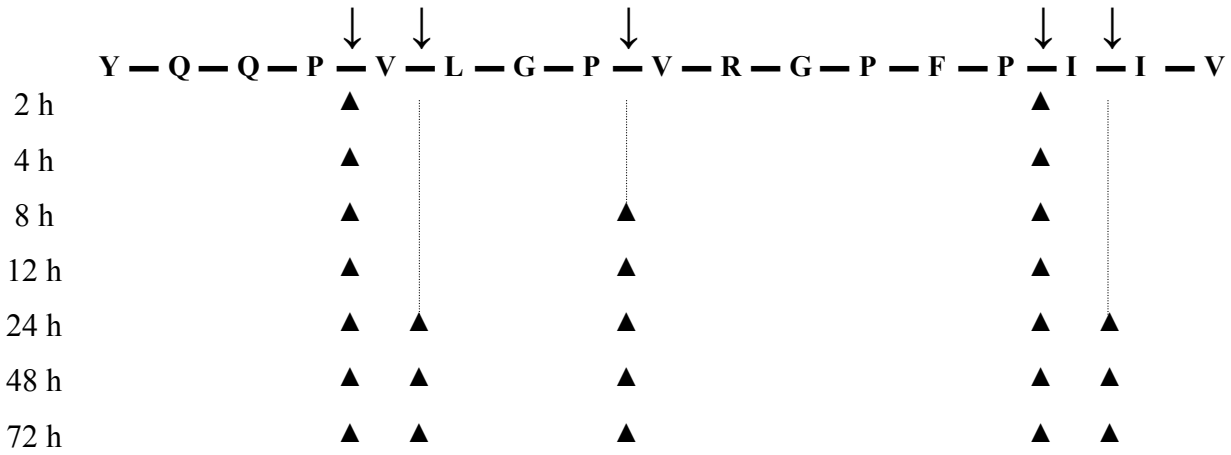

Figure 40. Cleavage sites of PepO3 from *Lb. helveticus* WSU19 in β-CN f193-209 as a function of incubation time (▲). ↓ indicates the overall peptide bonds in β-CN f193-209 cleaved by PepO3 from *Lb. helveticus* WSU19.

Table 13. Peptide fragments formed during hydrolysis of β-CN f193-209 by PepN from *Lb. helveticus* WSU19 at 37°C under simulated cheese conditions (4% salt, w/v; 50mM citrate buffer pH 5.2)

Time (h)	m/z (Da)	193 Y	194 Q	195 Q	P	V	L	G	P	V	R	G	P	F	P	I	I	209 V	β-casein fragment
0	1881.3																		f193-209
2	1881.3																		f193-209
	1718.2																		f194-209
	1701.1																		PCA[a]-f195-209
	1589.8																		f195-209
	1572.8																		PCA[a]-f196-209
4	1881.3																		f193-209
	1718.6																		f194-209
	1700.8																		PCA[a]-f195-209
	1589.9																		f195-209
	1572.6																		PCA[a]-f196-209
8	1718.1																		f194-209
	1700.5																		PCA[a]-f195-209
	1589.9																		f195-209
	1572.4																		PCA[a]-f196-209
12	1718.0																		f194-209
	1701.0																		PCA[a]-f195-209
	1590.0																		f195-209
	1572.9																		PCA[a]-f196-209
24	1717.6																		f194-209
	1700.5																		PCA[a]-f195-209
	1590.0																		f195-209
	1572.6																		PCA[a]-f196-209
48	1701.0																		PCA[a]-f195-209
	1590.0																		f195-209
	1573.0																		PCA[a]-f196-209
72	1699.7																		PCA[a]-f195-209
	1589.3																		f195-209
	1572.4																		PCA[a]-f196-209

Bitter peptide

Non-bitter peptide

The highest intensity peak in MALDI-TOF spectrum for each incubation time

[a]PCA, pyrrolidonecarboxylic acid

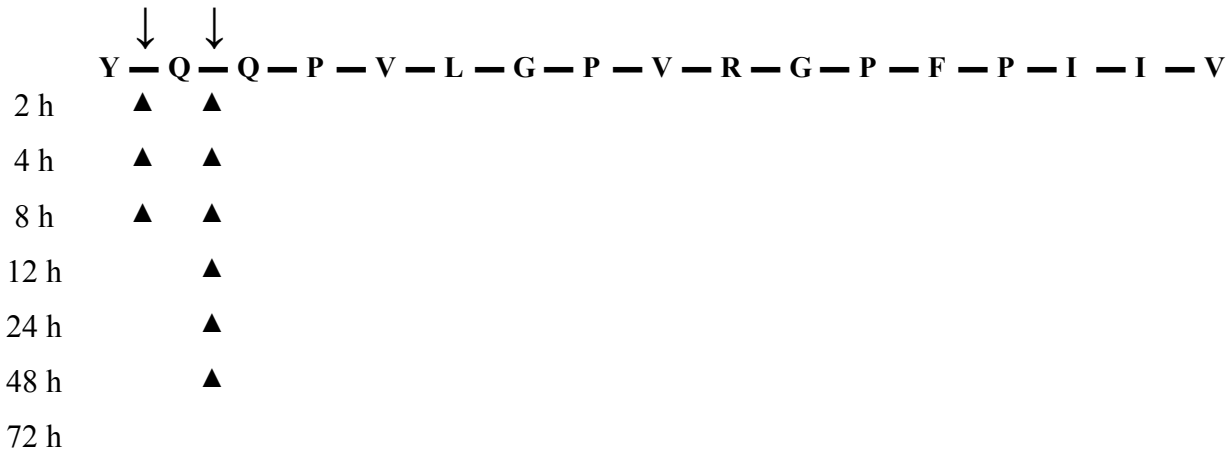

Figure 41. Cleavage sites of PepN from *Lb. helveticus* WSU19 in β-CN f193-209 as a function of incubation time (▲). ↓ indicates the overall peptide bonds in β-CN f193-209 cleaved by PepN from *Lb. helveticus* WSU19.

Table 14. Peptide fragments formed during hydrolysis of β-CN f193-209 by PepN and PepO from *Lb. helveticus* WSU19 at 37°C under simulated cheese conditions (4% salt, w/v; 50mM citrate buffer pH 5.2)

Time (h)	m/z (Da)	193 Y	194 Q	195 Q	P	197 V	198 L	199 G	P	201 V	202 R	G	P	F	206 P	207 I	I	209 V	β-casein fragment
12	1718.2																		f194-209
	1590.0																		f195-209
	1392.6																		f194-206
	1376.2																		PCA[a]-f195-206
	1264.6																		f195-206
	1247.4																		PCA[a]-f196-206
	1152.2																		f197-207
	1039.0																		f197-206
	939.5																		f198-206
	826.5																		f199-206
	672.3																		f201-206
	573.2																		f202-206
24	1589.9																		f195-209
	939.8																		f198-206
	827.0																		f199-206
	672.3																		f201-206
	573.8																		f202-206

Bitter peptide

Non-bitter peptide

The highest intensity peak in MALDI-TOF spectrum for each incubation time

[a]PCA, pyrrolidonecarboxylic acid

Table 15. Peptide fragments formed during hydrolysis of β-CN f193-209 by PepN and PepO2 from *Lb. helveticus* WSU19 at 37°C under simulated cheese conditions (4% salt, w/v; 50mM citrate buffer pH 5.2)

Time (h)	m/z (Da)	193 Y	194 Q	195 Q	P	V	L	199 G	P	V	R	G	P	F	206 P	I	I	209 V	β-casein fragment
24	1701.1																		PCA[a]-f195-209
	1590.0																		f195-209
	1572.9																		PCA[a]-f196-209
	1152.4																		f199-209
48	1700.5																		PCA[a]-f195-209
	1590.0																		f195-209
	1572.9																		PCA[a]-f196-209
	1152.2																		f199-209
	1264.3																		f195-206

Bitter peptide

Non-bitter peptide

The highest intensity peak in MALDI-TOF spectrum for each incubation time

[a]PCA, pyrrolidonecarboxylic acid

Table 16. Peptide fragments formed during hydrolysis of β-CN f193-209 by PepN and PepO3 from *Lb. helveticus* WSU19 at 37°C under simulated cheese conditions (4% salt, w/v; 50mM citrate buffer pH 5.2)

Time (h)	m/z (Da)	193 Y	194 Q	195 Q	P	197 V	198 L	199 G	P	201 V	202 R	G	P	F	206 P	207 I	I	209 V	β-casein fragment
12	1718.2																		f194-209
	1590.0																		f195-209
	1392.8																		f194-206
	1376.4																		PCA[a]-f195-206
	1264.8																		f195-206
	1247.4																		PCA[a]-f196-206
	1152.3																		f197-207
	1039.1																		f197-206
	940.0																		f198-206
	827.0																		f199-206
	672.7																		f201-206
	573.7																		f202-206
24	1589.9																		f195-209
	939.7																		f198-206
	827.0																		f199-206
	672.3																		f201-206
	573.8																		f202-206

Bitter peptide

Non-bitter peptide

The highest intensity peak in MALDI-TOF spectrum for each incubation time

[a]PCA, pyrrolidonecarboxylic acid

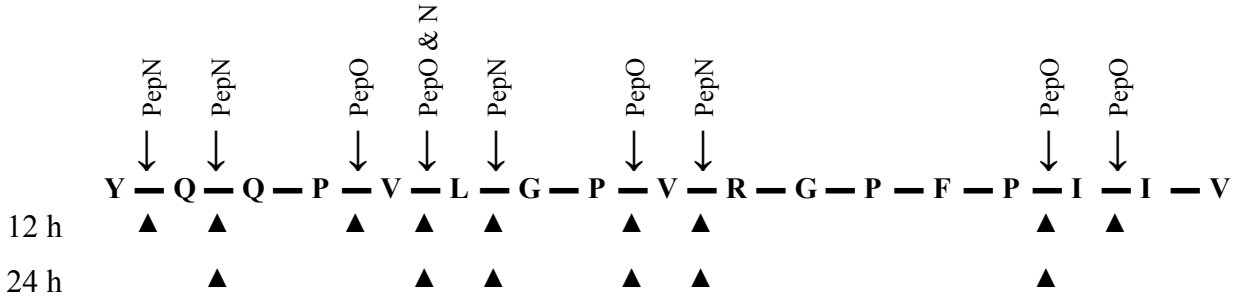

Figure 42. Cleavage sites of PepN and PepO from *Lb. helveticus* WSU19 in β-CN f193-209 as a function of incubation time (▲). ↓ indicates the overall peptide bonds in β-CN f193-209 cleaved by PepN and/or PepO from *Lb. helveticus* WSU19.

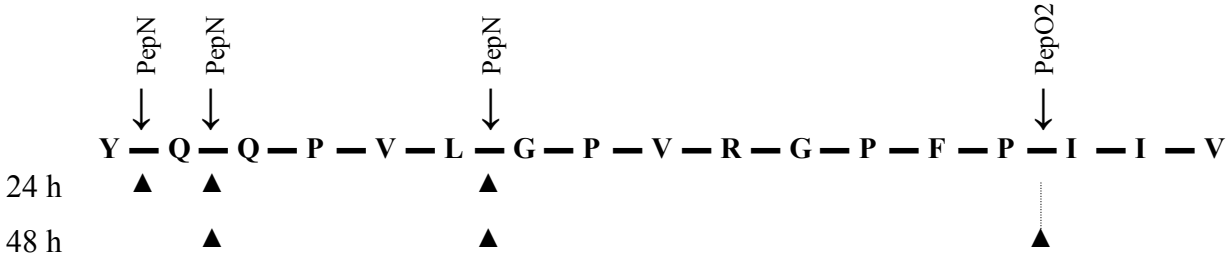

Figure 43. Cleavage sites of PepN and PepO2 from *Lb. helveticus* WSU19 in β-CN f193-209 as a function of incubation time (▲). ↓ indicates the overall peptide bonds in β-CN f193-209 cleaved by PepN and/or PepO2 from *Lb. helveticus* WSU19.

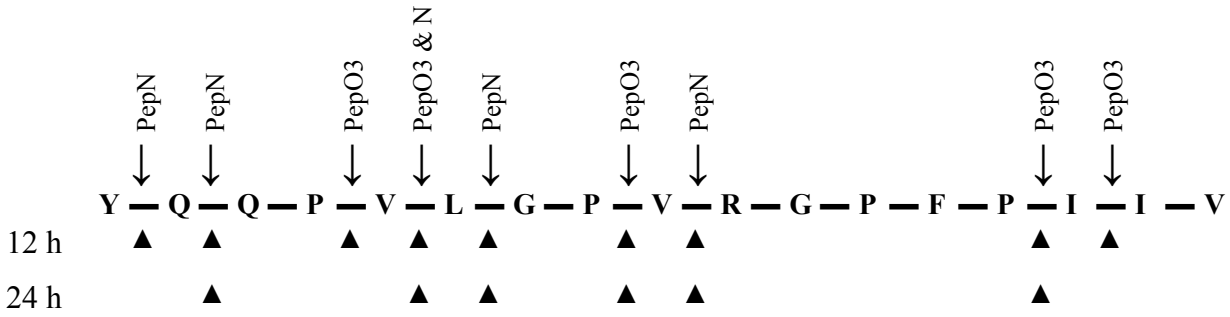

Figure 44. Cleavage sites of PepN and PepO3 from *Lb. helveticus* WSU19 in β-CN f193-209 as a function of incubation time (▲). ↓ indicates the overall peptide bonds in β-CN f193-209 cleaved by PepN and/or PepO3 from *Lb. helveticus* WSU19.

Table 17. Peptide fragments formed during hydrolysis of β-CN f193-209 by PepE and PepN from *Lb. helveticus* WSU19 at 37°C under simulated cheese conditions (4% salt, w/v; 50mM citrate buffer pH 5.2)

Time (h)	m/z (Da)	193 Y	194 Q	195 Q	P	V	L	199 G	P	V	202 R	G	P	F	P	I	I	209 V	β-casein fragment
2	1881.3																		f193-209
	1718.4																		f194-209
	1701.1																		PCA[a]-f195-209
	1589.9																		f195-209
	1572.8																		PCA[a]-f196-209
4	1881.5																		f193-209
	1718.1																		f194-209
	1700.9																		PCA[a]-f195-209
	1589.8																		f195-209
	1572.7																		PCA[a]-f196-209
	1151.9																		f199-209
8	1718.1																		f194-209
	1701.0																		PCA[a]-f195-209
	1590.0																		f195-209
	1573.0																		PCA[a]-f196-209
	1152.0																		f199-209
12	1718.1																		f194-209
	1700.9																		PCA[a]-f195-209
	1590.0																		f195-209
	1572.9																		PCA[a]-f196-209
	1151.8																		f199-209
24	1701.0																		PCA[a]-f195-209
	1590.0																		f195-209
	1572.7																		PCA[a]-f196-209
	1152.0																		f199-209
48	1700.0																		PCA[a]-f195-209
	1589.5																		f195-209
	1572.4																		PCA[a]-f196-209
	1151.9																		f199-209
	898.0																		f202-209

Bitter peptide

Non-bitter peptide

The highest intensity peak in MALDI-TOF spectrum for each incubation time

[a]PCA, pyrrolidonecarboxylic acid

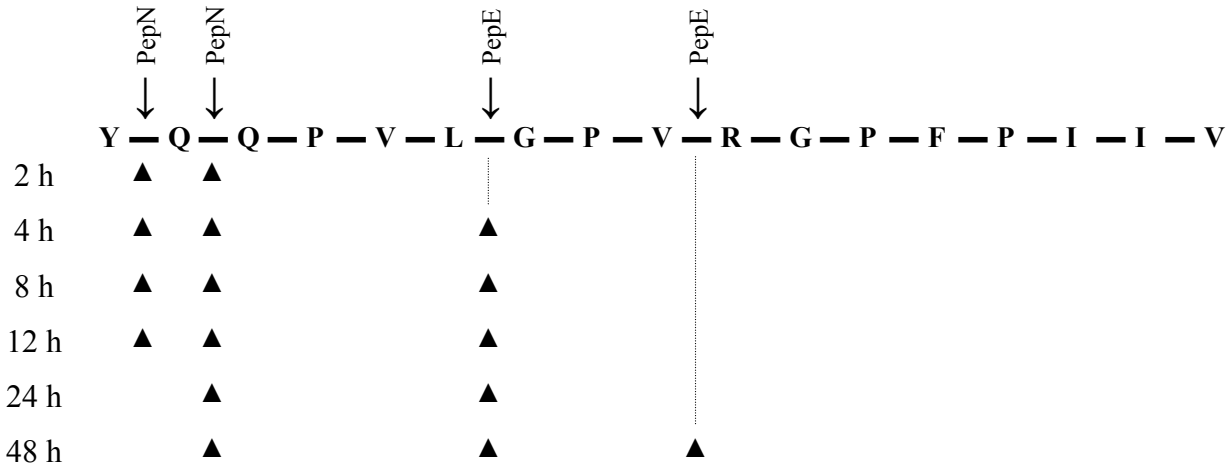

Figure 45. Cleavage sites of PepE and PepN from *Lb. helveticus* WSU19 in β-CN f193-209 as a function of incubation time (▲). ↓ indicates the overall peptide bonds in β-CN f193-209 cleaved by PepE and/or PepN from *Lb. helveticus* WSU19.

Table 18. Peptide fragments formed during hydrolysis of β-CN f193-209 by PepE and PepO from *Lb. helveticus* WSU19 at 37°C under simulated cheese conditions (4% salt, w/v; 50mM citrate buffer pH 5.2)

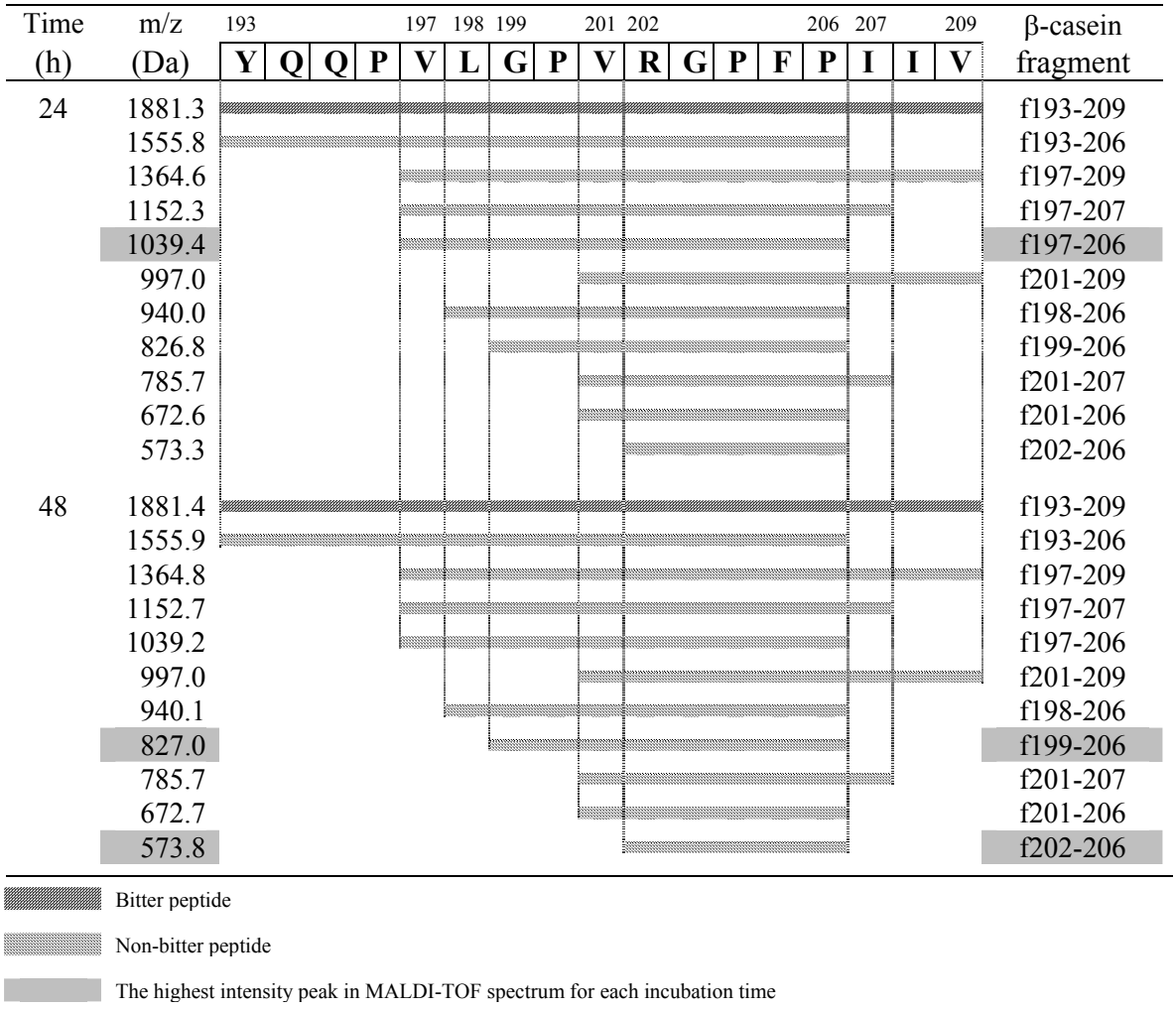

Table 19. Peptide fragments formed during hydrolysis of β-CN f193-209 by PepE and PepO2 from *Lb. helveticus* WSU19 at 37°C under simulated cheese conditions (4% salt, w/v; 50mM citrate buffer pH 5.2)

Time (h)	m/z (Da)	193 Y	Q	Q	P	197 V	198 L	199 G	P	V	202 R	G	P	F	206 P	207 I	I	209 V	β-casein fragment
24	1881.3																		f193-209
	1555.4																		f193-206
	1363.6																		f197-209
	1152.2																		f199-209
	898.6																		f202-209
48	1881.3																		f193-209
	1555.7																		f193-206
	1363.6																		f197-209
	1151.3																		f199-209
	898.2																		f202-209

Bitter peptide

Non-bitter peptide

The highest intensity peak in MALDI-TOF spectrum for each incubation time

Table 20. Peptide fragments formed during hydrolysis of β-CN f193-209 by PepE and PepO3 from *Lb. helveticus* WSU19 at 37°C under simulated cheese conditions (4% salt, w/v; 50mM citrate buffer pH 5.2)

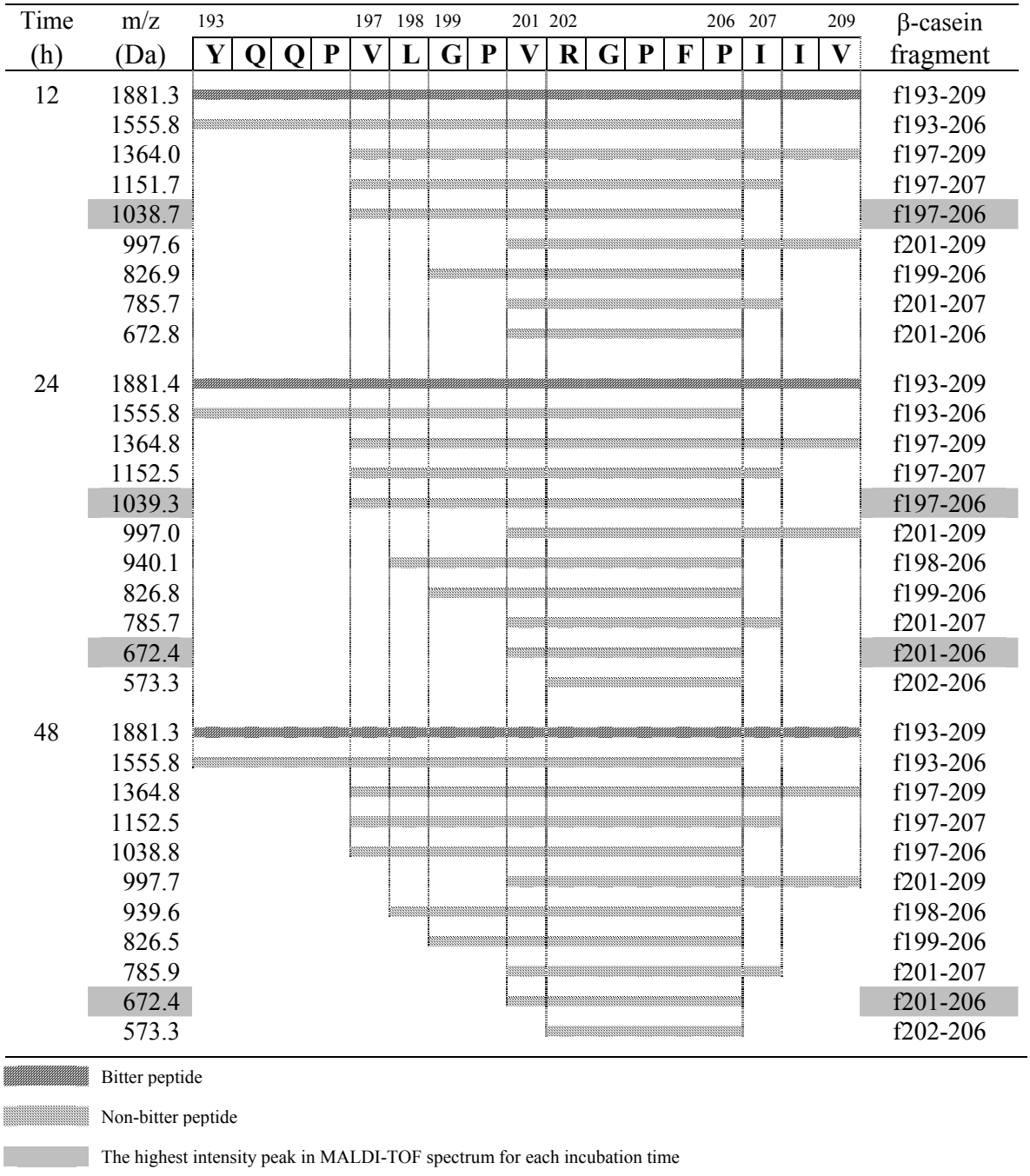

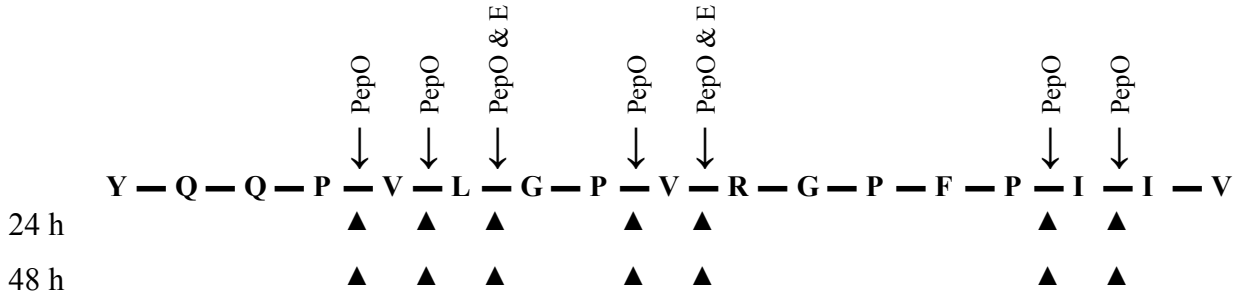

Figure 46. Cleavage sites of PepE and PepO from *Lb. helveticus* WSU19 in β-CN f193-209 as a function of incubation time (▲). ↓ indicates the overall peptide bonds in β-CN f193-209 cleaved by PepE and/or PepO from *Lb. helveticus* WSU19.

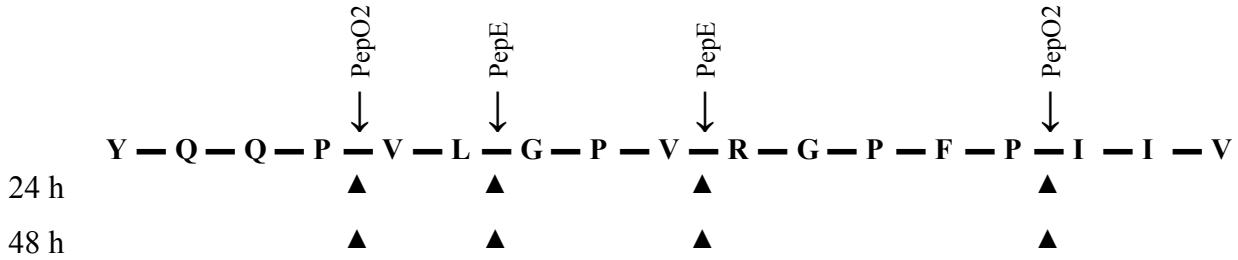

Figure 47. Cleavage sites of PepE and PepO2 from *Lb. helveticus* WSU19 in β-CN f193-209 as a function of incubation time (▲). ↓ indicates the overall peptide bonds in β-CN f193-209 cleaved by PepE and/or PepO2 from *Lb. helveticus* WSU19.

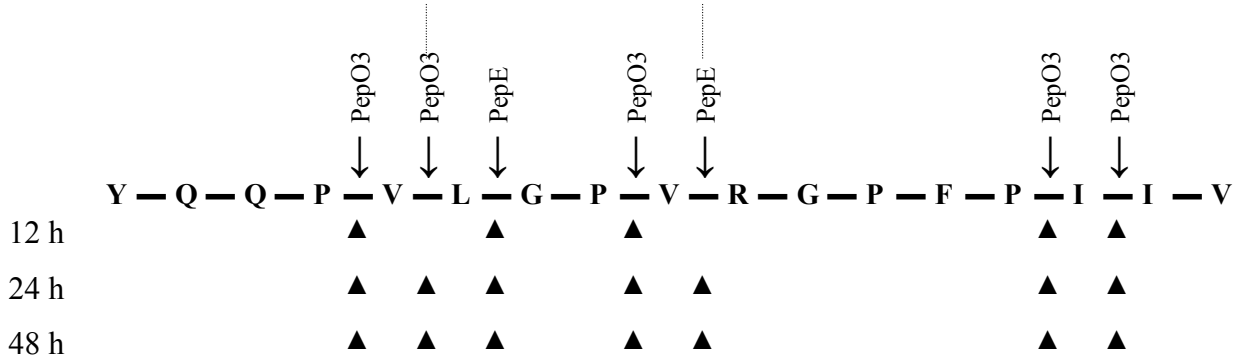

Figure 48. Cleavage sites of PepE and PepO3 from *Lb. helveticus* WSU19 in β-CN f193-209 as a function of incubation time (▲). ↓ indicates the overall peptide bonds in β-CN f193-209 cleaved by PepE and/or PepO3 from *Lb. helveticus* WSU19.

11. Degradation of α_{s1}-CN f1-23 by PepO, PepO2, and PepO3

The 1-23 fragment of α_{s1}-CN is the primary product of α_{s1}-CN hydrolysis by chymosin (Exterkate, 1987). The α_{s1}-CN f1-23 peptide in cheese is further hydrolyzed, primarily by starter proteinases (Exterkate and Alting, 1993; 1995). In addition to the proteinases, hydrolysis of α_{s1}-CN f1-23 occurs by the action of starter peptidases (Exterkate and Alting 1993; 1995). In contrast to β-CN f193-209, α_{s1}-CN f1-23 is not a bitter peptide. However, some peptides derived from α_{s1}-CN f1-23 have been determined to be bitter, including α_{s1}-CN f1-7 (m/z 876 Da), α_{s1}-CN f1-9 (m/z 1142 Da), α_{s1}-CN f1-13 (m/z 1537 Da), α_{s1}-CN f11−14 (m/z 484 Da), α_{s1}-CN f14-17 (m/z 475 Da), α_{s1}-CN f17-21 (m/z 603 Da), and α_{s1}-CN f21-23 (436 Da) (Lemieux and Simard, 1992; Lee et al., 1996; Broadbent et al., 1998). Christensson et al. (2002) hypothesized that fragment 1-14 of α_{s1}-CN (m/z of 1666 Da) is bitter because the peptide has a similar structure and hydrophobicity to α_{s1}-CN f1-13. In addition, the latter group also reported that α_{s1}-CN f1-17 (m/z of 1992 Da) tastes bitter. In contrast to Christensson et al. (2002), Broadbent et al. (1998) reported a negative correlation between the concentrations of fragments 1-13 and 1-14 of α_{s1}-CN and the bitterness intensity of cheese. In addition, Broadbent et al. (1998) reported no correlation between the concentration of α_{s1}-CN f1-17 and the bitterness of cheese. In the present study, the peptide fragments 1-13, 1-14, and 1-17 are considered bitter peptides.

Tables 21-23 list the mass-to-charge ratio (m/z) of peaks in the MALDI-TOF spectra and the corresponding peptide fragments formed during hydrolysis of α_{s1}-CN f1-23 by CFEs from *E. coli* DH5α(pES5), *E. coli* DH5α(pES2), and *E. coli* DH5α(pES6). These *E. coli* clones express the *pepO*, *pepO2*, and *pepO3* genes from *Lb. helveticus* WSU19, respectively.

Hydrolysis of α_{s1}-CN f1-23 by CFE from *E. coli* DH5α(pJDC9) served as the control. No peaks corresponding to peptide fragments derived from α_{s1}-CN f1-23 were observed in the control. Peptides with m/z ratio less than 500 Da were not detected by the MALDI-TOF analyses in this study due to the mass acquisition being set at 500 Da to 4000 Da. The 2765-Da peak, corresponding to the mass of α_{s1}-CN f1-23, exhibits the greatest intensity in all of the MALDI-TOF spectra. Thus, to demonstrate the dynamics of α_{s1}-CN f1-23 hydrolysis, the data are presented in the Tables such that the second most intense peak is highlighted. In the case of β-CN f193-209, the highlighted peak represented the peak exhibiting the greatest intensity in the MALDI-TOF spectrum.

In contrast to the MALDI-TOF analyses of peptides from β-CN f193-209, Tables 21-23 display peptides mostly from the C-terminus of α_{s1}-CN f1-23. For example, at 2-h incubation with PepO (Table 21), the MALDI-TOF spectrum displayed peptides with m/z ratios of 1907.8, 1770.8, 1246.5, and 1117.5 Da, corresponding to the masses of α_{s1}-CN f8-23, f9-23, f14-23, and f15-23, respectively. The complementary sequences from the N-terminus of α_{s1}-CN f1-23, namely f1-7, f1-8, f-13, and f1-14, respectively, were not observed. This observation indicates a suppression effect on peptide ions from the N-terminus of α_{s1}-CN f1-23. Although the peptide fragments observed in the MALDI-TOF spectra are not bitter (Tables 21-23), the complementary peptides from the N-terminus of α_{s1}-CN f1-23 may be bitter.

Knochenmuss et al. (2000) explained that analyte-analyte suppression effect is the result of secondary proton transfer during ionization process in MALDI. The transfer of proton occurs via direct analyte-analyte collisions or matrix-mediated process. Proton affinities or gas-phase basicity of the analytes are important in determining the direction of

suppression. Thus, the presence of basic amino acids, including arginine, lysine, and histidine, in a peptide is expected to enhance the peak intensity of the peptide in the MALDI-TOF spectrum. In contrast, Valero et al. (1999), Burkitt et al. (2003), and Baumgart et al. (2004) reported that suppression effect does not relate directly to peptide basicity or hydrophobicity.

Valero et al. (1999) reported that an efficient peptide ionization is determined by the ease of peptide desorption from the matrix, which in turn is affected by the amino acid side chains. Peptide desorption is enhanced by aliphatic apolar amino acids (leucine, isoleucine, and valine), aromatic amino acids (tyrosine and phenylalanine), proline, and arginine. On the other hand, the presence of acidic amino acids (glutamic and aspartic acids) and basic amino acids (lysine and histidine) exhibited the opposite effect. The impact of arginine on peptide desorption is due to electrostatic stabilization of the carboxylate group of the matrix by the positively charged guanidine group via hydrogen bonding. Primary amino groups cannot perform this stabilization. The matrix stabilization increases co-crystalllization of matrix and peptide, which promotes desorption.

Baumgart et al. (2004) supported the findings reported by Valero et al. (1999). The presence of arginine, phenylalanine, leucine, and proline were reported to increase the peak intensity of a peptide in a MALDI-TOF spectrum. Furthermore, the signal-enhancing effect of arginine depends on the adjacent amino acids. When arginine is attached to an acidic amino acid, the peak intensity decreases because the positively charged guanidine group interacts with the adjacent carboxylate anion via a tight salt bridge. Baumgart et al. (2004) also reported low peak intensities of peptides containing lysine residue(s).

Burkitt et al. (2003) hypothesized that peptide ion mobility and proton affinity are two important factors in peptide ion suppression. Peptides resulting from ablation by laser irradiation undergo competition for charge. The protonated matrix acts as the charge donor. Peptide mobility determines the extent of peptide-peptide and peptide-matrix interactions. The mobility of a peptide relates to its mass. Small peptides tend to run ahead, while large peptides lag behind and are separated from the charged matrix molecules.

Several factors might account for the suppression of peptides from the N-terminus of α_{s1}-CN f1-23 by the C-terminal peptides. Although the C-terminus of α_{s1}-CN f1-23 contains 2 glutamic acid residues, the presence of valine (1), leucine (3), arginine (1), and phenylalanine (1) residues might compensate for the effect of glutamic acid on peptide desorption and ionization. Moreover, the arginine residue on the C-terminus is located between leucine and phenylalanine, which might strengthen the impact of arginine. In contrast to the C-terminus, the N-terminus of α_{s1}-CN f1-23 contains 2 lysine and 2 histidine residues, which prevent peptide desorption. The presence of lysine and histidine might negate the signal-enhancing effect of arginine and proline residues. In addition to the amino acid composition, the size of peptide fragments derived from the C-terminus of α_{s1}-CN f1-23, except for f8-23, f9-23, and f10-23, are smaller than the complementary fragments from the N-terminus. Consequently, the C-terminus peptides possess mobilities that enable rapid interaction with the protonated matrix.

The following results (Tables 21-23) show the different activities of PepO, PepO2, and PepO3 in the early stage of α_{s1}-CN f1-23 hydrolysis. Incubation of α_{s1}-CN f1-23 with PepO from *Lb. helveticus* WSU19 produced peaks at m/z of 1908, 1771, 1247, and 1118 Da after 2 h. These peaks correspond to α_{s1}-CN f8-23, f9-23, f14-23, and f15-23, respectively.

Hydrolysis of α_{s1}-CN f1-23 by PepO2 from *Lb. helveticus* WSU19 produced 1771-Da and 1118-Da peaks at 2-h incubation, while a peak at m/z of 1247 Da was observed after 12 h (Table 22). The 1908-Da peak, corresponding to α_{s1}-CN f8-23, was not observed during the 72-h incubation with PepO2 from *Lb. helveticus* WSU19. A peak at m/z of 1118 Da and 1247 Da were formed after 2-h and 4-h incubation with PepO3 from *Lb. helveticus* WSU19, respectively, while the formation of 1908-Da and 1770-Da peaks were observed after 12-h and 24-h incubations, respectively (Table 23). Based on these observations, during the first 2-h incubation, the Glu_{14}-Val_{15} bond in α_{s1}-CN f1-23 was cleaved by PepO, PepO2, or PepO3; His_8-Gln_9 was cleaved by PepO or PepO2; and Lys_7-His_8 and Gln_{13}-Glu_{14} bonds were cleaved by PepO only (Figures 49-51). In addition, hydrolysis on the Lys_7-His_8 bond never occurred during 72-h incubation with PepO2 (Figure 50).

Because of the sampling interval and the activity of PepO, it is not clear which site is the first cleavage site of PepO in α_{s1}-CN f1-23. Incubation of α_{s1}-CN f1-23 with PepO produced the fragments 8-23, 9-23, 14-23, and 15-23 as early as 2 h (Table 21). However, the peak corresponding to f15-23 (m/z of 1118 Da) was the most intense among the peptides derived from α_{s1}-CN f1-23 up to 12-h incubation (Table 21). It can be interpreted that PepO most readily cleaves the Glu_{14}-Val_{15} bond in α_{s1}-CN f1-23 (Figure 49). Compared to the 1908-Da and 1771-Da peaks, the 1247-Da peak exhibited a greater intensity in the MALDI-TOF spectra, indicating the possibility that the Gln_{13}-Glu_{14} bond in α_{s1}-CN f1-23 is the second preferred cleavage site of PepO from *Lb. helveticus* WSU19 (Figure 49).

At 24-h incubation of α_{s1}-CN f1-23 with PepO, the peak at m/z of 1666 Da was dominant (Table 21). The m/z ratio of 1666 Da corresponds to the mass of α_{s1}-CN f1-14, which is the complementary sequence of α_{s1}-CN f15-23. The 1666-Da peak was observed

initially after 8-h incubation at a much lower intensity than its complementary 1118-Da peak. The emergence of the α_{s1}-CN f1-14 peptide (m/z of 1666 Da) as dominant in the spectra at or after 24 h shows that the peptide is less readily broken down compared to its complementary peptide α_{s1}-CN f15-23. The α_{s1}-CN f15-23 peptide is cleaved at Asn_{17}-Glu_{18}, Glu_{18}-Asn_{19}, and Asn_{19}-Leu_{20} bonds to form α_{s1}-CN f18-23, f19-23, and 20-23, respectively (Figure 49; Table 21). The appearance of peaks at m/z of 791, 662, and 548 Da correspond to the masses of α_{s1}-CN f18-23, f19-23, and f20-23, respectively (Table 21). These peaks were observed as early as 8-h incubation, at which time the 1666-Da peak was initially observed.

The low susceptibility of α_{s1}-CN f1-14 to be further hydrolyzed by PepO is in agreement with Baankreis et al. (1995). The 1-12 fragment of α_{s1}-CN observed at 48-h was more likely produced by hydrolysis of α_{s1}-CN f1-23 than α_{s1}-CN f1-14 at the Pro_{12}-Gln_{13} bond. The complementary sequence of α_{s1}-CN f1-12, i.e., α_{s1}-CN f13-23, was further hydrolyzed at Leu_{21}-Arg_{22} to form α_{s1}-CN f13-21. The α_{s1}-CN f13-21 peptide (m/z of 1072 Da) was observed in the MALDI-TOF spectra at 48 h and 72 h. The cleavage at the Leu_{21}-Arg_{22} bond after 48 h might explain the disappearance of α_{s1}-CN f18-23, f19-23, and f20-23 (Table 21). In contrast to α_{s1}-CN f1-12, α_{s1}-CN 6-14 (m/z of 1050 Da), first observed at 48-h incubation, may indicate poor cleavage of α_{s1}-CN f1-14 at the Pro_5-Ile_6 bond.

In addition to α_{s1}-CN f15-23, PepO from *Lb. helveticus* WSU19 also hydrolyzed α_{s1}-CN f14-23, f8-23, and f9-23. The complementary sequence of α_{s1}-CN f14-23, i.e., f1-13 (m/z of 1537 Da), was observed after 48-h incubation of α_{s1}-CN f1-23 with PepO (Table 21). A peak with m/z of 1072 Da was observed at 48-h incubation (Table 21). This m/z ratio corresponds to the mass of α_{s1}-CN f14-20, suggesting that hydrolysis occurs at Leu_{20}-Leu_{21}.

The fragments 8-23 and 9-23 of α_{s1}-CN were cleaved at the Glu_{14}-Val_{15} bond, forming α_{s1}-CN f8-14 (m/z of 808 Da) and α_{s1}-CN f9-14 (m/z of 672 Da), respectively (Table 21). These peptides were observed initially at 48-h incubation. In addition to the above cleavage sites, PepO from *Lb. helveticus* WSU19 also exhibited poor cleavage at the Gln_9-Gly_{10} bond, forming α_{s1}-CN f10-23 (m/z of 1642 Da), after 24-h incubation (Table 21).

The formation of α_{s1}-CN f15-23, f14-23, f8-23, and f10-23 by PepO may be important for cheese quality since the complementary sequences of these peptides, namely α_{s1}-CN f1-14, f1-13, f1-7, and f1-9, respectively, potentially contribute to the bitterness intensity of cheese. The fragments 1-13, 1-14, 14-23, and 19-23 of α_{s1}-CN were identified in a one year-old commercial Cheddar cheese (Gouldsworthy et al., 1996).

A peak at m/z of 1118 Da, corresponding to α_{s1}-CN f15-23, exhibited the greatest intensity among PepO2 hydrolysis products of α_{s1}-CN f1-23 in the first 24 h (Table 22). This observation indicates that Glu_{14}-Val_{15} is the preferred cleavage site of PepO2 in α_{s1}-CN f1-23. PepO2 seemed to hydrolyze the α_{s1}-CN f15-23 at Glu_{18}-Asn_{19}, Asn_{19}-Leu_{20}, and Arg_{22}-Phe_{23} bonds to form α_{s1}-CN f19-23, f20-23, and f15-22, respectively (Figure 50; Table 22). Table 22 demonstrates the formation of 662-Da, 548-Da, and 971-Da peaks, initially observed at 12-h, 24-h, and 48-h incubations, respectively. These m/z ratios correspond to the masses of α_{s1}-CN f19-23, f20-23, and f15-22, respectively (Table 22). The cleavage at the Arg_{22}-Phe_{23} bond might indicate that PepO2 possesses a weak carboxypeptidase activity.

The appearance of the 662-Da peak at 12-h incubation was accompanied by the appearance of a 1666-Da peak, corresponding to the mass of α_{s1}-CN f1-14. The α_{s1}-CN f1-14 peptide is the complementary sequence of α_{s1}-CN f15-23. The simultaneous appearance of 1666-Da and 662-Da peaks supports the assumption that the appearance of the N-terminus of

a peptide sequence occurs upon hydrolysis of the complementary C-terminus of the peptide. In contrast to the hydrolysis of α_{s1}-CN f1-23 by PepO, the 1666-Da peak was not the most intense peak among the peptide hydrolysates from α_{s1}-CN f1-23 up to 72-h incubation (Table 22). This observation indicates that α_{s1}-CN f15-23 is more resistant to hydrolysis by PepO2 than PepO.

In contrast to PepO, the second cleavage site preferred by PepO2 in the early hydrolysis of α_{s1}-CN f1-23 is His_8-Gln_9, resulting in the formation of α_{s1}-CN f9-23 (m/z of 1771 Da; Table 22). However, the f9-23 product of cleavage of the His_8-Gln_9 bond was observed only at or before 12 h. The disappearance of the 1771-Da peak after 12 h was accompanied by the appearance of a 1247-Da peak, corresponding to the mass of α_{s1}-CN f14-23 (Table 22). It is not clear what is responsible for the disappearance of the 1771-Da peak after 12-h incubation. It is possible that the α_{s1}-CN f9-23 peptide was completely hydrolyzed into f14-23 at 24 h. The occurrence of 14-23 fragment of α_{s1}-CN up to 72-h incubation, after the depletion of the parent peptide, suggests the resistance of this peptide to hydrolysis by PepO2. Moreover, the complementary sequence of α_{s1}-CN f14-23, i.e., f1-13 did not appear until 72-h incubation, supporting the resistance of f14-23 to PepO2 hydrolysis.

The fact that PepO2 did not continue hydrolyzing the His_8-Gln_9 bond after α_{s1}-CN f14-23 formation suggests an alteration of PepO2 specificities. PepO2 might prefer to cleave substrate smaller than α_{s1}-CN f1-23 or f9-23, which was not available initially (Table 22). As hydrolysis progressed, small peptide (f15-23) became available as a PepO2 substrate. PepO2 apparently preferred to hydrolyze α_{s1}-CN f15-23 at the Glu_{18}-Asn_{19} bond in the later stages of incubation (Figure 50). At 12-h incubation, a peak with m/z of 662 Da, corresponding to α_{s1}-CN f19-23, was first observed (Table 22). The 662-Da peak exhibited the same intensity

as the 1118-Da peak at 48-h incubation (Table 22). Similarly, the 662-Da, 1118-Da, and 1666-Da peaks exhibited the same intensities at 72-h incubation. The preferential cleavage at the Glu_{18}-Asn_{19} bond might account for the discontinuation of α_{s1}-CN f9-23 hydrolysis. The fact that PepO2 preferred to cleave the Glu_{18}-Asn_{19} bond differentiates PepO2 from PepO in the later stages of α_{s1}-CN f1-23 hydrolysis.

Compared to PepO and PepO2, hydrolysis of α_{s1}-CN f1-23 by PepO3 differed in that a smaller number of peptides were produced early in the incubation (Table 23). The 791-Da, 662-Da, and 548-Da peaks, corresponding to the fragments α_{s1}-CN f18-23, f19-23, and f20-23, respectively, were detected only after incubation for 72 h (Table 23). Similar to PepO and PepO2, the preferred cleavage site of PepO3 from *Lb. helveticus* WSU19 in the early hydrolysis of α_{s1}-CN f1-23 is the Glu_{14}-Val_{15} bond, forming α_{s1}-CN f15-23 (m/z of 1118 Da) (Figure 51). The fragment 15-23 of α_{s1}-CN f1-23 was the predominant peptide seen during the 72-h incubation with PepO3 (Table 23).

The second cleavage during the initial hydrolysis of α_{s1}-CN f1-23 by the PepO3 enzyme was at Gln_{13}-Glu_{14}, as indicated by the formation of a 1247-Da peak, corresponding to the mass of α_{s1}-CN f14-23, at 4-h incubation (Table 23). The pattern of peptidolytic action by PepO3 on α_{s1}-CN f1-23 also suggests that the fragments 8-23 and 9-23 of α_{s1}-CN are not the parent compounds for the formation of α_{s1}-CN f14-23 or α_{s1}-CN f15-23. The former 2 fragments were detected after 12-h and 24-h incubation, respectively, while the latter 2 fragments were initially seen at 2 h and 4 h, respectively. In general, the preferred cleavage sites of PepO3 in α_{s1}-CN f1-23 are more similar to PepO than PepO2.

Figures 49-51 illustrate the cleavage sites of PepO, PepO2, and PepO3 enzymes from *Lb. helveticus* WSU19 in α_{s1}-CN f1-23. Unlike their activities on β-CN f193-209, the -Pro-

X- bond is not the preferred cleavage site of these endopeptidases in α_{s1}-CN f1-23. While PepO did cleave the Pro_5-Ile_6 and Pro_{12}-Gln_{13} bonds, it was detected only after 48-h incubation (Figure 49). No cleavage at these proline bonds was observed during 72-h incubations with PepO2 and PepO3 (Figures 50, 51). Cleavages by PepO, PepO2, or PepO3 from *Lb. helveticus* WSU19 in α_{s1}-CN f1-23 preferentially occurred at the peptide bonds that involve glutamic acid, glutamine, or asparagine residues. Sridhar et al. (2005) reported cleavage at the Pro_5-Ile_6 bond by PepO2 and PepO3 from *Lb. helveticus* CNRZ32. However, the latter study used α_{s1}-CN f1-9 as the substrate. The different α_{s1}-CN fragments used as the substrates in the two studies might cause differences in the observed substrate specificities and the hydrolysis at particular bonds. Christensson et al. (2002) reported that the primary cleavage sites of PepO from *Lb. rhamnosus* HN001 in α_{s1}-CN f1-17 were identical to those in α_{s1}-CN f1-23. However, the rates of hydrolysis of the four primary sites, i.e., Pro_5-Ile_6, Lys_7-His_8, His_8-Gln_9, and Gln_9-Gly_{10}, were not the same for each substrate. The Lys_7-His_8 and Gln_9-Gly_{10} bonds were hydrolyzed more rapidly than the Pro_5-Ile_6 and His_8-Gln_9 bonds in α_{s1}-CN f1-17.

The PepO, PepO2, and PepO3 enzymes from *Lb. helveticus* WSU19 have as their primary cleavage site in α_{s1}-CN f1-23 the Glu_{14}-Val_{15} bond, followed by the Gln_{13}-Glu_{14} bond (Figures 49-51). The preferred cleavage site at the Glu_{14}-Val_{15} bond differentiates the metalloendopeptidase activities of PepO, PepO2, and PepO3 of *Lb. helveticus* WSU19 from the extracellular proteinase activities of *Lb. helveticus* (Oberg et al., 2002). Oberg et al. (2002) reported the primary cleavage sites of extracellular proteinases from 8 strains of *Lb. helveticus* in α_{s1}-CN f1-23 to be His_8-Gln_9, Gln_9-Gly_{10}, Gln_{13}-Glu_{14}, and Leu_{16}-Asn_{17} bonds. Exterkate and Alting (1993) reported the Gln_{13}-Glu_{14} and Glu_{14}-Val_{15} bonds were preferred

by the proteinase-negative variant of *Lc. lactis* subsp. *cremoris* strain HP at pH 5.2, while the Glu_{18}-Asn_{19} bond was the preferred site at pH 6.5. Exterkate and Alting (1995) reported that cleavages at the Glu_{14}-Val_{15} and Gln_{13}-Glu_{14} bonds of α_{s1}-CN f1-23 were due to the activity of an intracellular metalloendopeptidase. PrtP was also reported to cleave the Gln_{13}-Glu_{14} bond (Exterkate and Alting, 1995).

In addition to the Gln_{13}-Glu_{14} and Glu_{14}-Val_{15} bonds, the PepO enzyme from *Lb. helveticus* WSU19 cleaves α_{s1}-CN f1-23 at Lys_7-His_8, His_8-Gln_9, Gln_9-Gly_{10}, and Pro_{12}-Gln_{13} bonds. Further study is needed to confirm if the remaining cleavage sites of PepO from *Lb. helveticus* WSU19 (Figure 49) occur in α_{s1}-CN f1-23 or in the products of initial α_{s1}-CN f1-23 hydrolysis. The finding that the primary cleavage sites of PepO from *Lb. helveticus* WSU19 occur toward the N-terminus of α_{s1}-CN f1-23 is in agreement with the established cleavage sites of PepO from *Lb. rhamnosus* HN001 (Christensson et al., 2002). The latter enzyme was reported to have 4 primary cleavage sites near the N-terminus of α_{s1}-CN f1-23, i.e., the Pro_5-Ile_6, Lys_7-His_8, His_8-Gln_9, and Gln_9-Gly_{10} bonds. Besides PepO, the PepO2 and PepO3 enzymes from *Lb. helveticus* WSU19 also possess additional cleavage sites toward the N-terminus of α_{s1}-CN f1-23, i.e., His_8-Gln_9 bond for PepO2; Lys_7-His_8, His_8-Gln_9, and Gln_9-Gly_{10} bonds for PepO3 (Figures 50 and 51). In contrast to PepO from *Lactobacilli*, most of the cleavage sites of the PepO enzymes from *Lactococci* have been reported to be at the C-terminus of α_{s1}-CN f1-23 (Yan et al., 1987a and 1987b; Baankreis et al., 1995; Stepaniak and Fox, 1995). The NOP enzyme from *Lc. lactis* subsp. *cremoris* C13 was reported to cleave α_{s1}-CN f1-23 at the Gln_{13}-Glu_{14}, Glu_{14}-Val_{15}, Leu_{20}-Leu_{21}, Glu_{18}-Asn_{19}, and Asn_{19}-Leu_{20} bonds (in the order of decreasing susceptibility) (Baankreis, et al., 1995). Stepaniak and Fox (1995) reported that the cleavage specificities of a 70-kDa intracellular endopeptidase (PepO)

from *Lc. lactis* subsp. *lactis* MG1363 on α_{s1}-CN f1-23 were at Gln_{13}-Glu_{14}, Glu_{14}-Val_{15}, Asn_{19}-Leu_{20}, and Leu_{20}-Leu_{21} bonds. In addition, lactococcal endopeptidase (LEP) I was reported to cleave the α_{s1}-CN f1-23 at the Asn_{17}-Glu_{18} bond, while the LEP II cleaved the same substrate at the Gln_{10}-Gly_{11} bond (Yan et al., 1987a; Yan et al., 1987b).

The cleavage by PepO, PepO2, and PepO3 from *Lb. helveticus* WSU19 at Gln_{13}-Glu_{14} and Glu_{14}-Val_{15} bonds in α_{s1}-CN f1-23 produce peptide fragments f1-13 and f1-14 that are potentially bitter. Except for α_{s1}-CN f1-9, the bitterness thresholds of the bitter peptides from α_{s1}-CN f1-23 have not been reported. The α_{s1}-CN f1-9 has a bitter recognition threshold of 0.78 mg/mL in water, while the bitter recognition threshold of β-CN f193-209 is 0.35 mg/mL in water (Koka and Weimer, 2000). The bitter detection level of β-CN f193-209 is 0.03% or 0.30 mg/mL in water (Singh et al., 2005). The lower bitterness threshold of β-CN f193-209 than α_{s1}-CN f1-23 suggests that the β-CN f193-209 (and possibly the bitter peptides derived from β-CN f193-209) is more important than the bitter peptides from α_{s1}-CN f1-23 in affecting the bitterness of cheese. Thus, the production of bitter peptides from α_{s1}-CN f1-23 by PepO, PepO2, and PepO3 may not be as critical as the ones from β-CN f193-209 with respect to the sensory quality of cheese.

12. Degradation of α_{s1}-CN f1-23 by PepE

Table 24 demonstrates the mass-to-charge ratio (m/z) of peaks in the MALDI-TOF spectra and the corresponding peptide fragments formed during hydrolysis of α_{s1}-CN f1-23 by CFE from *E. coli* DH5α(pES1), expressing the *pepE* gene from *Lb. helveticus* WSU19. Hydrolysis of α_{s1}-CN f1-23 by CFE from *E. coli* DH5α(pJDC9) served as the control. No

peaks corresponding to the peptide fragments derived from α_{s1}-CN f1-23 were observed in the control. The m/z ratios of less than 500 Da were not detected by the MALDI-TOF analyses in this study due to the mass acquisition setting from 500 Da to 4000 Da.

Similar to the MALDI-TOF spectra of α_{s1}-CN f1-23 hydrolysis by the PepO, PepO2, and PepO3 enzymes, the substrate peak (m/z of 2765 Da) exhibited the highest intensity during the 72-h incubation of α_{s1}-CN f1-23 with PepE, while the 2384-Da peak was the hydrolysis product that exhibited the greatest intensity (Table 24). The m/z of 2384 Da is the mass of α_{s1}-CN f4-23, indicating the Lys_3-His_4 bond is the first cleavage site of PepE in α_{s1}-CN f1-23 (Figure 52). Besides the 2384-Da peak, the MALDI-TOF spectra show a second peak at m/z of 1247 Da, corresponding to the mass of α_{s1}-CN f14-23 (Table 24). This result indicates the Gln_{13}-Glu_{14} bond is the second cleavage site of PepE in α_{s1}-CN f1-23 (Figure 52). Incubation of α_{s1}-CN f1-23 with the PepE enzyme for 48 h revealed the production of a third peak at m/z of 2036 Da, corresponding to the mass of α_{s1}-CN f7-23 (Table 24). The latter result indicates Ile_6-Lys_7 is the third cleavage site of PepE in α_{s1}-CN f1-23 (Figure 52).

The first cleavage site by PepE from *Lb. helveticus* WSU19 at the Lys_3-His_4 bond of α_{s1}-CN f1-23 is in agreement with Sridhar et al. (2005) who explained the action of PepE from *Lb. helveticus* CNRZ32 on α_{s1}-CN f1-9. In contrast, the second cleavage of PepE was reported by Sridhar (2003) to be at the Lys_7-His_8 bond. The latter cleavage was not observed in our study until 72-h incubation. The occurrence of secondary structure in α_{s1}-CN f1-23 (Malin et al., 2001) might be responsible for the accessibility of the peptide bonds to the endopeptidases.

The cleavage by PepE of the Lys_3-His_4 bond indicates the ability of PepE to hydrolyze bitter peptides containing the N-terminus of α_{s1}-CN f1-23, such as α_{s1}-CN f1-9,

f1-13, and f1-14. Hence, the PepE activity may complement PepO, PepO2, or PepO3 activities in hydrolyzing α_{s1}-CN f1-23 and retarding bitter peptide accumulation.

Table 25 demonstrates the mass-to-charge ratio (m/z) of peaks in the MALDI-TOF spectra and the corresponding peptide fragments formed during hydrolysis of α_{s1}-CN f1-23 by CFE from *E. coli* DH5α(pES1) and *E. coli* DH5α(pES5), expressing the *pepE* and *pepO* genes from *Lb. helveticus* WSU19, respectively. The most intense peak was observed at m/z of 1666 Da after 12-h and 24-h incubations. The m/z of 1666 Da is the mass of α_{s1}-CN f1-14. The fact that the α_{s1}-CN f1-14 was dominant at 12-h and 24-h incubations is an indication of a larger PepO activity than PepE activity.

The MALDI-TOF spectra show the formation of peak at m/z of 1284 Da due to the combined PepE-PepO activities. The m/z ratio of 1284 Da corresponds to the mass of α_{s1}-CN f4-14. There are 2 possible mechanisms for α_{s1}-CN f4-14 formation. First, α_{s1}-CN f1-23 is hydrolyzed on Glu_{14}-Val_{15} by PepO to form α_{s1}-CN f1-14, which is further hydrolyzed on Lys_3-His_4 by PepE to form α_{s1}-CN f4-14 (Figure 53). Second, α_{s1}-CN f1-23 is hydrolyzed by PepE to form α_{s1}-CN f4-23, which is further hydrolyzed by PepO to form α_{s1}-CN f4-14 (Figure 53). Since the 1-14 fragment of α_{s1}-CN is resistant to hydrolysis, the formation of α_{s1}-CN f4-14 is more likely via the second mechanism.

Besides α_{s1}-CN f4-14, the combination of PepO and PepE produced α_{s1}-CN f4-13 (m/z of 1155 Da; Table 25), which might be due to hydrolysis at the Gln_{13}-Glu_{14} bond of α_{s1}-CN f4-23 by PepE. In addition, the PepE-PepO combination hydrolyzed α_{s1}-CN f1-23 to generate a new peak at m/z of 905 Da, corresponding to the α_{s1}-CN f17-23 (Table 25). This new peak was the result of cleavage at the Leu_{16}-Asn_{17} bond (Figure 53). However, it is not

clear which enzyme was responsible for the formation of α_{s1}-CN f17-23 since the cleavage at the Leu_{16}-Asn_{17} bond was not observed during incubations of PepE or PepO with α_{s1}-CN f1-23 (Tables 21 and 24). The 905-Da peak was reported by Gouldsworthy et al. (1996) in a 1 year-old commercial Cheddar cheese.

The combination of PepE and PepO enzymes did not cleave the Glu_{18}-Asn_{19} bond (Figure 53). The PepO enzyme cleaved poorly at the latter bond (Table 21; Figure 49). It is possible that combining the two enzymes altered the specificities of PepO on this minor cleavage site. The combined actions of PepE-PepO might have preferred the cleavage of Leu_{16}-Asn_{17} to form α_{s1}-CN f17-23 (Table 25; Figure 53).

In addition to the formation of new peptides, the PepE-PepO combination apparently increased the hydrolysis of the Gln_9-Gly_{10} bond (Figure 53). The 1642-Da peak was not observed in the hydrolysis of α_{s1}-CN f1-23 by PepO alone until 24-h incubation (Table 21). In contrast, the hydrolysis of α_{s1}-CN f1-23 by the combined action of PepE and PepO resulted in observation of the 1642-Da peak at 12 h (Table 25). The combination of PepE and PepO also evidently increased the hydrolysis of the complement α_{s1}-CN f15-23 (m/z 1118 Da). When hydrolyzed by PepO alone, the 1666-Da peak was not observed as the dominant peak until 24-h incubation (Table 21). Hydrolysis of α_{s1}-CN f1-23 by the combined PepE and PepO enzymes produced the 1666-Da peak as the dominant peak at 12-h incubation (Table 25). The increase of α_{s1}-CN f15-23 hydrolysis supports the assumption that the combination of PepE and PepO favors the cleavage at Leu_{16}-Asn_{17}.

Table 26 demonstrates the mass-to-charge ratio (m/z) of peaks in the MALDI-TOF spectra and the corresponding peptide fragments formed during hydrolysis of α_{s1}-CN f1-23 by CFE from *E. coli* DH5α(pES1) and *E. coli* DH5α(pES2), expressing the *pepE* and *pepO2*

genes from *Lb. helveticus* WSU19, respectively. The 1284-Da peak, corresponding to α_{s1}-CN f4-14, was observed as the product of α_{s1}-CN f1-23 degradation by the combined PepE and PepO2 activities. The most intense peak due to hydrolysis was observed at m/z of 1247 Da and 1666 Da after 12-h and 24-h incubations, respectively (Table 26). These peaks correspond to α_{s1}-CN f14-23 and α_{s1}-CN f1-14, respectively. The accumulation of α_{s1}-CN f14-23 occurred because PepE and PepO2 possess the same cleavage site, at the Gln_{13}-Glu_{14} bond (Figures 50 and 52). The 905-Da peak was observed as the product of α_{s1}-CN f1-23 hydrolysis by the combination of PepE and PepO2 (Table 26). In addition, a peak at m/z of 791 Da was observed, which corresponds to α_{s1}-CN f18-23. This peak was not observed in the 72-h incubation of α_{s1}-CN f1-23 with PepO2 alone. Figure 54 illustrates the cleavage sites due to the combined action of PepE and PepO2 enzymes from *Lb. helveticus* WSU19 on α_{s1}-CN f1-23. Similar to the combination of PepE and PepO enzymes, mixing PepE and PepO2 enzymes from *Lb. helveticus* WSU19 seemed to increase the hydrolysis of α_{s1}-CN f15-23 and produced a greater number of peptides than when these enzymes were used independently.

Table 27 demonstrates the mass-to-charge ratio (m/z) of peaks in the MALDI-TOF spectra and the corresponding peptide fragments formed during hydrolysis of α_{s1}-CN f1-23 by CFE from *E. coli* DH5α(pES1) and *E. coli* DH5α(pES6), expressing the *pepE* and *pepO3* genes from *Lb. helveticus* WSU19, respectively. The 1284-Da peak, corresponding to the α_{s1}-CN f4-14, was not observed as the product of α_{s1}-CN f1-23 degradation by combined activities of PepE and PepO3. The absence of the 1284-Da peak indicates a lower PepO3 activity than PepO or PepO2 on α_{s1}-CN f1-23. Hydrolysis of α_{s1}-CN f1-23 by PepE resulted in the accumulation of peak of α_{s1}-CN f4-23 peptide (m/z of 2384 Da; Table 24). Prolonged

incubation might promote the cleavage at Glu_{14}-Val_{15} or Gln_{13}-Glu_{14} bonds of α_{s1}-CN f4-23 by PepO3 or PepE, respectively.

The 2384-Da and 1247-Da peaks were the most intense of the hydrolysis products after 12-h and 24-h incubations of α_{s1}-CN f1-23 with PepE and PepO3 (Table 27). The accumulation of α_{s1}-CN f14-23 occurred because PepE and PepO3 share Gln_{13}-Glu_{14} as a cleavage site (Figures 51 and 52). The 905-Da peak was observed in the hydrolysis of α_{s1}-CN f1-23 by the combination of PepE and PepO3 enzymes (Table 27). In addition, the 791-Da peak was observed at 12-h incubation in the two-enzyme degradation of α_{s1}-CN f1-23, while the same peak was not observed at 72 h in the hydrolysis by PepO3 alone (Table 23). Figure 55 illustrates the cleavage sites of the PepE and PepO3 enzymes from *Lb. helveticus* WSU19 in α_{s1}-CN f1-23.

Although PepE predominantly cleaves at the Lys_3-His_4 bond, combining PepE with PepO, PepO2, or PepO3 enzyme does not prevent the accumulation of bitter peptides, particularly α_{s1}-CN f1-13 and f1-14. However, by adjusting the level of PepO, PepO2, or PepO3 activity, hydrolysis can be directed to promote the formation of α_{s1}-CN f4-14 or f4-13, which are non-bitter.

13. <u>Degradation of α_{s1}-CN f1-23 by PepN-an endopeptidase activities</u>

PepN activity was not observed on α_{s1}-CN f1-23. This observation coincided with the report of Baankreis (1992) concerning the activity of PepN from *Lc. lactis* subsp. *cremoris* C13. The presence of a proline residue as the second amino acid in α_{s1}-CN f1-23 precludes PepN from cleaving the substrate. Combining PepN with PepO, PepO2, or PepO3 resulted in additional peptides formed by PepN activity on α_{s1}-CN f1-23 (Table 28).

The combined activitites of PepN and PepO on α_{s1}-CN f1-23 produced peptides with m/z of 905, 1019, and 1585 Da. These peaks correspond to the masses of α_{s1}-CN f17-23, f16-23, and f11-23, respectively. The 1642-Da peak, corresponding to the α_{s1}-CN f10-23, might be formed by the activities of PepO and PepN enzymes. The PepO enzyme cleaves the Gln_9-Gly_{10} bond poorly (Tables 21 and 25), but the peak observed here is intense (Table 28), indicating cleavage by an enzyme with a high activity toward glutamine at the N-terminus. However, the accumulation of α_{s1}-CN f10-23 was not accompanied by the accumulation of α_{s1}-CN f1-9 (presumably) because the f10-23 peptide originated from the activity of PepO on α_{s1}-CN f8-23. Besides the 1642-Da peak, 1585-Da and 905-Da peaks accumulated at 12-h incubation with PepN and PepO enzymes. The accumulation of the 1585-Da peak was due to the inability of PepN to cleave beyond the Gly_{10} in the presence of Pro_{12} (Figure 56). The accumulation of the peptide with at m/z 905 Da was likely due to the N-terminus Glu_{18}, an amino acid that is not a preferred cleavage site of PepN (Christensen et al., 1999). Consequently, Glu_{18} will slow the cleavage of α_{s1}-CN f1-23 by PepN beyond Asn_{17} (Figure 56).

Incubation of α_{s1}-CN f1-23 with PepN and PepO2 produced peaks at m/z of 905 and 1019 Da, corresponding to α_{s1}-CN f17-23 and f16-23, respectively (Table 28; Figure 56). Unlike the PepN-PepO combination, the 1642-Da and 1585-Da peaks were not observed during incubation with PepN and PepO2. The PepO2 enzyme does not cleave at Lys_7-His_8 bond to form α_{s1}-CN f8-23 (Figure 50). Therefore, PepN could not readily cleave at the Gln_9-Gly_{10} and Gly_{10}-Leu_{11} bonds to form α_{s1}-CN f10-23 and f11-23, respectively. The incubation of α_{s1}-CN f1-23 with PepN and PepO2 enzymes accumulated the 1666-Da and 905-Da peaks, corresponding to the α_{s1}-CN f1-14 and f17-23, respectively (Table 56).

Incubation of α_{s1}-CN f1-23 with PepN and PepO3 enzymes resulted in prominent peak at m/z of 1585 Da after 12 h. In addition, the combined enzyme produced peaks at m/z of 1019 and 905 Da (Table 56). Unlike the incubation with PepO or PepO2, the 905-Da peak did not accumulate in the incubation with PepN and PepO3. Previous results indicated that PepO3 exhibited more restricted activity than PepO or PepO2 on α_{s1}-CN f1-23 (Table 23; Figure 51). The formation of α_{s1}-CN f17-23 by PepN depends largely on the cleavage of Glu_{14}-Val_{15} and Gln_{13}-Glu_{14}, the main cleavage sites of PepO3 in α_{s1}-CN f1-23.

Incubation of α_{s1}-CN f1-23 with PepN and PepE enzymes produced m/z of 2384 Da as the predominant hydrolysate peak (Table 29). The 2384-Da peak corresponds to the mass of α_{s1}-CN f4-23, formed by PepE activity (Figures 52; 57). The cleavage of PepE at the Lys_3-His_4 bond of α_{s1}-CN f1-23 does not remove Pro_5 (Figure 57). Therefore, the α_{s1}-CN f4-23 accumulated because PepN could not cleave this peptide fragment further.

In addition to m/z of 2384 Da, peaks at m/z of 1642, 1585, 905, and 791 Da were observed at a very low intensity, although the incubation was extended to 72-h. These peaks correspond to the α_{s1}-CN f10-23, f11-23, f17-23, and f18-23, respectively and were possibly formed by PepN activity. Due to the presence of Pro_5, PepN should not be able to cleave α_{s1}-CN f4-23. However, Figure 52 demonstrates that PepE cleaves α_{s1}-CN f1-23 poorly at the Ile_6-Lys_7 and Gln_{13}-Glu_{14} bonds, in addition to Lys_3-His_4. The cleavage at the Gln_9-Gly_{10} and Gly_{10}-Leu_{11} bonds by PepN was likely initiated by PepE cleavage at the Ile_6-Lys_7 bond, forming α_{s1}-CN f7-23 (Figure 57). Similarly, PepN cleavage at Leu_{16}-Asn_{17} and Asn_{17}-Glu_{18} bonds was possibly initiated by the cleavage at the Gln_{13}-Glu_{14} bond by PepE. The large PepN activity compared to the PepE activities at Ile_6-Lys_7 and Gln_{13}-Glu_{14} bonds might cause

the complete degradation of the intermediate peptides at Lys_7-His_8, His_8-Gln_9, Glu_{14}-Val_{15}, and Val_{15}-Leu_{16}.

Based on the above results, PepN activity seems to be less important in debittering peptide hydrolysates from α_{s1}-CN f1-23 than those from β-CN f193-209. The presence of proline residues in α_{s1}-CN f1-23, particularly at residues 2 and 5, strongly inhibits the ability of PepN to cleave the bitter peptides that are derived from the N-terminus of α_{s1}-CN f1-23. Degradation by PepN depends largely on the cleavage of Ile_6-Lys_7 or Lys_7-His_8. Although the PepO, PepO2, PepO3, and PepE from *Lb. helveticus* WSU19 possess the ability to cleave these bonds, the sites are not the preferred cleavage sites for these endopeptidases.

Table 21. Peptide fragments formed during hydrolysis of α_{s1}-CN f1-23 by PepO from *Lb. helveticus* WSU19 at 37°C under simulated cheese conditions (4% salt, w/v; 50 mM citrate buffer pH 5.2)

Time (h)	M/z (Da)	1 R	P	K	H	P	6 I	K	8 H	9 Q	10 G	L	12 P	13 Q	14 E	V	L	N	18 E	19 N	20 L	21 L	R	23 F	α_{s1}-casein fragment
0	2765.2																								f1-23
2	2765.2																								f1-23
	1907.8																								f8-23
	1770.8																								f9-23
	1246.5																								f14-23
	1117.5																								f15-23
4	2765.2																								f1-23
	1907.8																								f8-23
	1770.8																								f9-23
	1247.4																								f14-23
	1117.7																								f15-23
8	2765.2																								f1-23
	1907.9																								f8-23
	1770.8																								f9-23
	1247.3																								f14-23
	1117.6																								f15-23
	1665.5																								f1-14
	791.4																								f18-23
	662.4																								f19-23
12	2765.2																								f1-23
	1907.9																								f8-23
	1770.7																								f9-23
	1246.7																								f14-23
	1117.7																								f15-23
	1665.9																								f1-14
	791.4																								f18-23
	662.4																								f19-23
	548.3																								f20-23

Table 21 (continued)

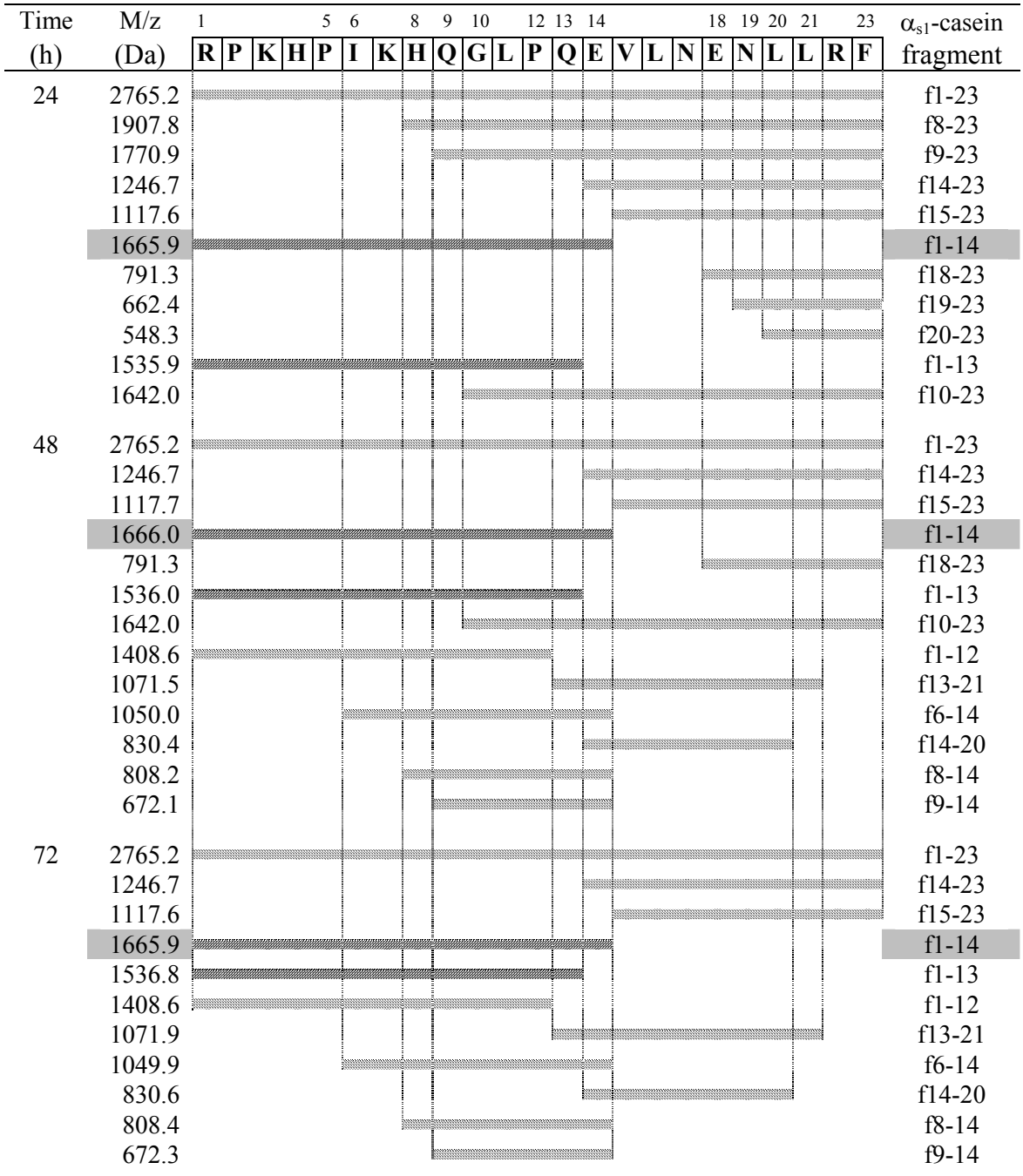

Table 22. Peptide fragments formed during hydrolysis of α_{s1}-CN f1-23 by PepO2 from *Lb. helveticus* WSU19 at 37°C under simulated cheese conditions (4% salt, w/v; 50 mM citrate buffer pH 5.2)

Time (h)	m/z (Da)	1 R	P	K	H	P	I	K	8 H	9 Q	G	L	P	13 Q	14 E	15 V	L	N	18 E	19 N	20 L	L	22 R	23 F	α_{s1}-casein Fragment
0	2765.2																								f1-23
2	2765.2																								f1-23
	1771.3																								f9-23
	1117.9																								f15-23
4	2765.2																								f1-23
	1770.8																								f9-23
	1118.1																								f15-23
8	2765.2																								f1-23
	1770.8																								f9-23
	1117.9																								f15-23
12	2765.2																								f1-23
	1770.7																								f9-23
	1117.6																								f15-23
	1665.7																								f1-14
	1247.5																								f14-23
	662.4																								f19-23
24	2765.2																								f1-23
	1117.7																								f15-23
	1665.9																								f1-14
	1246.8																								f14-23
	662.4																								f19-23
	548.3																								f20-23
48	2765.2																								f1-23
	1117.7																								f15-23
	1665.3																								f1-14
	1247.0																								f14-23
	662.3																								f19-23
	548.3																								f20-23
	970.7																								f15-22

Table 22 (continued)

Time (h)	m/z (Da)	1 R	2 P	3 K	4 H	5 P	6 I	7 K	8 H	9 Q	10 G	11 L	12 P	13 Q	14 E	15 V	16 L	17 N	18 E	19 N	20 L	21 L	22 R	23 F	α_{s1}-casein fragment
72	2765.2																								f1-23
	1117.7																								f15-23
	1665.1																								f1-14
	1247.3																								f14-23
	662.4																								f19-23
	548.2																								f20-23
	970.8																								f15-22

Bitter peptide

Non-bitter peptide

The most intense peak of hydrolysis products from α_{s1}-CN f1-23 in MALDI-TOF spectrum for each incubation time. (The greatest intensity peak was α_{s1}-CN f1-23.)

Table 23. Peptide fragments formed during hydrolysis of α_{s1}-CN f1-23 by PepO3 from *Lb. helveticus* WSU19 at 37°C under simulated cheese conditions (4% salt, w/v; 50 mM citrate buffer pH 5.2)

Time (h)	m/z (Da)	1 R	P	K	H	P	I	7 K	8 H	9 Q	10 G	L	P	13 Q	14 E	15 V	L	N	18 E	N	19 L	20 L	R	23 F	α_{s1}-casein fragment
0	2765.2																								f1-23
2	2765.2																								f1-23
	1117.7																								f15-23
4	2765.2																								f1-23
	1118.3																								f15-23
	1246.7																								f14-23
8	2765.2																								f1-23
	1118.3																								f15-23
	1246.7																								f14-23
12	2765.2																								f1-23
	1117.6																								f15-23
	1247.3																								f14-23
	1907.0																								f8-23
24	2765.2																								f1-23
	1117.8																								f15-23
	1246.7																								f14-23
	1907.7																								f8-23
	1770.0																								f9-23
48	2765.2																								f1-23
	1117.9																								f15-23
	1247.0																								f14-23
	1907.9																								f8-23
	1770.0																								f9-23
	1665.0																								f1-14
	1642.2																								f10-23

Table 23 (continued)

Time (h)	m/z (Da)	1 R	P	K	H	P	I	7 K	8 H	9 Q	10 G	L	P	13 Q	14 E	15 V	L	N	18 E	19 N	20 L	L	R	23 F	α_{s1}-casein fragment
72	2765.2																								f1-23
	1117.5																								f15-23
	1246.6																								f14-23
	1907.7																								f8-23
	1770.0																								f9-23
	1665.4																								f1-14
	1642.2																								f10-23
	2348.2																								f1-20
	791.2																								f18-23
	662.0																								f19-23
	548.2																								f20-23

Bitter peptide

Non-bitter peptide

The most intense peak of hydrolysis products from α_{s1}-CN f1-23 in MALDI-TOF spectrum for each incubation time. (The greatest intensity peak was α_{s1}-CN f1-23.)

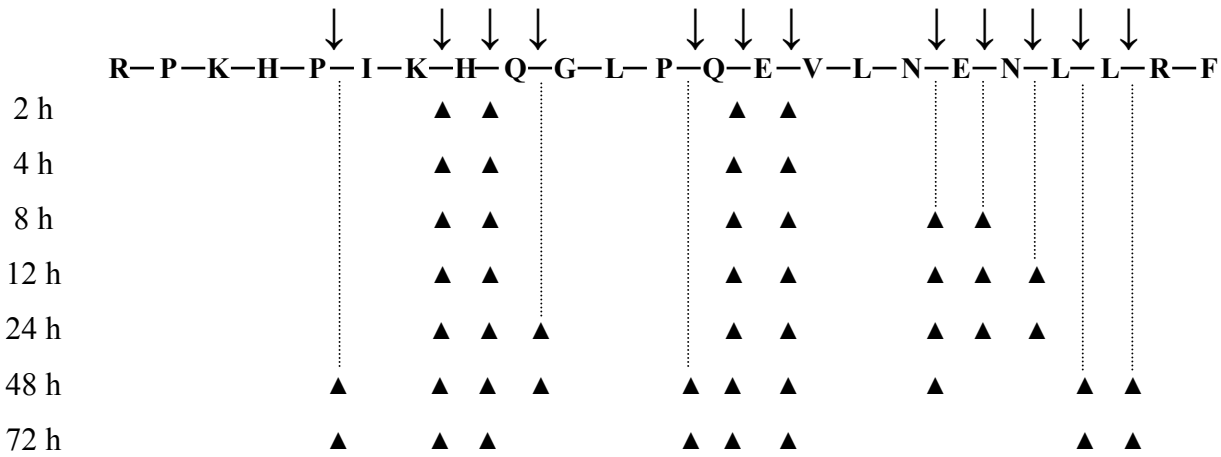

Figure 49. Cleavage sites of PepO from *Lb. helveticus* WSU19 in α_{s1}-CN f1-23 as a function of incubation time (▲). ↓ indicates the overall peptide bonds in α_{s1}-CN f1-23 cleaved by PepO from *Lb. helveticus* WSU19.

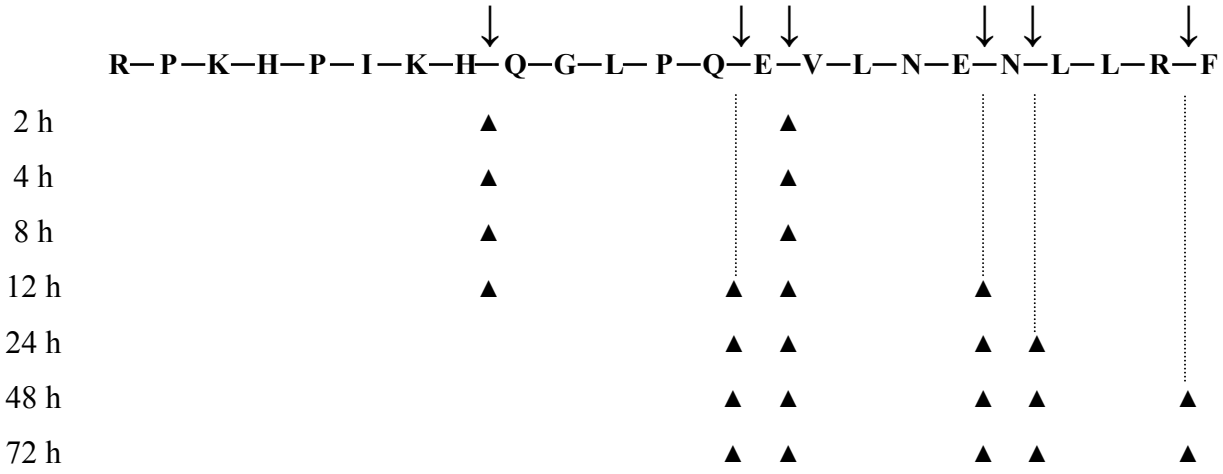

Figure 50. Cleavage sites of PepO2 from *Lb. helveticus* WSU19 in α_{s1}-CN f1-23 as a function of incubation time (▲). ↓ indicates the overall peptide bonds in α_{s1}-CN f1-23 cleaved by PepO2 from *Lb. helveticus* WSU19.

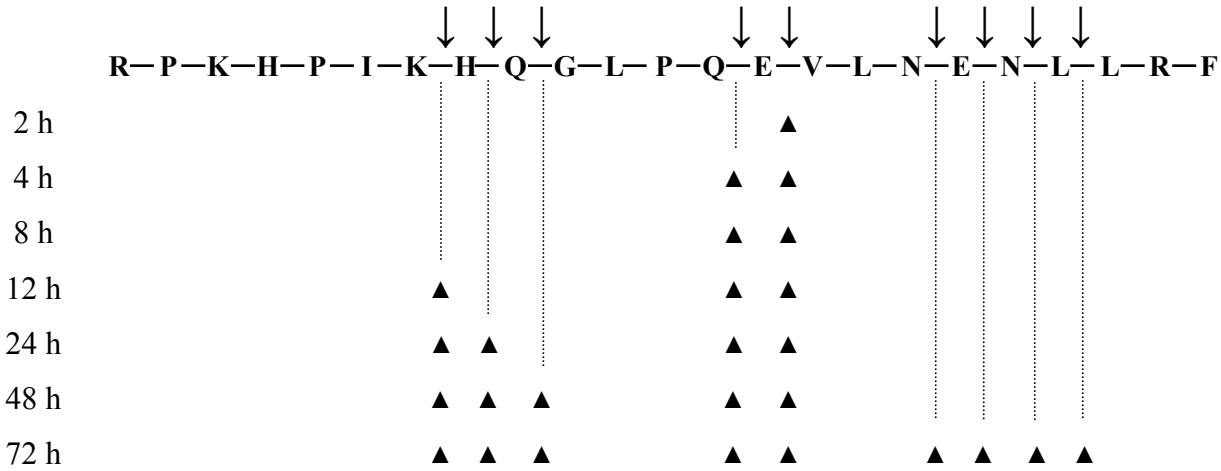

Figure 51. Cleavage sites of PepO3 from *Lb. helveticus* WSU19 in α_{s1}-CN f1-23 as a function of incubation time (▲). ↓ indicates the overall peptide bonds in α_{s1}-CN f1-23 cleaved by PepO3 from *Lb. helveticus* WSU19.

Table 24. Peptide fragments formed during hydrolysis of α_{s1}-CN f1-23 by PepE from *Lb. helveticus* WSU19 at 37°C under simulated cheese conditions (4% salt, w/v; 50 mM citrate buffer pH 5.2)

Time (h)	m/z (Da)	1 R	2 P	3 K	4 H	5 P	6 I	7 K	8 H	9 Q	10 G	11 L	12 P	13 Q	14 E	15 V	16 L	17 N	18 E	19 N	20 L	21 L	22 R	23 F	α_{s1}-casein fragment
0	2765.2																								f1-23
2	2765.2																								f1-23
4	2765.2																								f1-23
	2384.2																								f4-23
	1247.4																								f14-23
8	2765.2																								f1-23
	2383.5																								f4-23
	1247.4																								f14-23
12	2765.2																								f1-23
	2383.5																								f4-23
	1247.4																								f14-23
24	2765.2																								f1-23
	2383.5																								f4-23
	1247.2																								f14-23
48	2765.2																								f1-23
	2383.7																								f4-23
	1247.4																								f14-23
	2036.0																								f7-23
72	2765.2																								f1-23
	2383.6																								f4-23
	1246.7																								f14-23
	2036.2																								f7-23

Bitter peptide

Non-bitter peptide

The most intense peak of hydrolysis products from α_{s1}-CN f1-23 in MALDI-TOF spectrum for each incubation time. (The greatest intensity peak was α_{s1}-CN f1-23.)

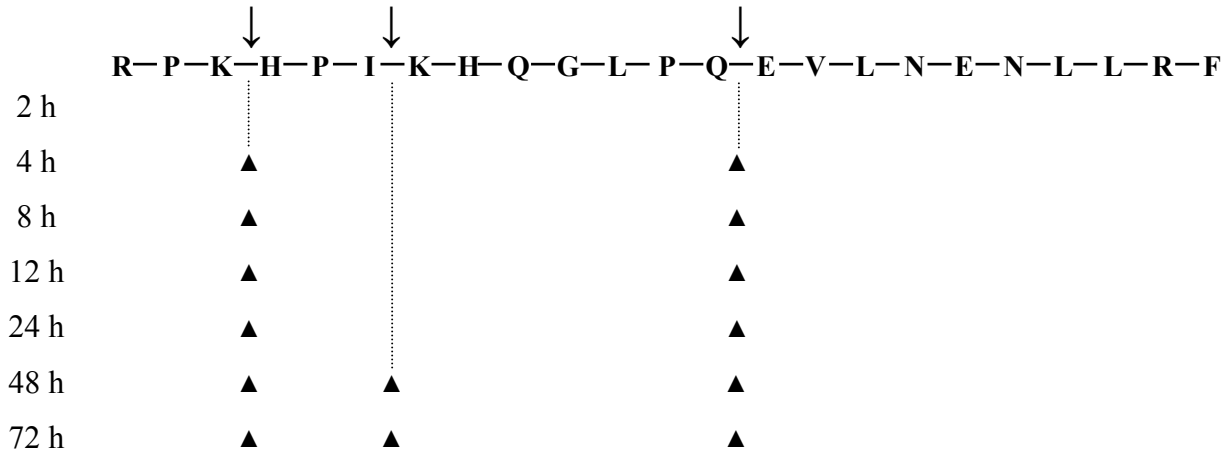

Figure 52. Cleavage sites of PepE from *Lb. helveticus* WSU19 in α_{s1}-CN f1-23 as a function of incubation time (▲). ↓ indicates the overall peptide bonds in α_{s1}-CN f1-23 cleaved by PepOE from *Lb. helveticus* WSU19.

Table 25. Peptide fragments formed during hydrolysis of α_{s1}-CN f1-23 by PepE and PepO from *Lb. helveticus* WSU19 at 37°C under simulated cheese conditions (4% salt, w/v; 50 mM citrate buffer pH 5.2)

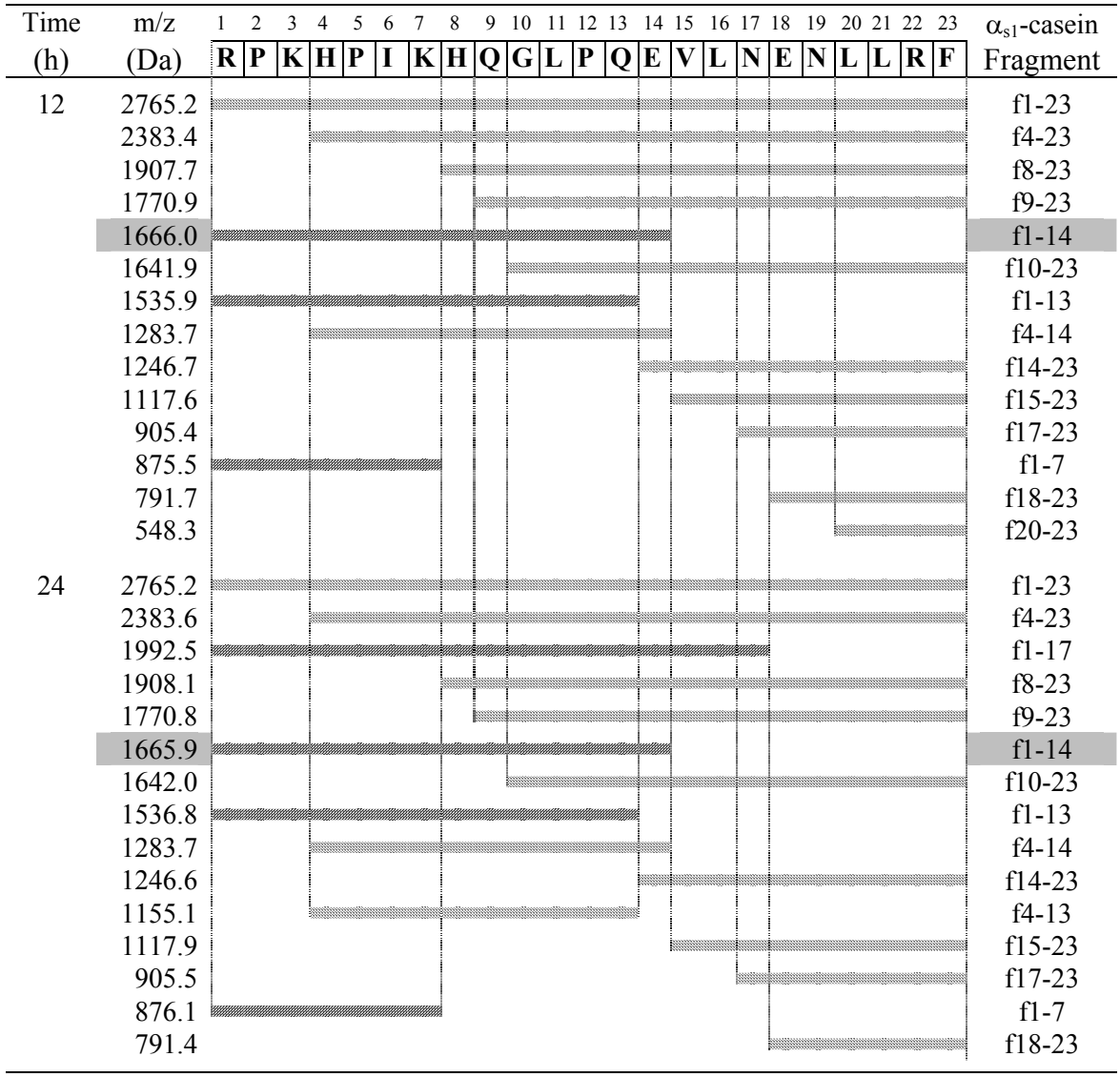

Table 26. Peptide fragments formed during hydrolysis of α_{s1}-CN f1-23 by PepE and PepO2 from *Lb. helveticus* WSU19 at 37°C under simulated cheese conditions (4% salt, w/v; 50 mM citrate buffer pH 5.2)

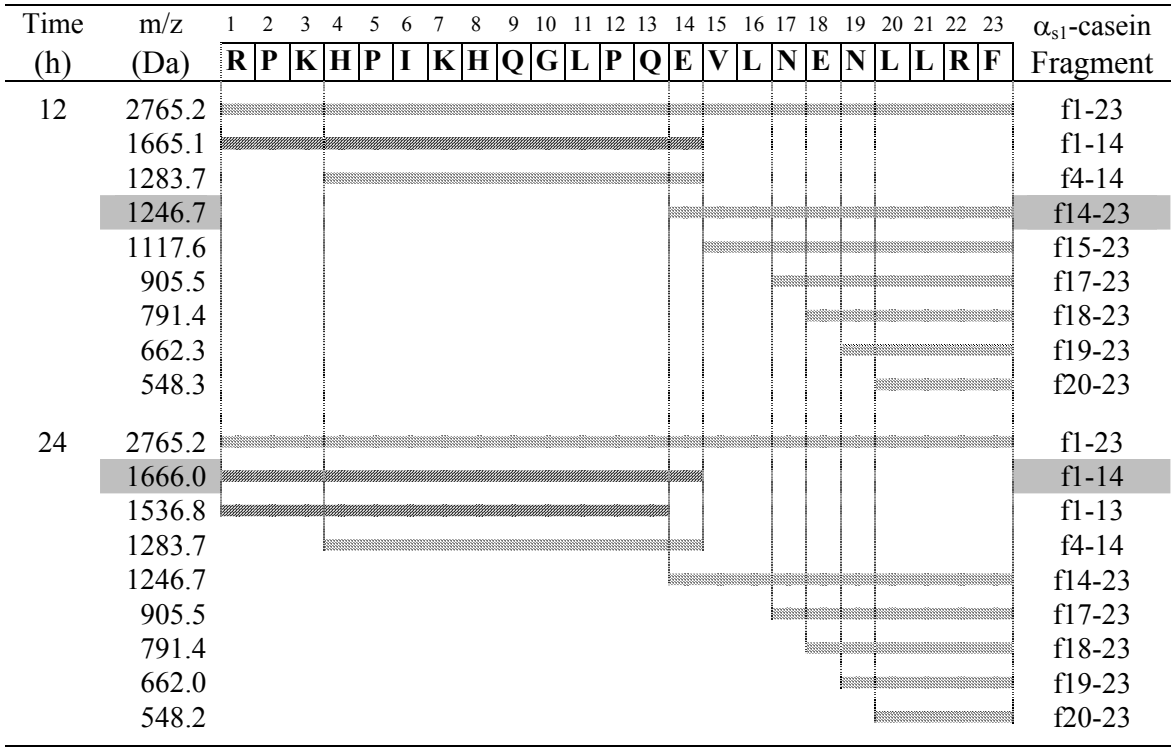

Table 27. Peptide fragments formed during hydrolysis of α_{s1}-CN f1-23 by PepE and PepO3 from *Lb. helveticus* WSU19 at 37°C under simulated cheese conditions (4% salt, w/v; 50 mM citrate buffer pH 5.2)

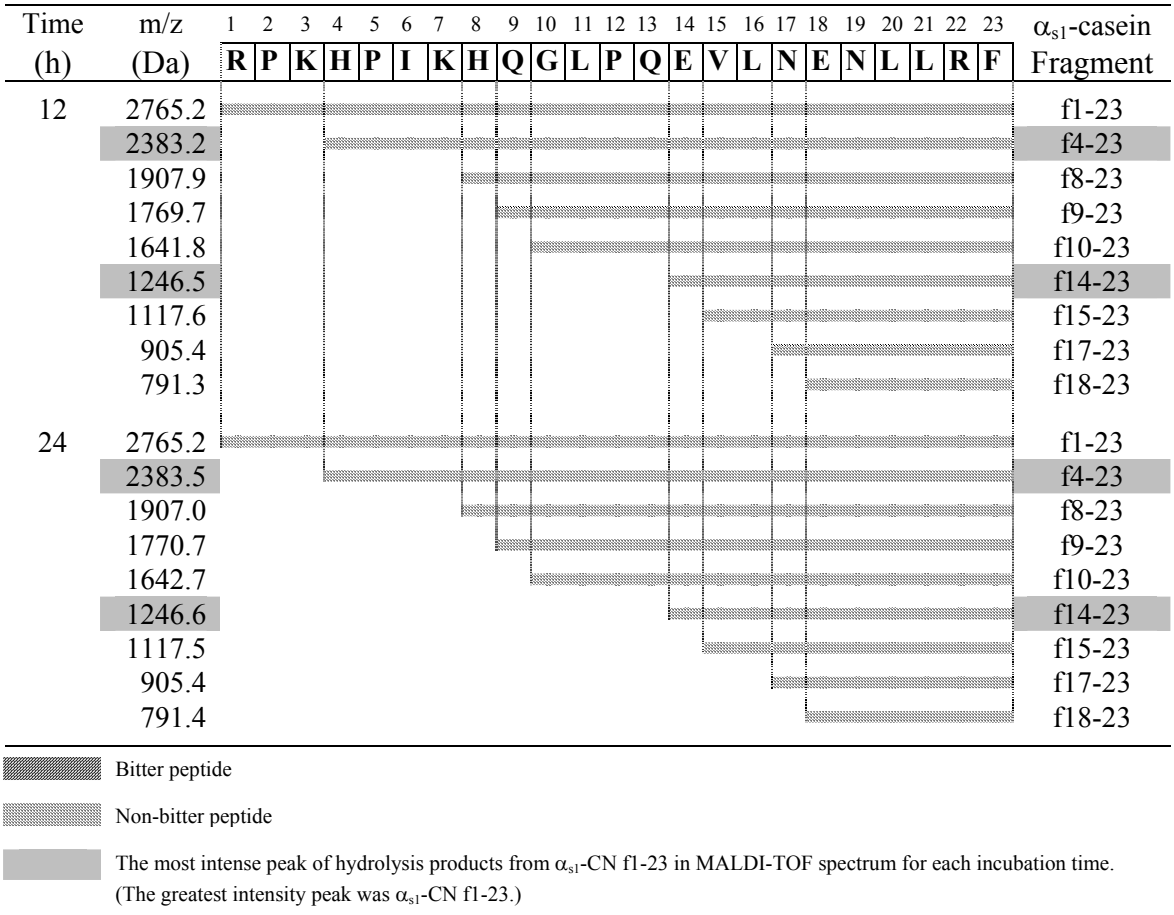

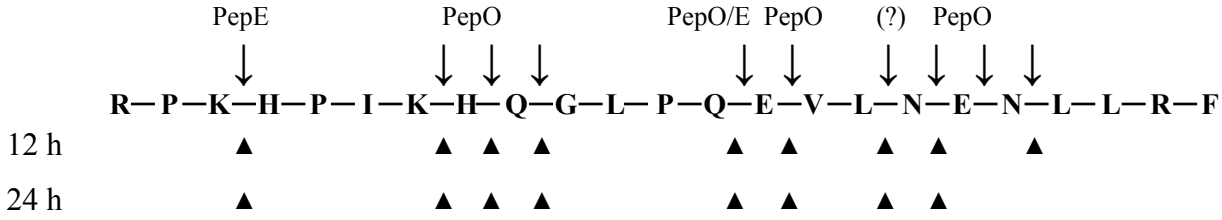

Figure 53. Cleavage sites of PepE and PepO from *Lb. helveticus* WSU19 in α_{s1}-CN f1-23 as a function of incubation time (▲). ↓ indicates the overall peptide bonds in α_{s1}-CN f1-23 cleaved by PepE and/or PepO from *Lb. helveticus* WSU19.

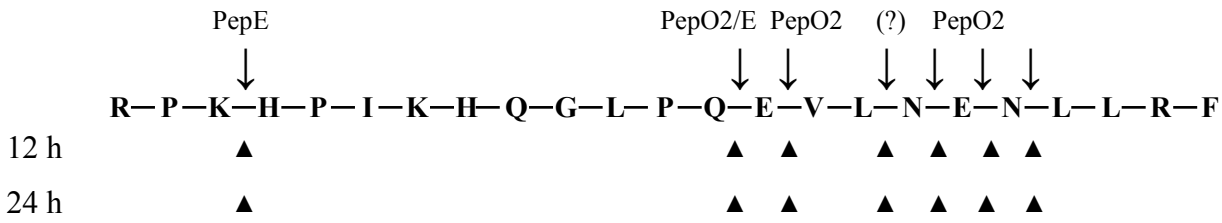

Figure 54. Cleavage sites of PepE and PepO2 from *Lb. helveticus* WSU19 in α_{s1}-CN f1-23 as a function of incubation time (▲). ↓ indicates the overall peptide bonds in α_{s1}-CN f1-23 cleaved by PepE and/or PepO2 from *Lb. helveticus* WSU19.

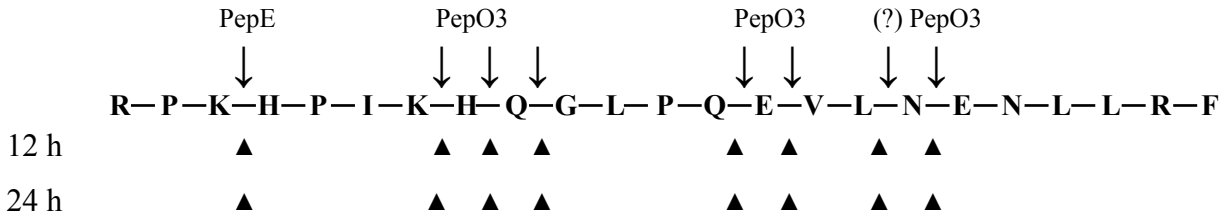

Figure 55. Cleavage sites of PepE and PepO3 from *Lb. helveticus* WSU19 in α_{s1}-CN f1-23 as a function of incubation time (▲). ↓ indicates the overall peptide bonds in α_{s1}-CN f1-23 cleaved by PepE and/or PepO3 from *Lb. helveticus* WSU19.

Table 28. Peptide fragments formed during hydrolysis of α_{s1}-CN f1-23 by a combination of PepN and indicated endopeptidase from *Lb. helveticus* WSU19 at 37°C under simulated cheese conditions (4% salt, w/v; 50 mM citrate buffer pH 5.2)

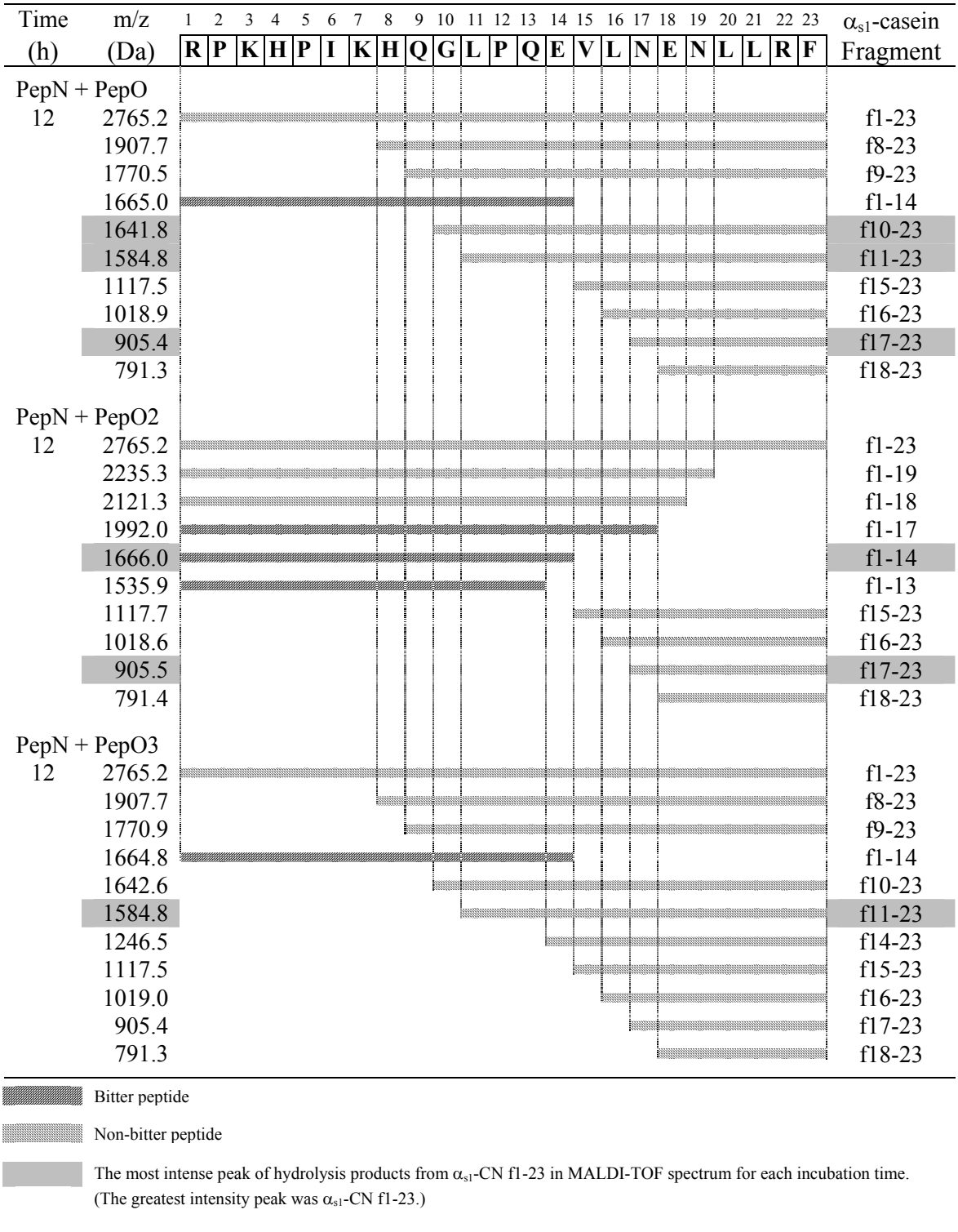

Table 29. Peptide fragments formed during hydrolysis of α_{s1}-CN f1-23 by PepN and PepE from *Lb. helveticus* WSU19 at 37°C under simulated cheese conditions (4% salt, w/v; 50mM citrate buffer pH 5.2)

Time (h)	m/z (Da)	1 R	2 P	3 K	4 H	5 P	6 I	7 K	8 H	9 Q	10 G	11 L	12 P	13 Q	14 E	15 V	16 L	17 N	18 E	19 N	20 L	21 L	22 R	23 F	α_{s1}-casein Fragment
24	2765.2																								f1-23
	2383.6																								f4-23
	1642.6																								f10-23
	1585.7																								f11-23
	905.4																								f17-23
	791.3																								f18-23
72	2765.2																								f1-23
	2383.7																								f4-23
	1642.6																								f10-23
	1585.7																								f11-23
	905.4																								f17-23
	791.3																								f18-23

Bitter peptide

Non-bitter peptide

The most intense peak of hydrolysis products from α_{s1}-CN f1-23 in MALDI-TOF spectrum for each incubation time. (The greatest intensity peak was α_{s1}-CN f1-23.)

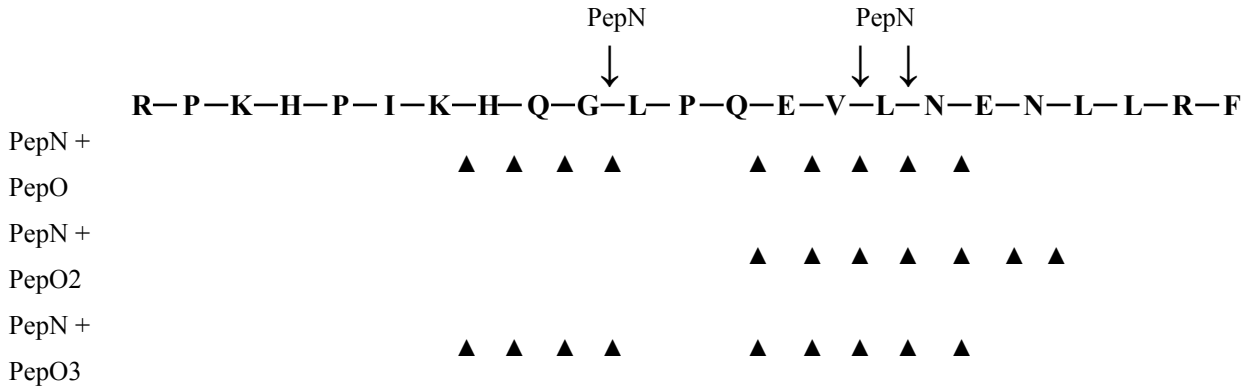

Figure 56. Cleavage sites of PepN and endopeptidases O, O2, or O3 from *Lb. helveticus* WSU19 in α_{s1}-CN f1-23 at 12-h incubation (▲). ↓ indicates the peptide bonds in α_{s1}-CN f1-23 cleaved by PepN from *Lb. helveticus* WSU19.

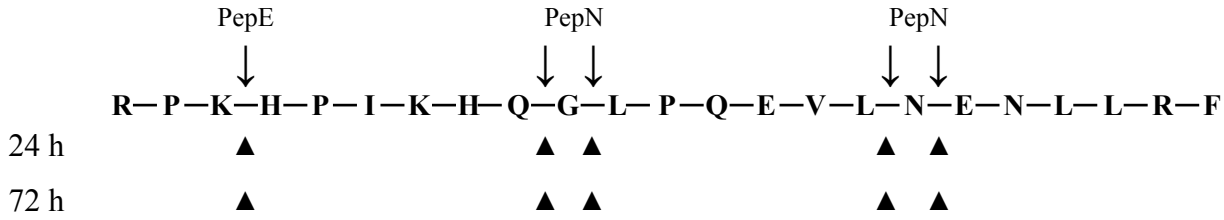

Figure 57. Cleavage sites of PepN and PepE from *Lb. helveticus* WSU19 in α_{s1}-CN f1-23 as a function of incubation time (▲). ↓ indicates the overall peptide bonds in α_{s1}-CN f1-23 cleaved by PepN and/or PepE from *Lb. helveticus* WSU19.

CHAPTER V:

Summary & Future Research

1. Summary

pepN, pepE, pepO, pepO2, and *pepO3* genes from *Lb. helveticus* WSU19 were successfully cloned in *E. coli* DH5α using the corresponding genes from *Lb. helveticus* CNRZ32 as probes. The presence of putative transcriptional promoters and putative transcriptional terminator in the nucleic acid sequence of each gene indicate the genes are transcribed monocistronically, not part of an operon.

Primer walking of a 5-kb *Sac*I-*Sph*I genomic insert revealed a 2532-bp ORF encoding for PepN, composed of 844 amino acids with a calculated MW of 95.8 kDa. The deduced amino acid sequence of PepN from *Lb. helveticus* WSU19 was determined to share 99%, 98%, and 90% identities with PepN from *Lb. helveticus* 53/7, *Lb. helveticus* CNRZ32, and *Lb. acidophilus* NCFM, respectively. PepN contains a zinc metallopeptidase motif, VitHELAHqW, at amino acid residues 286-295. PepN cleaves the bitter peptide, β-CN f193-209, at Tyr_{193}-Gln_{194} and Gln_{194}-Gln_{195} bonds to form β-CN f194-209 and f195-209, respectively, at 37°C under cheese ripening conditions (pH 5.2, 4%(w/v) salt). The glutamine residue at the N-terminus undergoes cyclization into pyrollidonecarboxylic acid (PCA) under acid condition used in the hydrolysis (pH 5.2). When incubated with PepO, PepO2, or PepO3, PepN cleaves α_{s1}-CN f1-23 at Gly_{10}-Leu_{11}, Val_{15}-Leu_{16}, and Leu_{16}-Asn_{17} bonds.

Primer walking of a 2.7-kb *Pst*I genomic insert revealed a 1314-bp ORF encoding for PepE, consisting of 438 amino acids with a calculated MW of 50 kDa. The deduced amino acid sequence of PepE from *Lb. helveticus* WSU19 shares 99% and 89% identities with PepE from *Lb. helveticus* CNRZ32 and *Lb. acidophilus* NCFM, respectively. The PepE enzyme contains the cysteine motif (QkhsGrCWlfAT) and histidine motif (VsHAMtLVGvD) of a thiol protease at amino acid residues 64-75 and 360-370, respectively. PepE cleaves β-CN

f193-209 at Leu_{198}-Gly_{199} and Val_{201}-Arg_{202} in the presence of PepN or PepO-like endopeptidases. Hydrolysis of α_{s1}-CN f1-23 by PepE occurs at Lys_3-His_4, Gln_{13}-Glu_{14}, and Ile_6-Lys_7 bonds (in the order of decreasing susceptibility).

Primer walking of a 4.3-kb *Hind*III-*Sal*I genomic insert revealed a 1941-bp ORF encoding for the PepO enzyme, a protein of 647 amino acids with a calculated MW of 73.6 kDa. The PepO enzyme contains a zinc metallopeptidase motif (TigHEVSHaF) at amino acid residues 493-502. The deduced amino acid sequence of PepO from *Lb. helveticus* WSU19 shares 99% and 60-85% identities with PepO from *Lb. helveticus* CNRZ32 and *Lb. acidophilus* NCFM, respectively. In addition, the PepO enzyme from *Lb. helveticus* WSU19 shares 56% and 62% identities with PepO2 and PepO3 enzymes from *Lb. helveticus* CNRZ32, respectively. Hydrolysis of β-CN f193-209 by PepO occurs predominantly at Pro_{196}-Val_{197}, Pro_{206}-Ile_{207}, and Pro_{200}-Val_{201} (in the order of decreasing susceptibility). In addition, PepO cleaves β-CN f193-209 at Val_{197}-Leu_{198}, Ile_{207}-Ile_{208}, Leu_{198}-Gly_{199}, and Val_{201}-Arg_{202}. Primary degradation of α_{s1}-CN f1-23 by PepO occurs at Gln_{13}-Glu_{14}, Glu_{14}-Val_{15}, Lys_7-His_8, and His_8-Gln_9 (in the order of decreasing susceptibility).

Primer walking of a 5.8-kb *Xba*I-*Sph*I genomic insert revealed a 1944-bp ORF encoding for PepO2 enzyme, a protein of 648 amino acids with a calculated MW of 73.8 kDa. The PepO2 enzyme possesses a zinc metallopeptidase motif, similar to PepO, at amino acid residues 494-503 (ViaHEISHaF). The deduced amino acid sequence of PepO2 enzyme from *Lb. helveticus* WSU19 shares 98% and 41% identities with PepO2 from *Lb. helveticus* CNRZ32 and *Lc. lactis* MG1363, respectively. In addition, PepO2 from *Lb. helveticus* WSU19 shares 56% and 62% identities with PepO and PepO3 from *Lb. helveticus* CNRZ32, respectively. Hydrolysis of β-CN f193-209 by PepO2 occurs at Pro_{196}-Val_{197} and Pro_{206}-Ile_{207}

bonds. Compared to PepO and PepO3, the β-CN f193-209 hydrolysis by PepO2 occurs more slowly. PepO2 cleaves α_{s1}-CN f1-23 most prominently at Gln_{13}-Glu_{14} and Glu_{14}-Val_{15}.

Primer walking of a 3.4-kb *Kpn*I genomic insert revealed a 1929 ORF encoding for PepO3 enzyme, comprised of 643 amino acids with a calculated MW of 72.6 kDa. The PepO3 enzyme contains a zinc metalloendopeptidase motif, similar to PepO and PepO2, at amino acid residues 489-498 (ViaHEISHaF). The deduced amino acid sequence of PepO3 from *Lb. helveticus* WSU19 shares 99% identity with PepO3 from *Lb. helveticus* CNRZ32. In addition, the PepO3 enzyme from *Lb. helveticus* WSU19 shares 62% identity with PepO and PepO2 enzymes from *Lb. helveticus* CNRZ32, respectively. PepO3 cleaves β-CN f193-209 preferentially after proline residues, as observed in the hydrolysate produced by PepO activity. Prolonged incubation of β-CN f193-209 with PepO3 produced cleavage at Val_{197}-Leu_{198} and Ile_{206}-Ile_{207} bonds. Hydrolysis of α_{s1}-CN f1-23 by PepO3 occurs primarily on Gln_{13}-Glu_{14} and Glu_{14}-Val_{15} bonds.

Combinations of PepN-PepO or PepN-PepO3 degrade β-CN f193-209 into peptides with MW less than 1000 Da. The proline at residue 206 occupies the C-terminus of the peptide produced by the combined actions of PepN-PepO or PepN-PepO3. Combining PepN and PepE produced a peptide with a MW of 898 Da, corresponding to the mass of β-CN f202-209. Although β-CN f202-209 was not the dominant product of β-CN f193-209 hydrolysis, the peptide has been reported to have a bitterness threshold of 0.004 mM (Kanehisa et al., 1972). The bitterness threshold of β-CN f202-209 is much lower than the bitterness threshold of β-CN f193-209, which is 0.16 mM (Singh et al., 2005). In contrast, none of the peptides formed by PepN-PepO or PepN-PepO3 combinations have been

identified as bitter, suggesting the combination of these enzymes may play an important role in debittering of Cougar Gold.

2. <u>Future research</u>

To evaluate the role(s) of PepN, PepE, PepO, PepO2, and PepO3 in the cheese matrix, it is necessary to delete the genes encoding for these enzymes from *Lb. helveticus* WSU19. However, construction of single peptidase mutants may not elucidate the key enzyme(s) in the debittering of Cougar Gold. Based on the results from the present study, double peptidase mutants of *Lb. helveticus* WSU19 (Δ*pepN*Δ*pepO*, Δ*pepN*Δ*pepO3*, Δ*pepN*Δ*pepO*, and Δ*pepN*Δ*pepE*) are recommended for study in cheese.

PepO, PepO2, and PepO3 exhibit similar peptidolytic patterns on β-CN f193-209 and α_{s1}-CN f1-23. It is likely that these enzymes have a similar pattern of activity on the peptides derived from β-CN f1-192 and α_{s1}-CN f24-199. Therefore, constructing isogenic strains of *Lb. helveticus* WSU19 having deficiency in PepO, PepO2, or PepO3 activity may not elucidate the role(s) of these enzymes in the growth of *Lb. helveticus* WSU19. Construction of double peptidase mutants, such as Δ*pepO*Δ*pepO2* or Δ*pepO*Δ*pepO3*, is a better approach to determine the functionalities of the enzymes.

Although, the current study identified 3 PepO-like endopeptidases in *Lb. helveticus* WSU19, it is not clear if the 3 endopeptidases are expressed at the same time. Northern hybridization as a function of growth time and growth condition will provide information on conditions that favor expression of these enzymes.

This study identified the activities of PepN, PepE, PepO, PepO2, and PepO3 enzymes from *Lb. helveticus* WSU19 on chymosin derived peptides, β-CN f193-209 and α_{s1}-

CN f1-23, under simulated cheese ripening conditions. In a real cheese matrix, peptides from β-CN f1-192 and α_{s1}-CN f24-199 produced by the action of starter proteinase may inhibit the general aminopeptidase and endopeptidases. Hydrolysis of the chymosin-derived peptides under simulated cheese conditions as done here does not encompass the effects of inhibitory cheese peptides on enzyme activities. Therefore, further study is recommended to elucidate the activity of PepN, PepE, PepO-like endopeptidases in a system more closely resembling the peptide composition in the cheese matrix.

Besides PepE and PepO-like endopeptidases, the presence of PepF has been reported in *Lb. helveticus* CNRZ32 (Sridhar et al., 2005). Because of its post-proline activity, PepF may be important to complement PepN activity. Thus, it would be useful to demonstrate the presence of PepF in *Lb. helveticus* WSU19 and determine the function(s) of this enzyme in the growth of *Lb. helveticus* WSU19 and the debittering of Cougar Gold.

Studies of the peptidases from *Lb. helveticus* WSU19 by Olson (1998), Fajarrini (1999), Soeryapranata et al. (2002a; 2002b; 2004) and the current study focused on their debittering activities. The peptidases may produce peptides with bioactive properties, which can have nutraceutical applications. Therefore, it is desirable to determine the bioactive properties of peptides produced by PepE, PepN, PepO, PepO2, and PepO3 activities on peptides derived from whey protein, β-CN f1-192, and α_{s1}-CN f24-199.

In addition to a lack of bitterness, Cougar Gold has a nutty, sharp flavor. Aminotransferases, which are key enzymes for the conversion of amino acids into flavor compounds, have not been studied in *Lb. helveticus* WSU19. Characterization of these enzymes from *Lb. helveticus* WSU19 will improve our understanding of the role of this bacterium in the ripening of Cougar Gold.

CHAPTER VI:

References

Altermann, E., Russell, W.M., Azcarate-Peril, M.A., Barrangou, R., Buck, B.L., McAuliffe, O., Souther, N., Dobson, A., Duong, T., Callanan, M., Lick, S., Hamrick, A., Cano, R., and Klaenhammer, T.R. 2005. Complete genome sequence of the probiotic lactic acid bacterium *Lactobacillus acidophilus* NCFM. *Proc. Natl. Acad. Sci. U.S.A.* 102: 3906-3912.

Awad, S., Luthi-Peng, Q.Q., and Puhan, Z. 1998. Proteolytic activities of chymosin and porcine pepsin on buffalo, cow, and goat whole and β-casein fractions. *J. Agric. Food Chem*. 46: 4997-5007.

Baankreis, R. 1992. The role of lactococcal peptidases in cheese ripening. Ph.D. Dissertation, University of Amsterdam, Amsterdam, Netherlands.

Baankreis, R., van Schalkwijk, S., Alting, A.C., and Exterkate, F.A. 1995. The occurrence of two intracellular oligoendopeptidases in *Lactococcus lactis* and their significance for peptide conversion in cheese. *Appl. Microbiol. Biotechnol*. 44: 386-392.

Bartels, H.J., Johnson, M.E., and Olson, N.F. 1987. Accelerated ripening of Gouda cheese. I. Effect of heat-shocked thermophilic lactobacilli and streptococci on proteolysis and flavor development. *Milchwissenschaft.* 42: 83-88.

Bastian, E.D. and Brown, R.J. 1996. Plasmin in milk and dairy products: an update. *Int. Dairy J*. 6: 435-457.

Baumgart, S., Lindner, Y., Kuhne, R., Oberemm, A., Wenschuh, H., and Krause, E. 2004. The contributions of specific amino acid side chains to signal intensities of peptides in matrix-assisted laser desorption/ionization mass spectrometry. *Rapid Commun. Mass Spectrom.* 18: 863-868.

Belitz, H.D., Chen, W., Jugel, H., Treleano, R., and Wieser, H. 1979. Sweet and bitter compounds: structure and taste relationship. Ch. 4, In *Food Taste Chemistry*, J.C. Boudreau (Ed.), 93-131. American Chemical Society, Washington, D.C.

Benech, R.-O., Kheadr, E.E., Lacroix, C., and Fliss, I. 2003. Impact of nisin producing culture and liposome-encapsulated nisin on ripening of *Lactobacillus* added-Cheddar cheese. *J. Dairy Sci.* 86: 1895-1909.

Bhowmik, T. and Marth, E.H. 1988. Protease and peptidase activity of *Micrococcus* species. *J. Dairy Sci*. 71: 2358-2365.

Bockelmann, W. 1995. The proteolytic system of starter and non-starter bacteria: components and their importance for cheese ripening. *Int. Dairy J*. 5: 977-994.

Bolotin, A., Wincker, P., Mauger, S., Jaillon, O., Malarme, K., Weissenbach, J., Ehrlich, S.D., and Sorokin, A. 2001. The complete genome sequence of the lactic acid

bacterium *Lactococcus lactis* ssp. *lactis* IL1403. *Genome Res.* 11: 731-753.

Bouchier, P.J., O'Cuinn, G., Harrington, D., and Fitzgerald, R.J. 2001. Debittering and hydrolysis of a tryptic hydrolysate of b-casein with purified general and proline specific aminopeptidases from *Lactococcus lactis* ssp. *cremoris* AM2. *J. Food Sci.* 66: 816-820.

Boutrou, R., Sepulchre, A., Pitel, G., Durier, C., Vassal, L., Gripon, J.C., and Monnet, V. 1998. Lactococcal lysis and curd proteolysis: two predictable events important for the development of cheese flavour. *Int. Dairy J.* 8: 609-616.

Bradford, M.M. 1976. A rapid and sensitive method for the quantitation of microgram quantities of protein utilizing the principle of dye binding. *Anal. Biochem*. 72: 248-254.

Broadbent, J.R., Barnes, M., Brennands, C., Strickland, M., Houck, K., Johnson, M.E., and Steele, J.L. 2002. Contribution of *Lactococcus lactis* cell envelope proteinase specificity to peptide accumulation and bitterness in reduced-fat Cheddar cheese. *Appl. Environ. Microbiol.* 68: 1778-1785.

Broadbent, J.R., Strickland, M., Weimer, B.C., Johnson, M.E., and Steele, J.L. 1998. Peptide accumulation and bitterness in Cheddar cheese made using single-strain *Lactococcus lactis* starters with distinct proteinase specificities. *J. Dairy Sci*. 81: 327-337.

Broome, M.C. and Limsowtin, G.K.Y. 1998. Starter peptidase activity in maturing cheese. *Aust. J. Dairy Technol*. 53: 79-82.

Burkitt, W.I., Giannakopulos, A.E., Sideridou, F., Bashir, S., and Derrick, P.J. 2003. Discrimination effects in MALDI-MS of mixtures of peptides-analysis of the proteome. *Aust. J. Chem.* 56: 369-377.

Chen, J.-D. and Morrison, D.A. 1987. Cloning of *Streptococcus pneumoniae* DNA fragments in *Escherichia coli* requires vectors protected by strong transcriptional terminators. *Gene*. 55: 179-187.

Chen, Y.-S., Christensen, J.E., Broadbent, J.R., and Steele, J.L. 2003. Identification and characterization of *Lactobacillus helveticus* PepO2, an endopeptidase with post-proline specificity. *Appl. Environ. Microbiol*. 69: 1276-1282.

Chen, Y.-S. and Steele, J.L. 1998. Genetic characterization and physiological role of endopeptidase O from *Lactobacillus helveticus* CNRZ32. *Appl. Environ. Microbiol.* 64: 3411-3415.

Chen, Y.-S. and Steele, J.L. 2005. Analysis of promoter sequences from *Lactobacillus helveticus* CNRZ32 and their activity in other lactic acid bacteria. *J. Appl. Microbiol*.

98: 64-72.

Chitpinityol, S. and Crabbe, M.J.C. 1998. Chymosin and aspartic proteinase: review. *Food Chem*. 61: 395-418.

Christensen, J.E., Dudley, E.G., Pederson, J.A., and Steele, J.L. 1999. Peptidases and amino acid catabolism in lactic acid bacteria. *Antonie van Leeuwenhoek*. 76: 217-246.

Christensen, J.E., Johnson, M.E., and Steele, J.L. 1995. Production of Cheddar cheese using a *Lactococcus lactis* ssp. *cremoris* SK11 derivative with enhanced aminopeptidase activity. *Int. Dairy J.* 5: 367-379.

Christensen, J.E., Lin, D.-I., Palva, A., and Steele, J.L. 1995. Sequence analysis, distribution and expression of an aminopeptidase N-encoding gene from *Lactobacillus helveticus* CNRZ32. *Gene*. 155: 89-93.

Christensson, C., Bratt, H., Collins, L.J., Coolbear, T., Holland, R., Lubbers, M.W., O'Toole, P.W., and Reid, J.R. 2002. Cloning and expression of an oligopeptidase, PepO, with novel specificity from *Lactobacillus rhamnosus* HN001 (DR20). *Appl. Environ. Microbiol*. 68: 254-262.

Cliffe, A.J. and Law, B.A. 1990. Peptide composition of enzyme-treated Cheddar cheese slurries, determined by reverse phase high performance liquid chromatography. *Food Chem.* 36: 73-80.

Courtin, P., Nardi, M., Wegmann, U., Joutsjoki, V., Ogier, J.C., Gripon, A, Palva, A., Henrich, B., and Monnet, V. 2002. Accelerating cheese proteolysis by enriching *Lactococcus lactis* proteolytic system with lactobacilli peptidases. *Int. Dairy J.* 12: 447-454.

Creamer, L.K. 1975. β-casein degradation in Gouda and Cheddar cheese. *J. Dairy Sci*. 58: 287-292.

Creamer, L.K. and MacGibbon, A.K.H. 1996. Some recent advances in the basic chemistry of milk proteins and lipids. *Int. Dairy J*. 6: 539-568.

Crow, V.L., Martley, F.G., Coolbear, T., and Roundhill, S.J. 1995. The influence of phage-assisted lysis of *Lactococcus lactis* subsp. *lactis* ML8 on Cheddar cheese ripening. *Int. Dairy J.* 5: 451-472.

Czulak, J. 1959. Bitter flavour in cheese. *Aust. J. Dairy Technol*. 14: 177-179.

Dako, E., El-Soda, M., Vuillemard, J.C., and Simard, R.E. 1995. Autolytic properties and aminopeptidase activities of lactic acid bacteria. *Food Res. Int*. 28: 503-509.

Dalgleish, D.G. 1997. Structure-function relationships of caseins. Ch. 7, In *Food Proteins and Their Applications*, S. Damodaran and A. Paraf (Eds.), 199-223. Marcel Dekker, NY.

Drake, M.A., Boylston, T.D., Spence, K.D., and Swanson, B.G. 1997. Improvement of sensory quality of reduced fat Cheddar cheese by a *Lactobacillus* adjunct. *Food Res. Int.* 30: 35-40.

El Abboudi, M., El Soda, M., Pandian, S., Barreau, M., Trepanier, G., and Simard, R.E. 1991. Peptidase activities in debittering and nondebittering strains of lactobacilli. *Int. Dairy J.* 1: 55-64.

El Soda, M., Madkor, S.A., and Tong, P.S. 2000. Adjunct cultures: recent development and potential significance to the cheese industry. *J. Dairy Sci*. 83: 609-619.

Exterkate, F.A. 1987. On the possibility of accelerating the ripening of Gouda Cheese; a comment. *Neth. Milk Dairy J.* 41: 189-194.

Exterkate, F.A. and Alting, A.C. 1993. The conversion of the as1-casein-(1-23)-fragment by the free and bound form of the cell-envelope proteinase of *Lactococcus lactis* subsp. *cremoris* under conditions prevailing in cheese. *System Appl. Microbiol.* 16: 1-8.

Exterkate, F.A. and Alting, A.C. 1995. The role of starter peptidases in the initial proteolytic events leading to amino acids in Gouda Cheese. *Int. Dairy J.* 5: 15-28.

Exterkate, F.A., Alting, A.C., and Bruinenberg, P.G. 1993. Diversity of cell envelope proteinase specificity among strains of *Lactococcus lactis* and its relationship to charge characteristics of the substrate-binding region. *Appl. Environ. Microbiol.* 59: 3640-3647.

Fajarrini, F. 1999. The influence of aminopeptidases from adjunct *Lactobacilli helveticus* on bitterness in Cheddar cheese. M.S. Thesis. Washington State Univ., Pullman, WA.

Fallico, V., McSweeney, P.L.H., Horne, J., Pediliggieri, C., Hannon, J.A., Carpino, S., and Licitra, G. 2005. Evaluation of bitterness in Ragusano Cheese. *J. Dairy Sci*. 88: 1288-1300.

Farkye, N. 1995. Contribution of milk-clotting enzymes and plasmin to cheese ripening. In *Chemistry of Structure-Function Relationships in Cheese*, E.L. Malin and M.H. Tunick (Eds.), 195-207. Plenum Press, NY.

Farrell, H.M., Qi, P.X., Brown, E.M., Cooke, P.H., Tunick, M.H., Wickham, E.D., and Unruh, J.J. 2002. Molten globule structures in milk proteins: implications for potential new structure-function relationships. *J. Dairy Sci*. 85: 459-471.

Fenster, K.M., Parkin, K.L., and Steele, J.L. 1997. Characterization of a thiol-dependent endopeptidase from *Lactobacillus helveticus* CNRZ32. *J. Bacteriol.* 179: 2529-2533.

Fernandez, L., Bhowmik, T., and Steele, J.L. 1994. Characterization of the *Lactobacillus helveticus* CNRZ32 *pepC* gene. *Appl. Environ. Microbiol.* 60: 333-336.

Forde, A. and Fitzgerald, G.F. 2000. *Curr. Opin. Biotechnol*. 11: 484-489.

Fortina, M.G., Nicastro, G., Carminati, D., Neviani, E., and Manachini, P.L. 1998. *Lactobacillus helveticus* heterogeneity in natural cheese starters: the diversity in phenotypic characteristics. *J. Appl. Microbiol.* 84: 72-80.

Fox, P.F., Guinee, T.P., Cogan, T.M., and McSweeney, P.L.H. 2000. Chemistry of milk constituents. Ch. 3, In *Fundamentals of Cheese Science*, 19-44. Aspen Publishers, Gaithersburg, MD.

Fox, P.F. and McSweeney, P.L.H. 1997. Rennets: their role in milk coagulation and cheese ripening. Ch. 9, In *Microbiology and Biochemistry of Cheese and Fermented Milk*, B.A. Law (Ed.), 299-314. Chapman and Hall, London, UK.

Fox, P.F., McSweeney, P.L.H., and Lynch, C.M. 1998. Significance of non-starter lactic acid bacteria in Cheddar cheese. *Aust. J. Dairy Technol.* 53: 83-89.

Fox, P.F., O'Connor, T.P., McSweeney, P.L.H., Guinee, T.P., and O'Brien, N.M. 1996. Cheese: physical, biochemical, and nutritional aspects. *Adv. Food Nutr. Res*. 39: 163-328.

Fox, P.F., Singh, T.K., and McSweeney, P.L.H. 1995. Biogenesis of flavour compounds in cheese. In *Chemistry of Structure-Function Relationship in Cheese*, E.L. Malin and M.H. Tunick (Eds.), 59-98. Plenum Press, NY.

Frister, H., Michaelis, M., Schwerdtfeger, T., Folkenberg, D.M., and Sorensen, N.K. 2000. Evaluation of bitterness in Cheddar cheese. *Milchwissenschaft*. 55: 691-695.

Gobbetti, M., Cossignani, L., Simonetti, M.S., and Damiani, P. 1995. Effect of the aminopeptidase from *Pseudomonas fluorescens* ATCC 948 on synthetic bitter peptides, bitter hydrolysate of UHT milk proteins and on the ripening of Italian Caciotta type cheese. *Lait*. 75: 169-179.

Gomez, M.J., Garde, S., Gaya, P., Medina, M., and Nunez, M. 1997. Relationship between level of hydrophobic peptides and bitterness in cheese made from pasteurized and raw milk. *J. Dairy Res*. 64: 289-297.

Gomez, M.J., Gaya, P., Nunez, M., and Medina, M. 1996. Debittering activity of peptidases from selected lactobacilli strains in model cheeses. *Milchiwissenschaft*. 51: 315-319.

Gouldsworthy, A.M., Leaver, J., and Banks, J.M. 1996. Application of a mass spectrometry sequencing technique for identifying peptides present in Cheddar cheese. *Int. Dairy J.* 6: 781-790.

Guigoz, Y. and Solm, J. 1974. Isolation of a bitter tasting peptide from "Alpkase", a Swiss mountain-cheese. *Lebensm. Wiss. Technol*. 7: 356-357.

Guinec, N., Nardi, M., Matos, J., Gripon, J.-C., and Monnet, V. 2000. Modulation of casein proteolysis by lactococcal peptidase gene inactivation. *Int. Dairy J.* 10: 607-615.

Guldfeldt, L.U., Sörensen, K.I., Ströman, P., Behrndt, H., Williams, D., and Johansen, E. 2001. Effect of starter cultures with a genetically modified peptidolytic or lytic system on Cheddar cheese ripening. *Int. Dairy J.* 11: 373-382.

Habibi-Najafi, M.B. and Lee, B.H. 1996. Bitterness in cheese: a review. *Crit. Rev. Food Sci. Nutr*. 36: 397-411.

Hamilton, J.S., Hill, R.D., and van Leeuwen, H. 1974. A bitter peptide from Cheddar cheese. *Agric. Biol. Chem*. 38: 375-379.

Hashimoto, A., Aoyagi, H., and Izumiya, N. 1980. Synthetic identification of bitter heptapeptide in tryptic hydrolysate of casein. *Bull. Chem. Soc. Jpn.* 53: 2926-2928.

Hebert, E.M, Raya, R.R., and deGoiri, G.S. 2002. Modulation of the cell-surface proteinase activity of thermophilic lactobacilli by the peptide supply. *Curr. Microbiol*. 45: 385-389.

Hellendoorn, M.A., Mierau, I., Van Der Horst, M., Venema, G., and Kok, J. 1996. A second endopeptidase PepO2 in *Lactococcus lactis* subsp. *cremoris* MG1363. Abstracts, Fifth Symposium on Lactic Acid Bacteria. Veldhoven, The Netherlands.

Holt, C. 1982. Structure and stability of bovine casein micelles. *Adv. Prot. Chem*. 43: 63-151.

Holt, C. and Sawyer, L. 1993. Caseins as rheomorphic proteins. *J. Chem. Soc. Faraday*. 89: 2683-2690.

Huber, L. and Klostermeyer, H. 1974. Isolation of a bitter peptide from the cheese "Butterkase" and its identification. *Milchwissenschaft*. 29: 449-455.

Hutkins, R.W. 2001. Metabolism of starter cultures. Ch. 7, In *Applied Dairy Microbiology*, E.H. Marth and J.L. Steele (Eds.), 207-241. Marcel Dekker, NY.

Ishibashi, N., Arita, Y., Kanehisa, H., Kouge, K., Okai, H., and Fukui, S. 1987. Bitterness of leucine-containing peptides. *Agric. Biol. Chem.* 51: 2389-2394.

Ishibashi, N., Kouge, K., Shinoda, I., Kanehisa, H., and Okai, H. 1988c. A mechanism for bitter taste sensibility in peptides. *Agric. Biol. Chem.* 52: 819-827.

Ishibashi, N., Kubo, T., Chino, M., Fukui, H., Shinoda, I., Kikuchi, E., Okai, H., and Fukui, S. 1988b. Taste of proline-containing peptides. *Agric. Biol. Chem.* 52: 95-98.

Ishibashi, N., Ono, I., Kato, K., Shigenaga, T., Shinoda, I., Okai, H., and Fukui, S. 1988a. Role of the hydrophobic amino acid residue in the bitterness of peptide. *Agric. Biol. Chem.* 52: 91-94.

Joutsjoki, V., Luoma, S., Tamminen, M., Kilpi, M., Johansen, E., and Palva, A. 2002. Recombinant *Lactococcus* starters as a potential source of additional peptidolytic activity in cheese ripening. *J. Appl. Microbiol.* 92: 1159-1166.

Juillard, V., Laan, H., Kunji, E.R.S., Jeronimus-Stratingh, C.M., Bruins, A.P., and Konings, W.N. 1995. The extracellular P_I-type proteinase of *Lactococcus lactis* hydrolyzes β-casein into more than one hundred different oligopeptides. *J. Bacteriol*. 177: 3472-3478.

Kanehisa, H., Miyake, I., Okai, H., Aoyagi, H., and Izumiya, N. 1984. Studies of bitter peptides from casein hydrolysate. X. Synthesis and bitter taste of H-Arg-Gly-Pro-Phe-Pro-Ile-Ile-Val-OH corresponding to C-terminal portion of β-casein. *Bull. Chem. Soc. Jpn.* 57: 819-822.

Kato, H., Shinoda, I., Fushimi, A., and Okai, H. 1985. Bitter taste of C-terminal tetradecapeptide of bovine β-casein, -Pro^{196}-Val-Leu-Gly-Pro-Val-Arg-Gly-Pro-Phe-Pro-Ile-Ile-Val^{209}. In *Peptide Chemistry 1985*, Y. Kiso (Ed.), 281-286. Protein Research Foundation, Osaka, Japan.

Kleerebezem, M., Boekhorst, J., van Kranenburg, R., Molenaar, D., Kuipers, O.P., Leer, R., Tarchini, R., Peters, S.A., Sandbrink, H.M., Fiers, M.W., Stiekema, W., Lankhorst, R.M., Bron, P.A., Hoffer, S.M., Groot, M.N., Kerkhoven, R., de Vries, M., Ursing, B., de Vos, W.M., and Siezen, R.J. 2004. Complete genome sequence of *Lactobacillus plantarum* WCFS1. *Proc. Natl. Acad. Sci. U.S.A.* 100: 1990-1995.

Klein, J.R., Henrich, B., and Plapp, R. 1994. Cloning and nucleotide sequence analysis of the *Lactobacillus delbrueckii* ssp. *lactis* DSM7290 cysteine aminopeptidase gene *pepC*. *FEMS Microbiol. Lett.* 124: 291-299.

Knochenmuss, R., Stortelder, A., Breuker, K., and Zenobi, R. 2000. Secondary ion-molecule reactions in matrix-assisted laser desorption/ionization. *J. Mass Spectrom*. 35: 1237-1245.

Koka, R. and Weimer, B.C. 2000. Investigation of the ability of a purified protease from *Pseudomonas fluorescens* RO98 to hydrolyze bitter peptides from cheese. *Int. Dairy*

J. 10: 75-79.

Kunji, E.R.S., Fang, G., Jeronimus-Stratingh, C.M., Bruins, A.P., Poolman, B., and Konings, W.N. 1998. Reconstruction of the proteolytic pathway for use of β-casein by *Lactococcus lactis*. *Mol. Microbiol*. 27: 1107-1118.

Law, J. and Haandrikman, A. 1997. Proteolytic enzymes of lactic acid bacteria: review article. *Int. Dairy J*. 7: 1-11.

Law, B.A. and Mulholland, F. 1995. Enzymology of lactococci in relation to flavour development from mik proteins. *Int. Dairy J*. 5: 833-854.

Lee, K.D., Lo, C.G., and Warthesen, J.J. 1996. Removal of bitterness from the bitter peptides extracted from Cheddar cheese with peptidases from *Lactococcus lactis* ssp. *cremoris* SK11. *J. Dairy Sci*. 79: 1521-1528.

Lee, K.D. and Warthesen, J.J. 1996. Preparative methods of isolating bitter peptides from Cheddar cheese. *J. Agric. Food Chem*. 44: 1058-1063.

Lemieux, L. and Simard, R.E. 1991. Bitter flavour in dairy products. I. A review of the factors likely to influence its development, mainly in cheese manufacture. *Lait*. 71: 599-636.

Lemieux, L. and Simard, R.E. 1992. Bitter flavour in dairy products. II. A review of bitter peptides from caseins: their formation, isolation and identification, structure masking and inhibition. *Lait*. 72: 335-382.

Lepeuple, A.-S., Vassal, L. Cesselin, B., Delacroix-Buchet, A., Gripon, J.-C., and Chapot-Chartier, M.-P. 1998. Involvement of a prophage in the lysis of *Lactococcus lactis* subsp. *cremoris* AM2 during cheese ripening. *Int. Dairy J.* 8: 667-674.

Lowrie, R.J. and Lawrence, R.C. 1972. Cheddar cheese flavour. IV. A new hypothesis to account for the development of bitterness. *N. Z. J. Dairy Sci. Technol*. 7: 51-53.

Lowrie, R.J., Lawrence, R.C., and Pearce, L.E. 1972. Cheddar cheese flavour. III. The growth of lactic streptococci during cheesemaking and the effect on bitterness development. *N. Z. J. Dairy Sci. Technol.* 7: 44-50.

Malin, E. L., Alaimo, M.H., Brown, E.M., Aramini, J.M., Germann, M.W., Farrell, H.M., McSweeney, P.L.H., and Fox, P.F. 2001. Solution structures of casein peptides: NMR, FTIR, CD, and molecular modeling studies of αs1-casein, 1-23. *J. Prot. Chem.* 20: 391-404.

Martley, F.G. and Lawrence, R.C. 1972. Cheddar cheese flavour. II. Characteristics of single strain starters associated with good or poor flavour development. *N. Z. J. Dairy Sci.*

Technol. 7: 38-44.

Matoba, T., Hayashi, R., and Hata, T. 1970. Isolation of bitter peptides from tryptic hydrolysate of casein and their chemical structure. *Agric. Biol. Chem.* 34: 1235-1243.

Mayo, B. 1993. The proteolytic system of lactic acid bacteria. *Microbiologia Sem*. 9: 90-106.

McGarry, A., Law, J., Coffey, A., Daly, C., Fox, P.F., and Fitzgerald, G.F. 1994. Effect of genetically modifying the lactococcal proteolytic system on ripening and flavor development in Cheddar cheese. *Appl. Environ. Microbiol.* 60: 4226-4233.

McSweeney, P.L.H. 1997. The flavour of milk and dairy products: III. Cheese: taste. *Int. J. Dairy Technol*. 50: 123-128.

McSweeney, P.L.H. 2004. Biochemistry of cheese ripening. *Int. J. Dairy Technol.* 57: 127-144.

McSweeney, P.L.H., Fox, P.F., and Law, J. 1993. Contribution of cell-wall associated proteinases of *Lactococcus* to the primary proteolysis of β-casein in Cheddar cheese. *Milchwissenschaft*. 48: 319-321.

Meijer, W., van de Bunt, B., Twigt, M., de Jonge, B., Smit, G., and Hugenholtz, J. 1998. Lysis of *Lactococcus lactis* subsp. *cremoris* SK110 and its nisin-immune transconjugant in relation to flavor development in cheese. *Appl. Environ. Microbiol.* 64: 1950-1953.

Mierau, I., Tan, P.S.T., Haandrikman, A.J., Kok, J., Leenhouts, K.J., Konings, W.N., and Venema, G. 1993. Cloning and sequencing of the gene for a lactococcal endopeptidase, an enzyme with sequence similarity to mammalian enkephalinase. *J. Bacteriol.* 175: 2087-2096.

Minamiura, N., Matsumura, Y., Fukumoto, J., and Yamamoto, T. 1972. Bitter peptides in cow milk digests with bacterial proteinase. *Agric. Biol. Chem.* 36: 588-595.

Miyake, I., Kouge, K., Kanehisa, H., and Okai, H. 1983. Studies of bitter peptides from casein hydrolyzate. III. Bitter taste of synthetic analogs of BPIa (Arg-Gly-Pro-Pro-Phe-Ile-Val) containing D-proline or glycine in place of L-proline. *Bull. Chem. Soc. Jpn*. 56: 1678-1681.

Morgan, S.M., O'Sullivan, L., Ross, R.P., and Hill, C. 2002. The design of a three strain starter system for Cheddar cheese manufacture exploiting bacteriocin-induced starter lysis. *Int. Dairy J.* 12: 985-993.

Mucchetti, G., Locci, F., Massara, P., Vitale, R., and Neviani, E. 2002. Production of pyroglutamic acid by thermophilic lactic acid bacteria in hard-cooked mini cheeses. *Int. Dairy J.* 85: 2489-2496.

Mulholland, F. 1997. Proteolytic systems of dairy lactic acid bacteria. Ch. 9, In *Microbiology and Biochemistry of Cheese and Fermented Milk*, B.A. Law (Ed.), 299-314. Chapman and Hall, London, UK.

Ney, K.H. 1979. Bitterness of peptides: amino acid composition and chain length. Ch. 6, In *Food Taste Chemistry*, J.C. Boudreau, 149-173. American Chemical Society, Washington, D.C.

Nielsen, S.S. 2002. Plasmin system and microbial proteases in milk: characteristics, roles, and relationship. *J. Agric. Food Chem.* 50: 6628-6634.

Oberg, C.J., Broadbent, J.R., Strickland, M., and McMahon, D.J. 2002. Diversity in specificity of the extracellular proteinase in *Lactobacillus helveticus* and *Lactobacillus delbrueckii* subsp. *bulgaricus. Lett. Appl. Microbiol*. 34: 455-460.

Olson, D.A. 1998. The ability of intracellular enzymes of *Lactobacillus helveticus* strains to degrade bitter peptides. M.S. Thesis. Washington State University, Pullman, WA.

Otagiri, K., Miyake, I., Ishibashi, N., Fukui, H., Kanehisa, H., and Okai, H. 1983. Studies of bitter peptides from casein hydrolysate. II. Syntheses of bitter peptide fragments and analogs of BPIa (Arg-Gly-Pro-Pro-Phe-Ile-Val) from casein hydrolysate. *Bull. Chem. Soc. Jpn.* 56: 1116-1119.

Parra, L., De Palencia, F., Casal, V., Requena, T., and Pelaez, C. 1999. Hydrolysis of β-casein (f193-209) fragment by whole cells and fractions of *Lactobacillus casei* and *Lactococcus lactis*. *J. Food Sci*. 64: 899-902.

Pillidge, C.J., Crow, V.L., Coolbear, T., and Reid, J.R. 2003. Exchanging lactocepin plasmids in lactococcal starters to study bitterness development in Gouda cheese: a preliminary investigation. *Int. Dairy J.* 13: 345-354.

Pouwels, P.H. and Chaillou, S. 2003. Gene expression in lactobacilli. Ch. 6, In *Genetics of Lactic Acid Bacteria*, B.B. Wood and P.J. Warner (Eds.), 143-188. Kluwer Academic/Plenum Publishers, New York, NY.

Pouwels, P.H. and Leer, R.J. 1993. Genetics of lactobacilli: plasmids and gene expression. *Antonie van Leeuwenhoek*. 64: 85-107.

Pridmore, R.D., Berger, B., Desiere, F., Vilanova, D., Barretto, C., Pittet, A.C., Zwahlen, M.C., Rouvet, M., Altermann, E., Barrangou, R., Mollet, B., Mercenier, A., Klaenhammer, T., Arigoni, F., and Schell, M.A. 2004. The genome sequence of the probiotic intestinal bacterium *Lactobacillus johnsonii* NCC 533. *Proc. Natl. Acad. Sci. U.S.A.* 101: 2512-2517.

Pritchard, G.G. and Coolbear, T. 1993. The physiology and biochemistry of the proteolytic system in lactic acid bacteria. *FEMS Microbiol. Rev*. 12: 179-206.

Ribadeau-Dumas, B., Brignon, F., Grosclaude, F., and Mercier, J.-C. 1972. Primary structure of bovine β-casein. Sequence complete. *Eur. J. Biochem*. 25: 505-514 (French).

Richardson, B.C. and Creamer, L.K. 1973. Casein proteolysis and bitter peptides in Cheddar cheese. *N. Z. J. Dairy Sci. Technol*. 8: 46-51.

Sambrook, J., Fritsch, E.F., and Maniatis, T. 1989. Molecular cloning: a laboratory manual, 2nd ed.. Cold Spring Harbor Laboratory, Cold Spring Harbor, NY.

Sasaki, M., Bosman, B.W., and Tan, P.T. 1995. Comparison of proteolytic activities in various lactobacilli. *J. Dairy Res*. 62: 601-610.

Shin, J.Y., Jeon, W.M., Kim, G.-B., and Lee, B.H. 2004. Purification and characterization of intracellular proteinase from *Lactobacillus casein* ssp. *casei* LLG. *J. Dairy Sci.* 87: 4097-4103.

Shinoda, I., Fushimi, A., Kato, H., Okai, H., and Fukui, S. 1985b. Bitter taste of synthetic C-terminal tetradecapeptide of bovine β-casein, H-Pro^{196}-Val-Leu-Gly-Pro-Val-Arg-Gly-Pro-Phe-Pro-Ile-Ile-Val^{209}-OH, and its related peptides. *Agric. Biol. Chem.* 49: 2587-2596.

Shinoda, I., Tada, M., Otagiri, K., and Okai, H. 1985a. Bitter taste of Pro-Phe-Pro-Gly-Pro-Ile-Pro corresponding to the partial sequence (positions 61-67) of bovine β-casein. In *Peptide Chemistry 1985*, Y. Kiso (Ed.), 287-290. Protein Research Foundation, Osaka, Japan.

Singh, T.K., Young, N.D., Drake, M., and Cadwallader, K.R. 2005. Production and sensory characterization of a bitter peptide from β-casein. *J. Agric. Food Chem.* 53: 1185-1189.

Smit, G., Kruyswijk, Z., Weerkamp, A.H., de Jong, C., and Neeter, R. 1996. Screening for and control of debittering properties of cheese culture. In *Flavour Science : Recent Developments*, A.J. Taylor and D.S. Mottram (Eds.), 8th ed., 25-31. Royal Society of Chemistry, Cambridge, UK.

Soeryapranata, E., Powers, J.R., Hill, H.H., Siems, W.F., Al-Saad, K., and Weller, K.M. 2002a. Matrix-assisted laser desorption/ionization time-of-flight mass spectrometry method for the quantification of beta-casein fragment (f193-209). *J. Food Sci*. 67: 534-538.

Soeryapranata, E., Powers, J.R., Fajarrini, F., Weller, K.M., Hill, H.H., and Siems, W.F. 2002b. Relationship between MALDI-TOF analysis of β-CN f193-209 concentration and sensory evaluation of bitterness intensity of aged Cheddar cheese. *J. Agric. Food*

Chem. 50: 4900-4905.

Soeryapranata, E., Powers, J.R., Weller, K.M., Hill, H.H., and Siems, W.F. 2004. Differentiation of intracellular peptidases of starter and adjunct cultures using matrix-assisted laser desorption/ ionization time-of-flight mass spectrometry. *Lebensm.-Wiss. Technol.* 37: 17-22.

Somers, J.M. and Kelly, A.L. 2002. Contribution of plasmin to primary proteolysis during ripening of cheese: effect of milk heat treatment and cheese cooking temperature. *Lait*. 82: 181-191.

Sorensen, N.K., Qvist, K.B., and Mulholland, F. 1996. Significance of low molecular weight nitrogen constituents in cheese milk and of proteinase-negative variants of a *Lactococcus lactis* subsp. *Cremoris* strain on the production and maturation of Danbo cheese. *Int. Dairy J.* 6: 113-128.

Sousa, M.J., Ardo, Y., and McSweeney, P.L.H. 2001. Advances in the study of protelysis during cheese ripening. *Int. Dairy J.* 11: 327-345.

Southern, E.M. 1975. Detection of specific sequences among DNA fragments separated by gel electrophoresis. *J. Mol. Biol*. 98: 503-517.

Sridhar, V.R. 2003. Development of food-grade starter system and role(s) of endopeptidase from *Lactobacillus helveticus* CNRZ32 to control bitterness in cheese. Ph.D. Dissertation, University of Wisconsin-Madison, Madison, WI.

Sridhar, V.R., Hughes, J.E., Welker, D.L., Broadbent, J.R., and Steele, J.L. 2005. Identification of endopeptidase genes from the genomic sequence of *Lactobacillus helveticus* CNRZ32 and the role of these genes in hydrolysis of model bitter peptides. *Appl. Environ. Microbiol.* 71: 3025-3032.

Stadhouders, J., Hup, G., Exterkate, F.A., and Visser, S. 1983. Bitter flavour in cheese. 1. Mechanism of the formation of the bitter flavour defect in cheese. *Neth. Milk. Dairy. J.* 37: 157-167.

Steele, J. 1995. Contribution of lactic acid bacteria to cheese ripening. In *Chemistry of Structure-Function Relationships in Cheese*, E.L. Malin and M.H. Tunick (Eds.), 209-220. Plenum Press, NY.

Stepaniak, L. 2004. Dairy enzymology. *Int. J. Dairy Technol.* 57: 153-171.

Stepaniak, L. and Fox, P.F. 1995. Characterization of the principal intracellular endopeptidase from *Lactococcus lactis* subsp. *lactis* MG1363. *Int. Dairy J*. 5: 699-713.

Stepaniak, L., Gobbetti, M., Sorhaug, T., Fox, P.F., and Hojrup, B. 1996. Peptides inhibitory to endopeptidase and aminopeptidase from *Lactococcus lactis* ssp. *lactis* MG1363, released from bovine beta-casein by chymosin, trypsin, or chymotrypsin. *Z. Lebensm.-Unters. forsch*. 202: 329-333.

Sullivan, J.J. and Jago, G.R. 1970. A model for bitter peptide formation and degradation in cultured dairy products. *Aust J. Dairy Technol.* 25: 111.

Sullivan, J.J. and Jago, G.R. 1972. The structure of bitter peptides and their formation from casein. *Aust. J. Dairy Technol*. 27: 98-104.

Swaisgood, H.E. 1992. Chemistry of the caseins. Ch. 2, In *Advanced Dairy Chemistry-1: Proteins*, P.F. Fox (Ed.), 63-110. Elsevier Applied Science, NY.

Takafuji, S., Iwasaki, T., Sasaki, M., and Tan, P.S.T. 1995. Proteolytic enzymes of lactic acid bacteria. In *Food Flavors: Generation, Analysis, and Process Influence*, G. Charalambous (Ed.), 753-767. Elsevier Science, NY.

Tan, P.S.T., Poolman, B., and Konings, W.N. 1993b. Proteolytic enzymes of *Lactococcus lactis*. *J. Dairy Res*. 60: 269-286.

Tan, P.S.T., Pos, K.M., and Konings, W.M. 1991. Purification and characterization of an endopeptidase from *Lactococcus lactis* subsp. *cremoris* WG2. *Appl. Environ. Microbiol.* 57: 3593-3599.

Tan, P.S.T., van Kessel, T.A.J.M., van de Veerdonk, F.L.M., Zuurendonk, P.F., Bruins, A.P., and Konings, W.N. 1993a. Degradation and debittering of a tryptic digest from β-casein by aminopeptidase N from *Lactococcus lactis* subsp. *Cremoris* Wg2. *Appl. Environ. Microbiol*. 59: 1430-1436.

Tsakalidou, E., Anastasiou, R., Vandenberghe, I., Van Beeumen, J., and Kalantzopoulos, G. 1999. Cell-wall-bound proteinase of *Lactobacillus delbrueckii* subsp. *lactis* ACA-DC 178: characterization and specificity for β-casein. *Appl. Environ. Microbiol*. 65: 2035-2040.

Tynkkynen, S., Buist, G., Kunji, E., Kok, J., Poolman, B., Venema, G., and Haandrikman, A. 1993. Genetic and biochemical characterization of the oligopeptide transport system of *Lactococcus lactis. J. Bacteriol.* 175: 7523-7532.

Valero, M.-L., Giralt, E., and Andreu, D. 1999. An investigation of residue-specific contributions to peptide desorption in MALDI-TOF mass spectrometry. *Lett. Peptide Sci.* 6: 109-115.

Varmanen, P., Vesanto, E., Steele, J.L., and Palva, A. 1994. Characterization and expression of the *pepN* gene encoding a general aminopeptidase from *Lactobacillus helveticus*.

FEMS Microbiol. Lett. 124: 315-320.

Vesanto, E., Varmanen, P., Steele, J.L., and Palva, A. 1994. Characterization and expression of the *Lactobacillus helveticus pepC* gene encoding a general aminopeptidase. *Eur. J. Biochem.* 224: 991-997.

Visser, S., Hup, G., Exterkate, F.A., and Stadhouders, J. 1983a. 3. Comparative gel-chromatographic analysis of hydrophobic peptide fractions from twelve Gouda-type cheeses and identification of bitter peptides isolated from a cheese made with *Streptococcus cremoris* strain HP. *Neth. Milk Dairy J*. 37: 181-192.

Visser, S., Slangen, K.J., Hup, G., and Stadhouders, J. 1983b. Bitter flavour in cheese. 2. Model studies on the formation and degradation of bitter peptides by proteolytic enzymes from calf rennet, starter cells and starter cell fractions. *Neth. Milk Dairy J.* 37: 169-180.

Walstra, P. 1990. On the stability of casein micelles. *J. Dairy Sci*. 73: 1965-1979.

Walstra, P. 1999. Casein sub-micelles: do they exist? *Int. Dairy J*. 9: 189-192.

Whitney, R.M. 1999. Proteins of milk. Ch.3, In *Fundamentals of Dairy Chemistry*, 3rd ed., N.P. Wong (Ed.), 81-169. Aspen Publishers Inc., MD.

Wilkinson, M.G., Guinee, T.P., O'Callaghan, D.M., and Fox, P.F. 1992. Effects of commercial enzymes on proteolysis and ripening in Cheddar cheese. *Lait*. 72: 449-459.

Yan, T.-R., Azuma, N., Kaminogawa, S., and Yamauchi, K. 1987a. Purification and characterization of a substrate-size-recognizing metalloendopeptidase from *Streptococcus cremoris* H61. *Appl. Environ. Microbiol.* 53: 2296-2302.

Yan, T.-R., Azuma, N., Kaminogawa, S., and Yamauchi, K. 1987b. Purification and characterization of a novel metalloendopeptidase from *Streptococcus cremoris* H61. *Eur. J. Biochem.* 163: 259-265.

Zevaco, X. and Desmazeaud, M.J. 1980. Hydrolysis of β-casein and peptides by intracellular neutral protease of *Streptococcus diacetylactis*. *J. Dairy Sci*. 63: 15-24.